
Dépôt Institutionnel de l'Université libre de Bruxelles /
Université libre de Bruxelles Institutional Repository
Thèse de doctorat/ PhD Thesis

Citation APA:

Depreter, F. (2012). *Development of dry powder formulations of proteins for inhalation* (Unpublished doctoral dissertation). Université libre de Bruxelles, Faculté de Pharmacie, Bruxelles.

Disponible à / Available at permalink : <https://dipot.ulb.ac.be/dspace/bitstream/2013/209719/4/f159caa6-ba41-4d28-9968-05f092b72ad9.txt>

(English version below)

Cette thèse de doctorat a été numérisée par l'Université libre de Bruxelles. L'auteur qui s'opposerait à sa mise en ligne dans DI-fusion est invité à prendre contact avec l'Université (di-fusion@ulb.be).

Dans le cas où une version électronique native de la thèse existe, l'Université ne peut garantir que la présente version numérisée soit identique à la version électronique native, ni qu'elle soit la version officielle définitive de la thèse.

DI-fusion, le Dépôt Institutionnel de l'Université libre de Bruxelles, recueille la production scientifique de l'Université, mise à disposition en libre accès autant que possible. Les œuvres accessibles dans DI-fusion sont protégées par la législation belge relative aux droits d'auteur et aux droits voisins. Toute personne peut, sans avoir à demander l'autorisation de l'auteur ou de l'ayant-droit, à des fins d'usage privé ou à des fins d'illustration de l'enseignement ou de recherche scientifique, dans la mesure justifiée par le but non lucratif poursuivi, lire, télécharger ou reproduire sur papier ou sur tout autre support, les articles ou des fragments d'autres œuvres, disponibles dans DI-fusion, pour autant que :

- Le nom des auteurs, le titre et la référence bibliographique complète soient cités;
- L'identifiant unique attribué aux métadonnées dans DI-fusion (permalink) soit indiqué;
- Le contenu ne soit pas modifié.

L'œuvre ne peut être stockée dans une autre base de données dans le but d'y donner accès ; l'identifiant unique (permalink) indiqué ci-dessus doit toujours être utilisé pour donner accès à l'œuvre. Toute autre utilisation non mentionnée ci-dessus nécessite l'autorisation de l'auteur de l'œuvre ou de l'ayant droit.

----- **English Version** -----

This Ph.D. thesis has been digitized by Université libre de Bruxelles. The author who would disagree on its online availability in DI-fusion is invited to contact the University (di-fusion@ulb.be).

If a native electronic version of the thesis exists, the University can guarantee neither that the present digitized version is identical to the native electronic version, nor that it is the definitive official version of the thesis.

DI-fusion is the Institutional Repository of Université libre de Bruxelles; it collects the research output of the University, available on open access as much as possible. The works included in DI-fusion are protected by the Belgian legislation relating to authors' rights and neighbouring rights. Any user may, without prior permission from the authors or copyright owners, for private usage or for educational or scientific research purposes, to the extent justified by the non-profit activity, read, download or reproduce on paper or on any other media, the articles or fragments of other works, available in DI-fusion, provided:

- The authors, title and full bibliographic details are credited in any copy;
- The unique identifier (permalink) for the original metadata page in DI-fusion is indicated;
- The content is not changed in any way.

It is not permitted to store the work in another database in order to provide access to it; the unique identifier (permalink) indicated above must always be used to provide access to the work. Any other use not mentioned above requires the authors' or copyright owners' permission.

ULB

UNIVERSITÉ LIBRE DE BRUXELLES,
UNIVERSITÉ D'EUROPE



Faculté de Pharmacie
Ecole Doctorale en Sciences Pharmaceutiques

**DEVELOPMENT OF DRY POWDER FORMULATIONS OF
PROTEINS FOR INHALATION**

Flore DEPRETER

Thèse présentée en vue de l'obtention du grade de Docteur en Sciences Biomédicales
et Pharmaceutiques

Promoteur: Prof. Karim AMIGHI

Laboratoire de Pharmacie Galénique et Biopharmacie

Composition du jury :

Prof. Jean NEVE (Président)

Prof. Véronique FONTAINE (Secrétaire)

Prof. Jean-Michel KAUFFMANN

Prof. Franck MEYER

Michel DELEERS, Ph.D., D.Sc., B.A.

Prof. Rita VANBEVER (membre externe, Faculté de Pharmacie et des sciences biomédicales – UCL)

Prof. Didier CATALDO (membre externe, Faculté de Médecine, GIGA Research – ULg)

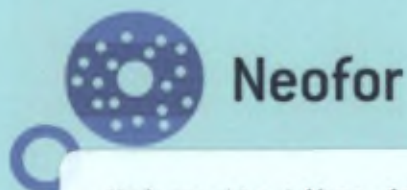


Wallonie



Service public
de Wallonie

Avec le soutien de la DGO6
Département du Développement
Technologique



Universite Libre de Bruxelles



003320678

Année académique 2011-2012



Faculté de Pharmacie Ecole Doctorale en Sciences Pharmaceutiques

DEVELOPMENT OF DRY POWDER FORMULATIONS OF PROTEINS FOR INHALATION

Flore DEPRETER

Thèse présentée en vue de l'obtention du grade de Docteur en Sciences Biomédicales
et Pharmaceutiques

Promoteur: Prof. Karim AMIGHI

Laboratoire de Pharmacie Galénique et Biopharmacie

Composition du jury :

Prof. Jean NEVE (Président)

Prof. Véronique FONTAINE (Secrétaire)

Prof. Jean-Michel KAUFFMANN

Prof. Franck MEYER

Michel DELEERS, Ph.D., D.Sc., B.A.

Prof. Rita VANBEVER (membre externe, Faculté de Pharmacie et des sciences biomédicales – UCL)

Prof. Didier CATALDO (membre externe, Faculté de Médecine, GIGA Research – ULg)



Wallonie



Service public
de Wallonie

Avec le soutien de la DGO6
Département du Développement
Technologique



Neofor

REMERCIEMENTS

J'adresse mes plus sincères remerciements au Professeur Karim Amighi, qui m'a permis de réaliser ce travail de thèse sous sa supervision, au sein du Laboratoire de Pharmacie Galénique et de Biopharmacie. Ses conseils avisés, sa patience et sa disponibilité malgré une charge de travail toujours plus importante ont été des atouts précieux. En tant que directeur du laboratoire, il m'a également permis de bénéficier d'un environnement et de conditions de travail toujours optimales. Peu de chercheurs ont malheureusement cette chance...

Mes plus vifs remerciements vont également à la Région Wallonne, qui a financé ce travail par l'intermédiaire du projet BioWin NEOFOR. Merci en particulier à Monsieur Alain De Mol et Madame Sylvie Ponchaut pour leur suivi du projet.

Je tiens à exprimer ma gratitude à l'entreprise UCB qui a assuré la coordination du projet NEOFOR et a fourni l'anticorps utilisé dans une partie de ce travail. Je remercie tout particulièrement le Docteur Michel Deleers, qui a très largement contribué au bon déroulement du projet par son implication massive, son esprit d'entreprendre, et son indéfectible enthousiasme. Il a toujours été là pour motiver les troupes. Merci aussi à Barbara Camerman pour sa gentillesse et son efficacité dans la gestion des nombreuses réunions passées ensemble.

D'une manière générale, j'adresse des remerciements chargés d'émotion à tous les partenaires du projet NEOFOR pour ces quatre années de collaboration. J'ai pris beaucoup de plaisir à découvrir tous ces différents univers. Merci donc à Daniel Zimmermann, de Cosysys sprl, à Olivier Verhoyen et Jean Vroomen, de Optim Test Center, aux Professeurs Pierre Mathys et Pierre Lambert, et à Michel Pierobon et Nicolas Julémont, de l'ULB-BEAMS, au Professeur André Luxen et au Docteur Jérôme Paris, du Centre de Recherches du Cyclotron (ULg), et enfin au Professeur Brigitte Evrard, au Docteur Séverine Jaspard, et à Amandine Berton, du Laboratoire de Technologie Pharmaceutique (ULg).

Au sein de cette équipe NEOFOR, j'adresse plus particulièrement mes remerciements au Laboratoire de Biologie des Tumeurs et du Développement, dirigé par le Professeur Didier Cataldo, et à Jonathan Hacha, pour les études de toxicité sur souris effectuées sur nos excipients lipidiques.

De même, je remercie chaleureusement le Professeur Serge Goldman, directeur du Département de Médecine Nucléaire de l'hôpital Erasme, ainsi que le Docteur Didier Blocklet et le Docteur Simon Lacroix, pour leur aide dans le radio-marquage des formulations d'insuline, et dans la préparation et la réalisation de l'étude clinique. Un grand merci aussi au personnel infirmier du département pour leur assistance dans la prise en charge des patients.

D'autre part, je remercie vivement le service d'endocrinologie de l'hôpital Erasme, en particulier le Docteur Agnès Burniat et Madame Nicole Hussain, infirmière en chef, pour leur suivi des patients durant l'étude clinique. Merci également aux Docteurs Françoise Fery et Myriam Cnop pour leur aide dans la rédaction du protocole de l'étude et dans le recrutement des patients.

Merci au Professeur Bertrand Blankert, directeur du Laboratoire d'Analyse Pharmaceutique de l'UMons, pour son aide dans la mise au point et la réalisation d'un test de dosage par électrochimie.

Je tiens aussi à remercier l'ensemble des membres du Laboratoire de Pharmacie Galénique et de Biopharmacie, côtoyés quotidiennement durant ces quelques années. Merci en particulier à Nancy Van Aelst et Véronique De Bueger, techniciennes du laboratoire, pour leur aide et leur bonne humeur à toute épreuve.

Un merci spécial à Gabrielle Pilcer et Laurence Durand, collègues devenues amies, pour tous les bons moments passés ensemble au laboratoire, mais aussi en congrès dans les vents tumultueux de l'Ecosse ou de Blankenberge, le froid des gares allemandes, le chaud des spas allemands, et partout ailleurs...

A mes parents, mes deux grand-mères, ma famille et mes amis, pour leur affection et leur aide dans tout ce que la vie peut comporter de petits ou gros soucis. Merci aussi de partager avec moi les petits, et gros, moments de bonheur !

A mon mari, Colin, pour son soutien, sa patience, ses conseils, sa patience, son attention de tous les instants, et sa patience.

TABLE OF CONTENTS

LIST OF ABBREVIATIONS	4
I. SUMMARY	6
II. INTRODUCTION	15
II.1. BASICS OF PULMONARY DRUG DELIVERY	16
II.1.1. ANATOMY AND PHYSIOLOGY OF THE RESPIRATORY TRACT.....	16
<u>II.1.1.1. Respiratory tree</u>	16
<u>II.1.1.2. Epithelium</u>	16
<u>II.1.1.3. Lung surfactant</u>	18
<u>II.1.1.4. Lung volumes</u>	18
II.1.2. LUNG DEPOSITION OF INHALED PARTICLES.....	19
<u>II.1.2.1. Mechanisms</u>	19
<u>II.1.2.2. Parameters influencing lung deposition</u>	21
II.1.2.2.1. Patient features.....	21
II.1.2.2.2. Aerosol features.....	22
II.1.3. DRUG DELIVERY DEVICES	23
<u>II.1.3.1. Nebulisers</u>	23
<u>II.1.3.2. Pressurised Metered Dose Inhalers (pMDI)</u>	26
<u>II.1.3.3. Dry Powder Inhalers (DPIs)</u>	27
II.1.4. MAIN ISSUES IN DPI FORMULATIONS.....	32
<u>II.1.4.1. Overcoming inter-particle interactions</u>	32
II.1.4.1.1. Interaction mechanisms.....	33
II.1.4.1.2. Formulation strategies.....	34
<u>II.1.4.2. Providing controlled release of the drug</u>	36
II.2. PEPTIDES AND PROTEINS FOR PULMONARY DELIVERY	40
II.2.1. STATE OF THE ART	40
<u>II.2.1.1. Topical applications</u>	41
<u>II.2.1.2. Systemic applications</u>	42
II.2.2. MAIN ISSUES IN DPI FORMULATION OF PEPTIDES AND PROTEINS.....	45
<u>II.2.2.1. Crossing the alveolar epithelium</u>	45
II.2.2.1.1. Absorption mechanisms.....	46
II.2.2.1.2. Formulation strategies.....	47
<u>II.2.2.2. Maintaining protein stability</u>	51
II.2.2.2.1. Degradation mechanisms.....	51
II.2.2.2.2. Formulation strategies.....	55
II.3. DIABETES MELLITUS: AN APPLICATION FOR SYSTEMIC PULMONARY DELIVERY OF PROTEIN.....	61
II.3.1. INSULIN IN DIABETES MELLITUS.....	61
II.3.2. PLACE OF INHALED INSULINS	63
<u>II.3.2.1. Insulin absorption through alveolar epithelium</u>	64
<u>II.3.2.2. Examples of inhaled insulins</u>	67
II.3.2.2.1. Exubera®.....	67
II.3.2.2.2. Afrezza®.....	69
II.3.2.2.3. Others.....	72
<u>II.3.2.3. Safety issues</u>	72
II.4. ASTHMA: AN APPLICATION FOR LOCAL PULMONARY DELIVERY OF PROTEIN	74
II.4.1. PHYSIOPATHOLOGY OF ASTHMA	74
II.4.2. CURRENT TREATMENTS.....	75
<u>II.4.2.1. Relievers</u>	75
<u>II.4.2.2. Controllers</u>	76

<u>II.4.2.3. Monoclonal antibodies: a new class of asthma controller</u>	77
II.4.3. PLACE OF INHALED PEPTIDES AND PROTEINS	79
III. AIM OF THE WORK	83
IV. EXPERIMENTAL PART	86
IV.1. DEVELOPMENT AND IN VITRO EVALUATION OF HIGHLY DISPERSIVE INSULIN DRY POWDER FORMULATIONS FOR LUNG ADMINISTRATION	87
IV.1.1. INTRODUCTION	88
IV.1.2. MATERIALS AND METHODS	90
<u>IV.1.2.1. Materials</u>	90
<u>IV.1.2.2. Methods</u>	90
IV.1.2.2.1. Production of the formulations	90
IV.1.2.2.2. Particle size analysis	94
IV.1.2.2.3. Particle morphology	96
IV.1.2.2.4. Insulin content	97
IV.1.2.2.5. Degradation products	98
IV.1.2.2.6. Crystalline state	99
IV.1.2.2.7. Residual solvents	100
IV.1.2.2.8. Aerodynamic features	101
IV.1.2.2.9. Stability study	106
IV.1.3. RESULTS AND DISCUSSION	107
<u>IV.1.3.1. Physicochemical characterisation of the formulations</u>	108
<u>IV.1.3.2. Selection of the inhalation device</u>	113
<u>IV.1.3.3. Aerodynamic characterisation</u>	114
<u>IV.1.3.4. Stability study</u>	118
IV.1.4. CONCLUSION	119
IV.2. COMPARATIVE PHARMACOSCINTIGRAPHIC AND PHARMACOKINETIC EVALUATION OF TWO NEW FORMULATIONS OF INHALED INSULIN IN TYPE 1 DIABETIC PATIENTS	120
IV.2.1. INTRODUCTION	121
IV.2.2. MATERIALS AND METHODS	122
<u>IV.2.2.1. Materials</u>	122
<u>IV.2.2.2. Methods</u>	124
IV.2.2.2.1. Study design	124
IV.2.2.2.2. Patients	125
IV.2.2.2.3. Safety assessment	126
IV.2.2.2.4. Radiolabelling of the formulations	126
IV.2.2.2.5. Validation of the radiolabelling process	127
IV.2.2.2.6. Scintigraphic analysis	128
IV.2.2.2.7. Pharmacokinetic analysis	129
IV.2.2.2.8. In vitro evaluation of the influence of the airflow rate on the aerodynamic behaviour of the formulations	130
IV.2.2.2.9. Dissolution test	130
IV.2.3. RESULTS	132
<u>IV.2.3.1. Validation of the radiolabelling process</u>	132
<u>IV.2.3.2. Adverse events</u>	133
<u>IV.2.3.3. Scintigraphic results</u>	134
<u>IV.2.3.4. Pharmacokinetic results</u>	135
<u>IV.2.3.5. In vitro aerodynamic evaluation</u>	136
<u>IV.2.3.6. Dissolution</u>	137
IV.2.4. DISCUSSION	137
IV.2.5. CONCLUSION	142
IV.3. FORMULATION AND IN VITRO EVALUATION OF DPI FORMULATIONS OF AN ANTI-IL13 MAB FRAGMENT	143
IV.3.1. INTRODUCTION	144
IV.3.2. MATERIALS AND METHODS	144
<u>IV.3.2.1. Materials</u>	144

<u>IV.3.2.2. Methods</u>	145
IV.3.2.2.1. Desalting the antibody solution	145
IV.3.2.2.2. Production of the formulations	148
IV.3.2.2.3. Physico-chemical characterisation	152
IV.3.2.2.4. Stability study	160
IV.3.2.2.5. Aerodynamic features	160
IV.3.3. RESULTS AND DISCUSSION	162
<u>IV.3.3.1. Influence of the folding state on UV absorbance</u>	162
<u>IV.3.3.2. Characterisation of the CA582 reference material</u>	163
<u>IV.3.3.3. Efficacy of the desalting procedure</u>	164
<u>IV.3.3.4. Stability of the desalted CA582 solutions</u>	165
<u>IV.3.3.5. Freeze-drying of the CA582 molecule</u>	167
IV.3.3.5.1. Influence of the buffering conditions on CA582 stability	167
IV.3.3.5.2. Influence of the concentration of stabilising sugar on CA582 stability	168
IV.3.3.5.3. Influence of the type of stabilising excipient on CA582 stability	169
IV.3.3.5.4. Crystalline state of the freeze-dried powders	170
IV.3.3.5.5. Stability study on the freeze-dried powders	171
<u>IV.3.3.6. High pressure homogenisation of the freeze-dried CA582</u>	172
IV.3.3.6.1. Evaluation of CA582 stability in isopropanol	172
IV.3.3.6.2. Particle size distribution of the CA582 homogenised suspensions	173
IV.3.3.6.3. Influence of the type of stabilising excipient on CA582 stability and particle size after HPH	173
IV.3.3.6.4. Influence of the type of liquid-phase dispersing agent on CA582 stability and particle size after HPH	174
IV.3.3.6.5. Influence of the concentration of liquid-phase dispersing agent on CA582 stability	176
IV.3.3.6.6. Influence of the processing pressure and temperature on CA582 stability	176
IV.3.3.6.7. Influence of the content of stabilising excipient on CA582 stability	177
<u>IV.3.3.7. Spray-drying of the CA582 formulations</u>	178
IV.3.3.7.1. Selection and composition of the formulations	178
IV.3.3.7.2. Particle size of the formulations	178
IV.3.3.7.3. Stability of the formulations	179
IV.3.3.7.4. Dispersion properties and aerodynamic features of the dry powder formulations	182
IV.3.4. CONCLUSION	184
V. GENERAL CONCLUSION	186
VI. REFERENCES	191
VII. APPENDICES	219
APPENDIX I: CURRENT DPI DEVICES AVAILABLE ON THE MARKET	220
APPENDIX II: FUTURE/NEXT GENERATION DPIs (IN DEVELOPMENT STAGE)	221
APPENDIX III: RELATIVE EFFICACY AND TOXICITY OF VARIOUS AGENTS IN PROMOTING PULMONARY PROTEIN ABSORPTION	222
APPENDIX IV: EXAMPLES OF INHIBITION OF PROTEIN AGGREGATION IN THE DRY STATE	223
APPENDIX V: EFFECT OF ABSORPTION ENHANCERS ON PULMONARY INSULIN ABSORPTION	224
APPENDIX VI: DISCONTINUED FORMULATION/DEVICE SYSTEMS FOR INHALED ADMINISTRATION OF INSULIN	225
APPENDIX VII: VALIDATION OF THE HPLC METHOD USED FOR THE DOSAGE OF INSULIN	227
APPENDIX VIII: CERTIFICATE OF ANALYSIS OF THE RAW INSULIN INCELLIGENT AF	241
APPENDIX IX: ASSESSMENT OF THE MICROBIAL QUALITY OF THE INSULIN FORMULATIONS USED IN THE PHARMACOSCINTIGRAPHIC STUDY	242

List of abbreviations

ACI	Andersen Cascade Impactor	HSH	high shear homogenisation
ACT	air classifier technology	HMWP	high molecular weight proteins
ARDS	acute respiratory distress syndrome	ICS	inhaled corticosteroid
		IgG	immunoglobulin G
BDP	beclomethasone dipropionate	IL	interleukin
BSA	bovine serum albumin	ISE	ion-selective electrode
CD	cyclodextrin	IU	international units
CEX	cation-exchange HPLC	i.v.	intravenous
CF	cystic fibrosis	LABA	long-acting β_2 agonist
CFC	chlorofluorocarbon	LAR	late allergen response
COPD	chronic obstructive pulmonary disease	LHRH	luteinizing hormone-releasing hormone
DD	delivered dose	LTRA	leukotriene receptor antagonist
D_{lco}	diffusing capacity of the lung for CO	MAb	monoclonal antibody
DM	diabetes mellitus	MMAD	mass median aerodynamic diameter
DPI	dry powder inhaler	MsLI	Multi-stage Liquid Impinger
DSPC	distearoylphosphatidylcholine	MWCO	molecular weight cut-off
DPPC	dipalmitoylphosphatidylcholine	NGI	Next Generation Impactor
DTT	dithiothreitol	NPH	neutral protamine insulin
DV	diafiltration volume	PD	pharmacodynamic
EAR	early allergen response	PDE	phosphodiesterase
ECP	eosinophil cationic protein	PEFR	peak expiratory flow rate
EMEA	European Medicines Evaluation Agency	PIFR	peak inspiratory flow rate
Epo	erythropoietin	PK	pharmacokinetic
EGP	endogenous glucose production	PLGA	poly(lactide-co-glycolide acid
FcRn	neonatal Fc receptor	pMDI	pressurised metered dose inhalers
FDA	food and drug administration	PTH	parathyroid hormone
FDKP	3,6-bis(N-fumaryl-N-(n-butyl)amino-2,5-diketopiperazine	PXRD	powder X-ray diffraction
FEV₁	forced expiratory volume in 1 second	QL	quantification limit
FPD	fine particle dose	RH	relative humidity
FPF	fine particle fraction	rHA	recombinant human albumin
GC	gas chromatography	rhGH	recombinant human growth hormone
G-CSF	granulocyte colony stimulating factor	R_i	intrinsic resistance
GH	growth hormone	SABA	short-acting β_2 agonist
GIR	glucose infusion rate	s.c.	subcutaneous
GLP-1	glucagon-like peptide-1	SD	spray-dried
GM-CSF	granulocyte-macrophage colony-stimulating factor	SDS-PAGE	sodium dodecyl sulphate polyacrylamide gel electrophoresis
HbA1C	glycosylated haemoglobin	SEC	size-exclusion HPLC
HFA	hydrofluoroalkane	SEM	scanning electron microscopy
HLA	human leucocyte antigens	SLMs	solid lipid microparticles
HMAP	hydroxy methyl amino propionic acid	SLNs	solid lipid nanoparticles
HPH	high pressure homogenisation	SOD	superoxide dismutase
HPLC	high pressure liquid chromatography	SSA	specific surface area
		TGA	thermogravimetric analysis
		UDD	uniformity of the delivered dose
		VC	vital capacity
		VIP	vasoactive intestinal peptide

FOREWORD

This work was realised as part of the NEOFOR project, which was supported by the Walloon Region (BIOWIN health cluster). The aim of the NEOFOR project was to develop a technological platform for the administration of peptides and proteins by inhalation. It involved academic partners from ULB (Brussels, Belgium) and ULg (Liège, Belgium), as well as SMEs and a large pharmaceutical company (UCB s.a., Brussels, Belgium). The partners were in the field of formulation (ULB-LPB Laboratory of Pharmaceutics and Biopharmaceutics, and ULg-LPT Laboratory of Pharmaceutical Technology) but also in inhalation devices design (Optim Test Center s.a., Cosysys sprl, ULB-BEAMS Bio-, Electro- And Mechanical Systems), and in assessment of in vivo efficacy and safety of the formulations developed. This last point was covered by partners involved in animal studies (ULg-LTDB Laboratory of Tumor and Development Biology) and partners involved in imaging techniques in humans (ULB-NMI Nuclear Medicine Imaging, and ULg-CRC Cyclotron Research Center). Finally, coordination of the project was realised by the partner UCB. The role of ULB-LPB in the NEOFOR project was to develop and evaluate in vitro original formulations for pulmonary administration of peptides and proteins, in particular monoclonal antibodies. Collaborations with the other partners were intended to evaluate the developed formulations in vivo. Our collaboration with partners involved in device design was also required, mainly for analytical support (particle size measurement techniques).

I. SUMMARY

SUMMARY

A number of therapeutic proteins are used for long in clinical practice. These include for example insulin, calcitonine, growth hormone, and parathyroid hormone for the treatment of various systemic disorders, as well as protein antigens in vaccine formulations. Due to the recent developments in biochemical engineering and in the comprehension of the physiopathology of many diseases, peptides and proteins are expected to become a drug class of increasing importance. Recently, novel biological drugs have for example been developed such as monoclonal antibodies, antibody fragments, soluble receptors, and receptor agonists or antagonists. These are mainly used for the treatment of auto-immune and inflammatory diseases (asthma, rheumatoid arthritis) and for the treatment of cancers. However, a major drawback of these biomolecules is the need to use parenteral administration. This is mainly due to the harsh pH conditions that proteins undergo by oral administration, leading to various physico-chemical degradations and loss of biological activity.

Pulmonary delivery of these proteins could constitute an alternative to parenteral delivery. Due to the very high surface area of the lungs, the low thickness of the alveolar epithelium and the high level of lung vascularisation, pulmonary administration can indeed provide fast systemic absorption of drugs, while avoiding hepatic first pass metabolism. On the other hand, drugs for local treatment can also be administered directly into the lung, which allows delivering high doses while limiting systemic side effects. Nevertheless, administration of drugs to the lungs requires some challenges to be taken up. It is indeed necessary to provide the drug as very small solid or liquid microparticles (1-5 μm) in order to reach the lungs. For solid microparticles, it is also needed to overcome the very high inter-particle interactions by using appropriate formulation strategies and by including deaggregation mechanisms in the inhalation device. Other issues are more specifically related to the pulmonary administration of proteins. These can indeed undergo physico-chemical degradations during processing, administration, and/or storage. Moreover, if systemic action is required, proteins will often need addition of an absorption enhancer to cross the alveolar epithelium because of their large molecular weight and hydrophilicity.

In this work, we developed formulations for pulmonary delivery of proteins using two model proteins. Insulin (5.8 kDa) was chosen as a model of small protein. It is also an application of systemic pulmonary delivery. On the other hand, an anti-IL13 monoclonal antibody fragment (54 kDa) was used as a model of larger protein. This molecule is currently in development for the treatment of asthma and provided an application for local pulmonary delivery. The formulation strategy was to produce dry powders using a combination of micronisation techniques (high speed and high pressure homogenisations), drying techniques (spray-drying, freeze-drying), and addition of lipid excipients. These lipid excipients were added as a coating around the protein particles and were expected to prevent protein degradations during processing and/or storage, essentially by avoiding contact with water. It could also improve the aerodynamic properties of the powders by modification of the surface properties of the particles and/or limitation of the capillary forces.

First, we evaluated insulin lipid-coated formulations and formulations without excipients, produced using high pressure homogenisation and spray-drying. In the case of lipid-coated formulations, a physiological lipid composition based on a mixture of cholesterol and phospholipids was used. We were able to obtain good aerodynamic features for the different formulations tested, with fine particle fractions between 46% and 63% versus 11% for raw insulin powder. These are high FPF values in comparison with those obtained for other protein formulations for inhalation currently under development, which often have an *in vitro* deposition of around 30%. Insulin presented a good stability in the dry state, even when no lipid coating was added.

The presence of a lipid coating of up to 30% (w/w) did not significantly improve the aerodynamic behaviour of the powders, but the coated formulations exhibited decreased residual moisture content after 3-month storage, which should be of interest for the long-term stability of the formulations.

In a second step, two of the developed insulin formulations were evaluated in a clinical study to determine whether the formulations give high deep lung deposition *in vivo*, and how insulin is absorbed into the systemic blood stream. This pharmaco-scintigraphic trial was performed on twelve type 1 diabetic patients using an uncoated formulation and a formulation coated with 20% (w/w) of lipids. The two formulations showed interesting

features, with pharmacokinetic profiles that mimic the natural insulin secretion pattern. Bioavailability was within the ranges of two of the three dry powder insulins that have reached phase III clinical development. However, the formulation with a lipid coating exhibited a lower lung deposition in comparison with the uncoated formulation, which was not expected from the previous in vitro results. Additional in vitro experiments indicated that this lower performance was related to a decrease in the disaggregation efficiency of the powder at a sub-optimal inhalation flow-rate. An extensive training of the patients to the inhalation procedure could therefore improve the lung deposition of the coated formulation.

Finally, we developed and evaluated dry powder formulations of the anti-IL13 antibody fragment. These were produced using, successively, freeze-drying, high pressure homogenisation (HPH), and spray-drying. The influence of different types and concentrations of stabilising excipients was evaluated for each production step. Due to its more elaborated structure, the antibody fragment was found to be more sensitive than insulin to physico-chemical degradation, particularly during the HPH process, which led to different types of degradation products. These could partly be avoided by adding 50% sucrose during freeze-drying and 10% Na glycocholate or palmitic acid in the liquid phase during HPH (dispersing agents). However, the presence of a small fraction of insoluble aggregates could not be fully avoided. Further spray-drying of the suspensions in the presence of 10% Na glycocholate or palmitic acid led to the formation of a hydrophilic or hydrophobic coating around the particles, respectively. Na glycocholate was found to be particularly effective in protecting the antibody during spray-drying, which was found to be at least partly related to its ability to inhibit sucrose recrystallisation. However, the best formulation still presented a small fraction of insoluble aggregates (6%). The aerodynamic evaluation of the formulations showed FPFs that were compatible with lung deposition, with the formulation containing Na glycocholate presenting the highest FPF (42%). The formulation coated with palmitic acid presented a slightly lower FPF (35%). The aerodynamic properties of this formulation remained unchanged at a sub-optimal inspiratory flow rate, to the contrary of what was observed for the insulin formulation coated with 20% (w/w) cholesterol and phospholipids. Palmitic acid could therefore be of interest as a hydrophobic coating material, and provide long-term stability of protein drugs.

The work performed with the insulin and anti-IL13 molecules provided the proof-of-concept that it was possible to obtain dry powder protein formulations with appropriate aerodynamic properties and good overall physico-chemical stability, using simple production techniques and few selected excipients. The formulation strategy presented in this work could therefore be of interest for the future development of inhaled proteins for local or systemic applications.

RESUME

Grâce aux récents progrès dans le domaine de l'ingénierie biologique et dans la compréhension des mécanismes moléculaires impliqués dans certaines pathologies, les protéines sont appelées à prendre dans le futur une place importante au sein de l'arsenal thérapeutique. De nouveaux médicaments issus des biotechnologies ont ainsi été développés, tel que des anticorps monoclonaux, des récepteurs solubles, ou des agonistes et antagonistes de récepteurs. Ces molécules sont déjà utilisées couramment en pratique clinique, principalement pour le traitement d'affections auto-immunes et inflammatoires comme l'asthme et la polyarthrite rhumatoïde, ou pour le traitement de cancers. Cependant, un inconvénient majeur de ces molécules est qu'il est nécessaire de les administrer par voie parentérale. Leur administration par voie orale est en effet entravée par la présence de conditions extrêmes de pH dans l'estomac, qui mènent généralement à la dégradation physico-chimique de la protéine et à la perte partielle ou complète de son activité biologique.

L'administration pulmonaire de protéines pourrait constituer une alternative à l'administration parentérale. Les poumons possèdent en effet une très importante aire de surface, un épithélium très fin et une forte vascularisation permettant d'obtenir une absorption systémique rapide et d'éviter le premier passage hépatique. D'autre part, des traitements locaux peuvent aussi être délivrés directement dans le poumon, permettant de limiter les effets secondaires systémiques et d'administrer des doses importantes de principe actif. Cependant, un certain nombre d'obstacles doivent être surmontés en vue d'administrer une molécule par voie pulmonaire. Il est en effet nécessaire de délivrer le principe actif sous forme de microparticules (liquides ou solides) dont la taille doit être comprise entre 1 et 5 μm afin d'atteindre le poumon profond. Pour les microparticules solides, il est aussi nécessaire d'utiliser des stratégies de formulation appropriées afin de limiter les importantes interactions inter-particulaires liées aux poudres micronisées. Dans ce but, des mécanismes de désagrégation sont également introduits dans les dispositifs pour inhalation. D'autres obstacles sont plus spécifiques à l'administration pulmonaire de protéines. Celles-ci peuvent en effet subir des dégradations physico-chimiques durant la

production, l'administration et/ou le stockage de la formulation. De plus, si une action systémique est recherchée, l'ajout d'un promoteur d'absorption sera généralement nécessaire afin de franchir l'épithélium alvéolaire, de par le haut poids moléculaire et le caractère hydrophile des protéines.

Dans ce travail, des formulations pulmonaires de protéines ont été développées en utilisant deux protéines modèles. L'insuline (5.8 kDa) a été utilisée comme modèle de petite protéine. Il s'agit également d'une application d'administration systémique par voie pulmonaire. D'autre part, un fragment d'anticorps monoclonal anti-IL13 (54 kDa) a été utilisé comme modèle de plus grande protéine. Cette molécule est actuellement en cours d'étude pour le traitement de l'asthme et constitue une application d'administration locale par voie pulmonaire. La stratégie de formulation utilisée a été de produire des poudres sèches en utilisant une combinaison de techniques de micronisation (homogénéisations à haute vitesse et à haute pression), de techniques de séchage (atomisation, lyophilisation), et d'ajout d'excipients lipidiques. Ces excipients ont été utilisés sous forme d'enrobage autour des particules de protéine afin d'en éviter la dégradation durant la production et/ou le stockage. L'enrobage pourrait aussi améliorer les propriétés aérodynamiques des poudres en modifiant les propriétés de surface des particules et/ou en limitant l'apparition de forces capillaires.

Tout d'abord, des formulations d'insuline avec ou sans enrobage lipidique ont été produites par homogénéisation haute pression (HHP) et atomisation. Dans le cas des formulations enrobées, un mélange de lipides physiologiques (cholestérol et phospholipides) a été utilisé pour réaliser l'enrobage. Des caractéristiques aérodynamiques intéressantes ont été obtenues pour les différentes formulations testées, avec des fractions de particules fines (FPF) comprises entre 46% et 63% contre 11% pour l'insuline non formulée. Ces valeurs de FPF sont hautes en comparaison de celles obtenues pour d'autres formulations de protéines pour inhalation actuellement en développement, dont la FPF avoisine généralement 30%. Les formulations développées ont permis de maintenir la stabilité physico-chimique de l'insuline, et ce même sans ajout d'un enrobage lipidique. La présence d'un enrobage dans une proportion allant jusqu'à 30% en poids n'a pas permis d'améliorer les propriétés aérodynamiques des poudres, mais les formulations enrobées présentaient un taux

d'humidité résiduelle plus faible, et une adsorption d'eau moins importante après 3 mois de stockage en comparaison avec les formulations non enrobées. Cette propriété devrait permettre d'améliorer la stabilité à long terme de la protéine.

Dans un deuxième temps, deux des formulations d'insuline développées ont été utilisées dans une étude clinique afin d'évaluer leur déposition pulmonaire *in vivo* et leur biodisponibilité. Cette étude pharmaco-scintigraphique a été réalisée sur douze patients diabétiques de type 1 recevant une dose unique d'une formulation non enrobée ou enrobée avec 20% de lipides. Les deux formulations ont présenté des caractéristiques intéressantes, avec des profils pharmacocinétiques mimant le schéma naturel de sécrétion de l'insuline. Leur biodisponibilité se situe dans la même gamme que celle de deux des trois formulations d'insuline en poudre sèche qui ont atteint une phase III de développement clinique. Cependant, la formulation enrobée a présenté une déposition pulmonaire plus faible que celle de la formulation non enrobée, en contradiction avec les résultats *in vitro*. Des essais *in vitro* complémentaires ont montré que cette plus faible déposition était liée, au moins en partie, à une moindre désagrégation de cette formulation lorsqu'un flux inspiratoire sub-optimal est utilisé. Un apprentissage approfondi des patients à la technique d'inhalation devrait donc permettre d'améliorer la déposition pulmonaire de la formulation enrobée.

Enfin, des formulations sèches d'un fragment d'anticorps anti-IL13 ont été réalisées, en utilisant successivement la lyophilisation, l'HHP, et l'atomisation. L'influence de différents types et concentrations d'excipients stabilisants a été évaluée durant les différentes phases de production. Du fait de sa structure tertiaire plus élaborée, le fragment d'anticorps s'est en effet montré plus sensible à la dégradation physico-chimique que l'insuline, en particulier durant l'HHP (formation d'agrégats, de composés désamidés,...). La dégradation de la molécule a pu être partiellement limitée par l'ajout de 50% de sucrose lors de la lyophilisation et par l'ajout de 10% de glycocholate de sodium ou d'acide palmitique dans la phase liquide durant l'HHP (agents dispersants). L'atomisation consécutive des suspensions a mené à la formation d'un enrobage respectivement hydrophile en présence de 10% de glycocholate de sodium ou lipophile en présence de 10% d'acide palmitique. Le glycocholate de sodium s'est montré particulièrement efficace pour protéger l'anticorps durant l'atomisation, au moins en partie grâce à sa capacité à inhiber la recristallisation du sucrose.

Cependant, une fraction résiduelle d'agrégats insolubles dans la formulation (6%) n'a pas pu être évitée. La formulation contenant 10% de glycocholate de sodium a présenté la plus haute FPF (42%), tandis qu'une FPF légèrement inférieure (35%) a été obtenue pour la formulation enrobée avec de l'acide palmitique. Les propriétés aérodynamiques in vitro de cette formulation sont restées inchangées avec l'utilisation d'un flux inspiratoire sub-optimal, contrairement à ce qui avait été observé pour la formulation d'insuline enrobée avec 20% de lipides. L'acide palmitique pourrait dès lors présenter un intérêt comme agent d'enrobage hydrophobe, et être utilisé pour fournir une stabilisation à long terme de principes actifs protéiques.

En conclusion, le travail réalisé avec l'insuline et le fragment d'anticorps a permis de montrer qu'il était possible d'obtenir des formulations sèches de protéines pour inhalation présentant des propriétés aérodynamiques adéquates et une bonne stabilité physico-chimique globale. La stratégie de formulation utilisée pourrait donc présenter un intérêt pour le développement futur de protéines inhalées pour des applications locales ou systémiques.

II. INTRODUCTION

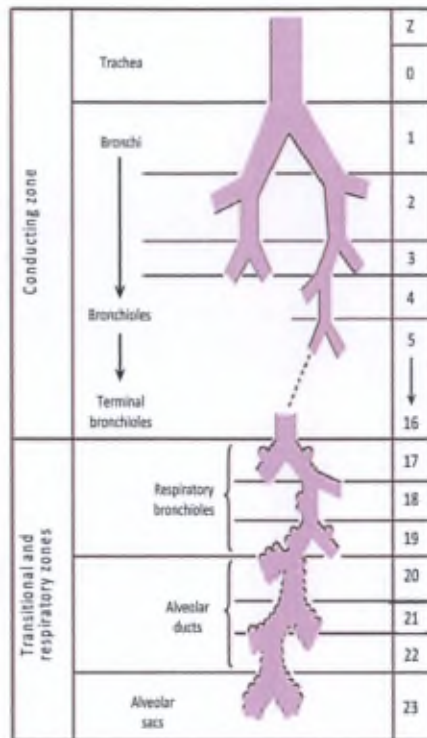


Figure 1. Schematic organisation of the tracheo-bronchial tree (Høiby et al., 2010) (Z: airway generation)

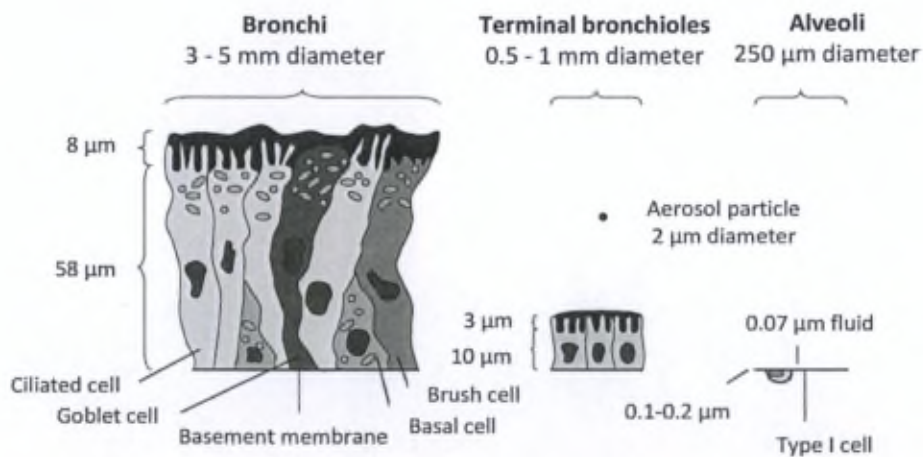


Figure 2. Lung epithelial cells of different regions, drawn at their relative sizes (Siekmeier and Scheuch, 2009)

II.1. Basics of pulmonary drug delivery

II.1.1. Anatomy and physiology of the respiratory tract

II.1.1.1. Respiratory tree

The respiratory tree is divided into the upper respiratory airways (nose, mouth, pharynx, larynx, and trachea) and the lower respiratory airways, which consist in the pulmonary region. This is constituted of the bronchi and several successive generations of bronchioles, whose numbers increase in inverse proportion to their size (**Figure 1**). Terminal bronchioles are at the end of the purely conductive part of the tract. They successively make way for a respiratory zone (~3000 ml; 95% of the lung volume), which comprises the respiratory bronchioles and the alveoli, which are the site of oxygen and carbone dioxyde exchanges with the blood (Høiby et al., 2010). These exchanges are made possible by the increased surface area within the alveolar zone (~140 m²), by its strong tissue vascularisation (100% of cardiac output, with 100 to 200 ml blood in contact with the alveoli), and by the very low thickness of the alveolar epithelium (0.1-1 μm) (Adjei et al., 1996).

II.1.1.2. Epithelium

In the **conducting zone**, there are a variety of cells that make up the epithelium: the *basal cells*, which are the stem cells for the epithelium and differentiate to form the other cells in the case of injury or apoptosis; the *goblet cells*, which secrete mucus; the *ciliated cells* (the most numerous cell type), which provide the mechanism for moving the mucus blanket; and the *brush cells*, which are involved in drug metabolism. These types of cells persist up to the terminal bronchioles, but with a decreasing size (**Figure 2**). Mucus is a viscous fluid, rich in polysaccharides and glycoproteins, that lies on the top of the aqueous layer that covers the luminal surface of the epithelium from the upper airways to terminal bronchioles. The thickness of the layer varies from 0.5 to 5 μm. The mucus functions are the moistening of inhaled air, hydration of the epithelium, and defence against microbial colonisation through the presence of antibacterial proteins such as lysozyme (Schutte and Cray, 2002). Mucus also protects the lungs from penetration of foreign particles.

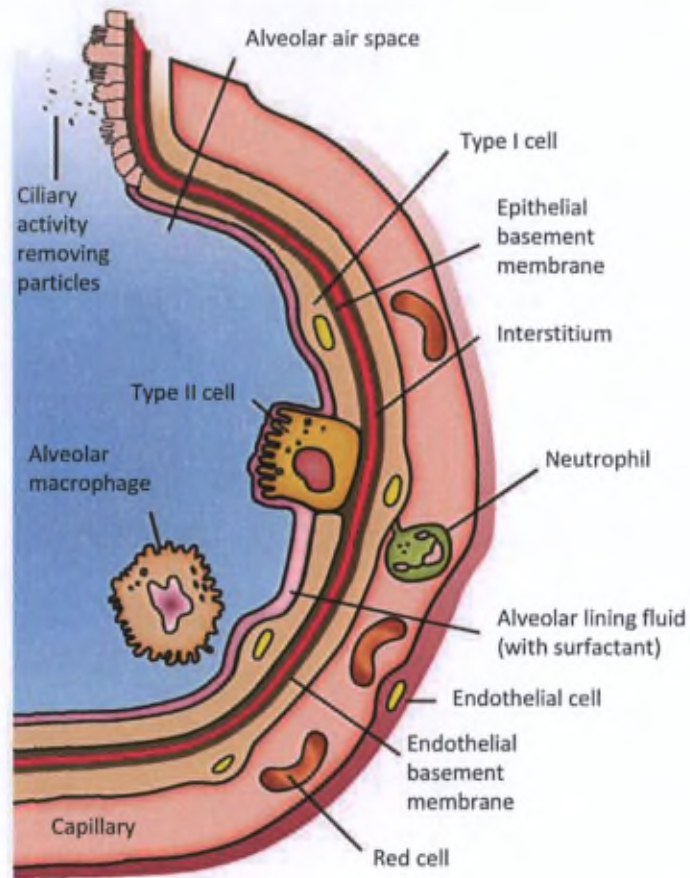


Figure 3. The alveolar-capillary membrane (Moss and Burnham, 2006)

Ciliated cells are involved in this latter function by driving the mucus – through coordinated ciliary beat – from the lower airways to the pharynx, where it can be either swallowed or ejected. This is called mucociliary clearance or the mucociliary escalator, and is the major defense system in the conducting zone (Yu and Chien, 1997; Høiby et al., 2010). Mucus clearance is faster in the large airways than in the smaller ones because of the presence of more ciliated cells and a higher ciliary beat frequency.

In the **respiratory zone**, alveoli possess the thinnest epithelium (~200 nm), which is made up of a single cellular layer and contains no cilia or goblet cells. The alveolar airspace is mainly covered by *type I pneumocytes* (95% of the surface area), which are joined together by tight junctions and sit on a basement membrane composed of an extracellular matrix of different biopolymers. This membrane is merged with the endothelium basement membrane of the blood capillaries that surround the alveoli. Together, the alveolar epithelium, the endothelial epithelium, and their basement membranes constitute the alveolar-capillary membrane, which is about 500 nm thick (**Figure 3**) (Patton and Byron, 2007). The alveolar epithelium also contains *type II pneumocytes* (5% of the surface area), which produce the alveolar surfactant.

Alveolar macrophages are in contact with the alveolar epithelial cells and are responsible for the clearance of particles deposited in the alveolar region, in which mucociliary clearance is absent. They constitute the major noninflammatory defense system in alveoli (Høiby et al., 2010). In response to deposited nanoparticles, alveolar macrophages will migrate to the particles and phagocytise them via chemotaxis involving opsonisation. Macrophage uptake is believed to complete in 6–12 h after deposition of particles in the alveoli. Once internalised in the macrophages, the particles are either disintegrated (e.g. by enzymes in lysosomes) or accumulated in the lymphatic system, which drains the airways and alveoli. A minor fraction of the particle-carrying macrophages migrate to the ciliated airways, where they are removed by mucociliary clearance (Zhang et al., 2011a). The uptake of deposited particles by alveolar macrophages depends on the size of particles and the composition of any coating material. It has been shown that particles of 1–3 μm in diameter are taken up far better by macrophages, which have cell diameters of about 15–22 μm , than particles of 6 μm . Particles of less than 0.26 μm , on the other hand, can escape phagocytosis by macrophages (Lauweryns and Baert, 1977; Yang et al., 2008).

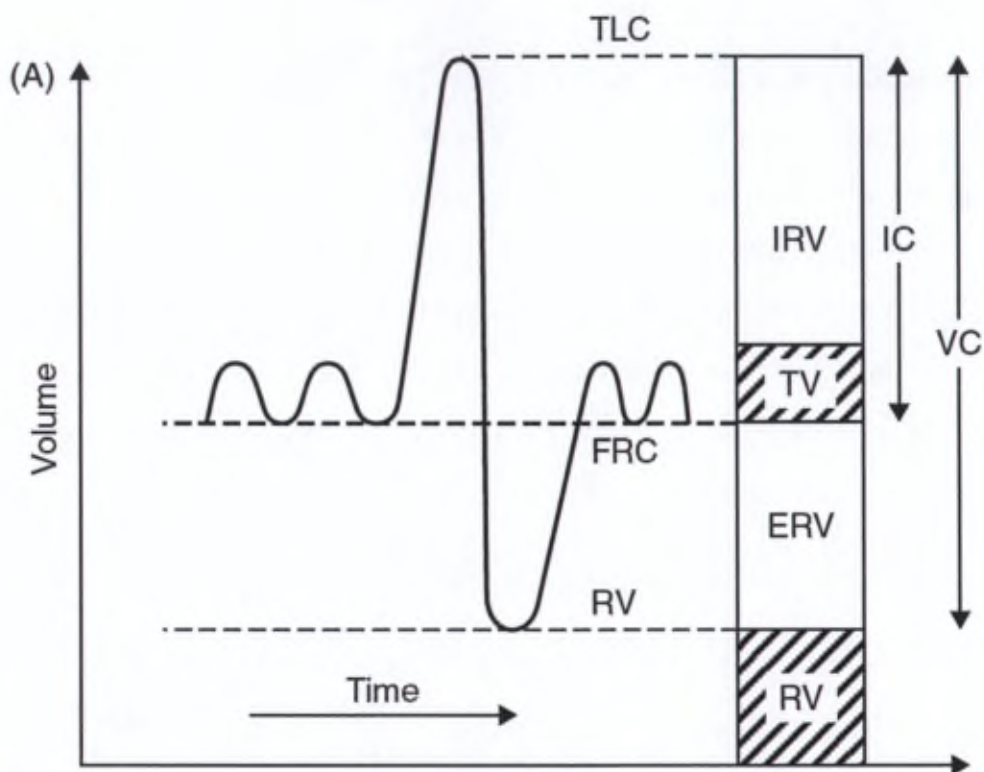


Figure 4. Trace of volume displacement as a function of time during quiet breathing followed by a maximal inspiration and exhalation (Irvin, 2009)

Tidal volume (TV ≈ 500 ml) is the volume of a quiet breath in and out. **Vital capacity (VC ≈ 5500 ml)** is the maximum (forced) tidal volume. **Total lung capacity (TLC ≈ 7300 ml)** is the volume in the lungs at the end of a maximal breath in. **Residual volume (RV ≈ 1800 ml)** is the volume left in the lungs after a maximal expiration. **Functional residual capacity (FRC ≈ 3500 ml)** is the volume in the lungs at the end of a normal expiration. **Expiratory reserve volume (ERV ≈ 1700 ml)** is the forced volume expired after a quiet expiration to reach RV. **Inspiratory reserve volume (IRV ≈ 3300 ml)** is the forced volume of air inspired after a quiet inspiration to reach TLC. **Inspiratory capacity (IC ≈ 3800 ml)** is the total volume of air inspired after a quiet expiration to reach TLC.

II.1.1.3. Lung surfactant

Alveolar epithelium is covered with a thin liquid layer ($< 0.1 \mu\text{m}$) that has a surfactant film on its top. This surfactant is a complex mixture of lipids and proteins. Its main function is to reduce the surface tension at the alveolar air-liquid interface of lungs to avoid alveolar collapse at the end of expiration and facilitate the work of breathing. It is synthesized by type II pneumocytes and it follows a regulated exocytic pathway leading to secretion into the thin aqueous layer covering the alveoli. The composition of surfactant is 80-86% phospholipids, 8% neutral lipids (mainly cholesterol), and 6-12% proteins. Saturated phosphatidylcholine accounts for 70% of the phospholipid portion of surfactant, with dipalmitoylphosphatidylcholine (DPPC) accounting for 60% of the phosphatidylcholine. DPPC is critical for lowering the surface tension and can reduce it to almost zero. Although DPPC is the primary component for surface activity, alone it adsorbs poorly onto the air-liquid interfaces within the alveoli. The presence of unsaturated phospholipids aids the adsorption and surface-active properties of surfactant (Bissinger and Carlson, 2006).

Surfactant contains four different proteins, which can be classified into two groups: the hydrophilic surfactant proteins, SP-A and SP-D, and the hydrophobic surfactant proteins, SP-B and SP-C. SP-B and SP-C also play critical roles in the formation and stabilization of pulmonary surfactant film, as they are mainly involved in promoting adsorption, stabilization, and re-spreading of the film. The other two proteins, SP-A and SP-D, have the ability to bind many different ligands, such as calcium, sugars or lipid molecules, in a concerted manner. This enables them to bind to a broad spectrum of pathogens including bacteria, viruses, and fungi. They therefore play an important role in the innate immune system (Serrano and Pérez-Gil, 2006).

II.1.1.4. Lung volumes

Figure 4 shows the spirometric trace when a subject breathes quietly and then takes a maximal breath in and out. The volumes mentioned are mean values for a healthy young male. They are somewhat smaller in women because women tend to have smaller thoracic cages (Ward, 2005).

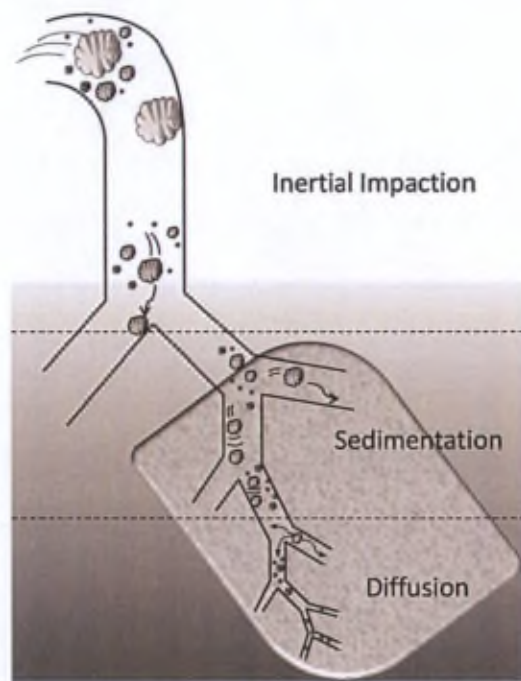


Figure 5. Schematic representation of particle deposition in the lungs according to different mechanisms related to particle size (Carvalho et al., 2011)

II.1.2. Lung deposition of inhaled particles

Understanding the processes and the factors influencing liquid and solid particle settlement on the surface of specific regions of the airway tree has implications for the assessment of the risk of air pollutants as well as for the development of pharmaceutical inhalation products.

II.1.2.1. Mechanisms

There are three main mechanisms by which particle deposition can occur in the lungs: inertial impaction, sedimentation, and diffusion (**Figure 5**). These are directly (or inversely) related to particle size whereas two other mechanisms – interception and electrostatic precipitation – are related, respectively, to particle shape and electrostatic charges (Carvalho et al., 2011).

Inertial impaction occurs when a particle has enough inertia to keep its trajectory despite changes in direction of the air stream, consequently impacting the walls of the respiratory tract. The probability of particle deposition in the airways via impaction rises when the dimensionless Stokes number (Stk) increases, as described in the following equation (Zeng et al., 2001):

$$\text{Stk} = \rho_p \cdot d^2 \cdot V / 18 \cdot \eta \cdot R$$

where ρ_p is the particle density, d is the particle diameter, V is the air velocity, η is the air viscosity, and R is the airway radius.

Therefore, considering the bifurcated architecture of the lungs, large particles – typically those over $5 \mu\text{m}$ – travelling through the airways at a high airflow velocity are more likely to impact in the proximal portion of the respiratory tract (upper airways) (Zeng et al., 2001).

Sedimentation is a time-dependent process in which particles settle due to the influence of gravity. It is governed by Stokes' law:

$$V_{ts} = (\rho_p - \rho_a) \cdot d^2 \cdot g / 18 \cdot \eta$$

where V_{ts} is the settling velocity, ρ_a is the density of air, and g is the gravitational acceleration (Gonda, 2004).

However, Stokes' law is only valid in conditions where a laminar flow is achieved within the airways. Sedimentation typically occurs in the lungs for particles in the range of 0.5-5 μm in the small conducting airways and alveoli (where the air velocity is low). Breath-holding after inhalation increases the extent of sedimentation whereas with increased air flow rate, the stream becomes turbulent and deposition by impaction increases (Zeng et al., 2001).

Diffusion occurs when particles are sufficiently small (typically under 0.5 μm) to undergo a random motion due to molecular bombardment by the air molecules. This process, also known as Brownian motion, is correlated to particle size, according to the Stokes–Einstein equation (Gonda, 2004):

$$\text{Dif} = k \cdot T / 3\pi \cdot \eta \cdot d$$

where Dif is the diffusion coefficient, k is the Boltzmann's constant, and T is the absolute temperature. Unlike the impaction and sedimentation mechanisms, diffusional deposition is therefore inversely related to particle size.

Interception is usually significant only for fibres and elongated particles, for which deposition can occur even though their centre of mass remains on the fluid streamline.

Electrostatic precipitation, which is a minor contributor to particle deposition, can occur for some freshly produced particles that are electrically charged during processing. These particles interact with charges on the airway surface, resulting in deposition on it (Carvalho et al., 2011).

II.1.2.2. Parameters influencing lung deposition

II.1.2.2.1. Patient features

The site and extent of lung deposition of particles depends on several patient-related factors. These are mainly the **breathing pattern** of the patient (i.e. flow rate, ventilation volume, and end-inspiratory breath-holding) (Scheuch and Siekmeier, 2007).

Fast inhalation (high flow rate, Q) leads to increased deposition by impaction in the larynx. This significantly reduces penetration into the deep lungs, even for particles with diameters of about 2-3 μm . Moreover, the residence time of inhaled particles also depends on the flow rate (slow flow rate = long residence time) and on the inhaled and exhaled volume (deep breath = longer residence time). A deep, slow breathing movement gives the inhaled particles much more time to deposit by sedimentation and diffusion, which increases deep lung delivery. This effect can also be obtained by implementation of an end-inspiratory breath-hold (5-10 seconds) in the breathing movement.

Another important factor affecting the lung deposition is the time of injection of the **aerosol bolus** into the inhaled volume. The first aerosol particles that enter the respiratory system penetrate deeper into the lungs than particles that are inhaled at the end of a breath.

In summary, a slow, deep inspiration, with aerosol bolus administration at the beginning of the inspiration and a slightly delayed expiration, will have a positive impact on the quantity of drug delivered at the alveolar level. The optimum conditions include an inspiratory flow rate of 200-400 ml/s and an inhaled volume of 1000-2000 ml (Scheuch, 2006).

It is to be noted that the site of lung deposition, and particularly extrathoracic deposition, has high intersubject variability because of large **anatomical and morphometrical differences** in the mouth and throat, and variations in the diameter and branching patterns of the airways. Moreover, some diseases, such as asthma, chronic obstructive pulmonary disease (COPD), cystic fibrosis (CF), and lung cancer, may cause changes in the pulmonary tract by obstruction due to excessive production of mucus or constriction of the airways.

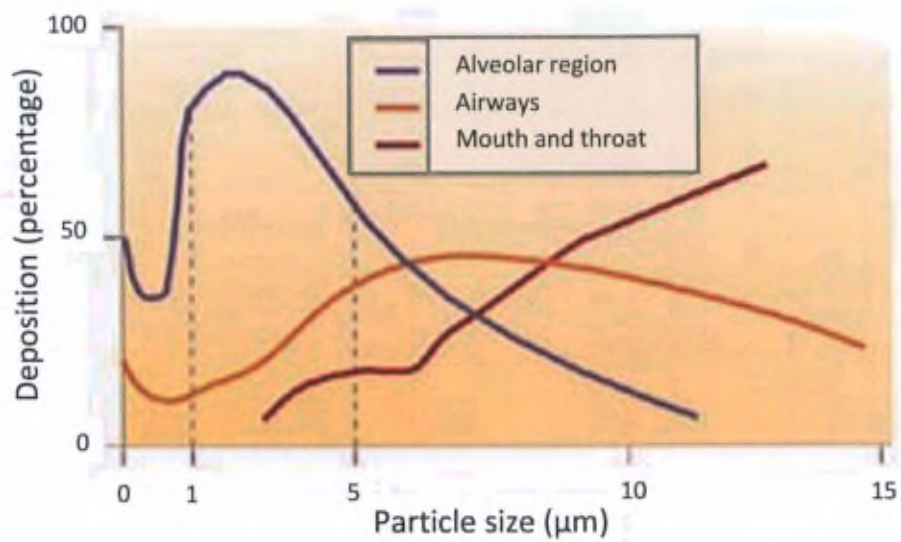


Figure 6. The effect of aerodynamic particle size on the deposition of aerosol particles in the human respiratory tract following a slow inhalation and a 5-second breath hold (Patton and Byron, 2007)

II.1.2.2.2. Aerosol features

The site and extent of lung deposition also depends strongly on the aerodynamic particle size distribution of the aerosol, which should be used in place of geometric diameters. The *aerodynamic diameter* of a particle is defined as the diameter of a sphere with a unit density that has the same settling velocity in still air as the particle in consideration (Timsina et al., 1994). It depends on the geometric diameter of the particle (d_{geo}), its density (ρ_p), and the dynamic shape factor (χ), which is a dimensionless measure of the deviation from sphericity:

$$d_{ae} = d_{geo} \sqrt{\left(\frac{\rho_p}{\rho_0 \chi}\right)}$$

Consequently, the aerodynamic diameter can be decreased by decreasing the particle size, decreasing particle density, and/or increasing the dynamic shape factor.

According to the deposition mechanisms previously mentioned, drug-containing particles need to have aerodynamic diameters of **between 1 and 5 μm** to reach the lower respiratory tract and optimise pulmonary drug deposition (**Figure 6**). Indeed, particles larger than 5 μm usually impact in the oropharynx, from which they are easily cleared. In contrast, particles smaller than 1 μm may not deposit at all because of Brownian motion: they stay in suspension in air until exhaled (Carvalho et al., 2011). If systemic action is sought for the drug to be delivered, the target aerodynamic diameter must even be as low as **1-3 μm** to reach the respiratory bronchioles and alveoli. Indeed, as an aerosol particle penetrates more deeply into the lung, the airway epithelium becomes thinner and the lung surface area becomes larger, which increases the rate and extent of absorption (Patton and Byron, 2007).

Experimental determination of aerodynamic diameters is generally performed using impaction techniques (see IV.1.2.2.8.3.). The particle size distribution of a formulation is then mainly characterised by its Mass Median Aerodynamic Diameter (MMAD), the Fine Particle Dose (FPD), and the Fine Particle Fraction (FPF). The FPD is the mass of particles with an aerodynamic diameter below 5.0 μm , which are therefore expected to reach the lungs. The FPF is the fraction of the total drug dose with a particle size below 5.0 μm (Dunbar et al., 1998).

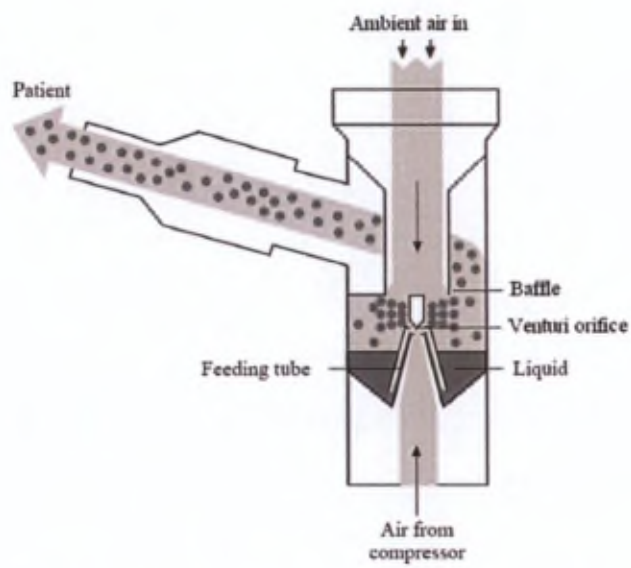


Figure 7: Schematic presentation of a jet nebuliser (Watts et al., 2008)

Interestingly, for a water droplet, the geometric and the aerodynamic particle diameter is identical. In contrast, large porous particles have a much smaller aerodynamic diameter compared to their geometric diameter. Aerosol particle design therefore involves two basic strategies: either particles are made with a standard unit density with a geometric size in the 1–5 μm range, or they are created with a lower density with geometric sizes over the standard range (Pilcer and Amighi, 2010). As an example, large porous particles exhibiting a high respirable fraction with mean geometric diameters ranging between 3 and 15 μm and tap densities between 0.04 and 0.6 g/cm^3 have been produced (Vanbever et al., 1999).

II.1.3. Drug delivery devices

Delivering drugs by inhalation requires not only a formulation that can be successfully aerosolised, but also a delivery system that produces a useful aerosol of the drug. Aerosolised drugs are designed for use in three different classes of inhaler devices, namely nebulisers, pressurised Metered Dose Inhalers (pMDI), and Dry Powder Inhalers (DPI).

II.1.3.1. Nebulisers

Nebulisers have been used in inhalation therapy since the 19th century to convert a liquid in solution or suspension into small inhalable droplets.

Pneumatic or jet nebulisers use compressed gas flow to break up the liquid into a fine mist. The driving force of jet nebulisers is based on negative pressure created by a high-velocity gas, drawing liquid from the reservoir up to a narrow opening (called a Venturi), through which the compressed air enters the nebuliser (**Figure 7**). This results in the aerosolisation of the formulation due to the Bernoulli effect (Watts et al., 2008). The protruding surfaces of primary and/or secondary baffles within the nebuliser are positioned in the path of the created aerosol so that the large liquid droplets impinge upon them, leading to a reduced, more useful particle size of the exiting aerosol (Dolovich and Dhand, 2011). The aerosol is continuously produced and the patient inhales it under normal breathing conditions from a mouthpiece or facial mask, which make these devices very useful for elderly and very young patients.

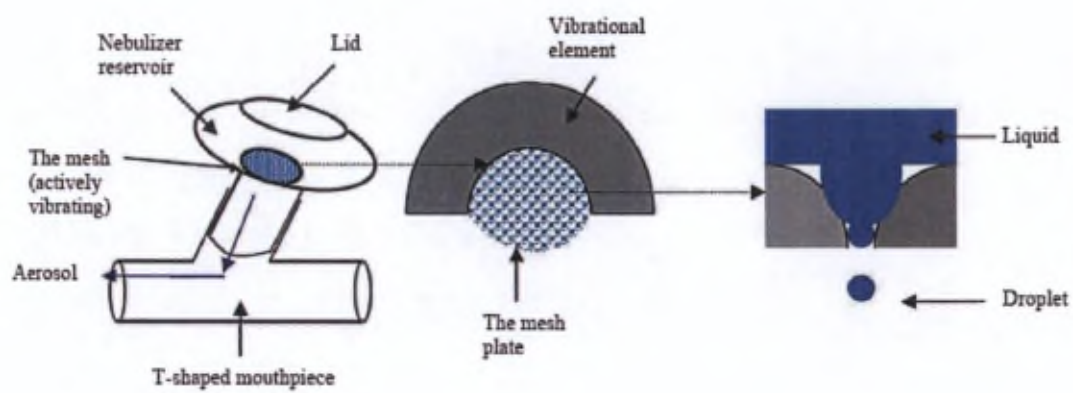


Figure 8. Diagram of the Aeroneb® Pro, a vibrating mesh nebuliser (Watts et al., 2008)

However, conventional jet nebulisers have many drawbacks. They need compressed gas or a compressor to operate and are therefore generally not portable. Treatment time is also usually around 5-15 min, which is much longer than for pMDIs and DPIs. Studies have also reported performance differences between nebulisers from different manufacturers and among nebulisers from the same manufacturer (Hess et al., 1996). Due to evaporative losses within the jet nebuliser, the solution also becomes increasingly concentrated and cools during nebulisation, which affects output and droplet size and leads to poor reproducibility. Jet nebulisers also have poor delivery efficiency, with only about 10% of the total reservoir dose actually reaching the lung (Watts et al., 2008). Indeed, nebulisers are characterised by a high dead volume (0.5-1 ml), with the wasted fraction accounting for up to 50% of the reservoir dose. Moreover, about 50% of the remaining dose is also lost because of the continuous generation of the aerosol, which cannot be administered during exhalation. Finally, only 50-60% of the particles produced are in the respirable range, which, in combination with the losses previously mentioned, explains the poor delivery efficiency.

Ultrasonic nebulisers incorporate a piezoelectric crystal vibrating at high frequencies (1-3 MHz). Aerosol production in these nebulisers is described by the capillary wave theory and the cavitation theory. The capillary wave theory describes aerosol formation with capillary waves forming on the fluid surface. As the amplitude of the waves reaches a threshold, the crest begins to break off into small droplets. In the cavitation theory, the implosion of small surface bubbles causes hydraulic shocks that create the droplets (Watts et al., 2008).

The above-mentioned drawbacks of jet nebulisers also apply to conventional ultrasonic nebulisers, except that no cooling effect occurs during nebulisation. The large energy input into ultrasonic nebulisers in turn causes a significant increase in the solution temperature, which can cause degradation of heat-sensitive materials (Dolovich and Dhand, 2011).

Recent adaptations of ultrasonic devices have led to the development of *vibrating mesh nebulisers*. These use a mesh or plate with multiple apertures to produce a liquid aerosol. This operating principle uses an aperture plate attached to a piezoelectric material that vibrates at a high frequency. The rapid vibration of the aperture plate creates a pumping action to produce the aerosol from a liquid solution (**Figure 8**). This mechanism is, for

example, used in the commercial Aeroneb® Pro nebuliser (Aerogen Inc., Galway, Ireland). This nebuliser has been shown to effectively aerosolise liposomal salbutamol sulfate, insulin, and other sensitive molecules that were prone to degradation from heat or shear produced by harsher nebulisation methods (Shaw, 2004; Elhissi et al., 2007; Watts et al., 2008).

Vibrating mesh nebulisers are able to generate aerosols with a high fine-particle fraction, which results in more efficient drug delivery compared to conventional nebulisers. They have a high rate of aerosol production, leading to shorter inhalation times, and they are portable and battery-operated. They also present minimal residual dead volume and can be coupled with adaptive aerosol delivery, which allow monitoring of the inhalation profile of the patient and delivery of the aerosol at the appropriate time (Watts et al., 2008, Dolovich and Dhand, 2011).

An alternative type of nebuliser is currently being developed that makes use of electrospray technology. It has notably been investigated by one of the partners of the NEOFOR project (Sausse Lhernould et al., 2009). Electrospraying refers to the atomisation of a liquid through the coulombic interaction of charges on the liquid and an applied electric field. It is implemented by applying a sufficiently high electric field to a metal capillary placed a few centimeters away from a ground electrode and by feeding a liquid of finite electric conductivity through the capillary. Depending on various parameters such as applied flow rate and electric field strength, different modes of electrospray can be obtained. The mode of most interest is the so-called cone-jet mode, in which monodisperse droplets in the micrometer range can be produced. The liquid meniscus at the capillary outlet then takes the shape of a cone from which emerges a very thin liquid jet. The microjet eventually breaks up into a spray of charged droplets because of the coulombic repulsion (Tang and Gomez, 1995). Nebulisation by electrospray is very simple to operate and produces very narrow particle size distributions (Gomez, 2002). However, no device has reached the market yet. Electrospray is indeed characterised by low flow rates in the range of 8-16 $\mu\text{l/s}$, which can represent a drawback for applications in drug inhalation. Moreover, the conductivity of the working fluids may have to be relatively large, which may conflict with other formulation constraints (e.g., pH-neutral solutions) (Deng et al., 2006).

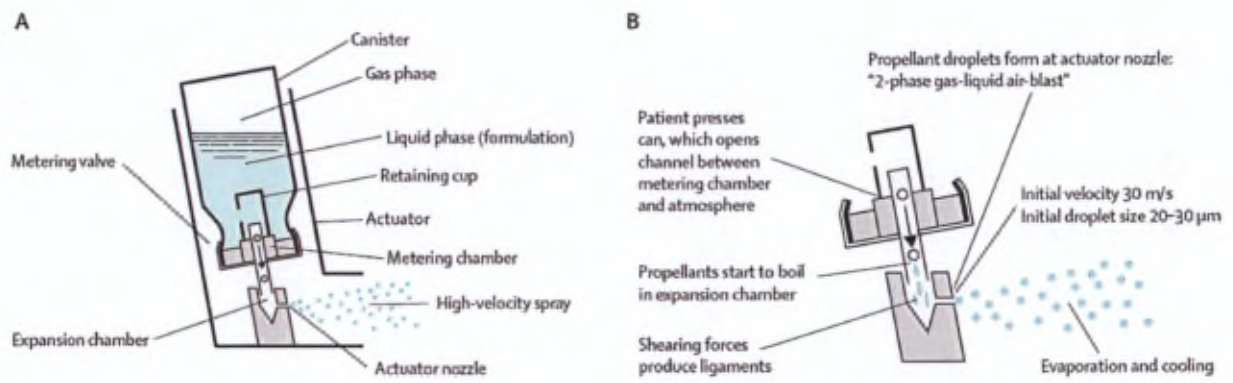


Figure 9. Key pMDI components and mechanism of aerosol generation (Dolovich and Dhand, 2011)

A) Key components of a pMDI B) Process by which the aerosol is formed

II.1.3.2. Pressurised Metered Dose Inhalers (pMDI)

Worldwide, pMDIs are the most widely-used inhalation devices for the treatment of asthma and COPD. In these systems, the drug is either dissolved or suspended in a liquefied propellant contained in a pressurised canister (**Figure 9**). When the metering valve is activated, the pressurised formulation is expelled rapidly into the expansion chamber in which the propellant begins to boil. This induces volume expansion and formation of a mixture of gas and liquid, which is discharged through the orifice of the device where a high-speed gas flow breaks up the liquid stream into droplets (Sackner and Kim, 1985). Chlorofluorocarbon (CFC)-propelled pMDIs were routinely prescribed for several decades. However, in accordance with the Montreal Protocol of 1987, CFC propellants are being replaced by hydrofluoroalkane (HFA) propellants, which do not have ozone-depleting properties. HFAs are non-toxic, non-flammable, and chemically stable and they are not carcinogenic or mutagenic (Dolovich and Dhand, 2011). A surfactant such as sorbitan trioleate (Span 85), oleic acid or lecithins, at levels between 0.1% and 2.0% w/w, is typically present to aid dispersion of suspended drug particles or dissolution of a partially soluble drug and to lubricate the metering mechanism (Newman, 2005).

pMDIs are compact pocket-sized devices that are disposable and designed for multi-dose use (generally a 1-month treatment). They allow a short inhalation time of the dose (a few seconds) and provide a more reproducible emitted dose compared to nebulisers. When used correctly, pMDIs deliver approximately 10-20% of the nominal dose to the lungs (Newman, 1985).

A major drawback of pMDIs is the need to precisely coordinate device actuation with inhalation. This can lead to poor drug delivery, increased inhaler use, and sub-optimum disease control, particularly in children and elderly patients. Breath-actuated pMDIs, such as the Maxair Autohaler® (Graceway Pharmaceuticals, Bristol, TN, USA) and Easibreathe® (IVAX, Miami, FL, USA), were developed to overcome this problem as they automatically actuate early during inspiration, at an inspiratory flow rate of about 30 l/min (500 ml/s) (Dolovich and Dhand, 2011). Another issue with pMDIs is the high velocity of the droplets exiting the device, which leads to high level of oropharyngeal impaction. To overcome this, several

types of spacer add-on devices have been developed. Among them, holding chambers, such as the AeroChamber Plus® Flow-Vu (Trudell Medical International, London, ON, Canada), possess a one-way valve that enables retention of the aerosol for a finite time after pMDI actuation. The overall effects of the chamber are to obtain particles with a decreased velocity and to produce an aerosol with a smaller aerodynamic size distribution, leading to lower oropharyngeal deposition and higher deep lung deposition. It also avoids the need to precisely coordinate device actuation with inhalation (Dolovich, 1993). However, it should be noted that impaction of the large particles within the chamber, as well as particle deposition due to electrostatic interaction with the plastic walls of the chamber, lead to a reduced total output of the aerosol. The decision to use a bulky spacer add-on should therefore be made on a case-by-case basis as it has been shown that lung deposition with a chamber is generally the same as that with a properly used pMDI without a chamber (Becker et al., 2005). Finally, another issue with pMDIs is that the usual valve volumes range from 25-100 µl, which only allows delivery of a small drug dose of about 50 µg to 5 mg.

II.1.3.3. Dry Powder Inhalers (DPIs)

The introduction of the first dry powder inhalers (DPIs) in the seventies was partly based on the need to find alternatives to ozone-destroying CFC propellants in pMDIs. A problem of hand-breath coordination was also frequently observed with incorrect use of pMDIs (Newman, 2004). DPIs avoid these two issues as they do not contain propellants and are generally breath-actuated. Presently, over 20 DPI devices are available on the market and more than 25 are in development (see **APPENDIX I** and **APPENDIX II**). In vitro lung deposition from current commercial DPIs varies from 12-40% of the recovered dose (Steckel and Müller, 1997; Islam and Gladki, 2008). There are essentially three types of DPIs, classified according to their metering system: **unit-dose devices**, in which the drug is packaged in capsules or foil blisters containing individual doses; **multiple-unit dose devices**, which contain multiple doses in multi-single-dose blister disks or strips; and **multi-dose devices**, in which the drug is contained in a reservoir from which the doses are metered out.

Unit-dose and multiple-unit dose inhalers are generally more effective than multidose reservoir devices as they better ensure dose uniformity and avoid the effects of moisture in

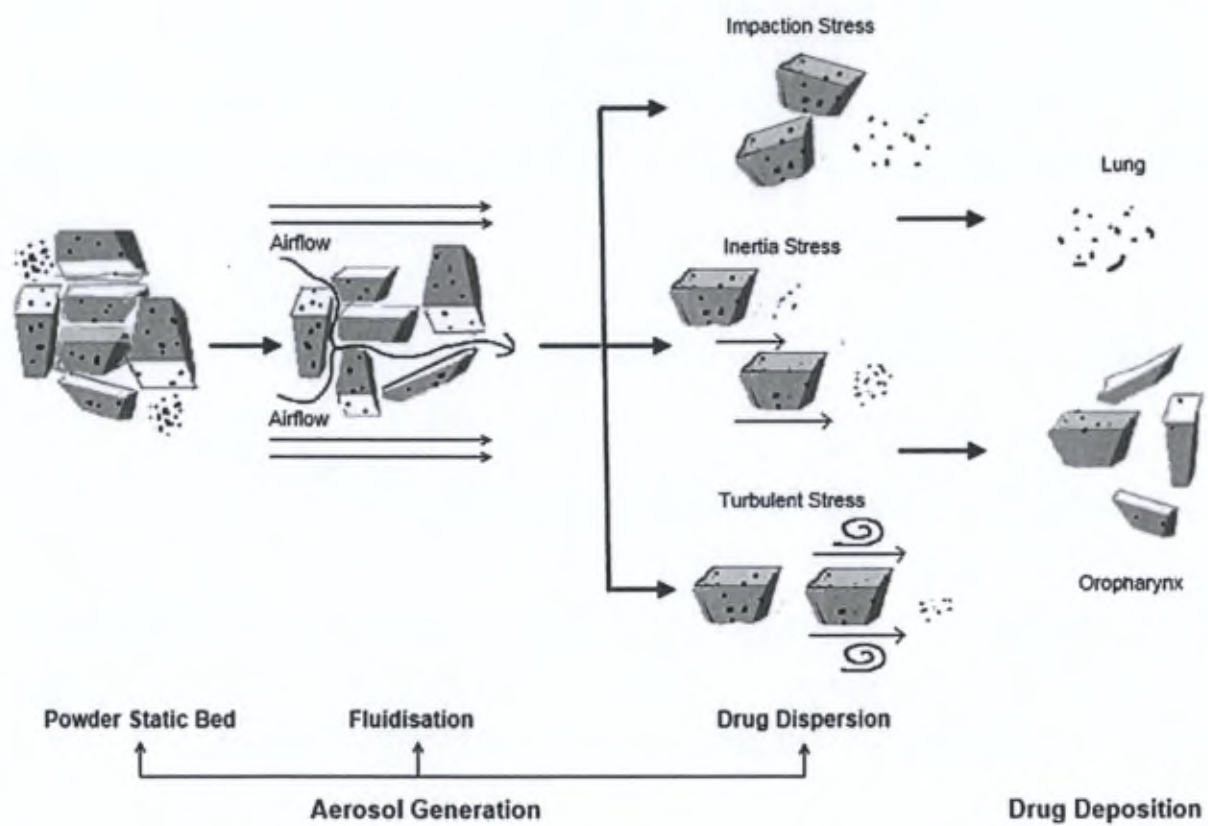


Figure 10. Mechanisms involved in aerosol generation (Pilcer et al., 2011)

the powder reservoir. Moisture can come from the ambient atmosphere or incorrect use of the DPI (e.g., expiration into the device) and can lead to powder aggregation (Steckel and Muller, 1997). The isolation of each dose also facilitates storage stability by protecting it from environmental degradation. In multi-dose devices, the issues of dose uniformity and storage stability then have to be limited by intensive development of the formulation to be used. On the other hand, unit-dose and multiple-unit dose devices are more complex to use due to the need to reload the device with a new cartridge/pack and patients (especially in the aged population) also need appropriate training to operate the device. These devices also have relatively higher cost than multi-dose reservoir designs (Islam and Gladki, 2008). A major classification of DPIs can also be made into passive and active devices.

Passive devices

In passive devices, the patient's inspiratory effort, both inspiratory flow and volume, provides the energy for dispersing and delivering the drug powder. Two consecutive mechanisms can be distinguished in powder dispersion from a passive DPI: entrainment of the particles from the powder bed (fluidisation) and breaking-up of aggregates (drug-carrier clusters) and agglomerates (drug-drug clusters) to form a fine respirable aerosol cloud (**Figure 10**). Shear force is the predominant mechanism of powder fluidisation in many passive devices (Dunbar et al., 1998). When the airstream passes over the powder bed, the viscous shear stresses in the boundary layer of the airstream cause the particles to lift from the powder bed surface. Shear force fluidisation is mainly dependent on the airflow velocity. Consecutively, the main mechanism involved in deaggregation and deagglomeration of particles is airflow turbulence (Dunbar et al., 1998; Louey et al., 2006). Another mechanism of deaggregation and deagglomeration is particle-device and particle-particle impaction (Voss and Finlay, 2002). On the other hand, inertial forces are the most effective type of separation force for drugs attached to carrier particles. They include vibration, centrifugal and collision forces (Pilcer et al., 2011). The majority of DPIs therefore contain specific design features, such as small-section and/or tortuous airflow paths, grids or impactor plates, to enhance the fluidisation and deaggregation of powder formulations (Dunbar et al., 1998; Louey et al., 2006).

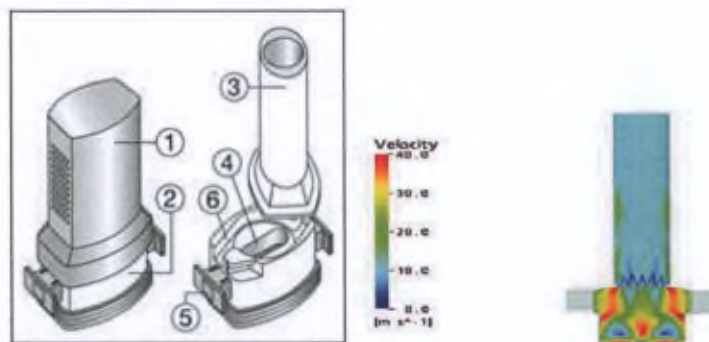


Figure 11. Device characteristics of the Aerolizer® and velocity profile of the flowfield generated in the device. 1. Mouthpiece cap, 2. Base, 3. Mouthpiece, 4. Capsule chamber, 5. Activation system of the piercing pins, 6. Air inlet channel. Velocity data obtained using Computational Fluid Dynamics (CFD) analysis (Coates et al., 2004; Rxlist, 2011)

All DPIs have an intrinsic resistance (R_i) to airflow, which determines the inspiratory flow rate occurring through the device for a given inspiratory effort. Devices with a low R_i used with maximal inspiratory effort result in a Peak Inspiratory Flow Rate (PIFR) through the device of 120 l/min, compared with values of only about 30 l/min for devices with very high R_i (Newman and Busse, 2002). This resistance differs among devices in relation to their internal design, with small internal sections in the airflow path leading to a higher resistance of the device. High inspiratory flow rates, obtained with low R_i devices, generally improve powder fluidisation, fine particle production, and lung delivery as they increase airflow velocity and turbulence. However, excessive inspiratory flow can increase impaction on the oral cavity and theoretically decrease lung deposition. Nevertheless, achievement of such excessive flow rates in current low-resistance devices is generally above the patient's capability (Borgström, 2001). On the other hand, for a given airflow rate, inhalers with a higher R_i are expected to generate greater turbulence and produce a higher fine particle fraction (Louey et al., 2006). A balance must therefore be made between the R_i of the device, on which its intrinsic dispersion efficacy depends, and the achievable airflow rate from the patient. Patients with severe asthma or COPD and children might indeed not be able to achieve sufficiently high flow rates in devices with a high R_i .

The first passive unit-dose device (developed in the seventies) was the **Spinhaler**[®], which delivers sodium cromoglycate (Lomudal[®], Sanofi-Aventis, Paris, France) in individual gelatin capsules. The patient places a capsule onto a propeller seated inside the inhalation channel, and the capsule is then pierced by two needles that are actuated by a sliding cam arrangement. When the patient inhales strongly through the mouthpiece, the propeller turns and vibrates, dispensing the drug as an aerosol (Newman and Busse, 2002).

Another unit-dose device is the **Aerolizer**[®] (Novartis, Basel, Switzerland) (**Figure 11**), in which the capsule is pierced on each side by four piercing pins. During inhalation, the capsule whirls and the particles are dispersed by turbulence generated by a spinning motion. Deagglomeration of the powder occurs through its passage through a plastic grid that also acts to straighten the flow and reduce the level of swirl generated in the device (Coates et al., 2004). It is commonly used for the delivery of budesonide (Miflonide[®]), formoterol (Foradil[®]), and beclometasone dipropionate (Beclophar[®]).

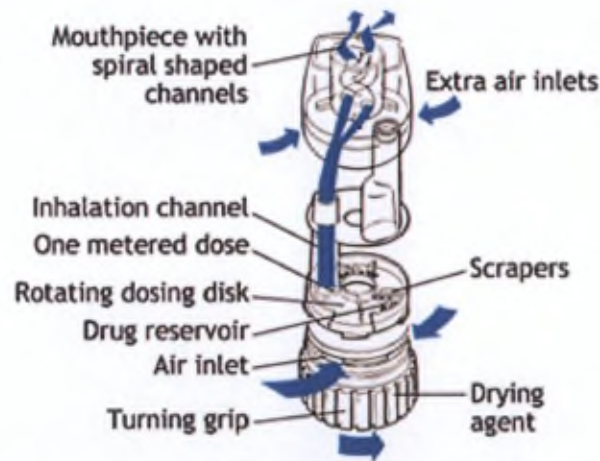
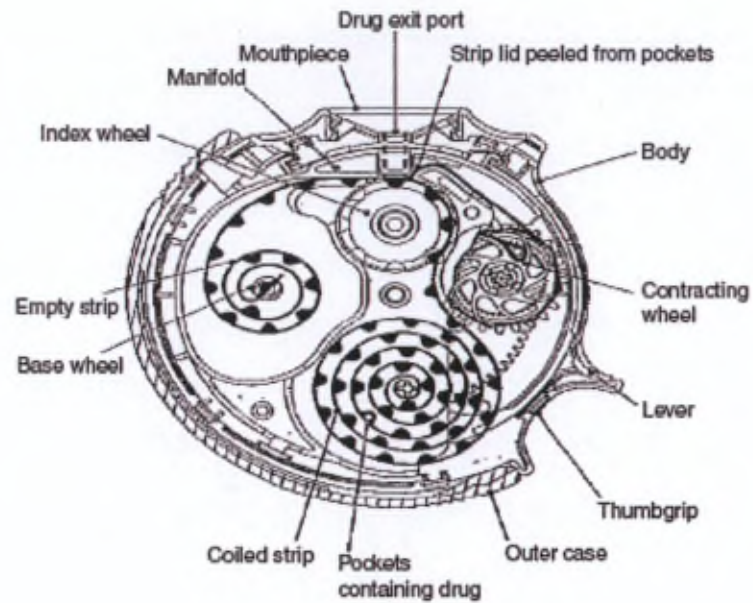


Figure 12. Device characteristics of the Diskus® (up) (Chrystyn, 2007) and Turbohaler® (down) (Asthma, 2012)

The **Diskus®**, presented in **Figure 12**, is a typical multiple-unit dose device that has been used since the mid-1990s for delivery of salmeterol (Serevent®), fluticasone propionate (Flixotide®), and a combination of these two molecules (Seretide®). The drug is metered into a tape of 60 double foil blisters, which corresponds to a one-month treatment. The patient operates the inhaler by sliding a lever that simultaneously moves the next dose-containing blister into place, peels the two layers of foil apart exposing the dose ready for inhalation, and decrements the dose counter (Chrystyn, 2007).

The first multidose device, the **Turbohaler®** (AstraZeneca, Lund, Sweden, **Figure 12**), was introduced in 1988. This inhaler incorporates up to 200 doses in a reservoir of drug powder and is used for the administration of terbutaline sulphate (Bricanyl®), formoterol (Oxis®), budesonide (Pulmicort®), and a combination of budesonide and formoterol (Symbicort®). When the patient activates the inhaler by twisting the base prior to inhalation, the Turbohaler® reservoir system deposits a single dose of the drug into a series of holes in a dosing disk. Most Turbohalers formulations are made of soft aggregates of micronised drug formed into pellets that are approximately 0.5 mm in diameter, without any excipients. The turbulence generated in spiral-formed channels in the mouthpiece during inhalation breaks up the agglomerates into fine particles, which are then inhaled into the lungs (Newman and Busse, 2002).

The **Novolizer®** multidose device (Sofotec GmbH, Frankfurt, Germany) is used to deliver salbutamol, formoterol, and budesonide. It provides a combination of technical features that ensure that every inhalation manoeuvre is performed with adequate inspiratory flow and that sufficient drug particles are delivered to the patient's lung. One of these technical features is an inspiratory flow rate threshold, triggering feedback mechanisms to the patient that confirm that an adequate inspiratory flow rate (minimum 35–50 l/min) has been achieved. A correct inhalation manoeuvre is confirmed to the patient by optical, acoustic, and taste feedback, which is likely to improve patient compliance. Unlike the other multidose systems, the Novolizer® also has a refillable cartridge system (up to 200 doses/cartridge), an accurate dose counter, low intrinsic resistance, and enables reliable and consistent dose delivery (Kohler, 2004).

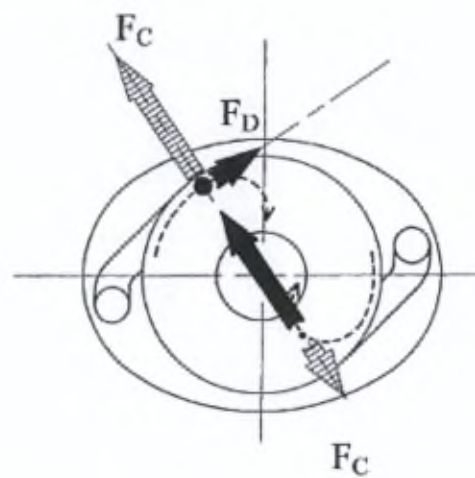
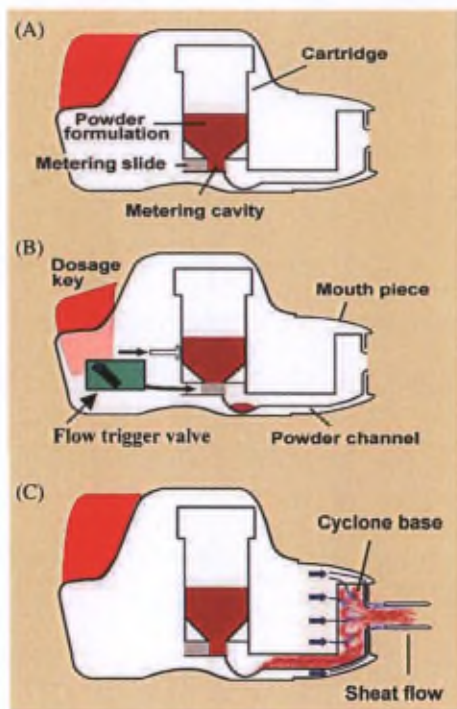


Figure 13. Device characteristics of the Novolizer® (Kohler, 2004) and schematic presentation of the forces acting on the particles during circulation in a basic air classifier (de Boer et al., 2003)
 F_C : centrifugal force, F_D : drag force

However, the most interesting feature of the Novolizer® is that it delivers high FPFs and has one of the highest lung deposition values obtained for DPIs, e.g. averaging 32.1% of the dose at an inspiratory flow rate of 99 l/min (Newman et al., 2000a). High deaggregation efficiency of the powder is achieved thanks to relatively low airflow resistance in comparison with other DPIs and thanks to the air classifier technology (ACT) located in the mouthpiece. The ACT is meant to classify particles by size. In its most basic design, it is a cylindrical chamber with a tangential air supply channel and a discharge channel starting from the centre of one of its circular ends. The larger carrier particles can be retained in the classifier and only detached drug particles are discharged with the inspiratory airstream. The classification is the result of the counter-acting of two forces (**Figure 13**): drag force (F_D) and centrifugal force (F_C). The drag force is proportional to the first power of the particle diameter and dominates for fine particles. Consequently, such particles are entrained by the air into the discharge channel of the classifier. The centrifugal force is proportional to the third power of the diameter and is strongest for the larger particles that are retained. The retention of large carrier particles has many advantages. Their continuous circulation within the classifier chamber for the whole duration of inhalation guarantees maximal utilisation of the available energy for deagglomeration. The break-up forces that are generated are thus a mix of centrifugal, collision, and friction forces (de Boer et al., 2003).

Active devices

As explained previously, an important drawback of DPIs is the dependency of their dispersion performance on the inhalation flow rate. This can lead to high intra- and inter-patient variability in dose delivery, particularly in patients with respiratory diseases. To overcome this, new generation DPIs are being developed that are active devices using an external energy input to disperse the powder. This generally provides higher dispersion efficiency than with passive DPI devices, allowing delivery of particles in the range of 1-3 μm . Many of them have therefore been developed for systemic applications. The mechanism employs compressed gas, motor driven impellers or vibrating piezoelectric crystals (Crowder et al., 2001; Young et al., 2004; Brown et al., 2004).

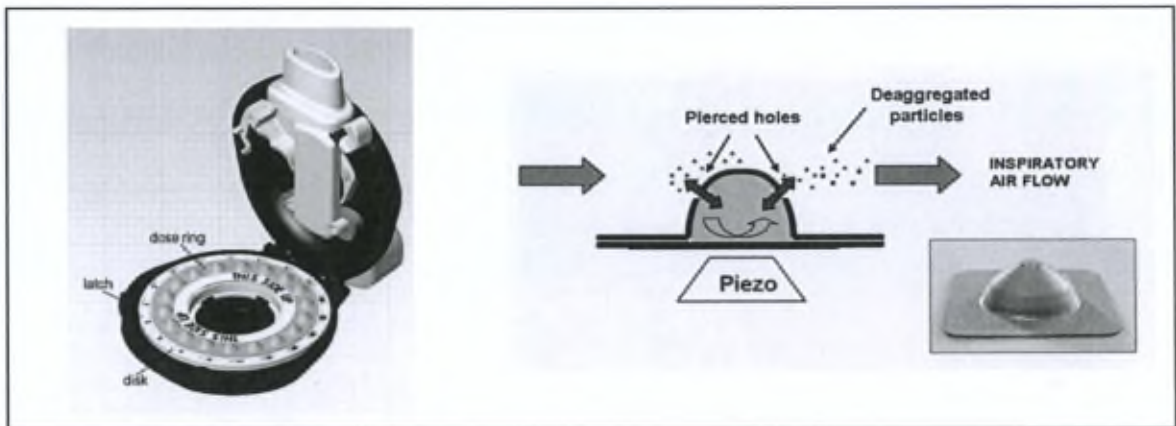


Figure 14. The MicroDose® active Dry Powder Inhaler (adapted from Fleming, 2007)

The first approved active device was the **Exubera**[®] device (Pfizer, New York, NY), which uses manually compressed air to disperse an insulin formulation in a retractable inhalation chamber (see also II.3.2.2.1.). Another active device, the **Aspirair**[®] (Vectura, Chippenham, Wiltshire, UK), utilises a vortex separation chamber and manually compressed air source that is triggered by an airflow sensor to deagglomerate drug particles and improve lung delivery of apomorphine hydrochloride for the treatment of erectile dysfunction (Tobyn et al., 2004). More recently, the development of the **NEXT**[®] multi-unit dose device (Chiesi, Parma, Italy) has been reported. This is a reservoir device in which the powder is metered into a dosing cup incorporated within the device. Another chamber helps compact the powder into the cup during dosing and the drug compact is deagglomerated during inhalation (Brambilla et al., 2006). A last example is the **MicroDose**[®] system (MicroDose Technologies, NJ, USA) (see **Figure 14**), which is a breath-actuated and piezo-electronic driven device. The drug powder, enclosed in a blister that protects the drug from the environment, is aerosolised by patient inspiratory force. Just before taking the drug, the blister is pierced and the patient takes a breath that, using an airflow sensor, turns on the piezo vibrator, which vibrates at high frequency to deagglomerate the powder particles. More than 25 chemical compounds, including insulin, other proteins and peptides, corticosteroids, and anti-cholinergic drugs, have been studied with this system. These compounds present high FPFs of between 50% and 90%, depending on the drug and formulation (Brown et al., 2004).

II.1.4. Main issues in DPI formulations

The formulation issues and formulation strategies that are specific to the development of protein formulations will be presented in section II.2.2. However, it is important to note that the general formulation issues for the development of inhaled dry powder formulations also apply to protein formulations. These are therefore presented in this section.

II.1.4.1. Overcoming inter-particle interactions

The main challenge in DPIs is to combine the DPI design with a suitable powder formulation that generates small particle aerosols. For dry powder formulations, agglomeration of the

drug particles is indeed a major obstacle in achieving appropriate aerosol generation and consecutive lung deposition as it causes an increase in the aerodynamic diameters. Agglomeration occurs as a consequence of inter-particle interactions, which are very high for micronised particles.

II.1.4.1.1. Interaction mechanisms

There are four types of inter-particle forces involved, namely the van der Waals, electrostatic, and capillary forces, and mechanical interlocking (Daniher and Zhu, 2008).

Van der Waals force becomes dominant when the particles are sufficiently close (< 100 nm) to each other and when the particles are small (20 μm or less). Surface roughness and geometrical structure can significantly affect this interaction by varying the separation distance between the particles. **Electrostatic force** can occur by tribo-electric charging or by the potential difference when particles of different work functions are brought into contact. The resulting Coulombic attraction makes the powder adhesive. **Capillary force** comes from fluid condensation at the surface of the particles, resulting in the formation of liquid bridges between them (Daniher and Zhu, 2008). The extent of the fluid condensation mainly depends on the specific surface area of the material, its hygroscopicity, and on storage conditions (Relative Humidity, RH). Moisture uptake and loss due to changes in RH can also result in local dissolution and recrystallisation, leading to irreversible agglomeration through solid bridge formation, which adversely affects aerodynamic diameter and lung deposition (Pilcer and Amighi, 2010). Controlling moisture content helps to reduce capillary forces. However, care must be taken to avoid increasing the surface charge of the particles since the magnitude of electrostatic forces is reciprocally related to capillary forces (Pilcer and Amighi, 2010). **Mechanical interlocking**, which comes from surface asperities or roughness, is also an important mechanism in preventing particle dispersion.

However, it is important to note that the relative importance of the different interaction forces varies on a case-by-case basis, as they are very dependent on particle size, shape, surface properties, and RH.

II.1.4.1.2. Formulation strategies

Adhesive mixtures

The most widespread formulation approach to overcoming inter-particle interactions and obtaining optimal aerosol generation is to blend the micronised drug particles with lactose to create adhesive mixtures. More than three-quarters of the most common DPIs on the market, such as Beclophar[®], Flixotide[®], Relenza[®], Seretide[®], Spiriva[®], and Symbicort[®], use this strategy. Lactose indeed has an established safety and stability profile as well as different manufacturing processes with tight controls over purity and physical properties. It is also easily available in different grades and is inexpensive (Pilcer et al., 2011). The lactose used in such formulations is generally composed of coarse particles (approximately 40–200 μm). These act as carriers onto which small drug particles adhere to aid powder flow and fluidisation, and also act as a diluent to help in dose metering. During inhalation, the drug particles separate from the carrier particles and are carried deep into the lungs, while the larger carrier particles impact the oropharynx and are cleared (Zhou and Morton, 2011). The homogeneity of the blend and the deaggregation and dispersion properties of the respirable particles upon the patient's inspiration are governed by the balance between cohesive (drug–drug) and adhesive (drug–excipient) interaction forces within the formulation. Indeed, the interparticulate forces need to be strong enough to facilitate handling but also weak enough to enable separation of drug and excipient during inhalation, using the air flow through the inhaler device as an energy source (de Boer et al., 2011). The addition to these binary mixtures of a fine size fraction of lactose (in the range of 1–40 μm and in a proportion of 1.5–20% w/w relative to the powder formulation) has been empirically observed to boost the deaggregation efficiency of the micronised drug as it is released from the powder mass (Zhou and Morton, 2011). Other fine-size particles, such as magnesium stearate or the drug itself, have also been used as a ternary compound in place of lactose, with significant increase in drug particle dispersion (Guchardi et al., 2008; Young et al., 2005).

An alternative to the addition of fines to decrease drug adhesion to the carrier material is to decrease the surface roughness of the carrier particles. This can be achieved by several processes such as surface erosion, surface dissolution or mechanofusion (Pilcer et al., 2011). Mechanofusion consists of homogenising the particle surface using intensive compression

and shearing energy. A slightly melting or a very fine solid material such as magnesium stearate can be added, which will form nano-structured layers around the carrier particles (Kumon et al., 2006). Lactose grades with modified surface properties could rapidly find their way onto the market as they do not require extensive toxicological studies to be approved by the authorities.

Other formulation strategies

Production of **pellets** made of pure drug particle agglomerates is another strategy to overcome interparticle interactions. It avoids the use of any excipient, which is of particular interest as a limited choice of excipients is currently authorised for inhalation because of a lack of safety data. Some commercially available DPIs, Pulmicort® and Bricanyl®, use pellet formulations for the delivery of budesonide and terbutaline, respectively. The agglomerates are formed by spheronisation in rotating blenders and present good aerosolisation properties due to weak van der Waals interactions (Pilcer and Amighi, 2010).

Another way to decrease interparticulate forces in a powder formulation is to limit capillary forces by decreasing the adsorption of water at the surface of the particles. This can be achieved by the use of **Solid Lipid Microparticles** (SLMs). The hydrophobic nature of lipids indeed reduces adsorption of the ubiquitous vapour leading to a reduction in the aggregation of particles. SLMs can be formulated either as a lipid matrix that entraps the drug or as particles that are physically blended with the drug particles. As an example, SLMs made of cholesterol and phospholipids were prepared by spray-drying to form matrixial and blended formulations of budesonide (Sebti and Amighi, 2006). Phospholipids were added to the formulation to reduce the generation of electrostatic charges at the surface of the particles, which also improves the deaggregation properties of the powder. The lipid particles, which had a geometric diameter around 2 µm, allowed higher fine particle doses of budesonide to be obtained than with the commercial Pulmicort® formulation (Sebti and Amighi, 2006). Alternatively, the same lipid composition was used to form a coating (5% w/w) around tobramycin particles to decrease moisture adsorption for this highly hygroscopic drug. The fine particle doses obtained for coated particles were significantly higher than for micronised tobramycin alone. The smoothing of the particle surfaces by the

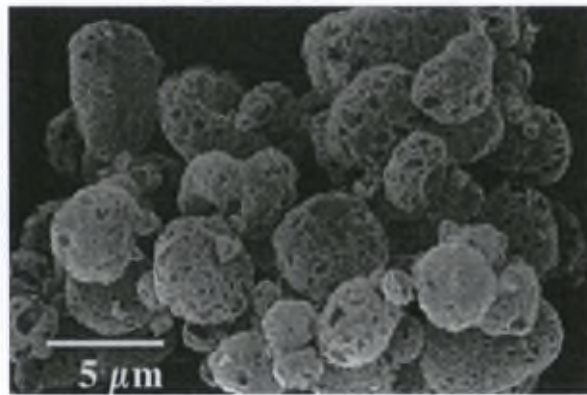


Figure 15. SEM of PulmoSphere budesonide formulation (Duddu et al., 2002)

lipid coating could also partly explain the better dispersibility results obtained for these formulations as it could reduce mechanical interlocking (Pilcer et al., 2006).

Large porous particles with a mass density significantly lower than 1 (0.1-0.5 g/cm³) have also been proposed to avoid deposition in the oropharynx. Porous particles with a geometric diameter of about 6-15 μm can indeed have aerodynamic diameters below 5 μm, and they aggregate less and deaggregate more easily under shear forces than smaller, non-porous particles. Spray-dried particles made of lactose, albumin, and DPPC have seemed particularly promising and have shown high respirable fractions of albuterol sulfate, estradiol, and insulin of 20%, 39% and 49%, respectively (Vanbever et al., 1999). Hollow porous microspheres (PulmoSpheres[®]) with a bulk density around 0.4 g/cm³ and a sponge-like appearance (**Figure 15**) were also obtained using a two-step process. First, a fluorocarbon-in-water emulsion was prepared by high pressure homogenisation, using a saturated phosphatidylcholine as surfactant. The emulsion was then combined with a second aqueous solution containing the active agent and other wall-forming materials (e.g., co-surfactants, sugars, and salts) and the aqueous dispersion obtained was spray-dried. The oil phase serves as a “blowing” or “inflating agent” during the drying process, retarding droplet shrinkage and simultaneously creating pores and voids in the particles (Dellamary et al., 2000; Pilcer and Amighi, 2010). Due to the hollow porous design of the particles, high respirable fractions were obtained *in vitro*. In a clinical evaluation of tobramycin pulmosphere particles on healthy volunteers, a mean whole lung deposition of 34 ± 6% was obtained (Newhouse et al., 2003).

II.1.4.2. Providing controlled release of the drug

Controlled drug delivery systems have become increasingly attractive options for inhalation therapies. A significant disadvantage of many existing inhaled drugs is indeed their relatively short duration of action, which requires inhalation at least twice daily and often leads to poor patient compliance. Reduction in the frequency of dosing would therefore be convenient, particularly for treatment of chronic diseases such as asthma. One of the strategies for achieving this goal is to develop molecules with an increased half-life. As an

example, ultra long-acting β_2 agonists (i.e. carmoterol, indacaterol) have been developed with a duration of action of up to 24 h, creating the possibility of once-daily dosing (Cazzola et al., 2005). However, appropriate formulation of short-acting molecules in sustained-release forms can also be a solution. An important issue to overcome is then to avoid mucociliary and/or macrophage clearance of the lung-deposited particles. Systems that allow the dissolution rate of the drug in the lining fluid of the lungs to be decreased are also being widely investigated.

Formulation strategies

Nanosystems seem particularly efficient in overcoming lung clearance mechanisms. It has indeed been shown that mucus clearance can be overcome by nanoparticles, possibly due to rapid displacement of particles to the airway epithelium via surface energetics (Schurch et al., 1990). On the other hand, the uptake of deposited particles by alveolar macrophages depends on particle size and nanoparticles of less than about 0.3 μm were shown to escape from phagocytosis (Lauweryns and Baert, 1977). Although particles below 1 μm are generally considered to be exhaled and not deposited in the respiratory tract because of the Brownian motion (see II.1.2.2.2.), particles with a diameter below about 500 nm may efficiently deposit in the small airways because of their increased diffusional mobility, particularly in cases where a breath-holding maneuver is applied (Byron, 1986; Carvalho et al., 2011). Although nanosystems are mainly administered as colloidal dispersions by nebulisation, dry formulations have also been investigated. The nanoparticles are formulated as micron-sized aggregates that can either be aerosolised as such or are blended with carrier particles to form an adhesive mixture (Huang et al., 2010). However, in order to recover the interesting release features associated with nanoparticles, the micron-size aggregates must be able to dissociate into primary particles either during inhalation (e.g. due to air turbulence in the inhaler) or after immersion in the lining fluid of the lungs.

Liposomes are one of the most extensively investigated nanosystems for controlled delivery of drug to the lungs. They are composed of small vesicles with an aqueous compartment enclosed by one or more concentric lipid bilayers and can be prepared using endogenous phospholipids such as distearoyl phosphatidylcholine (DSPC) and dipalmitoyl-phosphatidylcholine (DPPC). Liposomes have been shown to increase drug retention time

and/or reduce toxicity of drugs such as antibiotics and β 2-agonists (Zaru et al., 2007; Chimote and Banerjee, 2010; Huang et al., 2010). Their potential to provide sustained release comes from both their nano size and the encapsulation of the drug in their core or within their membrane bilayers, depending on the hydrophilicity of the drug. Several factors have been shown to influence drug release and absorption of liposome-encapsulated drugs, such as the composition of the lipids and the size of the liposomes used (Abra et al., 1990). Dry powder liposome formulations are generally prepared by lyophilisation of the aqueous liposome dispersions followed by micronisation by milling to achieve particles in the desired range. However, these formulations have to be processed with care, as deleterious effects on their integrity could be caused, thereby causing leakage of the entrapped drug (Desai et al., 2003; Pilcer and Amighi, 2010).

Solid Lipid Nanoparticles or SLNs have also been used to encapsulate drugs and provide sustained release. A sustained release effect was, for example, observed for interferon-alpha entrapped in hydrogenated castor oil (Li et al., 2010a). SLNs made of thymopentin, an immunomodulator, have also been administered in the form of hollow micron-size aggregates, which combines the delivery potential of nanoparticles with the aerosolisation properties of large porous particles (Li et al., 2010b).

However, a drawback of nanoparticles is that their very high surface area makes them very prone to fast dissolution in mucus and lining fluid, which implies that only insoluble or very poorly soluble nanomaterials could provide sustained release.

Interestingly, macrophage clearance can also be decreased by the use of **large particles** with a geometric diameter of over 6 μ m (Lauweryns and Baert, 1977). As an example, in vivo sustained release of insulin in rats was obtained with large porous particles fabricated from Poly(lactide-co-glycolide acid) (PLGA), which showed reduced macrophage uptake and immune response relative to non-porous controls (Edwards et al., 1997). Another formulation of large porous particles containing insulin (see II.3.2.2.3.) has also shown a prolonged insulin time-concentration profile in healthy volunteers (Rave et al., 2005).

A large number of other formulations have also been investigated to provide sustained release by decreasing the dissolution rate of the drug. These include SLMs, which have also been used to overcome inter-particle interactions (see II.1.4.1.2.). As an example, matrix

microparticles made of compritol and salbutamol acetone exhibited a sustained release of the drug. The particles were prepared by the hot emulsion technique followed by solidification at room temperature and freeze-drying (Sanna et al., 2004, Jaspert et al., 2007). Solid lipid microparticles made up of palm oil encapsulating terbutaline sulphate nanoparticles, produced by spray-drying, were also used to obtain a sustained release effect, with an appropriate FPF around 46% (Cook et al., 2005).

Poly(L-lactic acid) (PLA) and PLGA microparticles have also been delivered to the lung for sustained release applications. A prolonged protection against bronchoconstriction has been reported in rats at least 12 h post administration with PLGA/isoproterenol microspheres (Lai et al., 1993). In addition, microparticles made of beclomethasone dipropionate and nedocromil sodium entrapped in PLA have shown sustained release in vitro for 8 and 6 days, respectively (El-Baseir and Kellaway, 1998). However, PLA and PLGA microparticles have shown long residence in the lung due to slow degradation (Dunne et al., 2000), and pulmonary administration of PLA microspheres to rabbits has also been associated with inflammation at sites adjacent to microparticle deposition (Armstrong et al., 1996). This might lead to pulmonary accumulation of polymers and consecutive toxicity, especially with daily administration. Therefore, the use of slowly degrading or non-biodegradable polymers in the lungs should be considered very carefully, and the safety of the degradation products must also be considered (Pilcer and Amighi, 2010).

II.2. Peptides and proteins for pulmonary delivery

II.2.1. State of the Art

Over about 25 years, a number of methods for recombinant synthesis of peptides and proteins have been developed, allowing the production of large amounts of these compounds (e.g. hormones, growth factors, cytokines, and monoclonal antibodies), which play an important role in clinical treatment (Siekmeier and Scheuch, 2009). These molecules are thus widely investigated for pulmonary delivery, either for the treatment or prophylaxis of airway diseases (topical applications) or for absorption into the blood for the treatment or prophylaxis of systemic diseases (Onoue et al., 2008). The systemic delivery of proteins by inhalation has particularly attracted attention because it provides an alternative to parenteral administration, which is the conventional administration mode for biomolecules. The combination of their large molecular size, hydrophilicity, and lability (both chemical and enzymatic) indeed limits their formulation in traditional oral dosage forms (Agu et al., 2001). Pulmonary administration presents several advantages, namely a very large alveolar surface, low thickness of the epithelium, high blood perfusion, and avoidance of hepatic first-pass metabolism (Siekmeier and Scheuch, 2009). This leads to higher bioavailability of drugs in comparison with the other alternatives for systemic protein administration. These are mainly nasal and transdermal delivery. Even though nasally administered drugs are also thought to avoid first-pass hepatic metabolism, bioavailability of nasally administered proteins can be limited because a broad range of metabolic enzymes are located in the nasal mucosal cavity. Furthermore, nasal mucosa is considerably smaller compared to the absorption area of the lungs (i.e. 150 cm² vs. 100 m²) and the mucosa is thicker than the alveolar membrane. These drugs are also rapidly cleared from the nasal cavity after administration because of mucociliary clearance. Nevertheless, some drugs that use the nasal route of administration have already been approved and have reached the market. These are mainly salmon calcitonin, desmopressin, and buserelin (gonadotropin-releasing hormone agonist). Transdermal delivery can also be considered an attractive alternative administration route. The skin, although it contains aminopeptidases, exhibits considerably reduced enzymatic

activity and also avoids the hepatic first-pass effect, leading to increased bioavailability of drugs. However, the primary problem associated with transdermal delivery is that the skin is an excellent barrier for large, hydrophilic and polar compounds. The only biomolecule currently investigated clinically by transdermal administration is an interferon α -2b for the treatment of genital warts and cervical dysplasia (Antosova et al., 2009).

A summary of the currently investigated applications of therapeutic peptides and proteins by inhalation to the lungs is provided hereafter.

II.2.1.1. Topical applications

With respect to topically acting drugs, there are few biopharmaceuticals for inhalation currently available on the market. One is a nebulised formulation of DNase for the treatment of CF (Pulmozyme[®], Genentech, San Francisco, CA, USA) (Chan et al., 1997).

The other protein-containing products currently available by inhalation are modified bovine pulmonary surfactants that contain surfactant proteins (Yapicioğlu et al., 2003). These are administered by intra-tracheal instillation and are, namely, Survanta[®] (Abbott Laboratories, North Chicago, IL, USA), Curosurf[®] (Chiesi Farmaceutici, Parma, Italy), Infasurf[®] (ONY Inc., Amherst, NY, USA), and BLES[®] (BLES Biochemicals, London, ON, Canada). Surfactant replacement therapy has become the standard therapeutic intervention for treating Acute Respiratory Distress Syndrome (ARDS), which consists of a loss of integrity in the alveolar-capillary barrier (Carden et al., 1998). Patients with ARDS have dysfunctional surfactant, a problem that may contribute to airway instability. The addition of exogenous surfactant would be beneficial in reversing adverse pulmonary effects of ARDS. It is well known that SP-B and SP-C surfactant proteins play a crucial role in monolayer-to-multilayer transition upon film compression, adsorption, and readsorption/respreading of surfactant film upon film expansion (Zhang et al., 2011b). New generation synthetic surfactants that contain simplified peptides or recombinant surfactant protein analogs are also under development to avoid the potential antigenic and infectious complications that might be associated with animal-derived preparations (Kattwinkel, 2005).

Table I. Approved or potential applications of therapeutic peptides and proteins for local effect, administered by inhalation (adapted from Onoue et al., 2008)

Drug	Biological functions	Clinical application	Clinical status (sponsor)	Ref./Trial registry number
DNase	Viscosity of sputum	Cystic fibrosis	Approved (Genentech)	Chan et al., 1997
Modified bovine surfactant	Surfactant replacement	Acute Respiratory Distress Syndrome	Approved (Abbott, Chiesi, ONY, BLES Biochem.)	Zhang et al., 2011b
Ciclosporin	Immunosuppression	asthma and COPD, lung transplant	φ II ongoing, 2012 (NHLBI) φ III ongoing, 2012 (APT Pharm.) φ III ongoing, 2012 (Pari Pharm.) φ I completed, 2009 (Univ. Pittsburgh)	NCT01287078 NCT00755781 NCT01334892 NCT00783107
α_1 -Antitrypsin	Trypsin inhibition	COPD, cystic fibrosis, α_1 -A deficiency	φ III ongoing, 2012 (Kamada) φ II completed, 2004 (Talecris Biotherap.) φ II ongoing, 2012 (Rabin MC) φ I/ φ II completed, 2003 (Baxter Corp.) φ I completed, 2011 (CSL Behring)	NCT01217671 NCT00486837 NCT01394835 NCT00161707 NCT01347190
Interferon- β	Regulation of immune response	Respiratory viruses	φ II completed, 2012 (Synairgen Res.)	NCT01126177
Interferon- γ		Mycobacteria, cystic fibrosis, lung cancer	φ II completed, 2002 (NIAID) φ I/ φ II completed, 2002 (InterMune)	NCT00021567 NCT00043316
Interleukin-2 (recombinant Aldesleukin)	T-cell proliferation	Cancer, tuberculosis	φ I completed, 2009 (USC)	NCT00003009
Interleukin-4 receptor (recombinant α -subunit)	Suppression of IL-4 and IL-13 activities	Asthma	φ II completed, 2005 (Immunex Corp.) φ II completed, 2008 (NIAID)	NCT00017693 NCT00001909
Interleukin-4 mutein	Il-4 and IL-13 antagonist	Asthma	φ II completed, 2011 (Aerovance)	NCT00801853

A growing number of other peptides and proteins are currently being investigated and are in various phases of clinical development (**Table I**). Most of them are aimed at treating respiratory diseases (asthma, COPD, cystic fibrosis, and other respiratory inflammations). The current investigations on inhaled peptides and proteins for the treatment of asthma are discussed in point **II.4.3**. They mainly focus on the use of anti-cytokines and ciclosporin.

Another widely investigated molecule is α 1-Antitrypsin (α 1-A), which is the most relevant protease inhibitor in the lung. Patients with CF or hereditary deficiency in α 1-A suffer from a local excess of neutrophil elastase leading to a progressive loss of lung function. Administration of α 1-A by nebulisation was shown to be effective in several studies (**Table I**) and it is currently investigated with the use of novel nebulisers and optimised breathing techniques (Siekmeier, 2010).

Other biologics are developed for the treatment of respiratory infections (tuberculosis) or lung cancer. Cytokines are particularly investigated, including interferons and interleukin-2. Interferon- α administered in nebulisers has shown little clinical benefit so far in the treatment of lung cancer. However, it may enhance standard anti-tuberculous therapies, although additional trials are needed to verify and quantify its benefits in tuberculosis patients (Thippawong, 2006). Most of the trials performed with inhaled Interferon- γ also enhanced clinical response to anti-tuberculous chemotherapy (Koh et al., 2004). However, lack of efficacy was observed in other studies, e.g. for cystic fibrosis treatment. This could be related to the low delivered lung doses, as demonstrated with commercial devices in scintigraphic studies (Condos et al., 2004). Treatment of pulmonary metastases with inhaled interleukin-2 (IL-2) exhibited comparable clinical efficacy and less systemic toxicity than those receiving systemic IL-2, although additional well-controlled studies are needed to confirm these potential clinical advantages (Huland et al., 2000).

II.2.1.2. Systemic applications

An overview of the applications of proteins and peptides for inhalation is presented in **Table II**. However, none of these systemic applications is currently available on the market.

The most visible drug under development for systemic delivery via inhalation is **insulin** (5.8 kDa) to treat diabetes. Many products have reached clinical development, including both

Table II. Potential application of therapeutic peptides and proteins for systemic effect, administered by inhalation

Drug	Biological functions	Clinical application	Clinical status (sponsor)	Ref./Trial registry number
Insulin	Hypoglycemic effect			
Exubera®		Type I/II diabetes	Approved, discontinued in 2007 (Nektar/Pfizer)	Bellary and Barnett, 2006
AIR system		Type I/II diabetes	φ III discontinued in 2008 (Alkermes/Eli Lilly)	Muchmore et al., 2007
Afrezza®		Type I/II diabetes	φ III ongoing, 2012 (MannKind)	Steiner et al., 2002
AERx IDMS		Type I/II diabetes	φ III discontinued in 2008 (Aradigm)	Thippawong et al., 2002
Glucagon-like peptide-1 (GLP-1)	Hypoglycemic effect	Type II diabetes	φ I completed, 2008 (MannKind)	NCT00642538 ; Lee et al., 2009
Calcitonin	Bone mineral metabolism	Osteoporosis, Paget's disease	φ I completed, 1996 (Dura Pharm.)	Deftos et al., 1997
Parathyroid hormone (PTH)	Bone mineral metabolism	Osteoporosis	Preclinical	Patton et al., 1994
Human growth hormone	Bone growth	Growth deficiency	φ I completed, 2008 (Alkermes/Eli Lilly)	Nelson et al., 2009
Erythropoietin-Fc	Erythrocyte production	Anemia	φ I completed, 2005 (Syntonix Pharm./ Boehringer Ingelheim)	Dumont et al., 2005; Bitonti and Dumont, 2006
Live attenuated measles virus	Immune system stimulation	Measles vaccine	φ I ongoing, 2012 (Serum Institute of India Limited)	NCT01557699
Live attenuated <i>Mycobacterium bovis</i> bacillus	Immune system stimulation	Tuberculosis vaccine	φ I ongoing, 2012 (University of Oxford)	NCT01497769

DPIs (Exubera[®], Afrezza[®], AIR[®] inhaled insulin system) and liquid-type inhalers (AERx insulin and Alveair[®]). Although Exubera[®] had obtained approval by the FDA and EMEA and briefly reached the market in 2006, it was withdrawn in 2008 because of unexpectedly low sales. All other studies on inhaled insulin were subsequently aborted, except on Afrezza[®], which was in phase III development and is currently waiting for approval. These inhaled insulin systems are described in further detail in part II.3.2.2. Other inhaled molecules, such as a Glucagon-like peptide-1 (GLP-1), are also under investigation for the treatment of insulin-dependent diabetes. GLP-1 stimulates the release of insulin from pancreatic β -cells through the G-protein-coupled GLP-1 receptor only when blood glucose levels are high (Thorens et al., 1993). GLP-1 also suppresses the release of glucagon from the pancreas, preventing the dumping of glucose into the bloodstream by the liver, and slows stomach emptying, leading to satiety. In a proof-of-concept study, a GLP-1 derivative in a DPI system (Technosphere microparticles) has been attempted for the treatment of Type 2 diabetes. Inhaled GLP-1 produced plasma levels comparable to those of parenteral administration and sufficient to induce insulin secretion resulting in attenuation of postmeal glucose excursions (Marino et al., 2010). GLP-1 and related peptide therapies using DPI systems have been identified as ideal treatments for diabetes to avoid hypoglycemia or weight gain (Qian et al., 2009; Kim et al., 2011).

Other proteins that have been investigated for inhaled systemic delivery are **calcitonin** (MW: 4500 Da) and **parathyroid hormone** (PTH; MW: 9400 Da). Parenteral administrations of calcitonin and PTH have been used either alone or in combination with other existing oral therapies (biphosphonates, vitamin D, and calcium) for treatment of osteoporosis. Pulmonary delivery of calcitonin and PTH seems promising as an alternative to injections, and they have been shown to be well absorbed from the rat lung, as demonstrated by the high absolute bioavailabilities (17% for calcitonin and 40% for PTH) obtained by liquid intratracheal administration (Patton, 2000; Onoue et al., 2008). On the other hand, DPI administration of PTH presented an absolute bioavailability of up to 34% (Codrons et al., 2003). Although a number of animal studies have been performed, studies in which calcitonin or PTH were administered in humans are, up to now, sparse. Administration of a DPI of salmon calcitonin in 10 healthy volunteers exhibited 28% of the bioavailability of the intramuscularly administered compound (Deftos et al., 1997).

A first-in-man study has also been performed with an **EPO-Fc fusion protein** (see II.2.2.1.2.), showing dose-dependent concentrations of the fusion protein in the serum and an increase in circulating reticulocytes in the highest dose group (Dumont et al., 2005).

Another example is **human growth hormone** (hGH; MW: 22100 Da), which is used to promote growth in children with pituitary dwarfism due to GH deficiency. However, GH-deficient adults are also treated in order to restore/ameliorate abnormalities of energy metabolism, muscle mass and strength, and cardiovascular function, as well as bone metabolism. A non-invasive treatment for this long-term treatment would thus improve compliance of the patients. The bioavailability of GH after pulmonary administration in different animal studies was shown to be between 5% and 45 % (Siekmeier and Scheuch, 2009). In a short-term safety study in adults with asthma, non significant changes in pulmonary function or worsening of asthma occurred during treatment with inhaled GH (Nelson et al., 2009).

Finally, another potential application of inhaled peptide and proteins is vaccination, as most antigens are macromolecules. In comparison to parenteral vaccination, pulmonary delivery has indeed demonstrated attractive properties, including superior local mucosal immunity and systemic immunity, absence of complications associated with injectable delivery, and ease of administration. Although superior local immunity is particularly beneficial for protection against infections originating from the respiratory tract (e.g. influenza and tuberculosis), the connection of various mucosal sites through a compartmentalised mucosal immune system presents the opportunity to immunise against diseases originating from a remote mucosal site via the pulmonary route (Sou et al., 2011). The spray-dried influenza vaccine with inulin as a stabiliser was demonstrated to have good inhalation characteristics with a fine particle fraction of 37%. The inhaled formulation has been shown to induce significantly higher antibody titres in mouse than i.m. injection and liquid aerosol and it remains biochemically and physically stable after 3 years at 20°C (Saluja et al., 2010). A spray-dried vaccine for Hepatitis B virus (HBV) has also been tested in guinea pigs, which induced protective systemic immunity and superior local mucosal immunity (Muttill et al., 2010). Dry powder measles and tuberculosis vaccines have been successfully tested in macaque and guinea pig, respectively (de Swart et al., 2007; Lu et al., 2010). These latter vaccines are currently entering clinical trials in India and South Africa , respectively (Sou et al., 2011).

Table III. Time to reach peak serum concentration (t_{max}) for proteins with various molecular weights after intra-tracheal administration in rat (Patton et al., 1994)

Protein	Molecular weight (Da)	t_{max}
LHRH analogue	1,182	30 min
Human calcitonine	3,416	~ 15 min
Salmon calcitonine	3,430	~ 15 min
PTH-34	4,278	~ 15 min
Insulin	5,786	11 min
G-CSF	18,000	1-2 h
α -interferon	19,271	3-9 h
GH	22,125	0.5-6 h
Bovine serum albumin	67,000	16-24 h
Bovine IgG	150,000	16 h

II.2.2. Main issues in DPI formulation of peptides and proteins

Efficient delivery of biomolecules to the lung depends on the biophysical (aerosol particle size) and physiological (inspired volume, inspiratory flow, breath holding time) factors previously described (see II.1.2.2.). Therefore, conventional formulation issues also occur with these molecules and the formulation strategies described in II.1.4. can generally be applied. However, specific challenges have to be addressed, whether the protein is intended for local or systemic administration. These are mainly related to the absorption of the protein through the pulmonary epithelium (when systemic action is required) and to the physical and biochemical stability of the molecule, which has to be preserved to guarantee the bioactivity of the molecule.

II.2.2.1. Crossing the alveolar epithelium

A major obstacle to the widespread use of pulmonary drug delivery is the relative impermeability of the lungs to many peptides/macromolecular drugs when they are administered alone. Although the alveolar epithelium has a high permeability to water, gases, and lipophilic substances, the absorption by simple diffusion through the membrane of hydrophilic substances, and even more so of large-size molecules, is limited by the structure and hydrophobicity of the double-layer membrane. Despite the fact that endothelial and Type I epithelial cells look very similar under electron microscopy (i.e. same extreme thinness, same simple cytoplasm), studies show that for a variety of high and low molecular weight solutes, more than 90% of the alveolar absorption 'barrier' is in the epithelium (Patton, 1996). Absorption rates of macromolecules from the lung into the blood is globally inversely related to molecular mass, although there does not seem to be an effect of molecular weight on the absorption rate of small peptides (**Table III**). This inverse relation can partly be explained by the existence of different absorption mechanisms at cellular level (Patton, 1996).

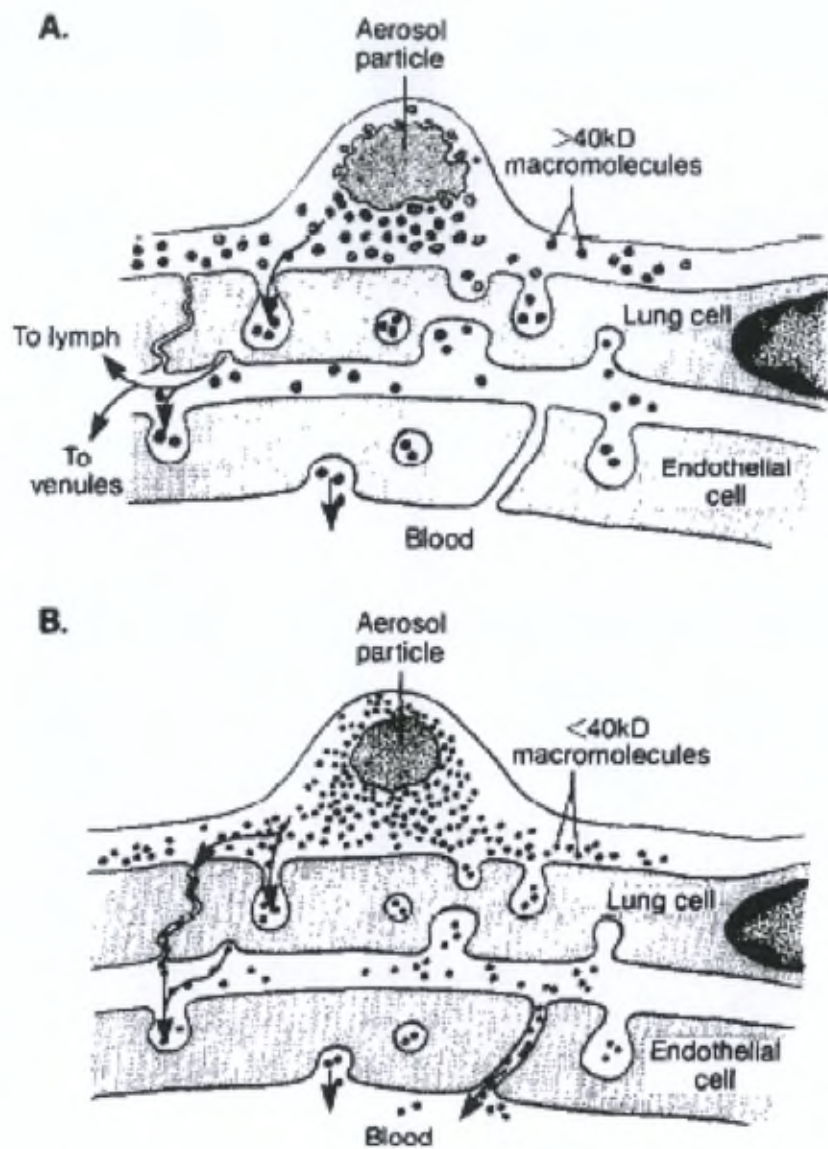


Figure 16. Models for the absorption of macromolecules across alveolar Type I cells (Patton, 1996). (A) Molecules larger than about 40 kDa may be absorbed by transcytosis and then enter blood either via transcytosis in the capillary, drainage into lymph or absorption through the leaky junctions of capillaries or post capillary venules. (B) Molecules smaller than about 40 kDa may directly enter the blood primarily via the tight junctions of both the Type I cell and the capillary. Transcytosis may be a minor route of transport for these small peptides

II.2.2.1.1. Absorption mechanisms

Even though the mechanisms of lung absorption of peptides and proteins are still poorly understood, it is generally accepted that they are poorly absorbed by simple diffusion, with the potential mechanisms being transcytosis (transport by endocytosis through the cells) and paracellular absorption (transport between the cells) (Wang and Zhang, 2004).

Transcytosis is characterised by the formation of vesicles that merge with the membrane, releasing molecules on the other side of the cell. Absorptive transcytosis may occur independent of a membrane receptor (fluid phase or adsorptive transcytosis) or it may involve receptor mediated binding followed by vesicular transport (receptor mediated transcytosis). Receptor-ligand complexes are generally localised into clathrin-coated pits and the complex is internalised and moved across the cell. Another kind of transcytosis occurs in non-coated vesicles called caveolae, with opening diameters of 40 nm and internal diameters of 50-100 nm (Lisanti et al., 1994; Schnitzer et al., 1995). Presumably macromolecules can be non-specifically captured in the solution space of both clathrin-coated vesicles and caveolae in a process referred to as fluid phase, non-receptor-mediated transcytosis. Alternatively, macromolecules may non-specifically adsorb to the plasma membrane and undergo transport through non-specific adsorptive transcytosis (Patton, 1996). Whether receptor-mediated or not, transcytosis is probably the mechanism used for proteins that exceed 40 kDa (**Figure 16**). The process seems to be relatively slow, taking hours to days to complete (Wang and Zhang, 2004).

Paracellular absorption is usually thought to occur through the junctional complexes between two cells (tight junctions) that allow interactions between cells and also provide a functional link between the basal and apical side of the cell surface. They form a kind of paracellular, semi-permeable "bridge", which restricts diffusion according to the size and charge of the molecule (Balda et al., 2007). This absorption system is generally limited to macromolecules not exceeding 40 kDa (**Figure 16**) (Wang and Zhang, 2004; Bur et al., 2006). It can be noted that the passage of molecules through the capillary endothelium is not the limiting factor because this has looser junctions than the alveolar epithelium. This

endothelium indeed contains gaps that are about 5-30 nm long and have a 4 nm diameter, which allows the passage of molecules approximately 10 times larger than those that can pass through the alveolar epithelium, which possesses openings with diameters of 0.5-2 nm between two Type I cells (Bundgaard et al., 1984; Agu et al., 2001). Another type of paracellular transport may occur at the junction of three cells, which occurs at specific spots on the circumference of both endothelial and epithelial cells. Paracellular transport may also occur when a cell dies, leaving a relatively large 'pore' on the basement membrane, which is soon filled as new cells spread and seal the monolayer. These mechanisms, which need further investigation, could allow proteins larger than 40 kDa to be absorbed by paracellular transport.

II.2.2.1.2. Formulation strategies

Absorption enhancers

Many potent absorption promoters have been investigated for the absorption of various proteins from the lungs. However, the mechanism of action of these absorption enhancers could be due to an irreversible distortion of the alveolar epithelial cell layer, which could potentially make the lungs susceptible to the entry of exogenous allergens and dust particles inhaled during respiration. Thus the use of absorption promoters in pulmonary drug delivery has generated safety concerns regarding possible long-term effects. Moreover, these molecules generally present a dose-dependent efficacy and toxicity, with high enhancer concentrations leading to higher bioavailability but also higher lung permeability. In some cases, however, the permeabilisation of the lungs has been demonstrated to be reversible after short-term use of the enhancer (Hussain et al., 2004). Efficacy and toxicity aspects of some agents widely-used in pulmonary peptide and protein delivery are tabulated and presented in **APPENDIX III**. Major classes of absorption enhancers include surface-active agents, liposomes and phospholipids, and cyclodextrins.

Among **surface-active agents**, bile salts and acids have been commonly employed as absorption enhancers. Possible mechanisms that could be involved in enhanced absorption

are: (i) alteration of the mucus layer, (ii) protection against enzymatic degradation, (iii) dissociation of high order protein multimers into oligomers or monomers, (iv) increased paracellular absorption due to opening of tight junctions between epithelial cells, and (v) extraction of membrane phospholipids and proteins by forming micelles, thereby facilitating transcellular passage of exogenous protein molecules (Gordon et al., 1985; Hersey and Jackson, 1987). As an example, a dose-dependent increase in the bioavailability of salmon calcitonin was obtained when co-administered with various doses of taurocholic acid by intratracheal instillation in rats (Kobayashi et al., 1996). The effect of sodium taurocholate on epithelial integrity and viability was also investigated using Caco-2 cell monolayers and demonstrated nonlinear concentration-dependent absorption enhancement of insulin, but also concentration-dependent toxicity (Johansson et al., 2002).

Co-administration of various fatty acids and nonionic surfactants has also been shown to increase protein and peptide absorption after inhalation in several animal experiments. Unsaturated fatty acids of oleic, palmitoleic, and linoleic acid have, for example, been shown to have potent effects on salmon calcitonin absorption (Kobayashi, 1994).

The use of **liposomes** has been suggested to provide sustained pulmonary release for various drugs. However, liposomes and phospholipids have also been investigated for the systemic absorption of different proteins after intratracheal delivery (Skubitz and Anderson, 2000; Guillaume et al., 2000). The mechanism of absorption enhancement by liposomes may be attributed to the presence of surfactants on the alveolar surface. The lung surfactants consist primarily of DPPC and low amounts of surfactant protein molecules A, B, and C, which undergo rapid recycling (Wright, 1990). The addition of exogenous liposomes hastens the surfactant recycling process in the alveolar cells, leading to enhanced uptake of the protein molecule into the systemic circulation. It has been demonstrated that the ability of liposomes to promote pulmonary protein absorption depends on the concentration, charge, and acyl chain length of the phospholipids (Li and Mitra, 1996).

Cyclodextrins (CD) are cyclic oligomers of glucose and form inclusion complexes with drugs whose molecules can fit into the lipophilic cavities of the cyclodextrin molecule. The potential of cyclodextrins, especially the methylated cyclodextrins, as absorption enhancers of proteins has been demonstrated for luteinizing hormone-releasing hormone (LHRH)

agonist (Matsubara et al., 1995), granulocyte colony stimulating factor (G-CSF) (Watanabe et al., 1995), and adrenocorticotrophic hormone analogue (Schipper et al., 1993). Cyclodextrins may have a direct disruption effect on alveolar epithelial membrane but the mechanisms involved are not fully elucidated (Hussain et al., 2004). The rank order of effectiveness of these agents in promoting transmucosal protein transport was found to be dimethyl- β -CD > α -CD > β -CD > γ -CD > hydroxypropyl- β -CD (Shao et al., 1994). The order of toxicity also followed a similar pattern, with dimethyl- β -CD being most toxic to the mucosal membrane (Shao et al., 1992).

Various other agents have also been tested as absorption enhancers for proteins, such as lanthanides ions and low molecular weight amino acids (hydroxy methyl amino propionic acid or HMAP), mainly for the delivery of insulin (Shen et al., 2000; Suarez et al., 2001)

Fusion proteins

Several studies have aimed to improve lung absorption of a protein by favouring transcytosis. The idea is to combine or merge the protein of interest with another protein that has specific receptors in the epithelium. In an in vitro study on alveolar epithelial cells monolayers, the binding of a peroxidase with a transferrin using a disulfide bridge was shown to increase endocytosis of the peroxidase using the transferrin's receptors. In the same study, adding brefeldin A (an antibiotic that affects the intracellular transport of proteins) to the system then produced an increase in the amount of peroxidase effectively absorbed by transcytose (Deshpande et al., 1994). More recently, the use of fusion proteins with the Fc domain of IgG immunoglobulin has been extensively investigated. The first molecule to be tested was erythropoietin (Epo), which is a cytokine used in the clinical treatment of anemia to stimulate erythropoiesis in the bone marrow, e.g. in patients with end-stage renal failure and with cancer. Due to its large molecular weight (epoetin α : MW: 14700 Da; epoetin β , γ , δ , ϵ , ω : MW: 18200 Da), the pulmonary absorption of Epo without absorption enhancement is low (Siekmeier and Scheuch, 2009). A novel drug delivery system has been developed that utilises a naturally occurring receptor known as the neonatal Fc receptor (FcRn). The receptor is specific for the Fc fragment of IgG and is expressed in epithelial cells, where it functions to transport immunoglobulins across these cell barriers. It

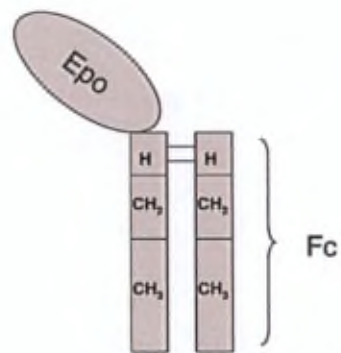


Figure 17. Composition of the EpoFc fusion protein comprised of full-length human erythropoietin fused recombinantly to the Fc domain of human IgG1 (Bitonti and Dumont, 2006)

has been shown that FcRn is expressed in both the upper and central airways in non-human primates as well as in humans. Pulmonary delivery of an erythropoietin-Fc fusion molecule (EpoFc, **Figure 17**) has been demonstrated in non-human primates using this FcRn pathway, with absolute bioavailability reaching 35% vs. 15% for inhaled Epo delivered alone (Bitonti et al., 2004). A phase I clinical study showed dose-dependent concentrations of the fusion protein in the serum, and an increase in circulating reticulocytes was evident in the highest dose group (Dumont et al., 2005). This demonstrates that large therapeutic molecules can be delivered to humans via the lung with retention of biological activity, using the FcRn-mediated transport pathway. Interestingly, the expression of the FcRn receptor is significantly more apparent in the epithelial cells of the upper and central airways than in those found in the lung periphery. In accordance with this, when the fusion protein was deposited in the lung periphery (small aerosol particle size and deep breathing), poor absorption was obtained in comparison with EpoFc administered with larger aerosol particle size and shallow breathing. The use of Fc-fusion proteins for systemic delivery could therefore require particles with aerodynamic diameters in the range of 4-6 μm instead of the usually recommended range of 1-3 μm (Bitonti and Dumont, 2006).

Delivery of other Fc-fusion proteins, such as interferon- α -Fc, interferon- β -Fc, and FSH-Fc, has been achieved, with promising results concerning retention of biological activity and increased circulating half-life (Bitoni and Dumont, 2006).

Protease inhibitors

In the lung, various enzymes, especially peptidases and proteases, degrade macromolecules by proteolysis. Addition of a protease inhibitor to the formulation can therefore be used to protect the protein and consequently increase its absorption and bioavailability (Siekmeier and Scheuch, 2009). The amount of absorption enhancement will typically rely on what enzyme the protease inhibitor inhibits (i.e. serine inhibitor, aminopeptidase inhibitor, etc.) as well as the specific vulnerabilities of the peptides that are being delivered. Some of the various protease inhibitors investigated have included nafamostat mesilate, bacitracin, soybean trypsin inhibitor, chymostatin, potato carboxy peptidase inhibitor (pCPI),

phosphoramidon, antipain, leupeptin, bestatin, foroxymithin, amastatin, and aprotonin. Nafamostat mesilate, which has been studied as an absorption enhancer for insulin, strongly inhibits a variety of proteases such as trypsin, plasmin, and kallikaren (Hussain et al., 2004). Studies have shown that when nafamostat was co-administered with insulin, the relative bioavailability of insulin was approximately twice that obtained when the peptide was administered alone, while bacitracin did not affect the bioavailability of insulin (Okumura et al., 1992). On the other hand, bacitracin has been shown to inhibit the activities of aminopeptidases such as trypsin and chymotrypsin in the pulmonary delivery of gonadorelin and buserelin (Raehs et al., 1988).

II.2.2.2. Maintaining protein stability

Protein drugs are very sensitive molecules that can undergo, in addition to enzymatic degradation, many physical and chemical degradations occurring during either processing or long-term storage of the formulation. These degradations can affect the primary, secondary, and/or tertiary structure of the molecule, possibly leading to partial or total loss of activity, or safety issues (e.g. immunogenicity caused by degradation products). Common degrading conditions include exposure to heat, freezing, light, pH extremes, agitation, shear stress, some metals, and organic solvents (Wang, 2005). It is important to note that all the degradation mechanisms described below can occur to proteins in both the liquid and the dry state. The type and extent of degradation involved is very dependent on the individual protein characteristics (hydrophobicity, presence of particular amino-acids or amino-acid sequences) and on the environmental conditions (concentration, pH, temperature, and various other processing or storage stresses). However, the extent of the degradation is generally limited by formulating the protein in the dry state (see II.2.2.2.2.).

II.2.2.2.1. Degradation mechanisms

The degradation mechanisms of proteins can be divided into two classes: chemical and physical. Chemical degradation involves the covalent modification of the primary structure via bond cleavage or formation. It includes thiol-disulfide exchanges, deamidation, oxidation,

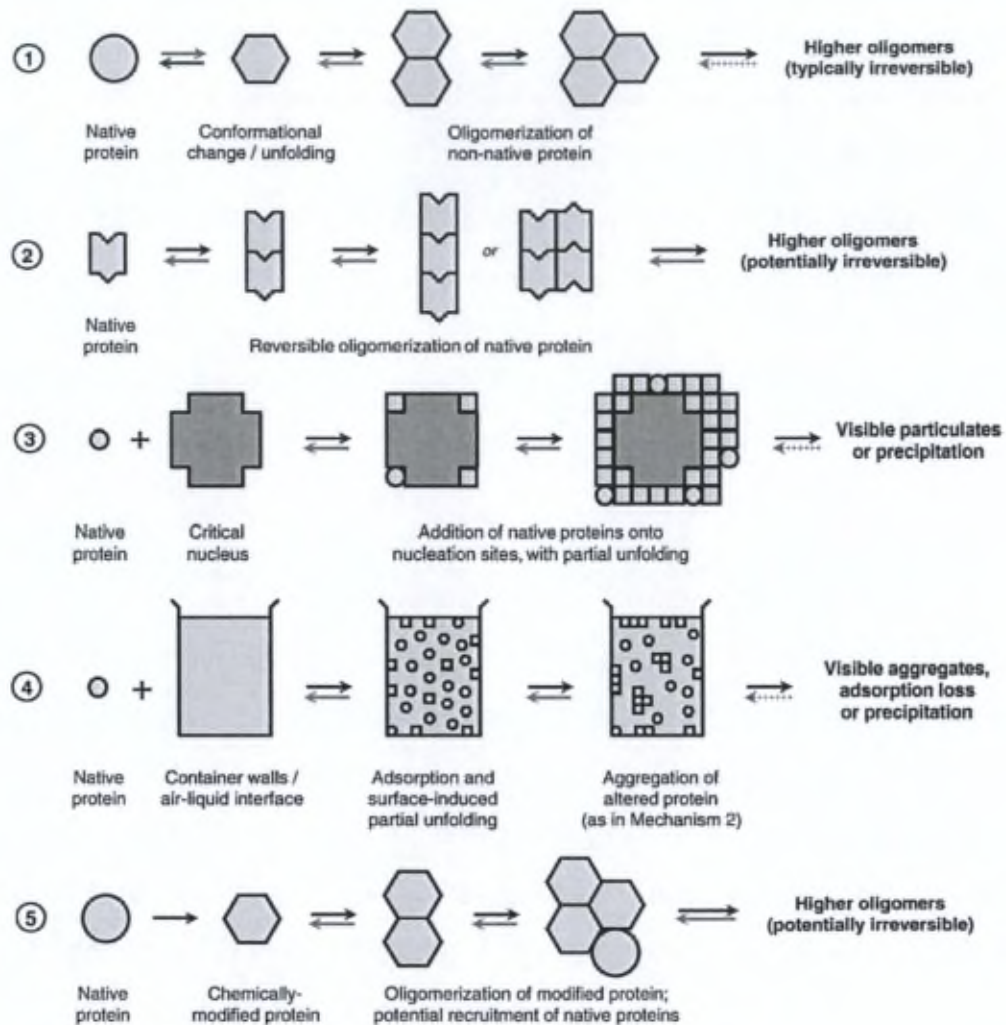


Figure 18. Schematic illustration of five common mechanisms of aggregation (Lee et al., 2011a). Multiple mechanisms may be at work in any given system

and glycation reactions. Physical degradation refers to changes in higher order structure (secondary and tertiary) by denaturation, and to noncovalent aggregation. Both denaturation and aggregation may be reversible changes. As an example, IgG antibodies have been observed to form reversible soluble aggregates in high concentration solutions due to the contribution of electrostatic interactions and hydrogen bonds (Lee et al., 2011a). Similarly, insulin aggregation is generally considered reversible at room temperature near its isoelectric point. This can be attributed to electrostatic interactions due to the marked charge anisotropy of the polypeptide (Lee et al., 2011a). However, aggregation is more often an irreversible phenomenon (Chang and Pikal, 2009). Protein aggregation is the most common manifestation of protein instability, encountered in almost all stages of protein drug development (Wang, 2005).

II.2.2.2.1.1. Physical instability

Denaturation/non-covalent aggregation

In general, hydrophobic residues are buried in the interior of a folded globular protein. Denaturation refers to the unfolding of this globular folded structure. The tertiary structure, and frequently the secondary structure, of proteins is then lost, at least in part (Chang and Pikal, 2009). Protein unfolding is a cooperative transition between the native and unfolded states of a protein, which may proceed through several intermediate states. There is overwhelming evidence that protein folding/unfolding intermediates are precursors in protein aggregation (**Figure 18, scheme 1**) (Fink, 1998; Wang, 2005), even though the intermediates are usually not stable and are poorly populated (Murphy et al., 1992; Wang, 2005). Transient surface exposure of hydrophobic domains can indeed lead to protein–protein contacts that hide these surfaces in a more energetically favorable manner. The consequence of these events is the stabilisation of these protein–protein contacts with the ultimate outcome of dimerisation, trimerisation, and further extended aggregation events. Association of a large number of monomers generally leads to precipitation of the aggregate (insoluble aggregates). The probability of energetically favorable contacts leading to aggregation generally increases with protein concentration and temperature (Daugherty and

Mrsny, 2006). It is to be noted that completely folded or unfolded proteins do not lead to aggregates as easily as intermediates because the hydrophobic side chains are either mostly buried away from contact with water or are randomly scattered (Uversky et al., 1999). However, aggregation of proteins from native monomers can also occur, forming reversible aggregates, especially in high concentration formulations, which is due to the surface-active properties of the protein. If protein concentration increases or time passes, the protein complex may become an irreversible aggregate (**Figure 18, scheme 2**) (Lee et al., 2011a). In contrast to the previous aggregation mechanisms, which are based on interactions between individual protein molecules, protein aggregation can also be attributed to a nucleation-dependent process. It is initiated when a “critical nucleus” is formed in solution, and native proteins are recruited, and often partially unfolded, to form aggregated species (**Figure 18, scheme 3**). A “lag phase” (often weeks or months) is characteristic of this mechanism. During this lag phase, the seed nucleus grows but no particles or precipitation can be observed. After the formation of a critical nucleus, the aggregation progresses rapidly, with the relatively sudden formation of visible aggregates or precipitates in solution. These nuclei may be denatured proteins, or solid contaminants (e.g. particles of silica from vials or metal from pumps). Finally, another common aggregation mechanism is surface-induced aggregation, in which native proteins first adsorb to an interface, after which they undergo conformational changes or partial unfolding (**Figure 18, scheme 4**). The resulting non-native conformation then serves as a starting point for aggregation (Lee et al., 2011a).

II.2.2.2.1.2. Chemical instability

Covalent aggregation

The most common covalent aggregation is through intermolecular thiol-disulfide exchange, which may occur for proteins containing both free thiol and disulfide bonds, such as bovine serum albumin (BSA) and recombinant human albumin (rHA) (Liu et al., 1991; Chang and Pikal, 2009). During this process, the (ionised) thiol of one albumin carries out a nucleophilic attack on a disulfide linkage of another albumin molecule. The result is a new intermolecular disulfide bond with conservation of the free thiolate ion. A further propagation of this process leads to high molecular weight aggregates, which are generally insoluble. These

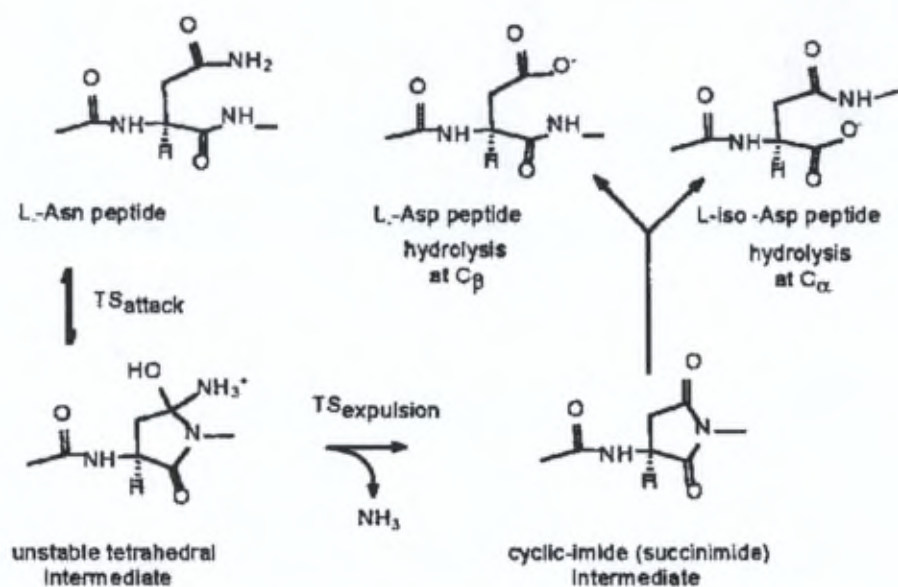


Figure 19. The mechanism of the Asn deamidation reaction at neutral and basic pH (Xie and Schowen, 1999). The Asn-containing peptide (top left) undergoes a base-catalysed nucleophilic attack at the backbone NH centre C-terminal to Asn on the side chain amide carbonyl. This step, passing through the transition state, TS_{attack} , leads to formation of the tetrahedral intermediate, an unstable species that never accumulates to observable concentrations. This unstable intermediate expels ammonia irreversibly in the transition state, $TS_{\text{expulsion}}$, to generate the more stable cyclic imide intermediate (bottom right). This species accumulates to observable levels in the pH region 4-5, but decomposes as rapidly as it forms at higher pH. The cyclic imide undergoes hydrolytic attack at both carbonyl centers, leading to the aspartic acid (Asp) product and the iso-aspartic acid (iso-Asp) product (upper right)

aggregates may also recruit native proteins by adsorption (**Figure 18, scheme 5**). Using methods such as lyophilisation from acidic pH or chemically blocking the free sulfhydryl groups, one can make it difficult for the thiol-disulfide interchange reaction to occur (Liu et al., 1991). It is to be noted that chemical modification such as oxidation and deamidation may also cause aggregation by altering protein properties such as solvent accessibility of hydrophobic patches, reduction in electrostatic repulsion due to modification of charged residues, or disruptions of the native structure that trigger unfolding (Lee et al., 2011a).

Deamidation

Deamidation is the hydrolysis of a side chain amide on glutamine or asparagine residues to yield a carboxylic acid (**Figure 19**) (Chang and Pikal, 2009). Deamidation stability problems nearly always involve asparagine residues. Non-enzymatic parameters of asparagine and glutamine deamidation in proteins have been defined in detail for factors such as pH, temperature, and ionic strength (Robinson and Robinson, 2004). In general, deamidation events appear to be relatively slow but are accelerated by unfolding of the protein (Chelius et al., 2005). Deamidation also depends on the primary sequence of the protein, which can be explained by a simple steric effect (Robinson and Robinson, 2004). In particular, asparagine–glycine sequences can demonstrate accelerated deamidation rates since glycine residues lack a side-chain structure that would otherwise act to decrease conformation interference for backbone-associated isoaspartyl formation (Radkiewicz et al., 2001).

Oxidation

Methionine and cysteine residues are frequently a site of oxidation in protein drugs. Oxidation of histidine, tyrosine, tryptophan, and phenylalanine residues can also occur (Griffiths, 2000). Factors such as pH, the nature of the buffers (Li et al., 1993), the presence of metal ions and metal ion chelators (Li et al., 1995), and neighbouring amino acid residues (Fransson, 1997) are critical variables in methionine oxidation for both small peptides and large proteins. It is expected that these factors will influence methionine oxidation in solid state as well. Oxidation in the solid state can be minimized by use of certain sugars and polyols such as sucrose, trehalose, lactose, sorbitol and mannitol (Li et al., 1996). It has been

suggested that these sugars may inhibit protein oxidation by complexation with metal ions or by hydrogen bonding to the surface of protein to preserve the native conformation, thereby protecting the buried amino residues from exposure to oxidation.

Glycation

Nonenzymatic glycation of a protein, also called the Maillard reaction, is a result of reducing sugars reacting with basic protein residues such as lysine, arginine, asparagine, and glutamine (Li et al., 1996). Reducing sugars include fructose, maltose, lactose, glucose, and xylose, and the reactivity for each sugar is different (Chang and Pikal, 2009). Even though sucrose is a nonreducing sugar, it is possible for it to hydrolyse into reducing sugars, especially at low pH. The Maillard reaction involves an aminocarbonyl condensation reaction between the carbonyl of a reducing sugar and an amino group to form a Schiff base and a molecule of water (Lai and Topp, 1999). Since water is produced, the material can be plasticized as the reaction proceeds, with a reduction of T_g and a possible increase in aggregation mechanisms. Methods such as removing reactive substrate, adjusting pH, limiting the water content, and maintaining low temperatures are usually used to control the Maillard reaction (Zhang and Zhang, 2007; Chang and Pikal, 2009).

II.2.2.2.2. Formulation strategies

Drying techniques

Proteins produced by recombinant technology are generally provided in solution with addition of stabilizing excipients. As most of the degradation mechanisms are water-mediated, a widely used strategy for protein stabilisation is formulation under the dry state. DPI administration of proteins seems particularly attractive in providing long-term stability of the drug (Daugherty and Mrsny, 2006).

Spray-drying (see IV.1.2.2.1.1.) is the drying process that has received the greatest attention for the production of DPI protein formulations owing to its relative simplicity, cost-

effectiveness, and scalability. Spray-drying also allows the engineering of particles with defined size, shape, surface properties, and density, providing appropriate aerodynamic characteristics for inhalation that cannot be readily achieved with other manufacturing processes. Furthermore, the incorporation of suitable stabilising excipients during spray-drying can help to preserve the integrity of macromolecules and improve the stability of dry powder formulations (Sou et al., 2011). However, drying of proteins is also associated with degradations. The three main sources of protein stress during spray-drying are heat stress, shear stress, and adsorption to the air–water interface during atomisation (Maltesen and van de Weert, 2008). Thermal denaturation is relatively rarely observed for proteins during the spray-drying process because the denaturation temperature of proteins is highly dependent on the water content and increases rapidly as the water is removed during the spray-drying process. Moreover, due to the evaporation process, the surface temperature of a droplet is kept at a temperature that is significantly lower than the drying gas temperature. Nonetheless, thermal stability is highly protein dependent and the drying temperature should be optimised for each protein (Maltesen and van de Weert, 2008). During the atomisation process the protein is also exposed to high shear stress. It is due to spatial differences in fluid velocities within the nozzle (zero velocity at the solid boundary layer). In general this would not cause any major stability issue, but in combination with adsorption to the air–water interface, significant aggregation of interfacially sensitive proteins may be observed (Maa and Hsu, 1996; Webb et al., 2002). Most proteins are amphiphilic and therefore surface active, and thus prone to adsorption at the air–water interface. Upon adsorption, the protein may change conformation, exposing the hydrophobic residues to the air–water interface to avoid contact with water. Interaction between hydrophobic regions may then lead to aggregation and ultimately precipitation. Owing to the rapid and large expansion of the air–water interface during atomisation, denaturation and aggregation at the air–water interface is often the dominant source of protein denaturation in the spray-drying process (Maltesen and van de Weert, 2008).

Freeze-drying (see IV.3.2.2.2.1.) is another drying method, which has routinely been used to dehydrate proteins in parenteral formulations (Tang and Pikal, 2004). Recently, it has also been used to obtain a dry powder for inhalation (Pfützner and Forst, 2005). The main source of protein stress during freeze-drying is associated with the freezing process. The

destabilising effects of freezing are not yet fully explained, but are known to be highly protein dependent. Cold denaturation of proteins is caused by a decrease in hydrophobic effects and the hydration of nonpolar residues and may explain the denaturation of some proteins (Roy and Gupta, 2004). The ice formation and concentration of solutes and proteins also affect protein stability during the freezing process. In particular, increase in ionic strength occurs during ice formation and can generate pH changes that may destabilise proteins (Bhatnagar et al., 2007; Wang, 2000). Furthermore, the cooling rate affects the crystal formation of the water molecules: a slow cooling rate yields larger crystals, whereas a rapid cooling rate enhances the formation of small crystals with a higher specific surface area (SSA). A larger SSA could result in larger protein adsorption to the interface, thereby increasing denaturation and aggregation (Abdul-Fattah et al., 2007). In contrast, a slow cooling rate tends to enhance phase separation between proteins and excipients, which can destabilise the protein. With both spray-drying and freeze-drying, an important issue is dehydration stress. It has been suggested that proteins should not be dried exhaustively, and that certain highly polar residues found on the protein surface should be maintained in the hydrated state to avoid denaturation and aggregation during drying (Hsu et al., 1991; Ma et al., 2001; Ohtake et al., 2011). The residual moisture content of the powder has been proved to be an important factor to control, particularly for the long-term stability of the dry protein powder. Studies have shown that freeze-drying antibodies to a specific percent of residual water (usually between 1% and 8%) allows for optimal stabilisation in the dry state (Breen et al., 2001). Higher and lower moisture content in lyophilised antibody preparations correlates with increased aggregation and asparagine deamidation. On the other hand, the storage stability of spray-dried IgG1/mannitol formulations has been evaluated at different residual moisture levels obtained by vacuum-drying or equilibration prior to storage. It has been found that the lower the residual moisture, the better was the stabilizing capability. Vacuum-drying at 32°C/0.1 mbar for 24 h reduced the moisture level to below 1%, constituting an optimal basis for improved storage stability (Schüle et al., 2008).

Careful selection of the drying process and drying conditions is thus required for both the spray-drying and freeze-drying methods. Addition of stabilising excipients is generally needed to maintain protein native structure during processing and/or for long-term storage of the formulation.

Table IV. Excipients and their stabilising effect for solid state protein preparation and storage (adapted from Pilcer and Amighi, 2010 and from Wang et al., 2012)

Excipient class	Excipient name	Stabilisation mechanism	Status for pulmonary use	Comments
Salts	<i>PBS</i>	Provide a buffering effect during freezing or drying	Na Cl and phosphate buffer approved in Flixotide®	
	<i>HBS</i>		Lack of sufficient data on lung toxicity	
	<i>Citrate</i>		Approved in Exubera® (DPI)	
Surfactants	<i>Tween 80</i>	Prevent protein unfolding/aggregation by exclusion of the protein from the air-liquid or ice/liquid interface	Approved in nebulised formulations (e.g. Pulmicort®)	Biocompatible and biodegradable
	<i>DPPC</i>		Lecithin approved in pMDIs (e.g. Combivent®, Serevent®)	
	<i>Na glycocholate</i>		Lack of sufficient data on lung toxicity, suspected to cause acute inflammation at high concentration (Suzuki et al., 2000)	Mainly investigated for its absorption enhancement properties
Polyols	<i>Mannitol</i>	Formation of a glass matrix (reduced molecular mobility) and/or water replacement effect (H-bonding of the protein with the hydroxyl groups of the stabiliser)	Approved in Exubera® (DPI)	Low T _g ; high concentration of mannitol displays increased crystallisation tendency, same is true at elevated temperature and moisture level
	<i>Sorbitol</i>		Lack of sufficient data on lung toxicity	Low T _g
Non-reducing sugars	<i>trehalose</i>			High T _g around 120°C, good water replacement property, but formation of sticky agglomerates
	<i>Sucrose</i>			Good water replacement property but fairly hygroscopic
	<i>Inulin</i>			High T _g , low crystallisation rate but weak water replacement property and contains a low number of reducing groups
	<i>Dextran</i>			
Reducing sugars	<i>Fructose</i>		Reducing sugars, potential for Maillard reaction that causes protein glycation, moisture-induced crystallisation	Approved in Bronchodual® (DPI)
	<i>Glucose (dextrose)</i>			
	<i>Lactose</i>	Approved and commonly used		
	<i>Maltodextrin</i>			
	<i>Maltose</i>			
Amino acids	<i>Histidine</i>	Water replacement effect	Lack of sufficient data on lung toxicity	Endogenous substances
	<i>Arginine</i>			
	<i>Alanine</i>			
	<i>Isoleucine</i>			
	<i>Glycine</i>		Approved in Exubera® (DPI)	Endogenous substances; hydrophobic properties that benefit the powder flow property

Stabilising excipients

The first step in optimising the protein's environment for both liquid and solid protein pharmaceuticals is to select a good buffering agent at a proper concentration to control the formulation pH. Most proteins are indeed stable in a narrow pH range (Fatouros et al., 1997), and the aggregation behavior of proteins can significantly vary in different buffer systems (Narhi et al., 1999) and at different buffer concentrations (Won et al., 1998). It should be noted that the pH of a protein solution for preparation of a solid formulation may affect the aggregation of proteins in solid states during storage. This is to say that the solid-state "acidity/basicity" may still affect protein aggregation, both physically and chemically (Wang, 2005). Therefore, the pH of a protein solution before drying may have to be carefully determined to prevent or inhibit protein aggregation during storage of the dried product. Such examples have been reported in the storage of lyophilised proteins such as RNase (Townsend et al., 1990), or recombinant human albumin (rHA) (Costantino et al., 1995a, 1995b).

The next step in protecting solid proteins from aggregation during storage is to select a suitable protein stabiliser(s). An overview of the various classes of stabilising excipients used in dry protein formulation is presented in **Table IV**. Examples of studies investigating the influence of these excipients on protein aggregation can also be found in **APPENDIX IV**, along with the excipient concentrations used,

Surfactants are often used to prevent protein adsorption at the air–water or ice–water interface during drying, and therefore circumvent unfolding and aggregation (Adler et al., 2000; Webb et al., 2002). Non-ionic surfactants seem particularly appropriate for pulmonary use due to their low potential mucosal toxicity. As an example, when 1 mg/ml solution of IL-1Ra was freeze dried with 0.1% polyoxyethylene sorbitan monooleate (Tween 80), less than 3% soluble aggregates was detected, while in the absence of the surfactant, approximately 50% of the protein was observed to form soluble aggregates (Chang et al., 1996a). In a study to minimise aggregation of recombinant human growth hormone (rhGH) during spray-drying, it was reported that insoluble aggregate formation decreased as polysorbate concentration was increased. The aggregate level reached a plateau at a certain critical

polysorbate concentration (cpc), which was independent of the protein concentration but was directly proportional to the air–water interfacial area, thus demonstrating that insoluble aggregate formation was linked to denaturation of rhGH at the air–water interface (Maa et al., 1998). The same protective effect by avoidance of surface denaturation has also been suggested for DPPC. It was indeed shown that albumin particles spray-dried with DPPC and a sugar stabiliser exhibited a surface enrichment in DPPC (Bosquillon et al., 2004).

The inclusion of **saccharides** or **polyols** in formulations of solid-state proteins has also been demonstrated to enhance stability of proteins (Chang and Pikal, 2009; Sou et al., 2011). In many cases, one excipient can serve to stabilise against various degradations. For example, sugars and polyols not only stabilise proteins against denaturation and aggregation, but also stabilise them against chemical degradation (Pikal et al., 1991; Li et al., 1996b; Cleland et al., 2001). Sugars and polyols stabilise macromolecules via two main mechanisms. Firstly, the glass-forming ability of these excipients stabilises the protein by trapping it in a rigid, amorphous glass matrix with high glass transition temperature (T_g) (Sou et al., 2011). This results in the separation of the protein molecules (dilution effect) and prevents significant motion, which leads to the preservation of the protein tridimensional structure (Chang and Pikal, 2009).

Secondly, these excipients can form hydrogen bonds with proteins in the dry solid state to replace the hydrogen bonds that water forms with proteins in solution to stabilise the tridimensional structure (Weers et al., 2007; Vehring, 2008; Chang and Pikal, 2009).

Common stabilising excipients include sucrose, trehalose, mannitol, and inulin (Wang, 2005; Vehring, 2008; Chang and Pikal, 2009). As an example, formulation efforts were made to produce fine dry powder particles of an anti-IgE monoclonal antibody in the size range desired for delivery to the lung (Costantino et al., 1998). This study showed the usefulness of mannitol as a protective excipient in spray-dried antibody formulations and that mannitol can play a role both in maintaining protein stability and in producing a suitable aerosol preparation. Further studies to assess carbohydrate excipients for spray-dried antibody aerosol formulations showed that excipient to protein ratios were critical (Andya et al., 1999). Carbohydrates are also attractive as freeze-drying excipients because they can be easily vitrified during freezing (T_g values of disaccharides and higher oligomeric sugars lie above $-30\text{ }^\circ\text{C}$) (Franks, 1998).

Small amino acids (particularly glycine, isoleucine, alanine, histidine, and arginine) have also been used as stabilisers, although there are limited reports on the effects of or understanding of the mechanisms involved in solid state stabilisation (Chen et al., 2003; Sane et al., 2004; Tian et al., 2007). To improve the solid state stability of a protein, the amino acid would need to be present in the same amorphous phase as the protein (Mattern et al., 1999; Daugherty and Mrsny, 2006; Tian et al., 2006). In a series of amino acid formulations, a good correlation was found between the structural changes of an antibody upon drying and its long-term storage stability (Sane et al., 2004; Tian et al., 2007). The data suggest that the amino acids can interact (i.e., hydrogen-bond) with the protein during drying to preserve the native protein structure in the dried state (Tian et al., 2006). Therefore, the long-term storage stability of protein is improved via the “water substitution mechanism”, as described above (Chang and Pikal, 2009).

It is important to note that the development of protein formulations for inhalation is limited by the small number of excipients that are currently approved for inhalation by the Food and Drug Administration because of the lack in toxicity studies conducted with inhaled excipients. Nowadays, the accepted excipients are sugars (lactose, mannitol and glucose) and, in much lower proportions, magnesium stearate, buffering agents (NaCl, HCl, Na citrate, Na phosphate, citric acid, tartaric acid, trometamol), surfactants (sorbitan esters, polysorbates, oleic acid and soya lecithin), and preservatives (Cl benzalkonium, EDTA and parabens) (Pilcer and Amighi, 2010). Nevertheless, most of these excipients are accepted for nebulisation and MDI formulations and some of them might not be used in DPI development due to their low melting point or their semi-solid or liquid state.

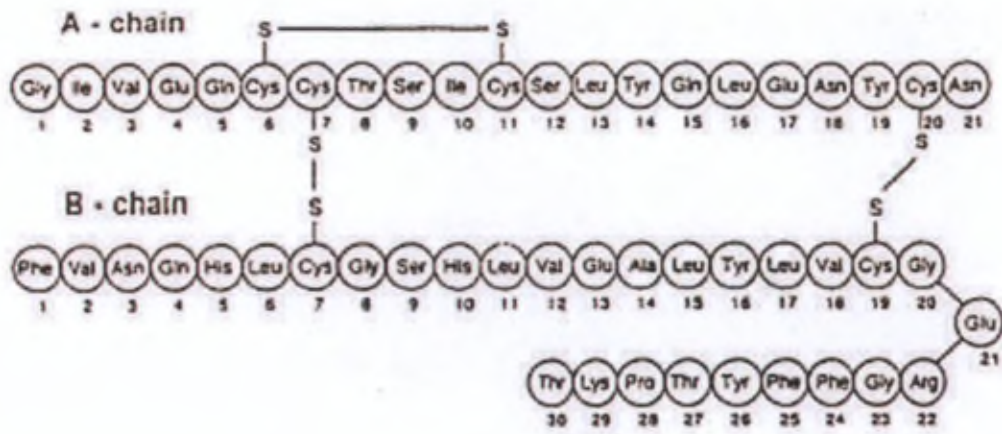


Figure 20. Structure of the human insulin molecule (Exubera SPC, 2007)

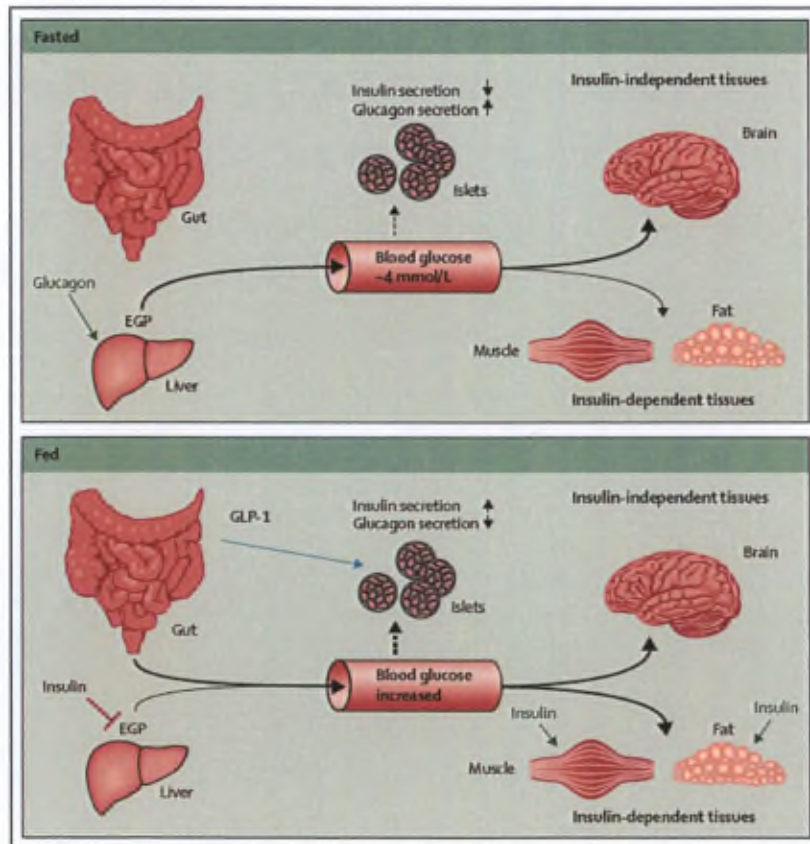


Figure 21: Overview of normal glucose homeostasis (Nolan et al., 2011). GLP-1: glucagon-like peptide, EGP: endogenous glucose production

II.3. Diabetes Mellitus: an application for systemic pulmonary delivery of protein

II.3.1. Insulin in Diabetes Mellitus

Human insulin is a peptide hormone composed of 51 amino acids and has a molecular weight of 5808 Da (**Figure 20**). It is synthesised in the endocrine portion of the pancreas, within the β -cells of the islets of Langerhans (Steiner and Oyer, 1967). Insulin is mainly involved in maintaining glucose homeostasis (**Figure 21**). The blood content of insulin can be measured in international units, such as $\mu\text{U}/\text{mL}$ or in molar concentration, such as pmol/L , where $1 \mu\text{U}/\text{mL}$ equals $6.945 \text{ pmol}/\text{l}$ (Rowlett, 2005). A typical blood level between meals is $8\text{--}11 \mu\text{U}/\text{ml}$ ($57\text{--}79 \text{ pmol}/\text{l}$) (Iwase et al., 2001). After an oligosaccharide-rich meal, a serum insulin peak occurs about 30 min after the meal, and a return to baseline is achieved in up to 3 h (**Figure 22**) (Westphal et al., 2004; Suckale and Solimena, 2008).

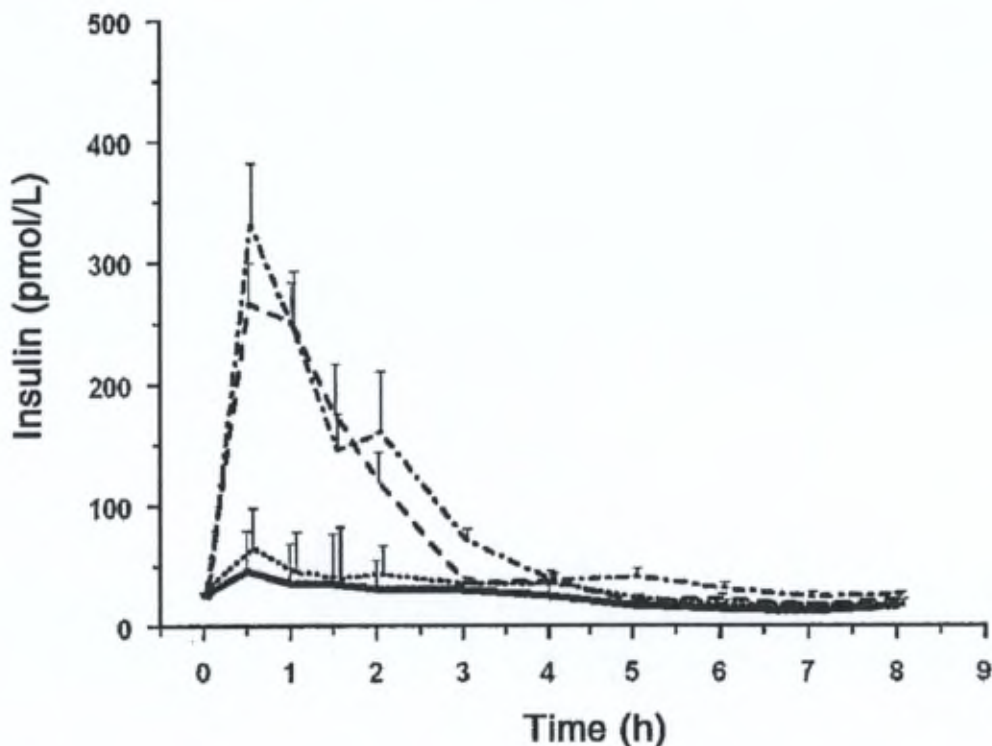


Figure 22. Mean (\pm SEM) postprandial concentrations of insulin in serum in 24 normolipidemic subjects after 4 different meals. 1) 1 g fat/kg b.w. (continuous line), 2) fat combined with 75 g oligosaccharides (broken line), 3) fat combined with 50 g sodium caseinate (dotted line), and 4) fat combined with oligosaccharides and caseinate (dot-dash line) (Westphal et al., 2004)

Table V. Incidence Rates of Diabetes-Related Complications. All complication rates (per 1000 patients) are reported at the 95% confidence interval (McAlpine et al., 2005).

Complication	Type 1 DM	Type 2 DM
Angina	8.8	38.4
Myocardial infarction	8.6	21.9
Cerebrovascular accident	1.1	3.1
Lower-extremity amputation	3.2	3.1
Peripheral vascular disease	5.5	13.6
Registered blindness	1.1	1.6
End-stage renal disease	6.4	5.0
Mortality	14.6	50.0

Diabetes Mellitus (DM) is a highly heterogeneous disease characterised by chronic hyperglycemia with disturbances of carbohydrate, fat, and protein metabolism resulting from defects in insulin secretion, insulin action or both. DM currently affects about 285 million adults worldwide, and this number is expected to increase to 439 million adults by the year 2030. It is the fifth leading cause of death in the United States (Shaw et al., 2010). Diagnosis is based on a value of the fasting plasma glucose concentration over 7 mmol/l (126 mg/dl) (Alberti and Zimmet, 1998). A glycosylated haemoglobin (HbA1C) percentage over 6.5% is also used as a diagnosis factor and provides an indication of the average plasma glucose concentration over prolonged periods of time (American Diabetes Association, 2011). The effects of diabetes mellitus include long-term damage to various organs resulting in microvascular and macrovascular complications, and an increased morbidity (**Table V**) (Patton et al., 1999; McAlpine et al., 2005). Several pathogenetic processes are involved in the development of diabetes, leading to its classification as either type 1 or type 2 DM. Among diagnosed patients, 90% to 95% have type 2 diabetes, while 5% to 10% have type 1 diabetes (Jonas et al., 2011).

Treatment of both type 1 and type 2 diabetes mainly aims at reducing blood glucose levels. A preprandial glucose value of 70–130 mg/dl (3.9–7.2 mmol/l), and a postprandial value below 180 mg/dl (< 10 mmol/l) are recommended to reach a target value of HbA1c < 7% in nonpregnant adults to prevent adverse microvascular outcomes (American Diabetes Association, 2011). For type 1 diabetic patients, administration of exogenous insulin is the only current treatment option for achieving this goal. Type 2 diabetes is initially managed by increasing exercise and dietary modification. If the condition progresses, glycemic control for type 2 DM can be achieved by medication with metformine (biguanide), sulfonylureas, thiazolidinediones (or glitazones), glinides, alpha-glucosidase inhibitors, dipeptidyl peptidase-4 (DPP-4) inhibitors, GLP-1 analogs, and insulin. It is estimated that more than 50% of persons with type 2 diabetes will require more than one oral hypoglycemic agent after 3 years from diagnosis and approximately 70% will require combination oral therapy, with or without insulin, 6 to 9 years from diagnosis (Jonas et al., 2011).

The benefits of tight glycemic control through the administration of exogenous insulin were shown in the landmark Diabetes Control and Complications Trial (DCCT) and the United Kingdom Prospective Diabetes Study (UKPDS) in patients with type 1 and type 2 DM,

Table VI. Action profile and composition of parenteral insulin preparations
(Robertson et al., 2003; Skyler, 2004; Heinemann, 2004)

Preparation	Time of action			Composition
	Onset (h)	Peak (h)	Duration (h)	
<i>Short-acting insulin</i>				
Regular	0.5-1.0	2-3	6-10	Soluble hexameric human insulin (+ 0.4% zinc)
<i>Rapid-acting insulin analogues</i>				
Lispro	0.25-0.5	0.5-1.5	2.5	Soluble human insulin with reversed proline and lysine at positions 28 and 29 of the B-chain
Aspart	0.25-0.5	0.5-1.5	2-5	Soluble human insulin with proline substituted with asparaginic acid at position 28 of the B-chain
Glulisine	0.25-0.5	0.5-1.5	2-5	Soluble human insulin with asparagine at position 3 of the B-chain replaced by lysine and lysine in position 29 of the B-chain replaced by glutamic acid
<i>Long-acting insulins</i>				
NPH	1-4	6-10	10-16	Human insulin suspension with 0.016 to 0.04 mg zinc, and 0.4 mg protamine per 100 U insulin
Lente	3	7-9	14-20	Human amorphous and crystalline insulin suspension with zinc excess
Ultralente	2-4	8-14	> 24	Human crystalline insulin suspension with zinc excess
<i>Long-acting insulin analogues</i>				
Glargine	1-4	/	20-24	Human microcrystalline insulin suspension with asparagine substituted with glycine at position 21 of the A-chain and two arginines added to the carboxy terminal of B-chain
Detemir	1-4	/	16-20	Soluble human insulin with acylation of the amino acid at position 29 of the B-chain with a 14-C fatty acid and removal of the amino acid at position 30 of the B-chain
<i>Premixed insulins or insulins analogues</i>				
70/30 – 70% NPH, 30% regular insulin	0.5-1	3-12	10-16	
50/50 – 50% NPH, 50% regular insulin	0.5-1	2-12	10-16	
75/25 – 75% protamine lispro, 25% lispro	0.2-0.5	1-4	10-16	
70/30 – 70% protamine aspart, 30% aspart	0.2-0.5	1-4	10-16	
50/50 – 50% protamine lispro, 50% lispro	0.2-0.5	1-4	10-16	

respectively. An “intensive” insulin therapy is generally prescribed, which consists of near-physiologic dosing with administration of long-acting/continuous insulin (basal insulin) and pre-meal boluses. It is accomplished by daily or twice-daily administration of long-acting insulin or insulin analogue, and pre-meal administration of short-acting insulin (regular insulin) or very rapid-acting insulin analogue. The doses are determined by the pre-meal glucose level, the composition of the impending meal, and the level of impending activity (Guntur and Dhand, 2007). The pharmacodynamic profiles of the different types of parenteral insulin preparations are summarised in **Table VI**.

II.3.2. Place of inhaled insulins

A recent report (Cheung et al., 2009) indicates that in the United States only 57% of diabetic adults achieve the treatment goal of less than 7% HbA1c. An important cause of this poor glycemic control is the difficulty in achieving plasma insulin profiles that resemble the natural prandial insulin secretion, despite the broad variety of s.c. insulins available (American Diabetes Association, 2011). Current s.c. insulin therapies do not provide the optimal pharmacokinetic profile. The absorption of regular human insulin is indeed too slow and its action is too prolonged to mimic early insulin release effectively. Rapid-acting insulins still have a relatively slow onset of action compared with prandial glucose absorption. In addition, these injected formulations present an intra-patient variability in the starting time of insulin action of up to 30% (Richardson and Boss, 2007). This is mainly due to the absorption rate from the s.c. depot, which depends on the insulin concentration, injection volume, and injection site, as well as on endogenous factors such as skin temperature, local blood flow, muscle activity, and thickness of the subcutaneous fat layer (Heinemann, 2004). The ideal prandial insulin would therefore have a pharmacokinetic profile that closely matches the body’s normal insulin response to a meal. It should have onset of action below 30 min after administration, high maximal activity, a duration of action below 4 h, and high reproducibility (Heinemann, 2004).

In recent years, several attempts have been made to develop insulin formulations that more closely meet these clinical requirements. Inhaled insulins seem particularly promising, as many formulations for pulmonary delivery exhibit pharmacokinetic profiles with fast

absorption rates. The pharmacokinetic (PK) and pharmacodynamic (PD) profiles of the inhaled insulin formulations that have reached advanced clinical evaluation are presented in **II.3.2.2**. In addition to the PK/PD considerations, this type of formulation might address compliance problems observed with s.c. insulin treatments, in particular when multiple daily injections are required or in type 2 diabetic patients, who often require insulin later in life (Pfützner and Forst, 2005).

II.3.2.1. Insulin absorption through alveolar epithelium

Mechanisms

Insulin is a peptide with a molecular weight of 5.8 kDa and an average size of between 2.2 and 2.6 nm (Patton, 1996). In the case of small proteins, both paracellular and transcellular routes may be involved in alveolar epithelial transport (Ikehata et al., 2009). Insulin is mainly absorbed by paracellular transport. It has indeed been reported that the P_{app}^1 of insulin in human primary cultured alveolar type I-like epithelial cells is comparable to that reported for dextran (4000 Da), and that no asymmetry in bi-directional permeability occurred. This indicates that a specific, transcellular transport process is not involved (Bur et al., 2006). However, it is to be noted that several studies also reported a transcellular transport of insulin but these used rat cells models (Orlando et al., 1998; Kolleck et al., 2002; Ikehata et al., 2009). The existence and extent of transcellular absorption of insulin in man has to be further investigated.

Absorption enhancement

The bioavailability of insulin after pulmonary deposition can be enhanced by a number of compounds, increasing its absorption or inhibiting proteolytic degradation.

APPENDIX V compiles the absorbance enhancing effect of various compounds and demonstrates that the intensity of their pharmacological effect depends on their type (e.g., different cyclodextrins and lanthanides) and their administered dose (e.g., sodium

¹ $P_{app}(\text{cm/s}) = (dQ/dt) (1/AC_0)$, where dQ/dt is the solute transfer rate, A is the membrane area, and C_0 is the initial solute concentration.

taurocholate and sodium glycocholate). However, it should be recalled that the toxicity of absorption enhancers often correlates with the strength of their pharmacological effect. This limits their clinical use, especially for a prolonged duration of treatment, which is necessary for patients with diabetes (Siekmeier and Scheuch, 2008). The majority of data was obtained in rats only, whereas results from other mammals or human studies are available for a few compounds only. Among the most relevant examples, citric acid or citrate buffering were found to increase effectively the hypoglycemic effect of insulin dry powders and insulin solutions administered in rats. Citric acid might decrease local pH in the lungs, which could increase the content in insulin monomers at the absorption site. Lower pH may also change the integrity of the epithelium membrane of the lungs and/or suppress enzyme activity for insulin degradation in alveolar epithelium and phagocytic activity of alveolar macrophages. Concerning the potential toxicity of citric acid, the lactate dehydrogenase activity, which is a sensitive indicator of acute toxicity in lung cells, was measured in the bronchoalveolar lavage and was as low as that observed after saline administration. Thus, citric acid appears to be a safe and potent absorption enhancer for insulin (Todo et al., 2001). It is included in the formulation of the Exubera® inhaled insulin (see II.3.2.2.1.). However, in this formulation citric acid is not claimed to be an absorption enhancer but serves as a buffering and stabilising agent.

The combination of sodium taurocholate with a powder insulin aerosol was also investigated in healthy individuals (Heinemann et al., 2000). Only a small increase in bioeffectivity was observed in comparison with powder insulin administered alone ($12.0 \pm 3.5\%$ vs. $7.6 \pm 2.9\%$). In contrast, a strongly increased bioavailability of insulin in dogs was observed if the substance was administered as a liquid aerosol - also containing taurocholate (taurocholate vs. control; $23.2 \pm 4.4\%$ vs. $2.6 \pm 0.3\%$) (Johansson et al., 2002).

The bioavailability and pharmacological activity of insulin can also be improved by addition of protease inhibitors preventing their inactivation by proteolytic cleavage. For example, selected protease inhibitors showed increased permeability of insulin across the rabbit trachea, with efficacies in the order di-peptidylaminopeptidase IV > leu-aminopeptidase > cathepsin B > trypsin (Morimoto et al., 2000). Another in vitro study demonstrated an inhibitory effect of the protease inhibitors bacitracin, aprotinin, soybean trypsin inhibitor, and sodium glycocholate on the degradation of insulin in lung homogenate in descending order (Fukuda et al., 1995). However, the antiproteolytic properties of these compounds on

insulin after tracheal or pulmonary administration were up to now only the subject of a few animal studies and not introduced into clinical investigations (Siekmeier and Scheuch, 2008).

Patient-related variability

It is important to note that some patient-related factors can also influence the absorption of inhaled insulin, such as asthma, COPD, and smoking. In clinical trials with the AERx® IDMS and Exubera® inhaled insulins, diminished absorption (with higher intra-subject variability) was seen in non-diabetic patients with mild to moderate asthma when compared with subjects with normal pulmonary function (Henry et al., 2003; Exubera® SPC, 2007). The absorption of inhaled insulin is also reduced in people with moderate COPD in comparison to healthy subjects (Rave et al., 2007a). Because of these findings, inhaled insulin should be contraindicated in patients with poorly controlled, unstable or severe asthma, or severe COPD.

A number of clinical trials investigated the impact of smoking, including smoking cessation and subsequent resumption, on inhaled insulin. These trials, with different inhaled insulin preparations, consistently showed that smoking substantially increased the rate and extent of absorption of inhaled insulin relative to non-smokers (three- to five-fold higher C_{max} and two- to three-fold higher AUCs) (Himmelman et al., 2003; Becker et al., 2006; Arnolds and Heise, 2007). The increase in bioavailability was dependent on the time interval between smoking and insulin inhalation: 'non-acute smoking' (last cigarette the day before inhalation of insulin) led to maximum insulin levels whereas 'acute smoking' (three cigarettes immediately before inhalation of insulin) increased absorption of inhaled insulin to a much lesser extent. As bioavailability also changes when smoking is stopped or resumed, inhaled insulin is contraindicated in smokers.

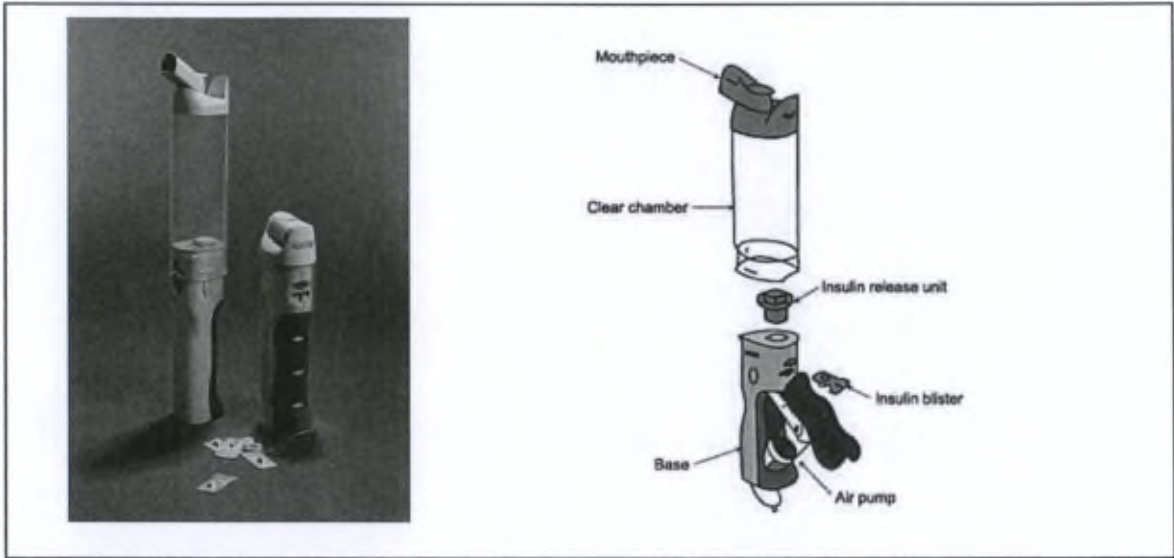


Figure 23. The Exubera® Dry Powder Inhaler (adapted from Strack, 2006 and Biotech, 2011)

II.3.2.2. Examples of inhaled insulins

II.3.2.2.1. Exubera®

Exubera® (Nektar Therapeutics/ Pfizer) was the only commercially-available inhaled insulin. However, it was taken off the market in October 2007, after one year of commercialisation, because of unexpectedly low sales (Bailey and Barnett, 2010). Because of its rather low bioavailability, treatment with Exubera® was indeed considerably more expensive than treatment with s.c. insulin. Together with this, a contemporaneous lack of evidence for superiority over s.c. insulin led to poor reimbursement of the product, despite increased treatment satisfaction compared to s.c. insulin being observed in several studies (Arnolds and Heise, 2007).

Formulation

The dry powder formulation consists of matrix particles containing amorphous insulin (approximately 60%), mannitol, glycine, Na citrate (stabilising excipients), and NaOH (pH adjustment). It is produced by a proprietary spray-drying process (PulmoSol) that provides low moisture content and allows room-temperature stability for two years. The powder is packaged into single-dose blisters containing 1 or 3 mg (approximately 28 and 84 units) of insulin (Onoue et al., 2008). In vitro aerodynamic evaluation of the formulation provided an MMAD between 2.8 and 3.4 μm and an FPF between 36% and 45% of the loaded dose at a flow rate of 57 l/min using an Andersen cascade impactor (Harper et al., 2007).

Inhaler

For delivery, an individual blister is placed into a slot on the Exubera® device (**Figure 23**), which uses compressed air to disperse the powder formulation into a spacer reservoir prior to inhalation. The patient then inhales the aerosol at the beginning of a slow, deep breath during which air is drawn into the chamber, extruding the aerosol into the pulmonary tree. The MMAD of the aerosol delivered is approximately 3 μm (Owens et al., 2003).

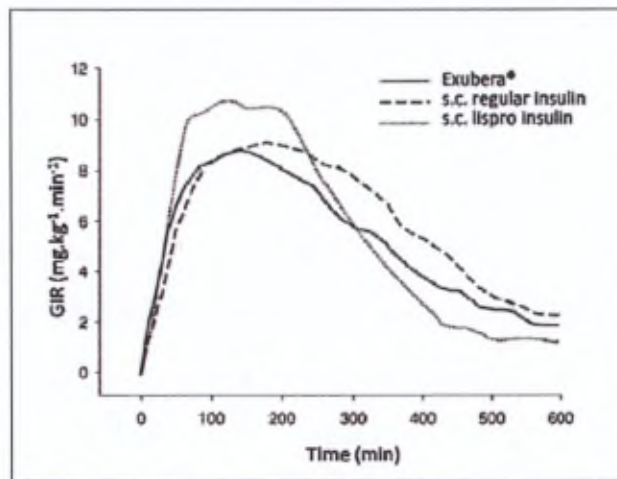


Figure 24. Time-action profile of Exubera[®], s.c. regular, and s.c. lispro insulins. Baseline-corrected glucose infusion rates (GIR) registered in 17 healthy volunteers after inhalation of 6mg Exubera (168 units), s.c. injection of 18 units regular insulin, and s.c.injection of 18 units insulin lispro (Rave et al., 2005)

PK/PD profile

The bioavailability of Exubera[®] has been estimated at 10% relative to s.c. insulin during a glucose clamp procedure in healthy, non-smoking subjects observed over a 10-h post-administration period (Rave et al., 2005).

In a study comparing pharmacokinetic profiles of Exubera[®], subcutaneous (s.c.), and intravenous (i.v.) insulin, maximum insulin concentrations were faster with the inhaled route than with s.c. regular insulin (Heinemann et al., 1997). In another study (Rave et al., 2005), time action profiles of Exubera[®], insulin lispro, and regular subcutaneous insulin were compared (see **Figure 24**). The onset of action was measured by the time to half of the maximum glucose infusion rate before the maximum glucose infusion rate (tGIR_{early 50%}). It was found that the tGIR_{early 50%} of Exubera[®] was shorter than that of s.c. regular insulin (32 min vs 48 min, respectively, $p < 0.001$) and was comparable to insulin lispro. The duration of action of Exubera[®], determined by the time to half of the maximum glucose infusion rate after the maximum glucose infusion rate (tGIR_{late 50%}), was longer than the duration of lispro (387 min vs 313 min, $p < 0.01$) and was comparable to s.c. regular insulin. In a study on type 2 diabetics, the reproducibility of the response to the pulmonary insulin was found to be similar to s.c. insulin (Gelfand et al., 2000).

Clinical efficacy

Studies demonstrating the equivalence of Exubera[®] to s.c. regular insulin have been conducted in both type 1 and type 2 diabetes patients. In these studies, the efficacy of inhaled insulin was shown to be comparable to s.c. insulin in reducing HbA1c levels (Quattrin et al., 2004; Hollander et al., 2004; Skyler et al., 2005). In patients with type 2 diabetes that were inadequately controlled through lifestyle modifications and oral therapies, addition of inhaled insulin even improved glycemic control (DeFronzo et al., 2005; Rosenstock et al., 2005).

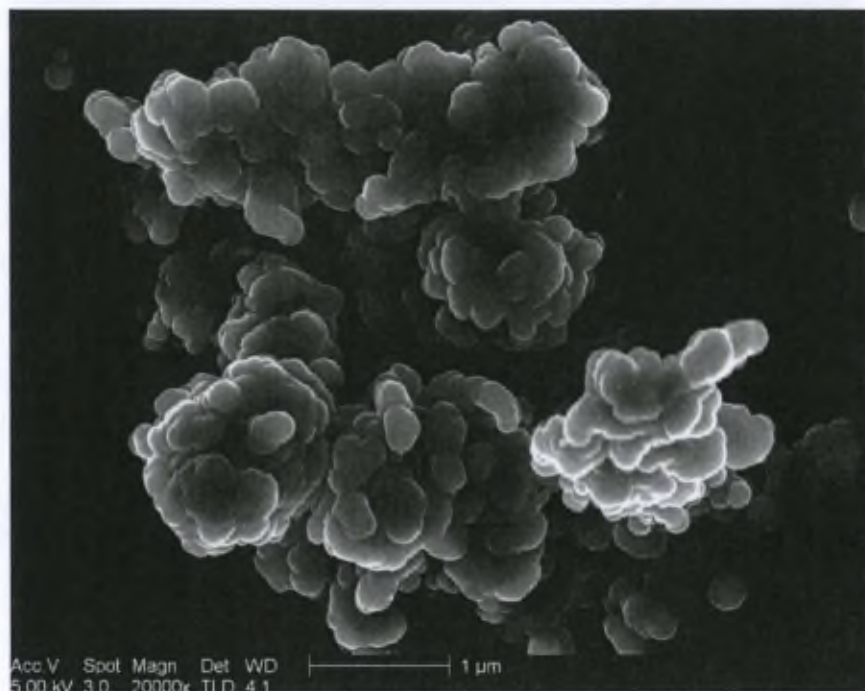


Figure 25. Technosphere-insulin particles in Afrezza® (Richardson and Boss, 2007)

II.3.2.2.2. Afrezza®

After the withdrawal of Exubera®, only one company, MannKind (Valencia, CA, USA), pursued the work on inhaled insulin and developed Afrezza®. Although most studies on Afrezza® were conducted with the MedTone® inhaler, clinical evaluation is currently being pursued with a new delivery device (Dreamboat®). The decision of the FDA to approve Afrezza® is expected for 2013.

Formulation

The formulation is based on the Technosphere™ drug carrier technology, in which peptides or proteins can be captured and stabilised in small precipitated particles (Pfützner and Forst, 2005; Cassidy et al., 2011). A well-characterised small organic molecule, 3,6-bis(N-fumaryl-N-(n-butyl)amino-2,5-diketopiperazine (FDKP), self-assembles by hydrogen binding in a mild acid environment into microspheres. In the precipitation process, it traps and microencapsulates insulin that is present in the solution during self assembly. The precipitates are freeze-dried and become a light powder predominantly composed of insulin and FDKP (1:9 ratio by dry weight), with residual amounts of water and polysorbate 80. The particles (**Figure 25**) present an internal porosity of ~ 70%, with a median diameter of approximately 2–2.5 µm. The MMAD measured with an Andersen cascade impactor is also 2–2.5 µm (Angelo et al., 2009). When administered by inhalation, the particles dissolve in the pH-neutral environment of the deep lung and rapidly liberate the insulin for absorption into the systemic circulation. The carrier molecules are not metabolised and are excreted as ammonium salts in the urine within hours of administration (Pfützner and Forst, 2005; Cassidy et al., 2011).

Inhaler

The MedTone® DPI was developed specifically for use with cartridges containing the Afrezza® formulation. This pocket-sized inhaler is a breath-powered, high-resistance, low-flow device with a passive powder de-agglomeration mechanism. Single-use cartridges are inserted into the dispersion chamber of the inhaler and patients administer the insulin by taking a deep breath, providing an aerosol cloud with a median aerodynamic diameter of 2–2.5 µm (Richardson and Boss, 2007; Cassidy et al., 2011). The Dreamboat® DPI is also a high-

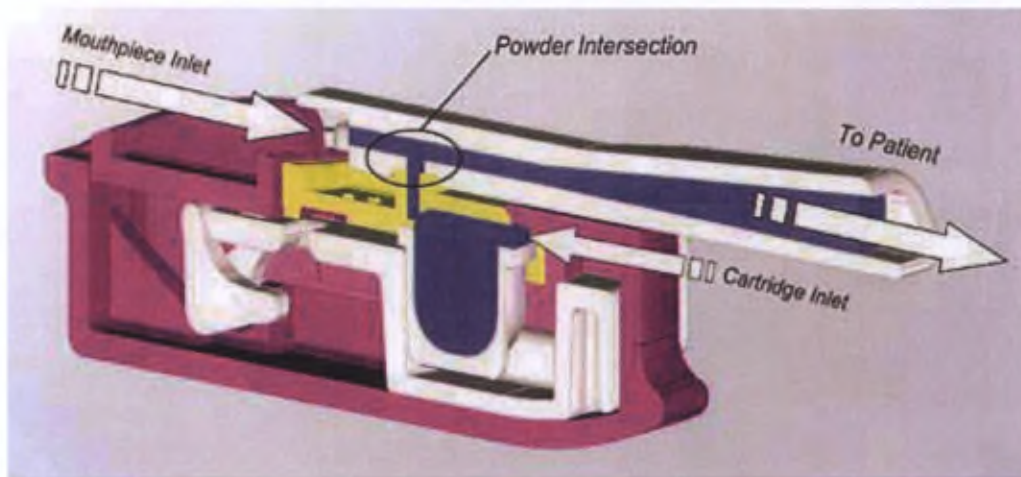


Figure 26. Inhalation system flow path of the Dreamboat® device (MannKind, 2010)

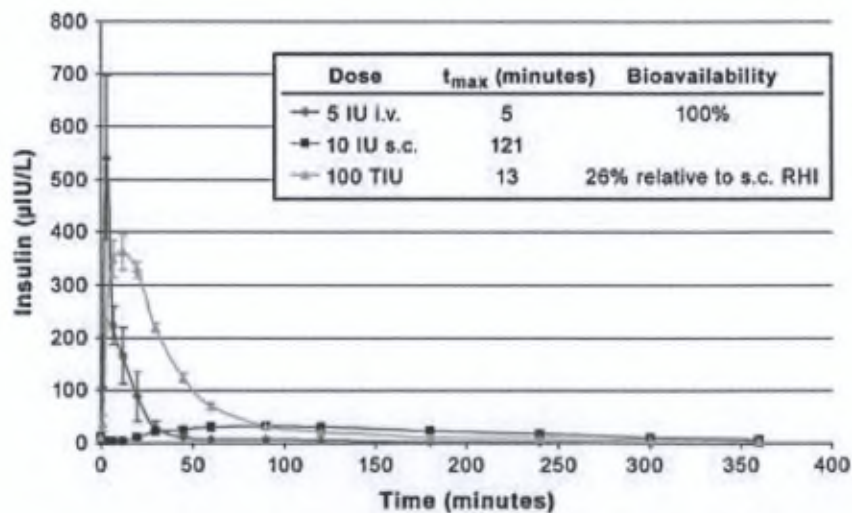


Figure 27. Absorption profile over time of 100 IU Afrezza (TIU), 10 IU s.c. regular insulin, and 5 IU i.v. regular insulin in healthy volunteers (Pfutzner and Forst, 2005)

resistance passive device that uses unit-dose plastic cartridges to load the formulation. Air flow moving through the cartridge initiates de-agglomeration and lifts the powder from the bottom of the cartridge to the top exit port. By-pass air flow moving down the mouthpiece intersects air flow moving from the cartridge exit. Here it is sheared to complete the de-agglomeration process before exiting the mouthpiece (**Figure 26**). This air-flow balance allows complete discharge of the cartridge contents as well as providing forces that are sufficient to de-agglomerate the powder into particles sized within the respirable range (Leone-Bay et al., 2006).

PK/PD profile

Afrezza® provides a high bioavailability of 26% relative to s.c. regular insulin (Boss et al., 2008). In a study of healthy subjects, the pharmacokinetics of 100 IU of Afrezza®, 10 IU s.c. regular insulin, and 5 IU of i.v. insulin were compared (Pfutzner and Forst, 2005). Afrezza® demonstrated a very rapid absorption, with a mean t_{max} of 13 min and a mean maximal concentration (C_{max}) of 371 mU/mL. In contrast, the mean t_{max} for 10 IU of s.c. regular insulin was 121 min, with a mean C_{max} of 34 mU/mL (**Figure 27**). The high bioavailability and fast absorption observed for Afrezza® is significantly higher than what is achievable with any other insulin to date, including Exubera®. The physicochemical basis of this observed pharmacokinetic profile is thought to result from the highly efficient delivery of Afrezza® particles to the deep lung (low MMAD of Afrezza® in comparison with the other formulations). As they are very small, particles can then dissolve rapidly and provide high local concentrations of insulin that can be quickly absorbed in the alveolae. However, it was shown that Afrezza® does not act as an absorption enhancer and that it has no cytotoxic effect in an in vitro human lung cell model (Angelo et al., 2009).

The postprandial pharmacodynamics of Afrezza® vs. s.c. regular insulin have been assessed with an isoglycemic glucose clamp study in subjects with type 2 diabetes (Rave et al., 2007b). The distribution of the total glucose lowering effect was significantly different between Afrezza® (48 IU) and s.c. insulin (24 IU) ($p < 0.05$). The adjusted mean time to maximal glucose-lowering effect (GIR- t_{max}) was approximately 200 min earlier with Afrezza® than with s.c. insulin ($p < 0.0001$). The majority (71%) of the total glucose-lowering effect of Afrezza® was delivered during the 0–3 h post-dosing period, compared with only about 27%

of the total effect of s.c insulin. Because the rise and fall in postprandial glycemia normally occurs over the first 3 h after a meal (Polonsky et al., 1988), the optimal time frame for insulin action is over that same time period. The time to maximal glucose-lowering activity is also reached more quickly with Afrezza® than with other inhaled insulins (Heinemann and Heise, 2004).

Clinical efficacy

In a 12-week randomised, controlled trial in 110 patients with type 1 diabetes, Afrezza® insulin was administered at mealtimes. The Afrezza®-treated subjects demonstrated significantly reduced HbA1c concentrations from baseline (-0.83%), without experiencing weight gain. The control group, which received prandial treatment with injected insulin, showed a similar statistically significant glycemic improvement from baseline (-0.99%). However, the injected group experienced a weight change of +0.89 kg compared with -0.41 kg for the Afrezza® group (Boss, 2006). Another study enrolled adult patients with type 2 diabetes mellitus and poor glycemic control. Patients were randomly allocated to receive 52 weeks of treatment with prandial Afrezza® plus bedtime insulin glargine (n=334) or twice-daily premixed bipart insulin (n=343). Over the 52 weeks, the change in HbA1c with inhaled insulin plus insulin glargine (-0.68%) was similar and not below that with bipart insulin (-0.76%). As reported in previous studies, patients had significantly lower weight gain and fewer mild-to-moderate and severe hypoglycemic events on inhaled insulin plus insulin glargine than on bipart insulin (Rosenstock et al., 2010).

It is to be noted that the clinical data available were all obtained using the MedTone® inhaler. In 2011, MannKind will conduct two clinical studies (one in patients with type 1 diabetes and one in patients with type 2 diabetes) to evaluate the efficacy and safety of Afrezza® administered using the Dreamboat® inhaler, with at least one trial including a treatment group using the previously studied MedTone® inhaler in order to obtain a head-to-head comparison of the two devices.

II.3.2.2.3. Others

After the withdrawal of Exubera[®], many formulation/device systems for the administration of inhaled insulin were discontinued, despite being in an advanced stage of development. An overview of their features is given in **APPENDIX VI**.

II.3.2.3. Safety issues

Recently, the use of inhaled insulin has been subject to controversy. This is mainly due to the fact that, in April 2008, a potentially increased risk of bronchial carcinoma in ex-smokers treated with Exubera[®] was reported compared to patients treated with injections. This increased risk of cancer could be related to the fact that insulin acts as a weak growth factor by binding to the IGF-1 receptor, even if its efficiency is only 1/100 of IGF-1 (Siekmeier and Scheuch, 2008). Because all six newly diagnosed cases of primary lung malignancies among Exubera[®]-treated patients had a history of cigarette smoking, the association with insulin therapy was regarded as inconclusive. In addition, there is to date no evidence for a significant action of inhaled insulin on IGF-1 receptors in the lung (Siekmeier and Scheuch, 2008; Bailey and Barnett, 2010).

Another potential issue with the use of inhaled insulin is the effect on lung function. In a long-term toxicity study (Skyler et al., 2008), patients received basal insulin plus either pre-meal Exubera[®] (n = 290) or a short-acting s.c. insulin (n = 290) for 2 years (comparative phase), followed by 6 months of s.c. insulin (washout) and 6 months of their original therapy (readministration). The results exhibited a decline in lung function that was slightly but significantly higher for the Exubera[®]-treated group. The FEV1 and the diffusing capacity of the lung for CO (D_{LCO}) indeed declined from baseline in both treatment groups but with treatment group differences equal to 0.9% and 1.5% of baseline values for FEV1 and D_{LCO} , respectively. However, these differences were non-progressive, resolved during washout, and recurred at the same magnitude during readministration. In a 1-year study on Afrezza[®] (Rosenstock et al., 2010), similar reversible, non-progressive, and non-pathological effects on

lung function were noted. Cough episodes were also reported in 25% of the patients treated with Exubera[®] and 33% of the patients treated with Afrezza[®]. These were however transient, disappearing with continued treatment, and did not result in discontinuation of treatment. The appearance of insulin antibodies is another common issue related to inhaled insulin. Higher levels of (IgG) insulin antibodies with inhaled insulin therapy compared to s.c. insulin were observed in several clinical trials with Exubera[®]. In the previously mentioned long-term toxicity study from Skyler et al., at baseline, median insulin antibody levels were 4.50 and 4.15 mU/ml for the Exubera[®] and s.c. insulin groups, respectively. Median antibody levels increased with respect to baseline in the Exubera[®] group but not in the s.c. insulin group during the 2-year comparative phase, reaching a peak at 12 months. In the Exubera[®] group, the median change from baseline was +128.20 mU/ml at 12 months, declining to a change from baseline of +52.95 mU/ml at 24 months. During the washout phase, median antibody levels declined further in the Exubera[®] group to levels near that of the s.c. insulin group. When Exubera[®] therapy was readministered, median antibody levels again increased to levels similar to those observed in the original comparative phase (Skyler et al., 2008). Increased antibody levels were also found for the AIR[®] and AERx[®] IDMS formulations (Arnolds and Heise, 2007). However, these antibodies were not associated with impairments in glycemic control, higher insulin doses or any adverse outcomes (hypoglycemia, pulmonary side-effects or allergic events).

In spite of the commercial failure of Exubera[®], novel and more potent inhaled insulins such as Afrezza[®] might thus achieve a place in the therapeutic arsenal. However, the assessment of the long-term safety of inhaled insulin still requires extensive and long evaluation before a product can be approved. Depending on the outcome for Afrezza[®], it would thus not be surprising if other pharmaceutical companies regained interest in developing an inhaled insulin formulation.

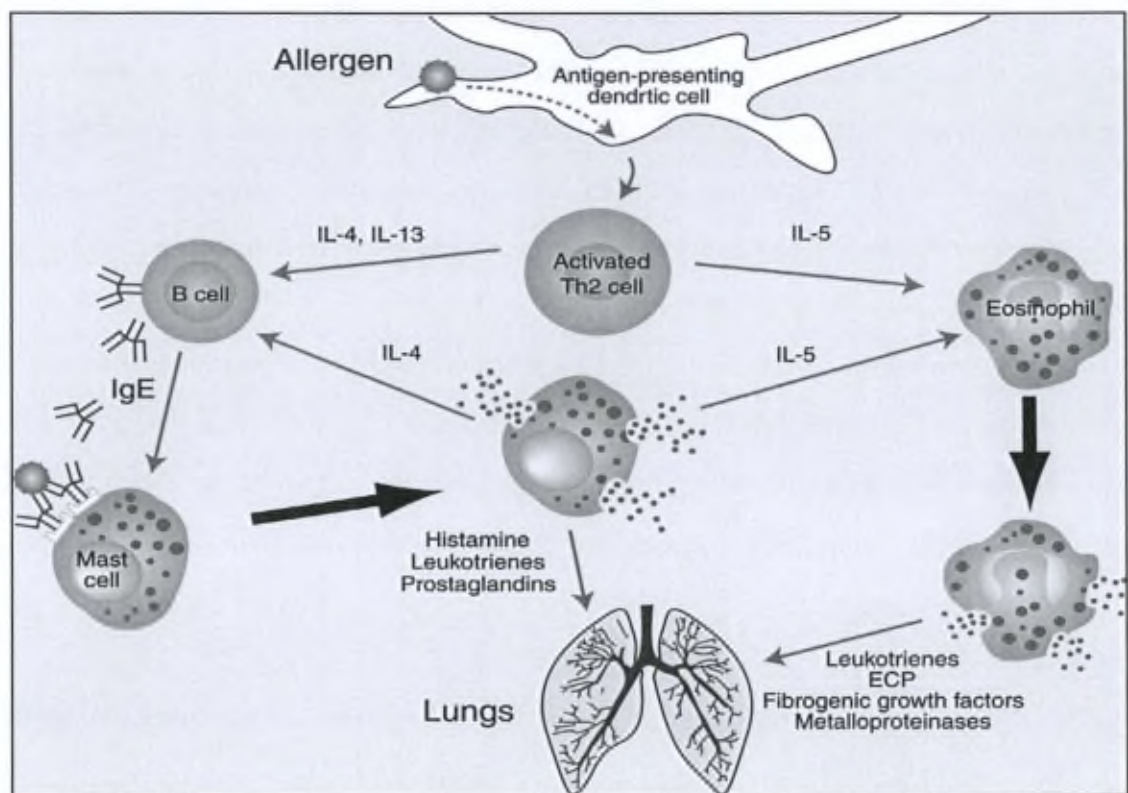


Figure 28. Simplified schematic version of how airway inflammation develops in patients with asthma (Hendeles et al., 2004)

II.4. Asthma: an application for local pulmonary delivery of protein

II.4.1. *Physiopathology of Asthma*

Asthma can simply be defined as recurrent reversible bronchospasm due to a triggering factor. These factors can be exposure to environmental allergens or viral respiratory infections (Diamant et al., 2007). However, asthma is a complex inflammatory syndrome involving the recruitment and activation of mast cells, macrophages, dendritic cells, neutrophils, eosinophils, and T lymphocytes. This results in inflammatory, cellular infiltration into the airways, which can involve potentially permanent airway obstruction and airway hyperresponsiveness (Linzer, 2007). Acute asthma exacerbations vary in severity and duration. Symptoms presented are wheezing and respiratory distress. Bronchospasm can also present as a cough, chest pain, shortness of breath, and fatigue. An asthma attack can be divided into 2 phases: early allergen response (EAR) and late allergen response (LAR).

Upon exposure to an allergen, IgE-mediated responses activate the EAR. This typically occurs within 1 hour of allergen exposure (Holgate et al., 2000). The allergen is presented to the type 2 helper T cell subtype (Th2) of CD4+ lymphocytes by an antigen-presenting cell such as a dendritic cell or a macrophage. The Th2 cell is activated and releases interleukins, such as IL-4, IL-5, and IL-13. IL-4 stimulates B cells to produce IgE, which then binds to the outside surface of mast cells. When the allergen subsequently comes in contact with the IgE bound to mast cells, the mast cell is activated and releases several broncho-constrictive substances including histamine, leukotrienes and prostaglandins, and interleukins IL-4 and IL-5 (**Figure 28**) (Hendeles et al., 2004). The IL-4 released from mast cells serves to perpetuate IgE production, while the IL-5 released from mast cells, as well as from activated Th2 lymphocytes, acts specifically on eosinophils to recruit them to the airways, activate them, and enhance their survival. The eosinophil, in turn, when activated, releases leukotrienes and other substances, such as eosinophil cationic protein (ECP), which is thought to cause mucosal damage and increase airway reactivity. In addition, eosinophils produce other

substances such as fibrogenic growth factors and matrix metalloproteinases, which may be involved in airway remodelling (Elias et al., 1999). Leukotrienes released by both mast cells and eosinophils are potent bronchoconstrictors and also perpetuate migration of the eosinophils into the airways. Thus the activated Th2 lymphocyte orchestrates the inflammatory cascade, communicating with the two primary effector cells, the mast cell, and the eosinophil by release of IL-4 and IL-5 cytokines (Hendeles et al., 2004).

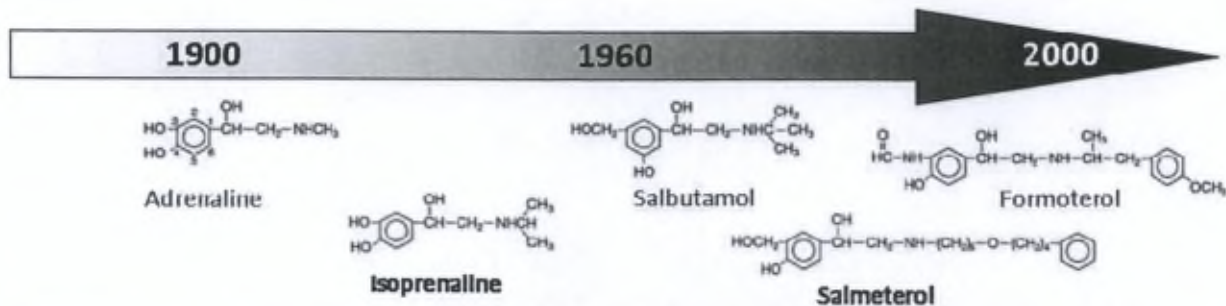
About 50% of patients go on to develop an LAR about 4 to 8 hours after exposure to the initial trigger. IgE is also postulated to be involved in the initiation of this late-phase response, even though its role in the pathogenesis is not well-defined (Rosenwasser and Nash, 2003). The LAR episode usually lasts 12-24 hours and leads to the infiltration of a number of preformed and generated inflammatory mediators, resulting in irreversible airway remodeling. It is characterised by the airway epithelium becoming fragile and denuded, thickening of the epithelial subbasement membranes (deposition of extracellular proteins), increased goblet cell and mucus production, smooth muscle hypertrophy, and endothelial leakage leading to mucosal oedema (**Figure 29**). Mediator-induced abnormalities in the parasympathetic and nonadrenergic noncholinergic nervous systems may also lead to increased bronchial hyperresponsiveness (Holgate et al., 2000; Rosenwasser and Nash, 2003; Linzer, 2007).

II.4.2. Current treatments

The goal of asthma treatments is to achieve and maintain clinical control. Medications to treat asthma can be classified as relievers or controllers. Relievers are medications used on an as-needed basis that act quickly to reverse bronchoconstriction and relieve its symptoms, whereas controllers are medications taken daily on a long-term basis to keep asthma under clinical control, chiefly through their anti-inflammatory effects.

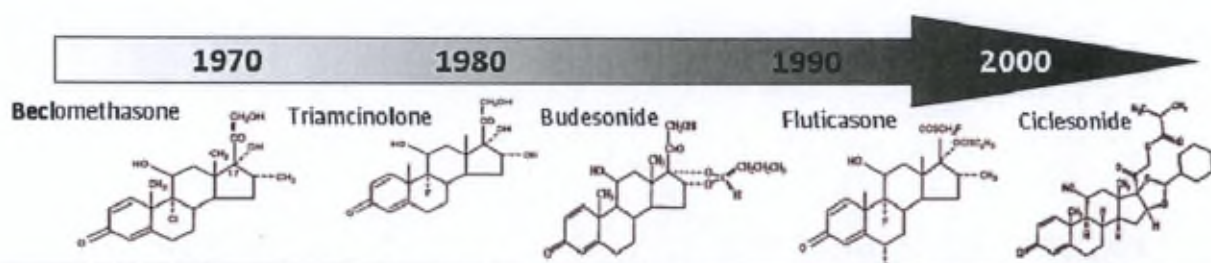
II.4.2.1. Relievers

These include intravenous theophylline (xanthine), short-acting inhaled β_2 agonists (SABAs), and inhaled anticholinergics. Among them, β_2 agonists are the most widely used (Diamant et al., 2007). They interact with the β_2 adrenergic receptors subset located on the bronchial



	Adrenaline	Isoprenaline	Salbutamol	Salmeterol	Formoterol
Specificity	α and β agonist	β_1 and β_2 agonist	Selective β_2 agonist	Selective β_2 agonist	Selective β_2 agonist
Action profile	Fast onset Short duration	Fast onset Short duration	Fast onset Short duration	Slow onset Long duration	Fast onset Long duration
Preferred administration	Injected or nebulised	Sublingual or nebulised	MDI or nebulised	MDI or DPI	MDI or DPI
Side-effects	Cardiotoxicity Hypertension Tachycardia Tremor	Tachycardia Tremor	Tremor	Tremor	Tremor

Figure 30. Structure and main properties of the major β -agonists (Diamant et al., 2007)



	Beclomethasone	Triamcinolone	Budesonide	Fluticasone	Ciclesonide
Administration	2-4 daily doses MDI/DPI	2-4 daily doses MDI/DPI	1-2 daily doses MDI/DPI	1-2 daily doses MDI/DPI	Once-daily MDI
Advantages	-Proven clinical efficacy -Low price -Moderate oral bioavailability	-Proven clinical efficacy -Low price	-Proven clinical efficacy -Moderate oral bioavailability -Available as combination therapy	-Proven clinical efficacy -Low oral bioavailability -Available as combination therapy -Most potent	-Low oral bioavailability -On site activation -Once daily dosing
Disadvantages	-Not available as combination therapy	-High oral bioavailability -Not available as combination therapy -Least potent	-Short lung residence time	-Greatest risk of HPA axis suppression	-Limited clinical experience -Not available as combination therapy

Figure 31. Structure and major advantages and disadvantages of the most widely used corticosteroids
 HPA: hypothalamic-pituitary-adrenal (Diamant et al., 2007)

smooth muscle, causing bronchodilatation. The success of SABAs such as salbutamol initiated the development of long-acting β_2 agonists (LABAs). Salmeterol was first launched with a duration of action of up to 12 h (Johnson, 1995), followed by formoterol. The latter drug combines long-lasting bronchodilator effects (> 12 h) with a fast onset of action similar to salbutamol (**Figure 30**) (Bartow and Brogden, 1998). Currently, several novel LABAs (i.e. carmoterol and indacaterol) are being developed with a duration of action of up to 24 h, creating the possibility of once-daily dosing (ultra long-acting β_2 agonists) (Cazzola et al., 2008).

II.4.2.2. Controllers

These include inhaled and systemic glucocorticosteroids, long-acting inhaled β_2 agonists in combination with inhaled glucocorticosteroids, oral antileukotrienes, oral sustained-release theophylline, and inhaled cromones. Among them, inhaled corticosteroids (ICS) are the most widely used and the most effective controller drugs for the treatment of persistent asthma (GINA, 2010). The effects of ICS are mediated through the intracellular glucocorticoid receptor in a large variety of (inflammatory) cells, resulting in both suppression of inflammatory gene transcription and activation of antiinflammatory gene transcription (Barnes, 2006a). In the past two decades, modification of the initial compounds and inhalers has increased their potency and first-pass metabolism in combination with improved lung deposition. Presently, available ICS differ little in clinical efficacy and side effects. Fluticasone and budesonide are the most widely used, alone or in combination with a LABA in one inhaler device (**Figure 31**) (Diamant et al., 2007). The recently launched ciclesonide combines the advantages of prolonged activity (once-daily use) with still fewer (local and systemic) side effects. Ciclesonide is a pro-drug with low glucocorticoid receptor affinity, and is activated primarily in the lung by esterases to an active metabolite, desisobutyryl-ciclesonide (des-CIC), with high glucocorticoid receptor affinity (Nave et al., 2005).

However, despite their established clinical effectivity, even prolonged treatment with high doses of ICS can neither fully reverse all chronic aspects of the airway inflammation nor cure the disease (Diamant et al., 2007). The main side-effects of ICS are related to their deposition in the oropharyngeal cavity, potentially leading to local complications such as dysphonia, pharyngitis, and oral candidiasis. Furthermore, corticosteroids deposited in the

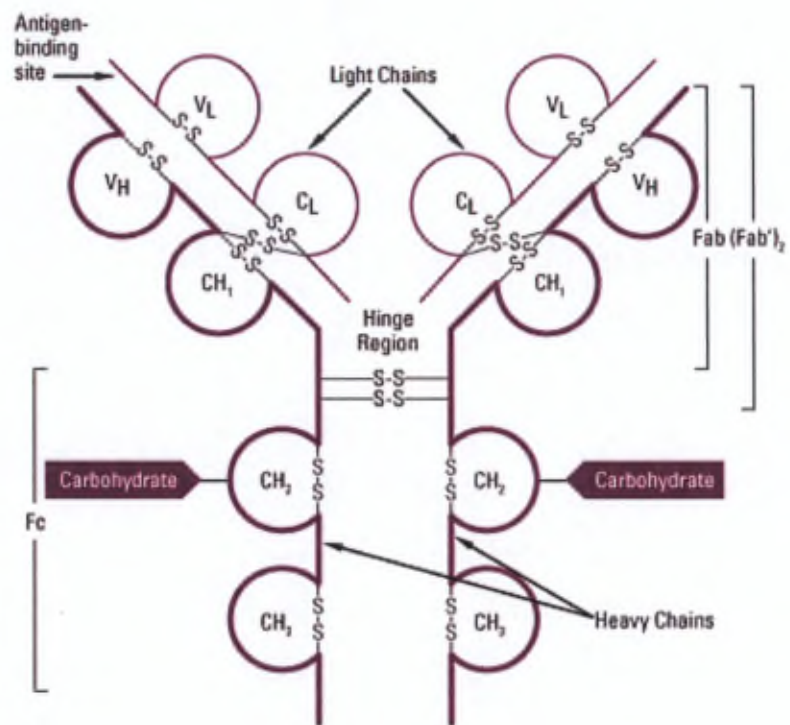


Figure 32. Structure of an immunoglobulin IgG (Piercenet, 2012)

oropharynx may be swallowed and absorbed into the systemic circulation, possibly resulting in the classical side-effects of systemic glucocorticoids (Jackson et al., 1999).

II.4.2.3. Monoclonal antibodies: a new class of asthma controller

Increased understanding of the immunological basis of asthma recently initiated the development of several targeted therapies such as monoclonal antibodies.

Structure and nomenclature of monoclonal antibodies

Antibodies are heavy (~150 kDa) globular plasma proteins that are also known as immunoglobulins (Ig). Antibodies can come in different varieties known as isotypes or classes. In mammals there are five antibody isotypes known as IgA, IgD, IgE, IgG and IgM, which differ in their biological properties, functional locations, and ability to deal with different antigens. IgG, IgD and IgE only contain one Ig monomer unit whereas IgA contains two Ig units. Antibodies can also be tetrameric with four Ig units, as with teleost fish IgM, or pentameric with five Ig units, as with mammalian IgM (Roux, 1999).

The Ig monomer is a "Y"-shaped molecule that consists of four polypeptide chains, two identical heavy chains and two identical light chains connected by disulfide bonds (see **Figure 32**) (Woof and Burton, 2004). There are five types of mammalian Ig heavy chain, denoted by the Greek letters: α , δ , ϵ , γ , and μ . The type of heavy chain that is present defines the class of antibody: these chains are found in IgA, IgD, IgE, IgG, and IgM antibodies, respectively (Rhoades and Pflanzner, 2002). Distinct heavy chains differ in size and composition: α and γ contain approximately 450 amino acids, while μ and ϵ have approximately 550 amino acids. Each heavy chain has two regions, the constant region and the variable region. The constant region is identical in all antibodies of the same isotype but differs in antibodies of different isotypes. Heavy chains γ , α and δ have a constant region composed of three tandem (in a line) Ig domains, and a hinge region for added flexibility (Woof and Burton, 2004). Heavy chains μ and ϵ have a constant region composed of four immunoglobulin domains (Janeway et al., 2001). The variable region of the heavy chain differs in antibodies produced by different B cells but is the same for all antibodies produced

Table VII. Nomenclature of monoclonal antibodies (World Health Organization, 2009)

Prefix	Target substem		Source substem		Stem
		Meaning		Meaning	
Variable	Angiogenesis	/	-a-	Rat	-mab
	Bacterium	-b(a)-	-e-	Hamster	
	Circulatory system	-c(i)-	-j-	Primate	
	Fungus	-f(u)-	-o-	mouse	
	Interleukins	-k(i)-	-u-	Human	
	Inflammatory lesions	/	-xi-	Chimeric (human/foreign)	
	Immune system	-l(i)	-zu-	Humanized	
	Musculoskeletal system	/	-xizu-	Chimeric/humanized hybrid	
	Nervous system	-n(e)-	-axo-	Rat/mouse hybrid	
	Bone	-s(o)-			
	Toxin	-tox(a)-			
	Tumors	-t(u)-			
	virus	-v(i)-			
Examples					
abciximab (Reopro®)	MAb for the circulatory system, chimeric (antagonist of glycoprotein IIb/IIIa receptor)				
Adalimumab (Humira®)	MAb for the immune system, human (TNF α inhibitor)				
Certolizumab (Cimzia®)	MAb for the immune system, humanized (TNF α inhibitor)				
Infliximab (Remicade®)	MAb for the immune system, chimeric (TNF α inhibitor)				
Denosumab (Prolia®)	MAb for bone disorders, human (inhibitor of a cytokine involved in osteoclast activation)				
Palivizumab (Synagis®)	MAb for viral infection, humanized (against respiratory syncytial virus)				
Trastuzumab (Herceptin®)	MAb for tumor treatment, humanized (inhibition of HER-2 growth factor)				
Cetuximab (Erbix®)	MAb for tumor treatment, chimeric (inhibition of EGF receptor)				

by a single B cell or B cell clone. The variable region of each heavy chain is approximately 110 amino acids long and is composed of a single Ig domain.

In mammals there are two types of light chain, which are called lambda (λ) and kappa (κ). A light chain has two successive domains: one constant domain and one variable domain. The approximate length of a light chain is 211-217 amino acids (Janeway et al., 2001). Each antibody contains two light chains that are always identical; only one type of light chain, κ or λ , is present per antibody in mammals.

Some parts of an antibody have unique functions. The tip of the Y, for example, contains the site that binds antigens and is therefore called the Fab (fragment, antigen binding) region. It is composed of one constant and one variable domain from each heavy and light chain of the antibody. The paratope, which is the part of the antibody which recognises the antigen, is shaped at the amino terminal end of the antibody monomer by the variable domains from the heavy and light chains (Janeway et al., 2001). On the other hand, the base of the Y plays a role in modulating immune cell activity. This region is called the Fc (Fragment, crystallizable) region, and is composed of two heavy chains that contain two or three constant domains, depending on the class of the antibody (Janeway et al., 2001). By binding to specific proteins, the Fc region ensures that each antibody generates an appropriate immune response for a given antigen. The Fc region also binds to various cell receptors, such as Fc receptors, and other immune molecules, such as complement proteins. By doing this, it mediates different physiological effects including opsonization, cell lysis, and degranulation of mast cells, basophils and eosinophils.

Monoclonal antibodies (MAb) are monospecific antibodies that have strictly the same primary structure because they are produced by clones of a unique parent cell. MAb are generally produced by recombinant technology in viruses or yeast cells. Nomenclature of monoclonal antibodies follows a scheme used by the World Health Organization. All monoclonal antibody names end with the stem *-mab*. Unlike most other pharmaceuticals, monoclonal antibody nomenclature uses different preceding word parts depending on structure and function (**Table VII**).

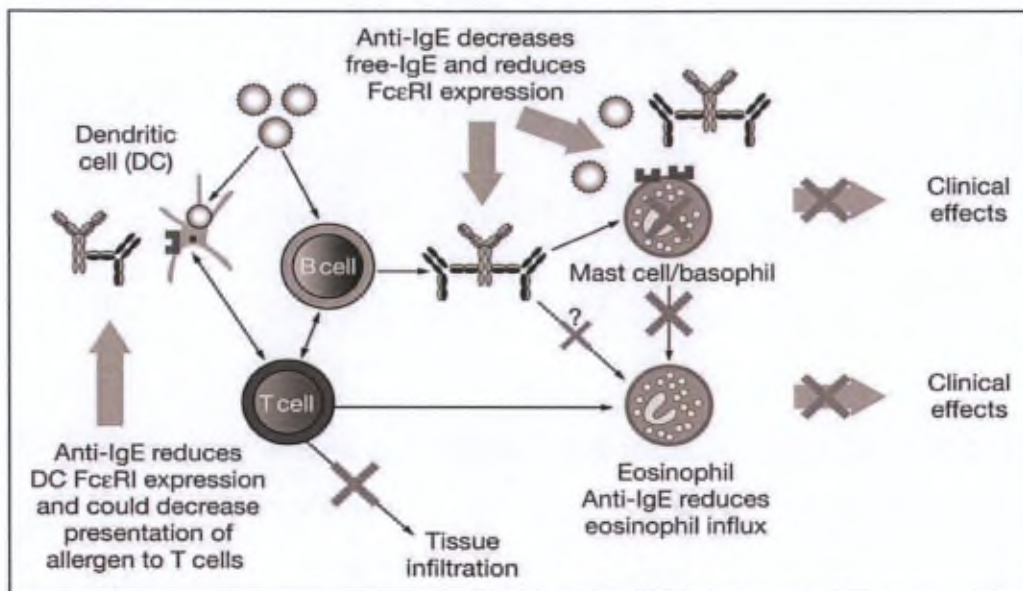


Figure 33. Proposed mechanisms of action of omalizumab (Holgate et al., 2009)

Monoclonal antibodies in asthma therapy

In 2003, subcutaneous Omalizumab (Xolair®), which is a humanised monoclonal antibody directed against IgE, was approved as an add-on therapy for the treatment of therapy-resistant, severe allergic asthma. Omalizumab inhibits the binding of IgE to Fc ϵ RI receptors (high-affinity receptors) on mast cells and basophils. Free IgE levels are rapidly reduced and, with less IgE available to bind, the expression of Fc ϵ RI on inflammatory cells, such as basophils, mast cells, and dendritic cells, is down regulated (**Figure 33**) (Holgate et al., 2009). Interrupting the interaction between IgE and Fc ϵ RI inhibits mast-cell and basophil activation and the subsequent release of their inflammatory mediators. By preventing the release of these mediators, omalizumab may reduce inflammatory cell recruitment (particularly eosinophils), tissue remodelling, and functional changes in the airways. When combined with regular maintenance therapy, Omalizumab effectively improved disease control, allowing reduction of the daily ICS dose in two-thirds of patients with allergic asthma (Nowak, 2006; Diamant et al., 2007). The major drawbacks are its subcutaneous administration (every 2–4 weeks) and the high costs involved. In 2011, the worldwide sales of Xolair® have reached 1.100 million USD.

11.4.3. Place of inhaled peptides and proteins

A number of studies have found that a substantial proportion of patients do not achieve asthma control with their medications. For example, the Gaining Optimal Asthma Control (GOAL) study compared ICS alone with an ICS/ β_2 agonist combination in over 3400 patients with varying severities of asthma. Despite dose-escalations and treatment for one year, 41% (ICS alone) to 29% (combination therapy) of subjects still did not achieve adequate control (Bateman et al., 2004). In another example, variations in response to fluticasone (ICS) and montelukast (antileukotriene) were evaluated in children with mild-to-moderate persistent asthma. It was found that 5% of children responded well to montelukast alone, 23% to fluticasone alone, and 17% to both medications, but 55% did not respond significantly to either medication (Szeffler et al., 2005). These findings highlight the importance of the continued search for new asthma therapeutics. Moreover, even patients whose asthma is

apparently well-controlled by existing therapies might benefit from more efficacious therapies that are easier to comply with (Adcock et al., 2008). Due to recent developments in biotechnology and to an increased knowledge of the mechanisms underlying asthma disease, research into future therapies of asthma is mainly focusing on targeted bioengineered products. In most studies, these new products are currently administered by injection. However, local lung delivery could optimise the therapeutic index by increasing local tissue drug concentrations at the same time as minimising systemic exposure, and could also increase compliance. Research on inhaled biologics for the treatment of asthma is therefore expected to increase in the years to come. A few drugs, presented below, have already been reported in the literature as being investigated via the pulmonary route.

Although **omalizumab** has entered clinical practice as parenteral add-on asthma therapy, this anti-IgE monoclonal antibody has also been investigated for direct administration to the lungs. Nebulised omalizumab was administered for 8 weeks to 33 patients with mild allergic asthma. It was concluded that aerosol administration of the antibody does not inhibit the airway responses to inhaled allergen (Fahy et al., 1999). This could be due to the route of delivery (nebulisation), which may not have delivered sufficient MAb to the lower airways, resulting in low concentrations in the tissue compartments surrounding IgE effector cells. DPI formulations of omalizumab have also been developed using spray-drying and with carbohydrates as stabilising excipients (Andya et al., 1999). However, an appropriate FPF of around 30% could only be obtained at the expense of protein biochemical stability and no further development of an anti-IgE administered by inhalation has been found in the literature.

There has recently been considerable interest in developing other inhibitors that could act at a former level of the inflammatory cascade, specifically **interleukins** (IL). Interleukin-4 (IL-4) and Interleukin-13 (IL-13) are indeed major stimuli for the production of IgE antibodies (Daugherty and Mrsny, 2006).

A variety of products that block the effect of IL-4 has been developed, including soluble IL-4 receptors (altrakcept, Immunex [Amgen], USA) and anti-IL-4 humanised monoclonal antibodies. Unfortunately, these products have not demonstrated adequate clinical efficacy (Colice, 2011). Because the IL-4 receptor α chain is used by both IL-4 and IL-13, antagonists

directed at IL-4R α have been developed. Phase I and Phase II studies have demonstrated that single inhalations of 1.5 mg of soluble IL-4R α were significantly more effective than 0.5 mg of IL-4R α and placebo in preventing asthma deterioration when corticosteroids were withdrawn (Borish et al., 1999). However further studies in patients with milder asthma proved disappointing and the development of this compound has now been discontinued (Caramori et al., 2008). IL-4 variants, also called IL-4 muteins, were also developed, such as pitrakinra, in which the tyrosine at 124 is replaced with aspartate and arginine at 121 is replaced with aspartate. IL-4 muteins act as antagonists for both IL4 and IL-13 because they are able to bind to IL-4R/IL13R but do not transduce the signal. Pitrakinra is now in phase IIa clinical trial for the treatment of asthma. Promising results have been published recently on the efficacy of this compound, administered either subcutaneously or by inhalation, in the prevention of late phase asthmatic responses to allergen (Wenzel et al., 2007).

Blocking the IL-13 pathway seems particularly promising as it is thought to contribute to many key features of asthma. Several specific monoclonal antibodies against interleukin 13, such as lebrikizumab, are also undergoing clinical trials for asthma. A significant increase in FEV₁ has been reported after 12 weeks subcutaneous lebrikizumab in asthmatic patients inadequately controlled with ICS (Corren et al., 2011). Other interleukin and cytokine antagonists are also being developed, such as anti-IL5, anti-IL2, and anti-TNF α , with promising results in early clinical trials (Colice, 2011). However, these have only been administered parenterally and it seems that none of them has already been investigated for inhalation application.

Dry powder formulations of **vasoactive intestinal peptide** (VIP) are also being developed to treat asthma and COPD. Deficiency of VIP in the respiratory system is indeed considered to be a pathogenetic factor in airway inflammatory disease, and VIP is abundantly present in normal human lung and monocyte-derived macrophages. It has been shown to possess potent anti-inflammatory efficacy in respiratory tissues by interaction with specific receptors (Groneberg et al., 2006). A FPF of around 29% has been reported, and the formulation showed efficient relaxant effect in guinea-pig isolated trachea, as well as an anti-inflammatory effect by markedly suppressing the antigen-evoked infiltration of granulocytes in the rat bronchiolar mucosa (Ohmori et al., 2004). More recently, a VIP derivative with improved chemical and metabolic stability was also developed as a dry powder, which

exhibited a FPF of around 30%. Intratracheal administration in rats led to significant reductions in recruited inflammatory cells in lung tissues and broncho-alveolar lavage fluid of 72% and 78%, respectively (Onoue et al., 2011). Although VIP-based drugs have not yet been used for clinical purposes, the combination of newly developed VIP derivatives and DPI systems might provide efficacious medication for the clinical treatment of asthma, while avoiding systemic side-effects of VIP such as hypotension (Barnes, 2006b).

The immunosuppressive agent **ciclosporin A** has been shown to be effective orally in asthma treatment by inhibition of T cell activation and blocking of the signal transduction pathway that results in de novo transcription of genes for proinflammatory cytokines (IL-3, IL-4, IL-5, IL-13, GM-CSF) and the IL-2 receptor (Wiederrecht et al., 1993). However, its oral use is limited by severe side effects (Lock et al., 1996). A new inhaled MDI formulation of ciclosporin A has been developed (ADI628) and has been shown to be a potent airway anti-inflammatory agent in both rats and mice, with no notable toxicity at doses of up to 40 mg/kg. Clinical data has suggested that repeated inhaled doses of ADI628 are also safe and generally well-tolerated in healthy subjects and mild asthmatic patients (Rohatagi et al., 2000). DPI formulations of ciclosporin A have also been investigated (Blair et al., 2000; Onoue et al., 2012). Inhaled ciclosporin A may provide an interesting alternative to oral therapy, with a better safety margin for the treatment of asthma.

Inhaled anti-oxidants, including superoxide dismutase (SOD) and catalase have also been investigated because oxidative stress has been implicated as a driving force behind the inflammatory response and lack of corticosteroid sensitivity in severe asthma. Moreover, oxidative stress and its byproducts may drive a Th2-dependent immune response (Onoue et al., 2008; Adcock et al., 2008). SOD administered by inhalation has been shown to provide a dose-dependent protection against various oxidative stresses in animal models (Tang et al., 1993; Kirkham and Rahman, 2006). However, current anti-oxidants effects on the redox balance in the airways of humans are still to be investigated.

III. AIM OF THE WORK

AIM OF THE WORK

Pulmonary delivery of protein and peptides could be of particular interest, either for the treatment of lung diseases (topical applications) or for the treatment of systemic diseases. This is due to recent advances in biotechnology and molecular biology that have led to the development of new clinical perspectives using biomolecules as targeted therapeutic agents. Topical pulmonary administration could limit systemic side-effects of some of these biomolecules, and could also deliver larger amounts of drug directly to the lungs. On the other hand, systemic delivery of proteins by inhalation has attracted particular attention because it provides an alternative to parenteral administration due to the advantages presented by this administration mode (large alveolar surface, thickness of the epithelium, high blood perfusion, and avoidance of hepatic first-pass metabolism).

However, lung delivery of peptides and proteins is still at an early stage of development, with only a very small number of products commercially available for local applications, and none at all for systemic application. The main issues to overcome in both cases are guaranteeing protein stability during processing and storage and, at the same time, obtaining particles with appropriate aerodynamic features and deposition profile in the lung.

In this work, we aimed to develop formulations for either local or systemic delivery of proteins that presented optimal aerodynamic features and stability. The formulation strategy was a combination of micronisation techniques (high speed and high pressure homogenisations), drying techniques (spray-drying, freeze-drying), and addition of lipid excipients, to produce DPI formulations.

Insulin was chosen as a model protein for systemic delivery because of the high therapeutic and economic potential generated by the use of inhaled formulations in patients with diabetes. Moreover, insulin is the biomolecule that has been the most extensively studied for inhalation, providing useful data for comparison with other formulation strategies. The formulations developed were characterised in terms of physical state, aerodynamic properties, and stability in order to determine which formulations could be the most suitable for pulmonary delivery. A clinical evaluation was then performed with the best insulin formulations to evaluate their lung deposition and pharmacokinetics in man.

However, insulin is only a small protein of 5.8 kDa. Due to their more elaborated primary, secondary, and tertiary structure, larger proteins are likely to be more sensitive molecules as they could undergo degradation in a larger extent or could be affected by degradation pathways other than those that affect small proteins. Therefore, a large protein was used to evaluate the potential of the formulation strategy to achieve optimal stability and aerodynamic features. The chosen molecule was an anti-IL13 monoclonal antibody fragment (code name: CA582), which was provided by our partner UCB s.a and is about 10 times larger than insulin.

This molecule was also chosen because it provides an example of local lung delivery of proteins. Anti-interleukins are indeed an interesting class of molecules for a new targeted therapy of asthma. The formulations were again characterised for physical state, aerodynamic properties, and stability.

IV. EXPERIMENTAL PART

IV.1. Development and in vitro evaluation of highly dispersive insulin dry powder formulations for lung administration

Depreter F., Amighi K. 2010. *Eur. J. Pharm. Biopharm.* 76(3): 454-63

IV.1.1. Introduction

Despite the recent failure of the Exubera® inhaled insulin for commercial reasons, there is still a benefit in developing insulin formulations for inhalation. It is indeed a non-invasive alternative therapy with treatment satisfaction that is higher than for s.c. insulin, as observed in open-label studies (Arnolds and Heise, 2007). It might be particularly useful in patients with type 2 diabetes who fail on oral antidiabetic therapy and whose switch to insulin treatment is often delayed. Patients with needle phobia, who represent at least 10% of the population, is another targeted population (Siekmeier and scheuch, 2008). Moreover, most inhaled insulins that have been investigated to date exhibit pharmacokinetics and pharmacodynamics that more closely fit the profile of natural insulin secretion than s.c. regular insulins. This close fit could allow inhaled insulin to control post-prandial glucose more efficiently (Rave et al., 2005; Bellary and Barnett, 2006).

It is estimated that the bioavailability and bioefficacy of the current inhalation systems is approximately 8-15% compared to s.c. insulin (Patton et al., 2004; Mastrandrea and Quattrin, 2006; Arnolds and Heise, 2007). This poor performance can be mainly attributed to losses within the device and in the patient's mouth and oropharynx (Patton et al., 2004; Mastrandrea and Quattrin, 2006). Therefore, improvements in formulations and/or delivery devices could lead to better performance. The most widespread formulation strategy for a DPI consists of blending the drug with coarse and fine carrier particles, which improves handling, dispensing, and metering of the drug (Adi et al., 2008). Carbohydrates, in particular lactose, are widely used for this purpose (Lohrmann et al., 2007). Another strategy for improving the dispersion properties of powders is to use lipids as an alternative excipient to lactose. Among them, cholesterol and phospholipids are expected to be well tolerated in the respiratory tract, thanks to their endogenous nature (lung surfactant is composed of about 90% phospholipids and 3% cholesterol) (Pilcer and Amighi, 2010). Phospholipids and cholesterol have been investigated to produce SLMs. These have been used as carriers to enhance deposition of budesonide in the deep lung (Sebti and Amighi, 2006). Unlike the hydrophilic sugar excipients, the hydrophobic nature of cholesterol allows the absorption of the ubiquitous vapour to be reduced, leading to a reduction in capillary forces and improved

powder aerosolisation properties. Phospholipids, on the other hand, may contribute to improving aerodynamic properties by reducing the generation of electrostatic charges at the surface of the particles. In another study, the same composition of lipids was used to coat tobramycin microparticles, leading to FPFs of up to 68% (Pilcer et al., 2006).

In this work, the proposed formulation alternative, which is promising in terms of particle dispersibility and potential tolerance in lung tissue, was used to produce lipid-coated DPI formulations of insulin. Although the use of cholesterol and phospholipids seeks to improve the aerosolisation properties of inhalation particles, the use of these two excipients in the formulation of proteins could present several other advantages. The hydrophobic nature of cholesterol, by reducing the adsorption of water vapour during storage, could improve the long-term stability of the encapsulated protein as water is involved in all of the major stability issues of proteins (Daugherty and Mrsny, 2006). In addition, surface-active properties of phospholipids could help avoid protein adsorption at the air-water interface during drying and prevent aggregation of the molecules. Phospholipids, on the other hand, could promote the dispersion and dissolution of the active ingredient in the lining fluid of the lungs and, perhaps, act as an absorption enhancer. Liposomes made up of cholesterol and phospholipids have indeed been shown to enhance absorption of insulin (Liu et al., 1993; Ji et al., 2007; Chono et al., 2009), probably thanks to the stimulation of the surfactant recycling process (Hussain et al., 2004).

The techniques chosen for production of the formulations were High Pressure Homogenisation (HPH) as a micronisation technique, and spray-drying, which allows drying and coating of particles in a single step. Several powder compositions were formulated, including two "reference" formulations spray-dried without excipients. These were spray-dried either from a solution or a suspension, with the aim of studying the influence of the physical state of insulin on the physicochemical and aerodynamic characteristics of the powders. The influence of the coating level (as a percentage) was also evaluated.

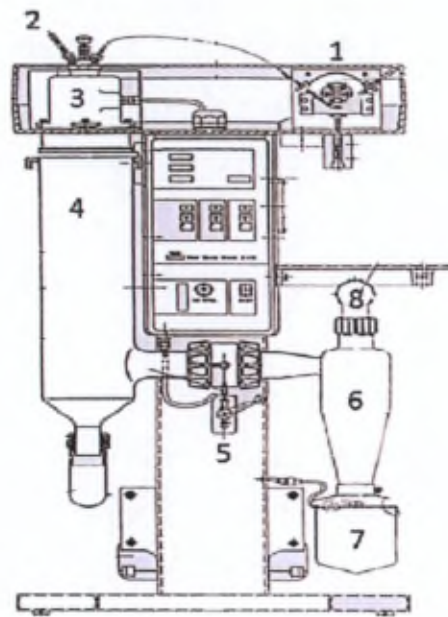


Figure 34: Representation of a Mini Spray-dryer (Buchi, 2008). 1) Peristaltic pump transporting the feed to the atomisation device, 2) compressed air input, 3) location of the atomisation device (two-fluid nozzle) and heated gas input, 4) drying chamber, 5) outlet temperature sensor, 6) cyclone for separation of the particles, 7) collecting vessel, 8) gas outlet connected to an aspiration motor

IV.1.2. Materials and Methods

IV.1.2.1. Materials

Raw recombinant human insulin was supplied as a micronised powder ($d_{(0.5)} = 9.30 \pm 0.03 \mu\text{m}$) from Sigma-Aldrich (St. Louis, MO). Cholesterol was purchased from Bufa (Uitgeest, The Netherlands). Phospholipon[®] 90H was purchased from Nattermann Phospholipids GmbH (Koln, Germany). This is a hydrogenated soy lecithin with more than 90% hydrogenated phosphatidylcholine, consisting of approximately 85% DSPC and 15% DPPC. Isopropanol and acetonitrile were of HPLC grade and were purchased respectively from Merck (Darmstadt, Germany) and Sigma-Aldrich (St. Louis, MO). Low viscosity silicone oil (20 cSt) was purchased from Dow Corning (Midland, Michigan). All other chemicals used were of analytical grade.

IV.1.2.2. Methods

IV.1.2.2.1. Production of the formulations

IV.1.2.2.1.1. Production of particles from a solution without excipients

A formulation of insulin particles without excipients was prepared by direct spray drying. **Spray-drying** is a process in which the compound of interest is first prepared in a liquid form, as a solution or suspension, and then sprayed in small droplets into a drying chamber where droplets are dried by heated air and then separated from the gas by means of a cyclone, electrostatic precipitator or bag filter (**Figure 34**) (Pilcer, 2008a; Sou et al., 2011). Droplet production causes the formation of very large surface areas that are exposed to the drying gas. This large surface area facilitates heat transfer from the heated drying gas to the atomised fluid particles, which results in evaporation of the solvent in seconds and mass transfer back into the gas phase. As a result, the drying material never reaches the inlet temperature of the drying gas, which makes the spray-drying process useful for drying heat sensitive substances such as proteins (Cal and Sollohub, 2010).

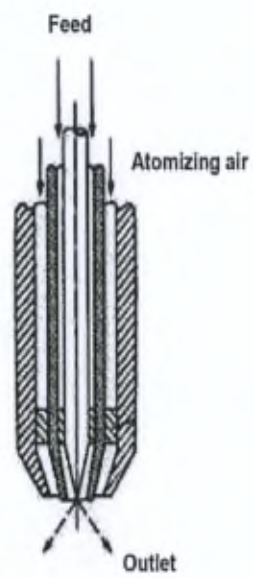


Figure 35. Atomisation principle of a two-fluid nozzle
(Cal and Sollohub, 2010)

Typical droplet mass median diameters in pharmaceutical spray-dryers range from less than 10 μm for pulmonary applications to upwards of 100 μm , which translates to a typical dry particle diameter range of 0.5-50 μm (Vehring, 2008). Four different types of atomisers are used for the majority of industrial spray-drying applications: rotary atomisers, pressure nozzles, two-fluid nozzles, and ultrasonic atomisers. In an atomiser with a two-fluid nozzle, the basic operation principle is based on the atomisation of the liquid feed within the stream of compressed carrier gas. Atomisation occurs due to the creation of high frictional forces over liquid surfaces, causing disintegration of the liquid into the spray droplets. In the example shown in **Figure 35**, the atomising gas meets the feed just beyond the nozzle, immediately at its outlet, resulting in the atomisation of the liquid (Cal and Sollohub, 2010).

There are many parameters that can be adjusted in the spray-drying process. The temperature and humidity of the drying gas affect the drying rate, which is a critical factor in the movement of compounds within the drying droplet and therefore the distribution of the compounds within the resulting particles (Vehring, 2008). Along with the flow rate of the drying gas, these factors also affect the final drying efficiency of the product (residual moisture content). Atomisation characteristics are other important parameters to control. In a two-fluid nozzle, the size of the droplets produced – and of the resulting particles – depends on the carrier gas properties (velocity and density) and the feed properties (solid content, surface tension, density, and viscosity) (Cal and Sollohub, 2010). The composition of actives and excipients in the feeding solution also influences the shape and density of the particles produced (Johnson, 1997). Hollow particles or particles with a sponge-like structure can, for example, be produced.

The insulin formulation was prepared using a Büchi mini spray dryer B-191 (Büchi Laboratory-Techniques, Flawil, Switzerland) equipped with a two-fluid nozzle and a high-performance centrifugation cyclone. The chosen operating conditions for spray-drying were inspired by the literature (Stahl et al., 2002) and were optimised for the feed flow rate, spraying air flow rate, inlet air temperature and drying air flow rate. The chosen parameters were: nozzle size, 0.7 mm; inlet temperature, 100 °C; resulting outlet temperature, 40 °C; spraying air flow rate, 800 l/h; drying air flow rate, 35 m³/h; feed flow rate, 5 g/min.

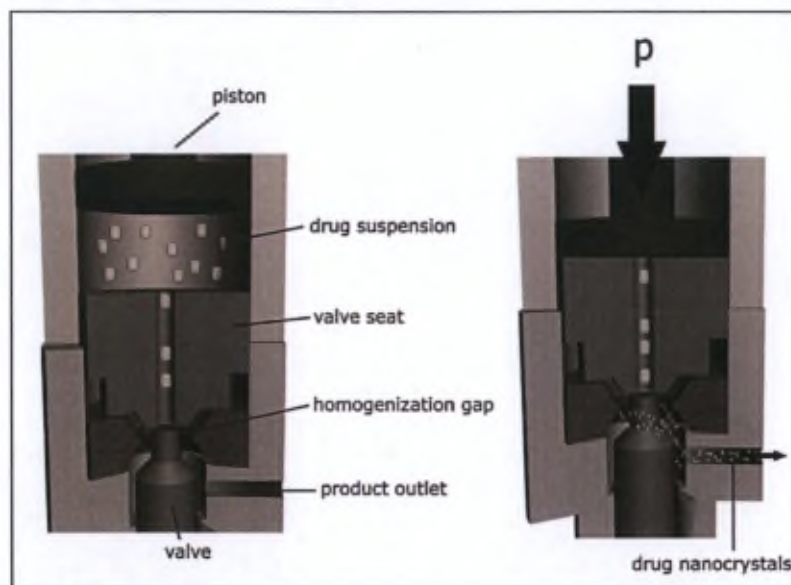


Figure 36. Basic principle of high pressure homogenisation using a piston-gap homogeniser (Junghanns and Müller, 2008)

The solution was composed of a 5 mg/ml insulin solution in water, prepared by alkalinisation with a few drops of 0.1 M NaOH followed by acidification to pH 7.4 with 0.1 M HCl. Batches of 100 ml were produced each time, resulting in the production of about 330 mg insulin powder (process yield around 66%).

IV.1.2.2.1.2. Production of particles from a suspension, with or without lipid coating

A lipid coating was made up of a mix of cholesterol and saturated phospholipids (Phospholipon® 90H). Saturated phospholipids have the advantage of presenting high transition temperatures ($T_c \sim 54$ °C for Phospholipon® 90H). However, a preponderant ratio of cholesterol was sought to limit the softening phenomenon during spray-drying as it has a melting temperature around 140 °C. A cholesterol/phospholipon ratio of 75:25 w/w was used, which has already been found to give appropriate size, density, and aerodynamic features to the coating of other active substances for inhalation, such as tobramycin and budesonide (Sebti and Amighi, 2006; Pilcer et al., 2006).

In order to obtain a final particle size distribution compatible with pulmonary administration, the particle size of the raw insulin powder was first reduced using HPH. HPH is a method for reducing the size of particles contained in a liquid medium, producing drug nano- or micro-suspensions. Effective particle size reduction in piston-gap high pressure homogenisers results from impaction forces brought in by intense interparticular collisions, fluid shear forces, and cavitation forces, the latter having the most pronounced effect in terms of size reduction (Kipp, 2004).

The suspension reservoir of the HPH (**Figure 36**) has a terminal diameter of approximately 3 mm and the diameter at the homogenising valve can be as narrow as 25 μm (size of the homogenising gap at a homogenising pressure of 1 500 bar or 22 000 PSI), thus leading to a very high streaming velocity (Müller et al., 2001). According to Bernouilli's law, which states that the flow volume of a liquid per cross-section is constant in a closed system, the reduction of the diameter through which the suspension is passed leads to a tremendous

increase in the fluid dynamic pressure and simultaneously to a decrease in the fluid static pressure at the homogenisation gap. This drop brings the static pressure below the vapour pressure of the liquid at ambient temperature, meaning that water starts to boil, with formation of gas bubbles (cavitation bubbles). When the suspension leaves the gap and the initial pressure is restored, these cavitation bubbles implode and the high energy accompanying this implosion (heat, turbulent flow, acoustic shockwaves) is responsible for breaking up the drug particles (Kipp, 2004; Keck and Müller, 2006; Pilcer, 2008a). The HPH particle size reduction efficiency is dependent upon the homogenising pressure applied, the number of homogenising cycles, the drug hardness characteristics, and possibly the processing temperature (Hecq, 2006). HPH is, in general, a rapid method of engineering drug nanosuspensions as reported protocols rarely exceed 20-30 homogenising cycles. These protocols generally involve the processing of previously micronised drugs and a gradual increase in homogenising pressure to prevent the blocking of the homogenising gap (since the gap aperture becomes smaller as the homogenising pressure is increased) (Hecq, 2006).

Insulin was suspended in isopropanol (2% w/v), and dispersion of the powder was ensured by 10 min of ultrasonication in a 40 kHz bath (Branson[®] 2510, Dietzenbach, Germany). The particle size was then reduced by HPH using an EmulsiFlex-C5 high-pressure homogeniser (Avestin Inc., Ottawa, Canada). Pre-milling low-pressure homogenisation cycles were first conducted on the insulin suspension to decrease further the particle size (10 cycles at 7 000 PSI and 10 cycles at 12 000 PSI). HPH was then finally applied for 30 cycles at 24 000 PSI. These cycles were conducted by recirculating the processed suspension directly into the sample tank (closed loop). Because HPH causes a sample temperature increase (increase of 30°C following 20 cycles at 24 000 PSI), all operations were carried out using a heat exchanger placed ahead of the homogenising valve, with the sample temperature maintained at 5 ± 1 °C. This permits limitation of the degradation of labile materials such as proteins. This protocol was chosen after particle size analysis of the samples between the different size reduction steps.

Lipids (cholesterol/phospholipids 75:25 w/w) in proportions of 0, 10, 20, 30 or 40% w/w in relation to the insulin load were then dissolved in a small volume (< 3 ml) of hot isopropanol (55 °C) before addition to the homogenised insulin suspension. Whereas insulin is insoluble

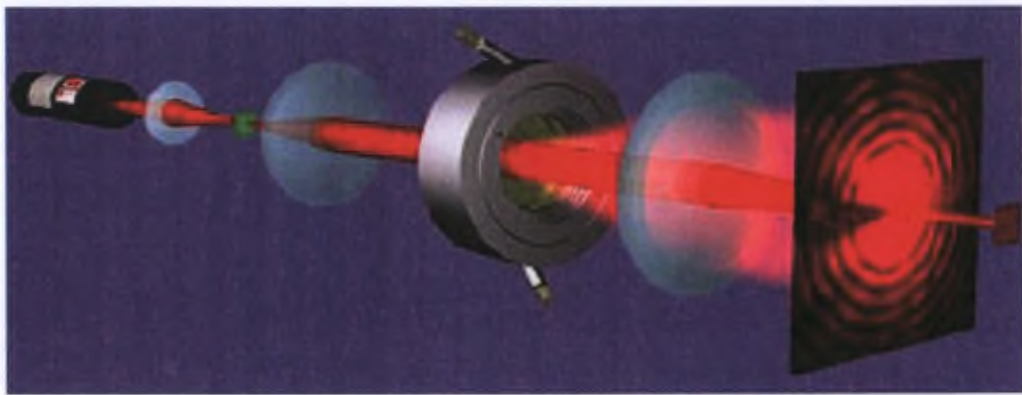


Figure 37: Simplified representation of laser diffraction equipment (Terry, 2007)

in isopropanol, lipids are soluble in it and will coat the micron-sized particles during atomisation. The suspension was then spray-dried using the same equipment as previously described. Some modifications were made to the commercial mini spray-dryer in order to improve its drying efficiency and to avoid partial melting or softening of the lipid excipients incorporated in the formulations (Sebti and Amighi, 2006; Pilcer et al., 2006). The following optimal spray-drying conditions were used for the coated and uncoated formulations: inlet temperature, 70 °C; resulting outlet temperature, 22-25 °C; spraying air flow rate, 800 l/h heated to 55 °C; drying air flow rate, 35 m³/h; solution feed rate, 2.5 g/min; nozzle size, 0.75 mm; cold air temperature, -5 °C, generated at 10 m³/h; cold water circulation in the jacketed cyclone, 5 °C. Following these conditions, the process yield was about 60% for an initial sample volume of 20 ml corresponding to 400 mg powder formulation.

IV.1.2.2.2. Particle size analysis

Particle size distributions were measured using laser diffraction. The principle of this technique is based on the diffraction in all directions of a monochromatic light beam by the particles being analysed. The sample is first dispersed at an adequate concentration in a suitable liquid or gas and is passed through the beam. The intensity of the diffracted light is proportional to the particle size. Larger particles correspond to a high intensity with a low angle of diffraction. By contrast, small particles diffract light with a small intensity but larger angles. Using an appropriate optical system (**Figure 37**), the diffracted light is measured using a multidetector, and the signal is converted into size distribution using a mathematical algorithm (taking into account the refractive and absorptive indices of the particle and the refractive index of the surrounding environment). The theories used to make this conversion (Mie theory and Fraunhofer theory) are complex and treat particle as spheres of equivalent volume. The size distribution is obtained as a volume distribution of particles (Terray, 2007).

The size of the particles is expressed in terms of volume mean diameter, $D_{[4,3]}$, which is the average diameter, balanced by the total volume of particles contained in each histogram class. This is the more representative value, since every single variation in size distribution will result in a change in $D_{[4,3]}$. Volume median diameter, $d_{(0,5)}$, corresponds to the size in

microns at which 50% of the sample is smaller and 50% is larger. In addition, $V\% < 5 \mu\text{m}$ is the total volume percentage of particles with a diameter below $5 \mu\text{m}$.

A liquid dispersion system was used in this work because it needs lower amounts of powder material than dry dispersion. However, this involves the control of many parameters, which have to be optimised for each particle type (Terry, 2007).

Dispersion: In order to measure the size of individual particles, powder must not contain any aggregates. If needed, surface-active agents and/or an ultrasonication sequence can be used to disperse particles. However, in some cases, an excessive ultrasonication time or intensity can also induce agglomeration or break the particles. Evaluation of particle diameters using various types and concentrations of surface-active agents has to be performed, as well as evaluation of the diameters over time by varying the duration and intensity of the ultrasonication step.

Dissolution: In order to avoid particle dissolution in the dispersion liquid during size measurement, the liquid has to be carefully selected and saturation of the liquid with the test substance has generally to be achieved. Dissolution phenomenon can be monitored by evaluation over time of the particle diameters and the obscuration rate of the laser beam.

Sedimentation: The agitation rate within the equipment must be sufficient to avoid particle sedimentation in the measurement cell. However, excessive turbulence of the liquid could lead to the formation of air bubbles, which introduces a bias in particle size measurement. Screening of the agitation rate has to be performed until a stable obscuration rate of the laser beam is obtained and no artefact peak from air bubbles is visible.

Particle size distributions were measured by laser diffraction using a Malvern Mastersizer 2000 laser diffractometer with a liquid sampling system (Hydro S, Malvern®, Malvern, Worcestershire, UK).

The insulin particles without lipid coating that were obtained from a solution or a suspension were measured using the following parameters: refractive index of insulin, 1.544; absorption index, 0.1; dispersing liquid, low viscosity silicone oil (20 cSt) containing 0.1% (m/v) Span 20 and 8% (v/v) isopropanol; agitation rate, 1 750 rpm; and obscuration, 4%. This low obscuration level was used to avoid multiple scattering. A 3 min ultrasonication sequence (70% power) was applied and the sizes were measured after stabilisation of the laser obscuration (2 or 3 minutes).

The insulin particles with a lipid coating were measured using the following parameters: refractive index of lipids, 1.6; absorption index, 0; dispersing liquid, distilled water containing 0.1% Polysorbate 80; agitation rate, 1 750 rpm; and obscuration, 4%. A 3 min ultrasonication sequence (70% power) was applied and the sizes were immediately measured.

IV.1.2.2.3. Particle morphology

Particle morphology was assessed by **Scanning Electron Microscopy (SEM)**, which is a technique that uses a beam of accelerated electrons to produce an image. The electron beam is produced by heating a metallic filament that functions as the cathode, generally a loop of tungsten. An anode placed immediately below the cathode forms powerful attractive forces for the electrons, causing them to accelerate down the microscope column towards the sample to be analysed. Before reaching the sample, the electron beam is condensed and focused to a very fine point on the material to be analysed. Once the electron beam hits the sample, the sample produces secondary electrons, which are collected, converted to voltage and amplified. The image viewed consists of thousands of spots of varying intensities that are dependent on the topography of the sample. The SEM column must always be in a vacuum in order to prevent electron beam instability. Moreover, since the SEM uses electrons to produce the image, it requires samples to be electrically conductive. In order to view non-conductive samples, such as most organic drugs, these must be covered with a thin layer of conductive material (gold, platinum, etc.) using a sputter coater (Goldstein, 2003; Pilcer, 2008a).

Evaluation of particle size and morphology was achieved by SEM (JSM-610, Jeol, Japan). Samples were scattered onto a carbon tape, which was then dusted to remove the excess. A 30 min depressurisation was applied in the coater (SCD030 sputter coater, Blazers Union, Liechtenstein) before coating with a platinum layer (pressure before coating, $3 \cdot 10^{-2}$ mbar; pressure under Ar, $6 \cdot 10^{-2}$ mbar; coating duration and power, 40 s and 40 mA). The acceleration voltage during observation was 8 kV.

IV.1.2.2.4. Insulin content

An evaluation of the content of insulin in the powders after the spray-drying process was carried out using a reverse-phase High Pressure Liquid Chromatography (HPLC) method, described in European Pharmacopoeia 6.0. This technique relies on the separation of proteins based on their net hydrophobicity. It can therefore be used for the evaluation of the global stability of the protein as degradation products such as unfolded, deamidated, and oxidated species all induce a change in the hydrophobicity or global charge of the molecule (Huff and Hannappel, 1997; Takemoto et al., 2001; Singh and Rao, 2002; Salnikova et al., 2008). Moreover, this technique also allows detection of insoluble aggregates. These are indeed removed before analysis through filtration on syringe filters (ProFill 0.22 μm , Alltech) and should therefore decrease the insulin content measured in the formulations. The equipment consisted of an HP 1100 series apparatus (Agilent Technologies, Santa Clara, CA, USA) equipped with a quaternary pump, an autosampler, an oven heated to 40 °C and a variable wavelength UV detector set at 214 nm. The separation system, as prescribed in the insulin monograph, was a 25 cm x 4.6 mm stainless steel (5 μm particle size) reversed-phase C18 column (Agilent Technologies, Santa Clara, CA, USA). The mobile phase (acetonitrile-phosphate buffer solution adjusted to pH 2.3 with phosphoric acid, 26:74) was run at a flow rate of 1.0 ml/min. Samples were dissolved in 0.01 M HCl. In the presence of lipids, a 15 min ultrasonication sequence in a 40 kHz Branson[®] 2510 bath was applied in order to dissolve the insulin, as well as a filtration step (ProFill 0.22 μm syringe filter, Alltech, Lexington, KY, USA) before injection of the samples. The mobile phase composition had to be adapted to a 28:72 acetonitrile/phosphate buffer ratio to avoid a small lipid peak appearing at the same retention time as insulin. The values presented are the average of at least 3 determinations.

A method validation was performed following guidelines from Caporal-Gautier et al., 1992. Linearity, accuracy, and precision were assessed and the results are presented in APPENDIX VII.

IV.1.2.2.5. Degradation products

Another important point to consider to assess conservation of the biological activity of insulin in the formulations is the possible presence of high molecular weight proteins (HMWP) arising from the aggregation of insulin. The formation of soluble and insoluble insulin aggregates has indeed been shown in accelerated stability studies of insulin in solution (Malik and Roy, 2011). Such insulin aggregates could modify the absorption kinetics of the insulin in the lungs or lead to a decreased bioavailability. Recently, protein aggregation has also been suspected to induce immunogenicity in the i.v. insulin preparations, although the type and size of aggregates involved (soluble or insoluble) is not yet determined (Sauerborn et al., 2010). The presence of HMWP was therefore investigated using size-exclusion chromatography (SEC), a method that can also help in detecting a loss of insulin tertiary structure as it is a separation technique based on the hydrodynamic diameter of the molecules.

The SEC HPLC method used is described in European Pharmacopoeia 6.0. We used an HP 1100 series apparatus (Agilent Technologies, Santa Clara, CA, USA) equipped with a quaternary pump, an autosampler, and a variable wavelength UV detector set at 276 nm. The separation system, prescribed in the insulin monograph, was a TSK-GEL® G2000SWXL column (Tosoh Bioscience, Tokyo, Japan) with hydrophilic silica beds (5 µm) and porosity of 125 Å, usable for globular protein separation between 5×10^3 and 1.5×10^5 Da, and run at 0.5 ml/min. The mobile phase was a mix of glacial acetic acid (15 V), acetonitrile (20 V), and an arginine R solution 1.0 g/l (65 V). Retention times were as follows: polymeric insulin complexes at 13-17 min; covalent insulin dimer at about 17.5 min; insulin monomer at about 20 min; salts at about 22 min.

System suitability was established using raw insulin (solution at 4 mg/ml in 0.01 M HCl) subjected to one week of stirring at 40 °C in order to obtain a sufficient percentage of covalent dimer to be detected (0.4%).

IV.1.2.2.6. Crystalline state

Powder X-Ray Diffraction (PXRD) is a powerful and widely-used tool for crystalline state evaluation. A parallel beam of monochromatic X-rays of a known wavelength is required for PXRD analysis. Striking a pure anode of a particular metal with high-energy electrons in a sealed vacuum tube generates X-rays that may be used for X-ray diffraction. By the right choice of metal anode and energy of accelerated electrons, a known wavelength (i.e., energy) will dominate the X-rays generated. Copper (Cu) X-ray tubes are most commonly used for X-ray diffraction of inorganic materials. The wavelength of the strongest Cu radiation emitted ($K\alpha$) is approximately 1.54 Å. The parallel beam of X-rays is directed at the powdered specimen. The interaction of X-rays with the sample creates secondary “diffracted” beams (actually generated in the form of cones) of X-rays related to interplanar spacings in the crystalline powder according to the mathematical relation Bragg’s Law:

$$n\lambda = 2d \sin\theta$$

where n is the order of reflection

λ is the wavelength of the incident X-rays

d is the interplanar spacing generating the diffraction and

θ is the diffraction angle (recorded as 2θ by convention)

The angles and intensities of diffractions are recorded electronically using a detector, resulting in a plot of 2θ (horizontal axis) vs. intensity (vertical axis) for the sample. If the sample is amorphous, then X-rays are not coherently scattered and no peak can be observed (Pecharsky and Zavalij, 2009).

Diffraction patterns were determined using a Siemens diffractometer D5000 (Siemens, Munich, Germany) with a Cu line as the source of radiation ($\lambda_1 = 1.5406$ Å, $\lambda_2 = 1.54439$ Å), and standard runs using a 40 kV voltage, a 40 mA current, and a scanning rate of $0.02^\circ/\text{min}$ over a 2θ angle range of $2-70^\circ$. The degree of crystallinity was evaluated by modelling the amorphous and crystalline areas using a pseudo-Voigt function (Topas fitting software) (Cerqueira et al., 2000).

IV.1.2.2.7. Residual solvents

IV.1.2.2.7.1. Water content

The residual water content of the powder formulations was assessed using **Thermogravimetric Analysis (TGA)**. TGA measures the amount and rate of weight change in a material, either as a function of increasing temperature or isothermally as a function of time, in a controlled atmosphere. It can be used to characterise any material that exhibits a weight change and to detect phase changes due to decomposition, oxidation, corrosion, moisture adsorption/desorption, and gas evolution. It is also able to determine the reaction kinetics associated with these transitions.

In this work, the residual water content in the formulations was assessed using a TGA Q500 apparatus (TA instruments, New Castle, USA). Runs in triplicate were set from 30 to 300 °C at 10 °C/min using samples of between 5 and 10 mg in a ceramic pan. The weight loss observed between 30 and 160 °C was attributed to water evaporation from the powder and the percentage of weight change was defined as the moisture content of the powder. However, this weight change was also expected to include a small loss of isopropanol, which is the only other potential solvent present in the powders. Weight loss occurring above 160 °C was probably due to thermal decomposition of insulin, which was observed through browning of the powder.

IV.1.2.2.7.2. Isopropanol content

As isopropanol was used as a dispersing solvent during the production of the formulations obtained from a suspension, the residual content was determined in two of these formulations, namely the 0% and 20% lipid-coated formulations. This was done in anticipation of the fact that these formulations were selected to be administered to patients for a phase I pharmaco-scintigraphic study. The isopropanol content was assessed using **gas chromatography (GC)**. GC is a method that allows the separation and quantification of molecules that are naturally present as a gas or that can be vaporised.

Table VIII. Commercial inhalation devices tested for comparison of their deaggregation efficiency.

Device	Type	Intrinsic resistance (approximative flow rate to reach 4 kPa pressure drop)	Main commercial formulations
Aerolizer® Novartis, Basel, Switzerland	Unit-dose	Low (100 l/min)	Foradil® (formoterol) Beclophar® (beclomethasone) Miflonide® (budesonide)
Spinhaler® Sanofi-Aventis, Paris, France	Unit-dose	Low (120 l/min)	Lomudal® (Na cromoglycate)
Handihaler® Boehringer Ingelheim, Ingelheim, Germany	Unit-dose	High (40 l/min)	Spiriva® (tiotropium)
Diskus® GSK, Brentford, UK	Multiple-unit dose	Intermediate (80 l/min)	Serevent® (salmeterol) Flixotide® (fluticasone propionate) Seretide® (salmeterol/fluticasone propionate)
Novolizer® Meda, Solna, Sweden	Multi-dose	Intermediate (70 l/min)	Novolizer budesonide® Novolizer Salbutamol® Novolizer Formoterol®
Turbohaler® AstraZeneca, Lund, Sweden	Multi-dose	High (45 l/min)	Pulmicort turbohaler® (budesonide) Symbicort turbohaler® (budesonide/formoterol) Oxis turbohaler® (formoterol) Bricanyl turbohaler® (terbutaline)

The following parameters were used: GC equipment, "Auto/HRG/MS" MFC 500 Instrument (Carlos Erba, Milano, Italy); capillary column, CP-Sil 5CB (polydimethyl siloxane phase) 25 m x 0.32 mm (Chromopack, Belgium); gas vehicle, He; pressure, 50 kPa; injector temperature, 200 °C; detector, flame ionisation (FID); detector temperature, 240 °C; column temperature, 40 °C for 10 min then a gradient of 30 °C/min to 200 °C, maintained for 15 min; acquisition time, 25 min; and injected volume, 1 µl.

Samples were put into solution in dimethylformamide (DMF) containing ethyl acetate as an internal standard. A calibration curve was constructed with standards of increasing concentrations in isopropanol (250 to 10 000 ppm).

IV.1.2.2.8. Aerodynamic features

IV.1.2.2.8.1. Selection of the inhalation device

An experiment was set up to compare the efficiency of several commercial inhalation devices in obtaining good powder dispersion. This was done to select the device to be used in the aerodynamic characterisation of the insulin formulations. The experiment also served as a support for the design of a DPI device by some of the research teams in the NEOFOR project. It was indeed useful to compare various devices currently on the market to select structural features that could be adopted.

Six commercial devices (**Table VIII**) were tested at three different flow rates (30, 60, 100 l/min) with a microfine inhalation grade lactose powder (Lactohale[®] LH300, Friesland Foods, The Netherland) with a median diameter ($d_{(0.5)}$) of $3.6 \pm 0.3 \mu\text{m}$ and a mean diameter ($D_{[4,3]}$) of $4.3 \pm 0.2 \mu\text{m}$, measured using a Malvern[®] Mastersizer 2000 laser Diffractometer (dry method). This micronised lactose material was chosen as it is in a size range comparable with the particle size of most active particles found in the formulations for inhalation. It is also, due to its small particle size, a highly cohesive powder that will therefore allow a large range of deaggregation efficiency to be seen. Two devices, derived from the Aerolizer[®] device but with reduced air inlet (1/3 and 2/3 of the original air inlet), were produced by one of the NEOFOR partners (Optim Test Center) and were also included in the study. This was

done to test the influence of increased airflow velocity within the device, which could increase the R_i of the device but could also increase its deaggregation efficiency.

The Spraytec[®] laser diffraction technique (see IV.1.2.2.8.4.) was chosen to assess device efficiency as it is designed to measure real agglomeration state and particle size distribution in an aerosol cloud under simulated breathing conditions.

For the testing of unit-dose devices (i.e. Aerolizer[®], Spinhaler[®], and Handihaler[®]), n° 3 HPMC capsules (Capsugel, Bornem, Belgium) were loaded with 25 ± 1 mg powder (Lactohale[®] LH300), which is a common powder load in commercial formulations for inhalation (e.g. Foradil[®], Lomudal[®]).

For the testing of the only multiple unit-dose device selected (i.e. Diskus[®]), the powder load was 3.0 ± 0.5 mg, which was the maximal dose that could be inserted in the blister cavity. A single empty blister was filled each time with the lactose and placed, without replacing the aluminium foil cover, in the inhalation chamber of the device. For the testing of multi-dose devices (i.e. Novolizer[®] and Turbohaler[®]), the powder reservoir was opened and loaded with the same powder mass as in the commercial formulations. The reservoir and device were then resealed, as hermetically as possible, using glue.

Measurements (n=10) were performed at three different flow rates (30, 60, and 90 l/min), with a duration adapted to each flow rate (8, 4 and 2.7 s, respectively) to obtain an air passage of 4 l within the device, which corresponds to a standardised vital capacity of the lungs. Test flow rates of 30 to 90 l/min were selected to study the variation in device efficiency over a range of inspiratory efforts. The device that presented the best deaggregation efficiency was selected for the characterisation of the formulations developed.

IV.1.2.2.8.2. Uniformity of the delivered dose

The delivered dose is the dose delivered from the inhaler. The Uniformity of the Delivered Dose (UDD) can be measured following a procedure described in European Pharmacopoeia

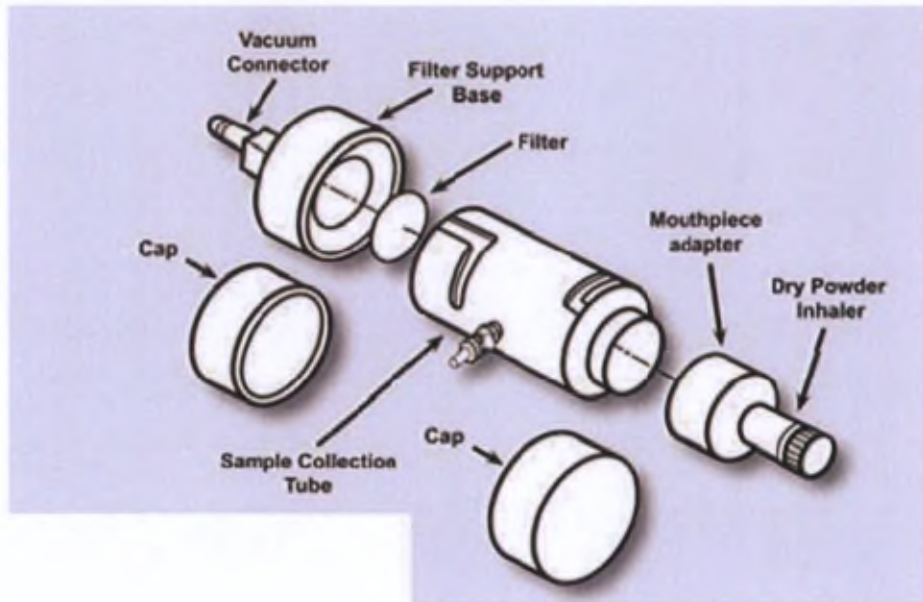


Figure 38. Schematic representation of a UDD device for DPIs testing (Copley Scientific, 2010)

6.0 for the assessment of powders for inhalation (section 2.9.18.). The dose collection apparatus must be capable of quantitatively capturing the delivered dose (DD). The apparatus consists of a glass fibre filter placed on an open-mesh filter-support, a collection tube that is screwed to the filter-support base, and a mouthpiece adapter to ensure an airtight seal between the collection tube and the mouthpiece (**Figure 38**). The UDD device is connected to an air pump that is operated at an airflow rate between 15 and 100 l/min (depending on the intrinsic resistance, R_i , of the device) to produce a pressure drop of 4 kPa over the inhaler, corresponding to a standardised inspiratory effort. The duration of the operation is chosen to achieve 4 l of air passing through the device. The content of the UDD device is quantitatively collected and the amount of active substance is determined. The procedure is repeated 10 times for each formulation and the preparation complies with the test if nine out of the ten results lie between 75% and 125% of the average value, and all lie between 65% and 135%.

A UDD device (Copley Scientific Ltd, Nottingham, UK) was used for collection of the doses. An Aerolizer[®] inhaler (Novartis, Switzerland) was first filled with a n° 3 HPMC capsule (Capsugel, Bornem, Belgium) loaded with powder corresponding to 5 ± 0.5 mg of insulin. HPMC capsules were used because gelatin capsules have a tendency to break during testing and to produce agglomerates during particle size measurements. The Aerolizer[®] is a unidose device of simple design with low internal resistance. The airflow rate was set to 100 l/min for 2.4 s. After particle deposition, the UDD device was rinsed with 0.01 M HCl and the liquid was quantitatively collected in a volumetric flask. This procedure was repeated for 9 other capsules. Drug deposition in the UDD device was then determined using the HPLC method previously described (section IV.1.2.2.4.). All of the formulations were tested in triplicate.

IV.1.2.2.8.3. Impaction measurements

Powder aerodynamic evaluation is generally performed using inertial impaction techniques, which predict the deposition of particles within the lungs. Aerosol exiting the device is suspended in an air stream with a defined airflow rate and passes through orifices of known dimensions. The output air stream is directed against a flat plate (impaction plate) that

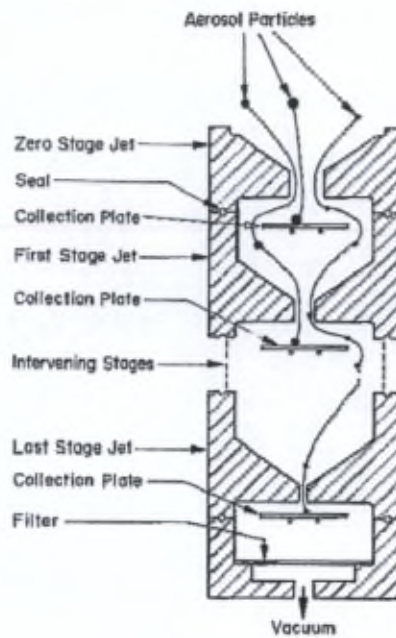


Figure 39. Schematic representation of the operating principle of impactors (US Pharmacopoeia 29th Edition, 2006)

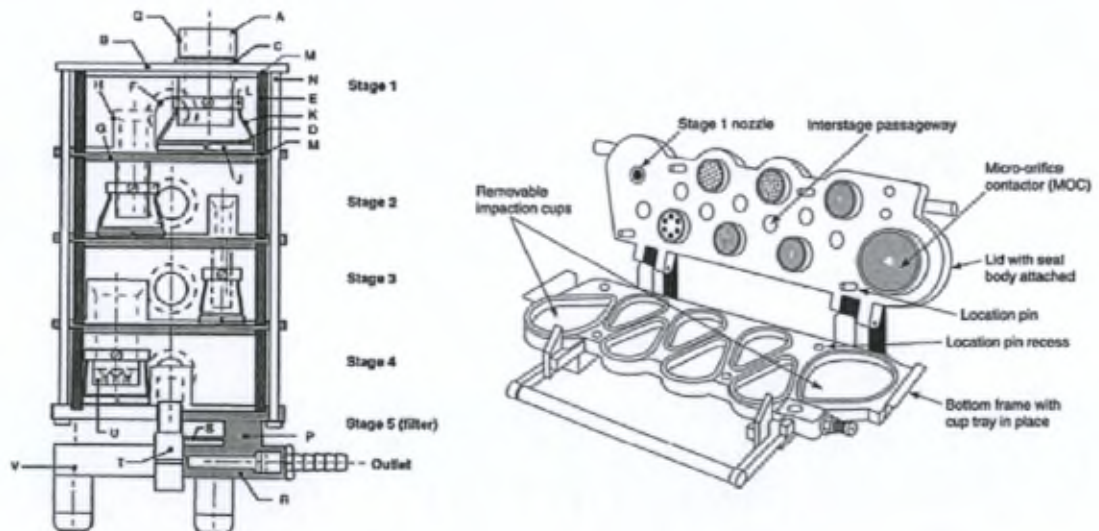


Figure 40. Representation of MsLI (left) and NGI (right) impactors (European Pharmacopoeia 7th Edition, 2011)

forms a 90° angle with the streamlines, which causes large particles to impact on the plate by inertia. Smaller particles, on the other hand, can follow the streamlines and avoid hitting the impaction plate. The principle can be repeated several times with decreasing orifice sizes, which creates increasingly higher air velocity and progressive impaction of smaller particles on the lower stages of the impactor (**Figure 39**) (Dunbar et al., 1998).

All impactors are made according to well-defined geometrical specifications (European Pharmacopeia 6.0., section 2.9.18), and the applied air flow rate is the only variable affecting the size of the particles impacted on a given stage of an impactor (Hinds, 1999). The flow rate and the duration of the experiment depends on the R_i of the inhaler and is chosen as described in the UDD experiment (IV.1.2.2.8.2.). Depending on the air flow applied, "cut-off" diameters can be calculated for each stage. They reflect the minimum aerodynamic diameter of the particles impacted at a given stage with 50% efficiency.

Four types of impaction devices are described in the European and US Pharmacopoeias: the glass impinger, the Andersen Cascade Impactor (ACI), the Multi-stage Liquid Impinger (MsLI), and the Next Generation Impactor (NGI), the latter two being the most widely used in continental Europe.

The **MsLI** apparatus (**Figure 40**) is arranged vertically and consists of 4 successive stages and a terminal filter (stage 5). An induction port or "throat", forming a 90° angle, is connected to the top of the MsLI to collect the largest particles. Samples are collected into an appropriate liquid medium in order to evaluate the influence of humidity on the aerodynamic behaviour of the particles. The MsLI can be operated at a range of flow rates, from 30 to 100 l/min.

The **NGI** apparatus (also presented in **Figure 40**) is arranged horizontally and consists of 7 successive stages and a micro-orifice collector (MOC). This MOC is a terminal impaction plate with 4032 holes of about 70 µm diameter, which eliminates the need for a final filter. A throat and an optional pre-separator are used to collect the largest particles before they enter the impactor. The device can be operated at a range of flow rates from 15 to 100 l/min, with at least 5 stages with cut-off diameters between 0.5 and 6.5 µm at all operating

flow rates. Unlike the MsLI, no liquid medium is used in the NGI. This impactor is equipped with removable impaction cups, which makes it easy to handle.

The Fine Particle Dose (FPD), Fine Particle Fraction (FPF), and Mass Median Aerodynamic Diameter (MMAD) are generally calculated by interpolation from the cumulative fraction curve of the active ingredient against the cut-off diameter of respective stages. The FPD is the mass of particles with an aerodynamic diameter of less than 5 μm , which are assumed to reach the lungs. The FPF expresses the percentage of particles with an aerodynamic diameter of less than 5 μm . In this work, the FPF is expressed as a percentage of the metered dose, which is the total drug dose collected after the impaction experiment (sum of the doses collected in device, throat, and stages 1-5). The MMAD corresponds to the diameter above and below which are each 50% of the powder mass (Courrier et al., 2002).

In this work, powder aerodynamic evaluation was performed using a MsLI (Copley Scientific Ltd, Nottingham, UK). An Aerolizer[®] inhaler (Novartis, Switzerland) was first filled with a n^o 3 HPMC capsule (Capsugel, Bornem, Belgium) loaded with powder corresponding to 5 ± 0.5 mg of insulin. Five capsules were taken for each test. The applied air flow rate was 100 l/min and the duration of the experiment was 2.4 s. At this flow rate, the cut-off diameters for stages 1, 2, 3, and 4 were, respectively, 10.1, 5.3, 2.4, and 1.3 μm .

The MsLI was filled with 20 ml of filtered 0.01 M HCl in each stage. After particle deposition, fractions were quantitatively collected in volumetric flasks and the volume adjusted with 0.01 M HCl. Two flasks were also dedicated to the collection of the powder that remained in the inhalation device and in the throat. Drug deposition in the device, the throat, the four stages, and the filter was determined by the HPLC method previously described. Each test was repeated three times. Data interpretation was performed using the CITDAS software (Copley Scientific Ltd, Nottingham, UK).

IV.1.2.2.8.4. Spraytec[®] measurements

The Spraytec[®] (Malvern, UK) is a laser diffraction apparatus equipped with an inhalation cell specifically modified for measuring the particle size distribution (PSD) generated from



Figure 41. Spraytec[®] device connected to a multi-stage liquid impinger (Pilcer, 2008a)

medicinal aerosols, including MDI, DPI, and nebulisers. It is equipped with an inhalation cell and uses a very rapid data acquisition rate (every 0.4 milliseconds) and a mathematical algorithm to measure sizes in large aerosol concentrations (obscuration of up to 95%). This allows the particle size properties of DPIs to be measured under simulated breathing conditions in order to collect information on the real agglomeration state of the powder. This is unlike the classic laser diffraction technique, in which particles are in the individualised state (Haynes et al., 2004). As in classical laser diffraction, the $d_{(0.5)}$, $D_{[4.3]}$, and $V\% < 5 \mu\text{m}$ can be determined.

The Spraytec[®] device is generally used in-line with an impaction device such as an MSLI (see **Figure 41**), which allows simultaneous sizing of the aerosol by the two techniques (Pilcer et al., 2008b). However, it is important to note that laser diffraction determines geometric size distributions, whereas impaction techniques provide aerodynamic diameters.

The acquisition parameters were as follows: triggering mode, level of 10%; data acquisition rate, 2 500 Hz; acquisition duty cycle, 50%; test duration, 3 000 ms; and refractive index, 1.50 (standard opaque particles).

IV.1.2.2.9. Stability study

A three-month stability study was performed on two of the formulations obtained from a suspension, namely the 0% and 20% lipid-coated formulations. This was done in anticipation of the fact that these formulations were selected to be administered to patients during a phase I pharmaco-scintigraphic study, and to evaluate the effect of a lipid coating on the moisture uptake of the powders. The two formulations were freshly produced and size 3 HPMC capsules (Capsugel, Bornem, Belgium) were filled with 5.0 mg ($\pm 2\%$) insulin. The capsules were shared out and stored in 50 ml high density polyethylene containers with tamper-evident airtight screw caps (30 capsules/container). The containers were stored in chambers with a controlled atmosphere for temperature and relative humidity (RH). Three storage conditions were chosen: 25 °C/60% RH, 40 °C/75% RH, and a fridge condition (2-8 °C, containers maintained in a dessicator containing silica gel beads). The formulations were

analysed at t=0, t=1 month and t=3 months for insulin content, HMWP content, residual water, and isopropanol content. Evaluation of the UDD and aerodynamic characterisation by impaction were also performed.

IV.1.3. Results and discussion

Table IX gives an overview of all spray-dried (SD) formulations studied. In the coated formulations, lipid coating represented 10-40% of the insulin mass. Two “reference” formulations without excipients were also produced, which were spray-dried either from a solution or a suspension of insulin.

Table IX. Physical state of insulin and composition of the insulin formulations (before and after spray-drying)

	physical state of Insulin (Before spray-drying)	Liquid Composition (Before spray-drying)		Solid Composition (After spray-drying)	Coating composition
		Insulin (%) (w/v)	Lipids (%) (w/v)	Lipids (%)*(w/w)	Cholesterol/ Phospholipon (%) (w/w)
F1	solution	0.5	0	0	/
F2	suspension	2	0	0	/
F3		2	0.2	10	75/25
F4		2	0.4	20	75/25
F5		2	0.6	30	75/25
F6		2	0.8	40	75/25

* Data expressed as a percentage of insulin weight

Table X. Particle size characteristics, insulin content, and water content of the formulations (mean \pm S.D., n=3)

	Particle size characteristics				HPLC insulin content (%)	Water content (%)
	Before spray-drying (suspension) <i>d</i> (0.5) (μm)	After spray-drying (powder)				
		<i>d</i> (0.5) (μm)	<i>D</i> [4, 3] (μm)	% < 5.0 μm (%)		
Raw insulin	/	9.30 \pm 0.03	9.55 \pm 0.05	21.8 \pm 0.8	100.0*	4.8 \pm 0.1
F1	/	2.05 \pm 0.07	2.25 \pm 0.08	97.5 \pm 0.9	98.4 \pm 1.1	6.1 \pm 0.1
F2	2.10 \pm 0.05	2.11 \pm 0.03	2.29 \pm 0.06	98.1 \pm 0.5	99.2 \pm 1.1	4.9 \pm 0.1
F3	2.10 \pm 0.04	2.09 \pm 0.05	2.37 \pm 0.06	95.9 \pm 0.6	100.4 \pm 0.4	3.7 \pm 0.1
F4	2.25 \pm 0.05	2.32 \pm 0.09	2.61 \pm 0.05	93.8 \pm 0.6	100.2 \pm 0.4	2.6 \pm 0.1
F5	2.15 \pm 0.07	2.18 \pm 0.05	2.65 \pm 0.06	92.4 \pm 0.6	100.5 \pm 0.6	2.4 \pm 0.1
F6	2.16 \pm 0.07	2.19 \pm 0.03	2.58 \pm 0.07	93.1 \pm 0.8	99.1 \pm 1.2	2.3 \pm 0.1

* Raw insulin (untreated material) was used as a reference for HPLC measurements

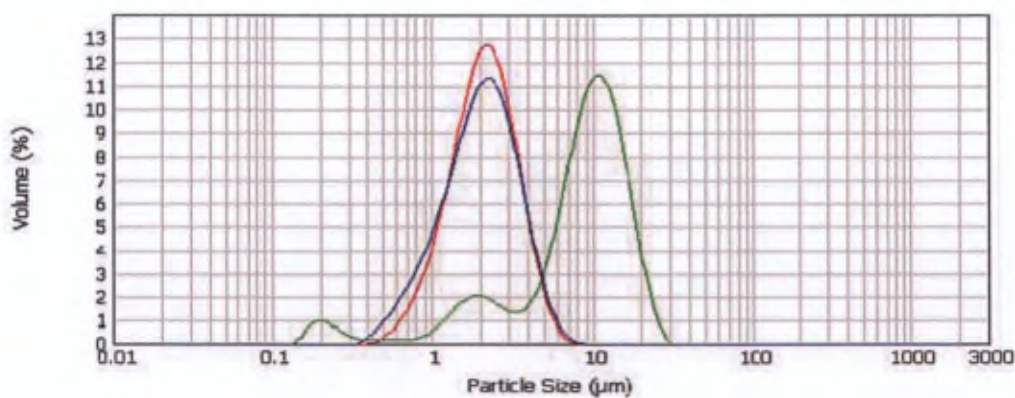


Figure 42. Particle size distributions measured by laser diffraction of raw insulin material (green line), formulation F1 (red line), and formulation F6 (blue line)

IV.1.3.1. Physicochemical characterisation of the formulations

The laser diffraction results presented in **Table X** and **Figure 42** show that the starting insulin material (raw insulin) had a median diameter of $9.30 \pm 0.03 \mu\text{m}$ and a bimodal distribution, which is not compatible with pulmonary administration. For all SD formulations, the median diameter could be reduced to values between $2.05 \pm 0.07 \mu\text{m}$ and $2.32 \pm 0.09 \mu\text{m}$, which is a size range well-suited for peripheral lung deposition and subsequent systemic absorption. The size distributions were monodisperse and exhibited quite a narrow range (**Figure 42**), with 83-90% of particles between 1.0 and 5.0 μm . No major differences were observed in the size distributions between the different formulation types, even for the coated formulations with a high content of lipid coating. The median particle sizes were 2.05 μm and 2.19 μm for the F1 (uncoated) and F6 (40% lipid coating) formulations, respectively. Particles obtained after spray-drying a suspension of insulin were as small as those obtained from a solution. This was achieved thanks to the size reduction step using HPH. Moreover, for each formulation, the median particle size was not significantly different before or after spray-drying (Student t-test, $p > 0.05$, N.S.), indicating that a single insulin particle was contained in each droplet during spray-drying of the suspensions and that no aggregation of particles occurred.

The absence of degradation of the insulin molecule during the HPH and spray-drying processes was evaluated using an reverse-phase HPLC method. The method exhibited appropriate linearity in the range 0.01-2 mg/ml (see APPENDIX VII). However, appropriate accuracy, characterised by a mean recovery of $99.4 \pm 1.7\%$, was only obtained between 0.05 and 2 mg/ml. On the other hand, appropriate precision of the method (inter-day CV% of 1.0%) was only found between 0.1 and 2 mg/ml. The HPLC method was therefore considered to be validated between 0.1 and 2 mg/ml. As shown in **Table X**, the content of insulin lies within pharmacopoeia requirements for all tested formulations, with insulin recovery between 98.4% and 100.5%. This indicates good global stability of the protein as regards degradation products such as unfolded, deamidated, and oxidated species, as well as insoluble aggregates.

In order to confirm the conservation of the biological activity of insulin in the formulations, we tested the presence of high molecular weight proteins using SEC. The formation of 0.4% soluble covalent dimer was obtained after 1 week's stirring at 40 °C of a 4 mg/ml solution in 0.01 M HCl. Appropriate resolution of the monomer and dimer peaks was achieved in this condition, with a peak-to-valley ratio of 2.0 (**Figure 43 A-B**). As a minimal value of 2.0 is required in the method description (Eur. Pharm. 6.0.), 0.4% was considered to be the quantification limit for the covalent dimer. Chromatograms obtained for all insulin formulations (**Figure 43 D-E**) did not exhibit detectable peaks, aside from the insulin monomer peak. The content of HMWP was therefore considered to be below the quantification limit of 0.4% in all cases. This is of interest, as formation of soluble covalent dimers can also occur with insulin in the dry state, as can be seen in **Figure 43 C**, where raw insulin powder stored at 40 °C for 6 months exhibited a covalent dimer content as high as 13.4%.

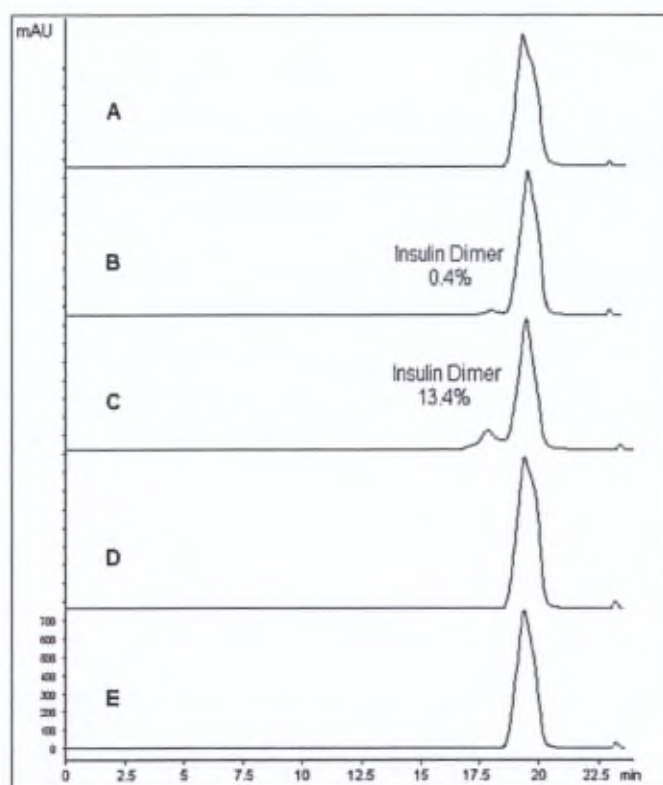


Figure 43. Size-exclusion chromatograms of raw insulin material: A) freshly prepared solution, B) solution under stirring at 40 °C for one week, C) powder stored at 40 °C for 6 months, and of insulin formulations: D) freshly prepared solution of F2, E) freshly prepared solution of F4

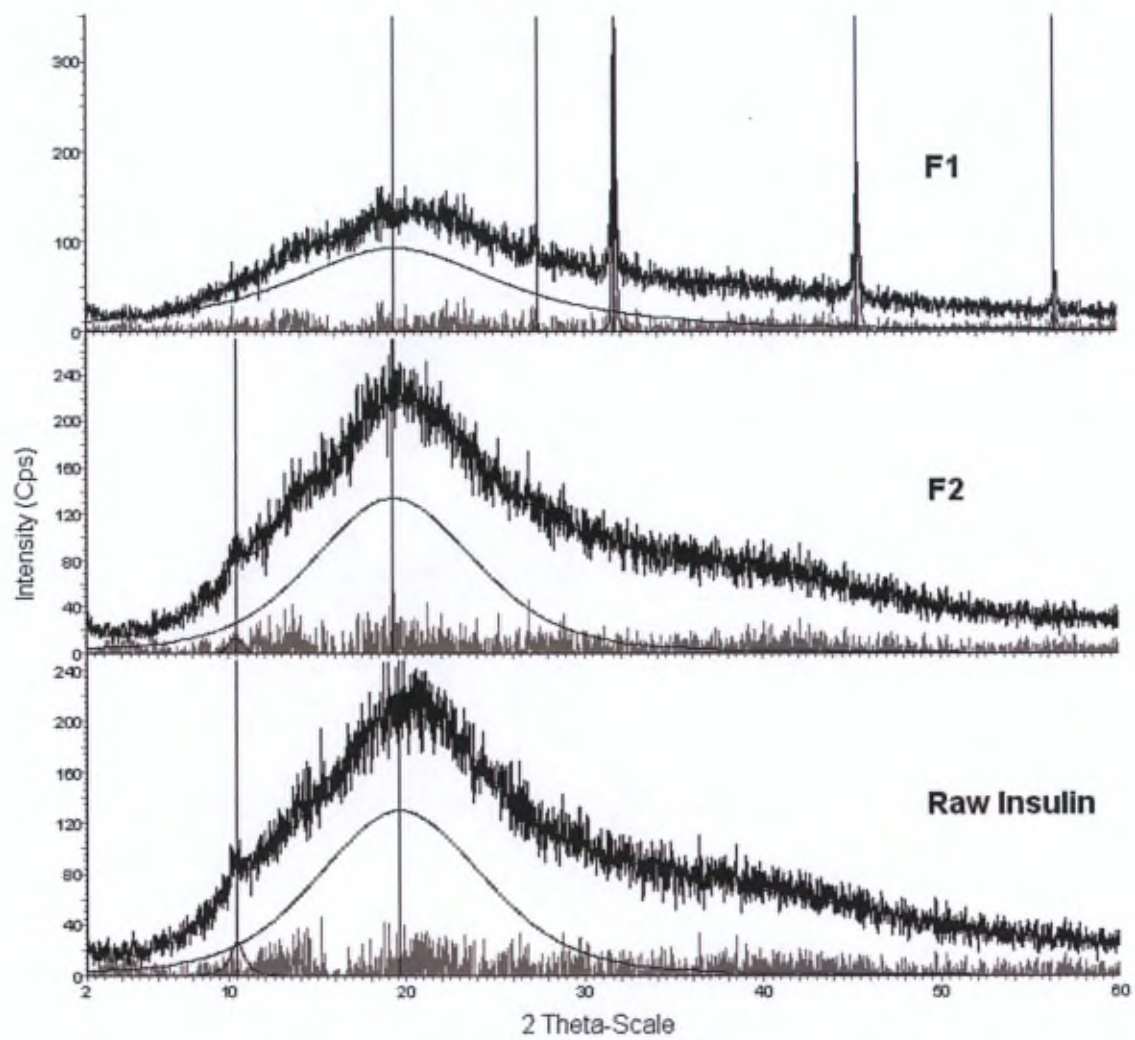


Figure 44. X-ray powder diffraction patterns of raw insulin, F1, and F2 formulations, and modelling of the amorphous and crystalline areas using a pseudo-Voigt function

The PXRD spectra of the untreated insulin (raw insulin) and the different formulation types are shown in **Figure 44**, with modelling of the amorphous and crystalline area using a pseudo-Voigt function. This is an empirical peak-shape function that fits the profile of each diffraction peak. The ratio of the area of the crystalline peaks to the total area of the spectrum is considered to be representative of the proportion of crystalline phase (Pecharsky and Zavalij, 2009). Some weak diffraction peaks appeared at 2θ angles of 10.4° and 19.5° for raw insulin, and the degree of crystallinity was determined to be $2.3 \pm 0.1\%$. For the F1 formulation produced from an insulin solution, these peaks almost fully disappeared, suggesting that the insulin was in amorphous form. This was probably due to the very fast solvent evaporation during spray-drying, which does not allow sufficient time for crystal nucleation, crystal growth, and polymorph transitions when the solubility limit of insulin is reached at the surface of the droplet. However, other peaks at 31.6° and 45.4° were detected in the XRD pattern, which were due to the presence of NaCl crystals (from neutralisation of the acidic solution of insulin with NaOH). These peaks were identified by comparison with a NaCl control sample. The pattern of the F2 formulation produced from an insulin suspension exhibited the same peaks as raw insulin, with a degree of crystallinity of $0.8 \pm 0.1\%$. This decreased crystallinity could be due to the decreased particle size in comparison with raw insulin powder. It is known that in X-ray diffraction, the peak height is affected by the crystal size and crystallinity of the particles (Lee et al., 2006).

In order to detect any potential change in the crystal state of the lipids, blank particles were first prepared by spray-drying a mixture of cholesterol and Phospholipon 90H (75:25) dissolved in isopropanol. The same spray-drying conditions were used as for the preparation of the insulin formulations. As shown in **Figure 45**, the PXRD pattern of the SD blank lipid particles exhibited peaks at 14.1° , 15.3° , 16.9° , 17.3° and 18.0° that could be attributed to the crystalline raw cholesterol, which contains only $2.1 \pm 0.3\%$ amorphous phase. However, the percentage of amorphous phase in the blank particles was evaluated to be $30.1 \pm 0.1\%$. Lipids were present in a partially amorphous state as they are dissolved in isopropanol and solidified by rapid solvent elimination during spray-drying. The lipid-coated insulin formulations all exhibited patterns that correspond to combining the pattern of the F2 formulation produced from an insulin suspension with that of the SD lipids, as can also be seen in **Figure 45**. The degree of crystallinity in these powders gradually increased from $6.8 \pm$

0.1% for the F3 formulation to $19.9 \pm 0.1\%$ for the F6 formulation, in accordance with the increased proportion of lipids. This proportional increase in the degree of crystallinity showed that the lipids are also about 30% in the amorphous phase in the coated formulations. The presence of amorphous insulin and lipids in the formulations could be an issue as these may have a tendency to crystallise slowly during storage and lead to a change in the physical properties of the powders. The conservation of these properties over time will therefore have to be evaluated. However, in a previous study carried out in our laboratory, it was shown that formulations made up of a physical blend of 98% SD lipid carrier particles (cholesterol/Phospholipon 90H in a ratio of 90:10 w/w) and 2% budesonide particles exhibited no change in their XRD patterns and degree of crystallinity after 12 months at 25 °C and 60% RH (Sebti and Amighi, 2006).

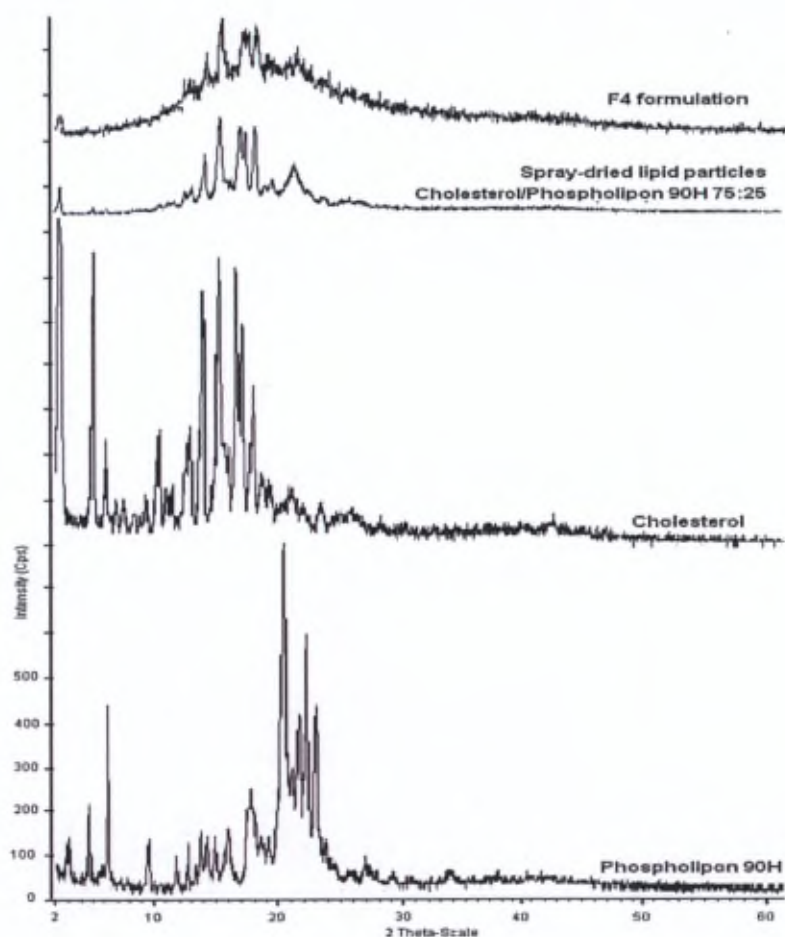


Figure 45. X-ray powder diffraction patterns of raw lipid excipients, spray-dried blank lipid particles (cholesterol/Phospholipon 90H 75:25 w/w), and the F4 formulation

As the amount of water adsorbed around the particles in a DPI formulation influences the stability of proteins and controls the magnitude of capillary forces that cause particle aggregation, the residual moisture content was measured using TGA. The water content was estimated to be about 4.8% for raw insulin, 6.1% for the F1 formulation, and 4.9% for the F2 formulation (**Table X**). The percentage of water in the lipid-coated formulations gradually decreased (from about 3.7% to 2.3%) with the increased proportion of lipid coating. The use of isopropanol rather than water as a dispersing solvent and the presence of a lipid coating around the insulin particles decreased the re-adsorption of water by the particles, which should enhance the physical stability of the macromolecule in long-term storage. More generally, the use of DPIs seems particularly favourable for the administration of peptides and proteins, due to the removal of water from the system. Their use also provides longer storage stability and avoids the need to store and distribute the final product in a cold-chain.

As isopropanol is used during the manufacture of the formulations obtained from a suspension, the residual solvent content was determined in the F2 and F4 formulations, which were selected to be administered to diabetic patients during a phase I pharmacoscintigraphic study. According to the ICH guidelines (CPMP/ICH/283/95), isopropanol is a class III solvent, a group that comprises solvents with low toxic potential in humans and for which the permitted daily exposure (PDE) is above 50 mg. No health-based exposure limit is required for class III solvents in final products but, as a precaution, we calculated the concentration limit in the same way as for class II solvents using the following equation:

$$\text{Concentration (ppm)} = 1.000 \times \text{PDE (mg)} / \text{Daily dose (g)}$$

The daily dose in this evaluation is generally fixed at 10.0 g and the concentration limit would therefore be 5 000 ppm. The two formulation types were under the limit of acceptable isopropanol residual content, with values of $2\,470 \pm 30$ ppm and $2\,810 \pm 30$ ppm for the uncoated and coated formulations, respectively.

Table XI. Comparison of the particle size distributions obtained for an inhalation grade lactose powder with different inhalation devices. Measured with the Spraytec[®] laser diffractometer using an acquisition rate of 2 500 Hz and an trigger set up on level 10.0 (mean \pm SD, n = 10).

	d(0.5) (μm)			D[4,3] (μm)			V < 5 μm (%)		
	30 l/min	60 l/min	90 l/min	30 l/min	60 l/min	90 l/min	30 l/min	60 l/min	90 l/min
Aerolizer [®] normal air inlet	6.0 \pm 0.5	4.37 \pm 0.18	5.4 \pm 0.5	6.7 \pm 0.9	6.9 \pm 0.8	8.4 \pm 1.4	42 \pm 3	56.6 \pm 1.4	49 \pm 2
Aerolizer [®] 2/3 air inlet	5.4 \pm 0.3	4.5 \pm 0.2	5.3 \pm 0.3	5.8 \pm 0.4	6.8 \pm 0.5	7.9 \pm 2.0	46 \pm 2	55 \pm 2	53 \pm 5
Aerolizer [®] 1/3 air inlet	4.9 \pm 0.3	4.9 \pm 0.3	5.5 \pm 0.5	5.1 \pm 0.4	6.4 \pm 0.6	8.5 \pm 1.2	51 \pm 2	51 \pm 3	53 \pm 3
Spinhaler [®]	-	43 \pm 12	4.2 \pm 0.7	-	50 \pm 13	6.3 \pm 1.3	-	27 \pm 4	62 \pm 5
Diskus [®]	-	76 \pm 34	58 \pm 49	-	75 \pm 30	63 \pm 41	-	17 \pm 9	19 \pm 15
Handihaler [®]	53 \pm 33	4.8 \pm 0.4	4.8 \pm 0.4	62 \pm 32	7.1 \pm 1.0	7.5 \pm 1.2	20 \pm 10	53 \pm 4	52 \pm 1
Novolizer [®]	4.9 \pm 0.3	3.6 \pm 0.6	2.9 \pm 0.2	5.2 \pm 0.2	4.4 \pm 0.9	3.4 \pm 0.2	52 \pm 4	67 \pm 8	78 \pm 2
Turbohaler [®]	4.7 \pm 0.3	4.5 \pm 1.7	2.4 \pm 0.2	5.1 \pm 0.4	4.8 \pm 1.5	3.1 \pm 0.3	54 \pm 4	56 \pm 22	82 \pm 3

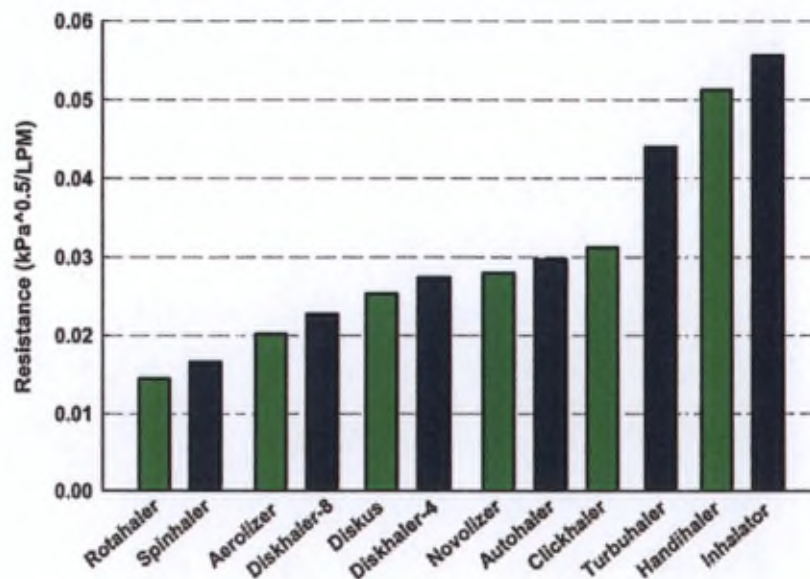


Figure 46. Internal resistances of some commercially available inhalers (Bellary and Barnett, 2006)

IV.1.3.2. Selection of the inhalation device

Particle size distributions obtained for the inhalation grade lactose powder (Lactohale[®] LH300) with various commercial devices were assessed using Spraytec[®] measurements. The particle size results are listed in **Table XI**.

It can be seen that the best particle deaggregation was obtained at 90 l/min with the Novolizer[®] and Turbohaler[®] devices, with a V% < 5 µm of 78 ± 2% and 82 ± 3%, respectively. In this condition, the $d_{(0.5)}$ was 2.9±0.2 µm and 2.4±0.2 µm, and the $D_{[4,3]}$ was 3.4 ± 0.2 µm and 3.1 ± 0.3 µm, respectively. These values are relatively well correlated to those obtained for the lactose by conventional laser diffraction, with a $d_{(0.5)}$ of 3.6 ± 0.3 µm and a $D_{[4,3]}$ of 4.3 ± 0.2 µm. These last values reflect the particle size distribution in a fully individualised state.

From this, we can say that an almost total deaggregation of the particles can be obtained at 90 l/min with the Novolizer[®] and Turbohaler[®] devices. The slightly lower values obtained with the Spraytec[®] laser diffractometer could be due to differences in the algorithm used for the determination of the particle size distributions for the two diffraction techniques. However, the Novolizer[®] and Turbohaler[®] devices possess a markedly higher R_i in comparison with other commercial devices, as can be seen in **Figure 46** and **Table VIII**. It is therefore not certain that all patients will be able to generate a sufficiently high flow rate through these devices. In the figure, it can be seen that the R_i of the tested devices is in the following order: Spinhaler[®] < Aerolizer[®] < Diskus[®] < Novolizer[®] < Turbohaler[®] < Handihaler[®].

For the devices showing lower resistance values, the Spinhaler[®] and Aerolizer[®], an intermediate deaggregation efficiency could be obtained at 90 l/min, with a V% < 5 µm of 62 ± 5% and 49 ± 2%, respectively. It is to be noted that the results obtained for the Aerolizer[®] with 2/3 and 1/3 air inlet did not lead to improved powder dispersion in comparison with the commercial Aerolizer[®] device, with V% < 5 µm of 53 ± 5% and 53 ± 3%, respectively. Although the Spinhaler[®] device led to better deaggregation than the Aerolizer[®] device at 90 l/min, when the flow rate was decreased at 60 l/min the Spinhaler[®] device presented a marked decrease in its deaggregation performance (V% < 5 µm of 27 ± 4%). At a flow rate of 30 l/min, it was even not possible to obtain fluidisation of the particles from the powder bed

with this device. This was also the case for the Diskus[®] device, for which we obtained the worse results of the study, with a $V\% < 5 \mu\text{m}$ of $17 \pm 9\%$ and $19 \pm 15\%$ at 60 l/min and 90 l/min, respectively. This could partly be due to the very small size of the blister cavity, which is not adapted to a sticky, unformulated powder.

Except for the Aerolizer[®] device, the performance of each device increased with the use of higher airflow rates. This can be explained by the fact that high flow rates generally lead to improved powder fluidisation and fine particle production as they increase airflow velocity and turbulence. However, an ideal inhaler should provide a dose to the airways that does not vary with the inspiratory flow rate. The Aerolizer[®] device exhibited the best results for this feature, with a $V\% < 5 \mu\text{m}$ of $42 \pm 3\%$, $56.6 \pm 1.4\%$ and $49 \pm 2\%$ at 30, 60 and 90 l/min. Similarly, the Aerolizer[®] with 2/3 and 1/3 air inlet did not exhibit significant changes in $V\% < 5 \mu\text{m}$ between 30 and 90 l/min. At a flow rate of 60 l/min or higher, the Handihaler[®] also showed interesting results, with a $V\% < 5 \mu\text{m}$ of $53 \pm 4\%$ and $52 \pm 1\%$ at 60 l/min and 90 l/min, respectively. However, the Handihaler[®] has a much higher R_i than the Aerolizer[®] device, which could make it less suitable for patients with decreased lung function.

Based on the above-mentioned results, the Aerolizer[®] device was selected for the aerodynamic evaluation of the insulin formulations. It indeed provided a good balance between deaggregation efficiency and intrinsic resistance, as well as good independency from airflow rate of deaggregation performance. Moreover, it is a very simple device that allows easy incorporation of a large powder dose in the capsule.

IV.1.3.3. Aerodynamic characterisation

Although the Spraytec[®] laser diffraction technique measures geometric particle size distributions, it provides useful information on the behaviour of the powders under simulated breathing conditions. Results presented in **Table XII** show that particle size values obtained for raw insulin were comparable to those obtained with the standard laser diffraction method. This indicated that the particles were easily dispersed in a fully individualised state, even under simulated breathing conditions, as shown in **Figure 47**.

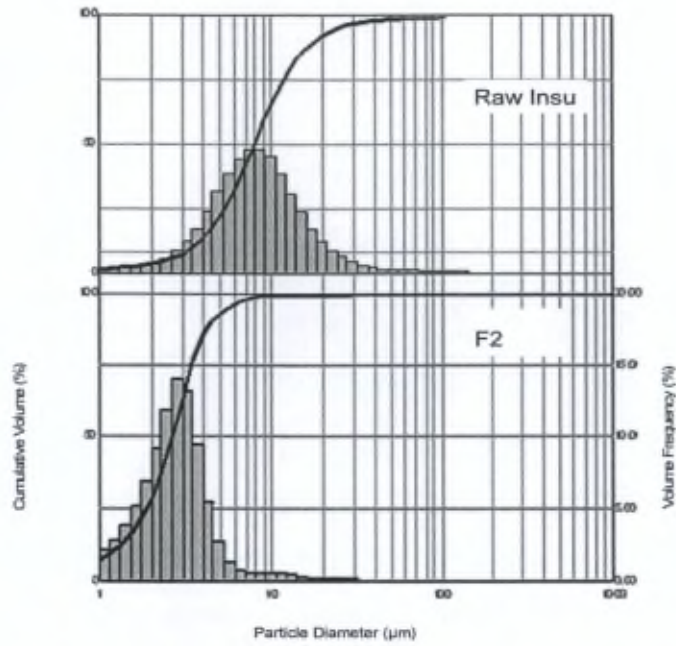


Figure 47. Average particle size distribution and undersize curve of raw insulin material and the F2 formulation measured with the Spraytec®

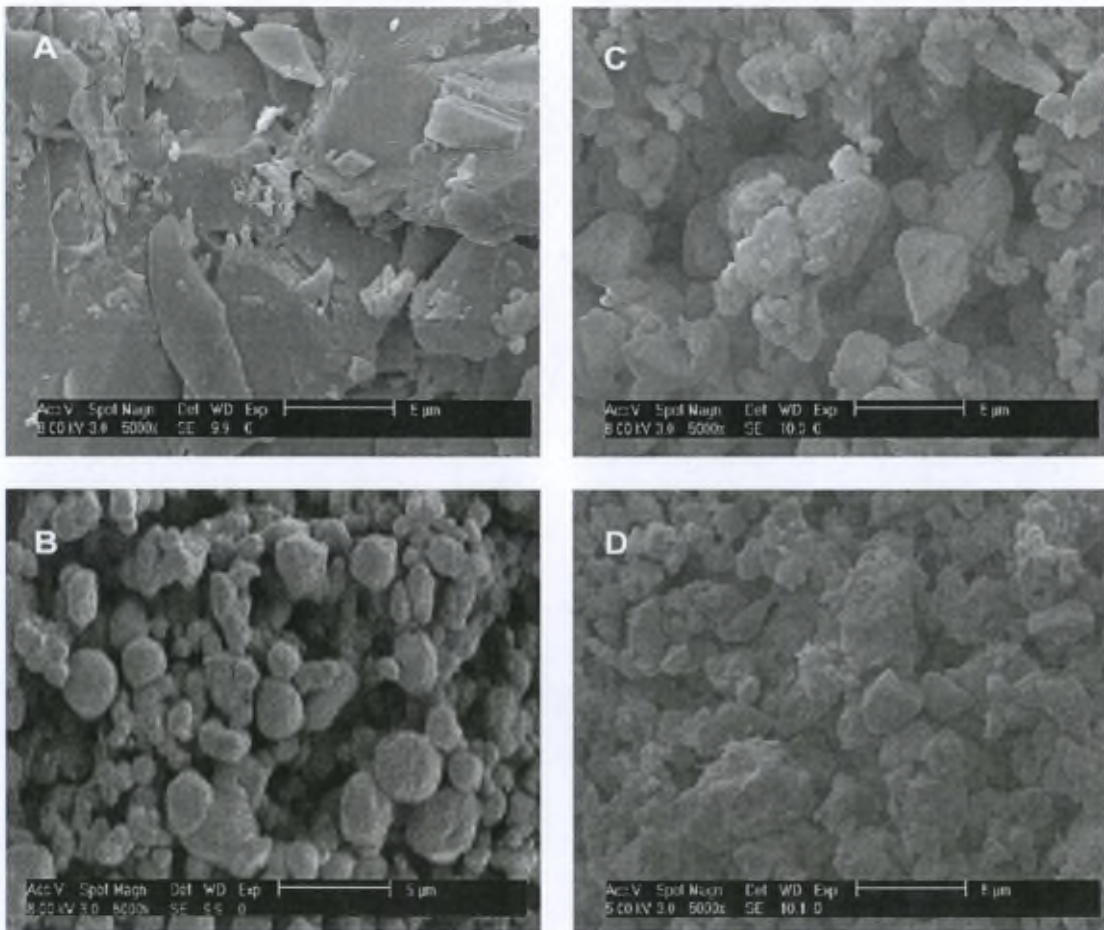


Figure 48. SEM pictures obtained at a magnification of 5 000 X of raw insulin (A) and from SD insulin formulations F1 (B), F2 (C), and F4 (D)

Table XII. Particle size characteristics of the formulations, $d_{(0,5)}$, $D_{[4,3]}$, and $V\% < 5 \mu\text{m}$ (mean \pm S.D., $n=3$) measured with the Spraytec[®] laser diffractometer. Results obtained at 100 l/min for 2.4 s using an Aerolizer[®] device. Acquisition parameters: triggering mode, 10% level; data acquisition rate, 2 500 Hz; acquisition duty cycle, 50%; test duration, 3 000 ms; refractive index, 1.50 (standard opaque particles).

	$d_{(0,5)}$	$D_{[4,3]}$	$\% < 5.0 \mu\text{m}$
Raw			
insulin	7.8 ± 0.3	10.5 ± 0.7	22.9 ± 1.6
F1	4.3 ± 0.4	6.1 ± 0.7	61 ± 6
F2	2.9 ± 0.2	3.22 ± 0.12	93.1 ± 1.4
F3	2.6 ± 0.3	3.8 ± 0.3	80.6 ± 1.7
F4	2.5 ± 0.2	3.7 ± 0.2	80.3 ± 1.3
F5	2.6 ± 0.4	4.0 ± 0.6	78 ± 4
F6	3.8 ± 0.4	6.0 ± 0.5	65 ± 5

Spraytec[®] results for the SD formulation from an insulin solution without excipient (F1) exhibited particle diameters that were higher in comparison with standard laser diffraction presented in **Table X** ($d_{(0,5)}$ of $4.3 \pm 0.4 \mu\text{m}$ and $2.05 \pm 0.07 \mu\text{m}$, respectively) and a much lower percentage of particles with a diameter below $5 \mu\text{m}$ ($61 \pm 6\%$ vs. $97.5 \pm 0.9\%$), whereas the SD formulation from an insulin suspension without excipient (F2) had only slightly higher median diameters ($2.9 \pm 0.2 \mu\text{m}$ vs. $2.11 \pm 0.03 \mu\text{m}$) and a slightly lower percentage of particles with a diameter below $5 \mu\text{m}$ ($93.1 \pm 1.4\%$ vs. $98.1 \pm 0.5\%$). The presence of powder aggregates in the formulations in simulated breathing conditions (100 l/min for 2.4 s) can be explained by the fact that inter-particle interactions are very high for micronised particles because of the increase in specific surface area. However, the different behaviours observed for the F1 and the F2 formulations could be explained by the differences in residual moisture content ($6.1 \pm 0.1\%$ and $4.9 \pm 0.1\%$, respectively), leading to the formation of more liquid bonds in the inter-particle gaps in the F1 formulation. The shape properties of the particles could also be involved. As shown in **Figure 48**, the F1 formulation had a fairly spherical shape with a smooth surface, whereas the F2 formulation, for which no insulin dissolution occurred in the solvent system used before spray-drying, retained a more corrugated surface, closer to the raw insulin powder features. This irregular shape could increase inter-particle

Table XIII. In vitro deposition characteristics of the different formulations. Results obtained using an Aerolizer® device loaded with nominal insulin doses of 5.0 mg in n°3 HPMC capsules. Experiment conducted at 100 l/min for 2.4 s (mean ± S.D., n=3).

	Raw Insulin	F1	F2	F3	F4	F5	F6
FPD (mg)	0.49 ± 0.16	2.17 ± 0.15	2.8 ± 0.2	2.8 ± 0.2	2.7 ± 0.3	2.6 ± 0.2	2.0 ± 0.2
MMAD (µm)	5.65 ± 0.06	3.53 ± 0.03	2.71 ± 0.05	2.68 ± 0.05	3.07 ± 0.06	3.02 ± 0.07	2.92 ± 0.07
Metered dose (mg)	4.5 ± 0.2	4.5 ± 0.2	4.5 ± 0.4	4.60 ± 0.11	4.6 ± 0.3	4.4 ± 0.2	4.4 ± 0.3
FPF (%)	11 ± 3	48 ± 4	63 ± 4	61 ± 4	59 ± 4	59 ± 3	46 ± 3

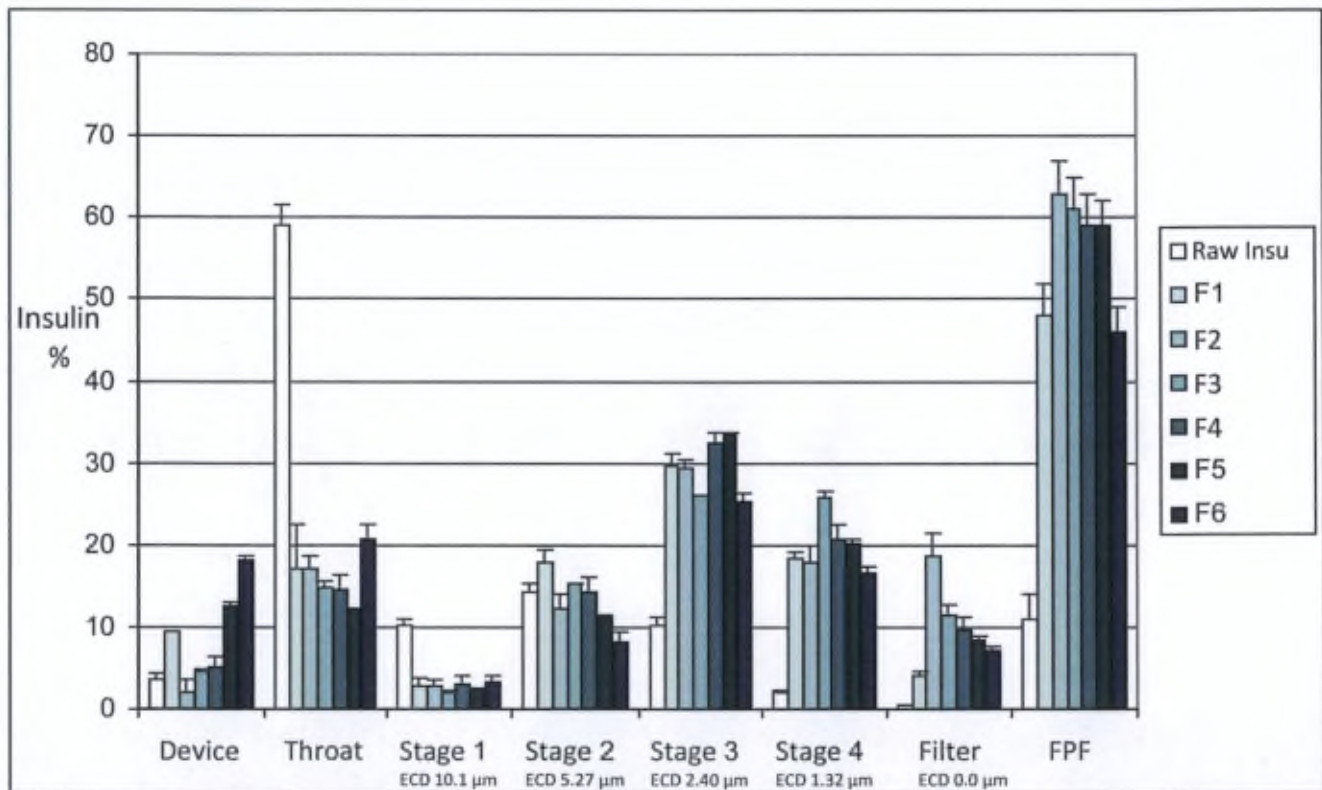


Figure 49. In vitro deposition patterns (Msl) of the different insulin formulations. Results obtained using an Aerolizer® device loaded with nominal insulin doses of 5.0 mg in n°3 HPMC capsules. Experiment conducted at 100 l/min for 2.4 s (mean ± S.D., n=3). ECD: effective cut-off diameter

distances and therefore reduce Van der Waals interactions, resulting in an increase in powder dispersibility (Chew et al., 2005).

The coated formulations (F3-F5) all showed a similar increase in particle aggregation in comparison with the uncoated F2 formulation, and a decrease of about 10% in the percentage of particles with a diameter below 5 μm (**Table XII**). The F6 formulation, which possesses the highest level of lipid coating (40%), exhibited higher aggregation, with a particle size distribution comparable to the F1 formulation. The sticky behaviour of lipid-coated powders has already been observed in previous papers (Sebti and Amighi, 2006; Pilcer et al., 2006) and is a function of the percentage of lipid coating and of the cholesterol/Phospholipon[®]90H ratio. This phenomenon is mainly attributed to the presence of phospholipids in the coating. Indeed, if a small proportion of these decreases the generation of electrostatic charges at the particle surface, an excessive proportion leads to the softening of the particles because of the low phase transition temperature (around 55 °C) of Phospholipon[®]90H.

It is important to note that Spraytec[®] laser diffraction only gives geometric particle dimensions, whereas MsLI measures aerodynamic diameters. Even if the Spraytec[®] could give a good indication of the aerosolisation properties of DPI formulations and be used as a quick preliminary test, we would still need impaction measurements to characterise the de-agglomeration behaviour of the powders in an air stream to understand how powder deposition in the lungs might occur.

The aerodynamic behaviour of the different insulin formulations analysed in an MsLI is shown in **Table XIII** and **Figure 49**. The results indicated that the MMAD were between 5.65 μm for raw insulin and around 2.7 μm for the F2 and F3 formulations. On the other hand, the FPF, which roughly corresponds to the drug deposition fraction at stages 3, 4, and at the filter (cut-off diameters of 5.3 μm , 2.4 μm , and 1.3 μm , respectively), varied within a range of 11% for raw insulin and 63% for the F2 uncoated formulation obtained from a suspension of insulin in isopropanol. The metered dose of insulin, which is the dose that is recovered from the inhaler and the different parts of the MsLI, was in all cases comprised between 88% and 92% of the total drug loaded.

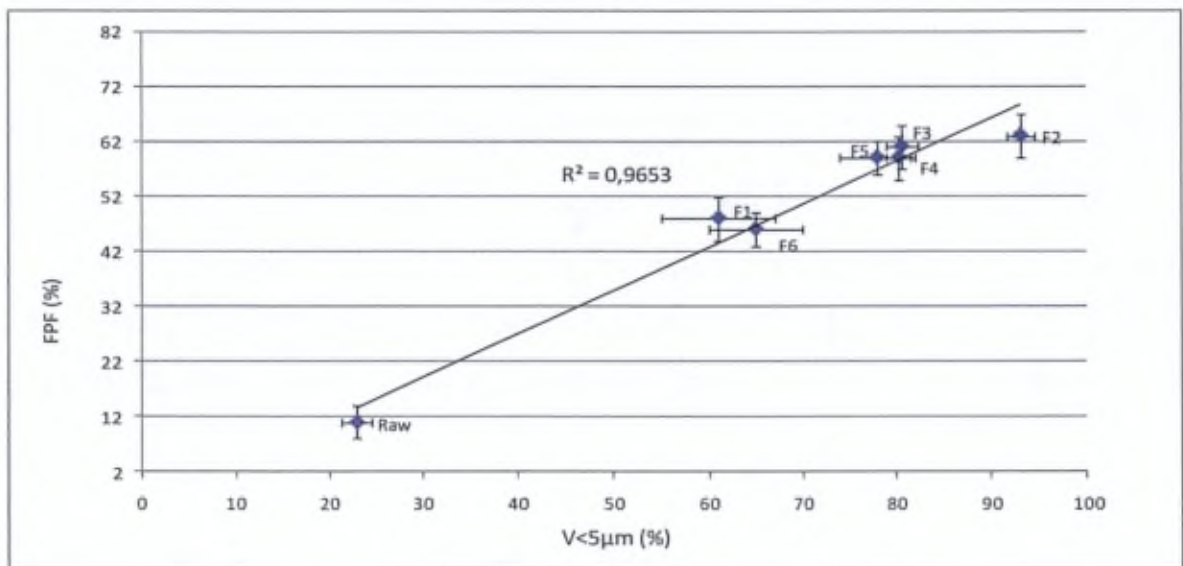
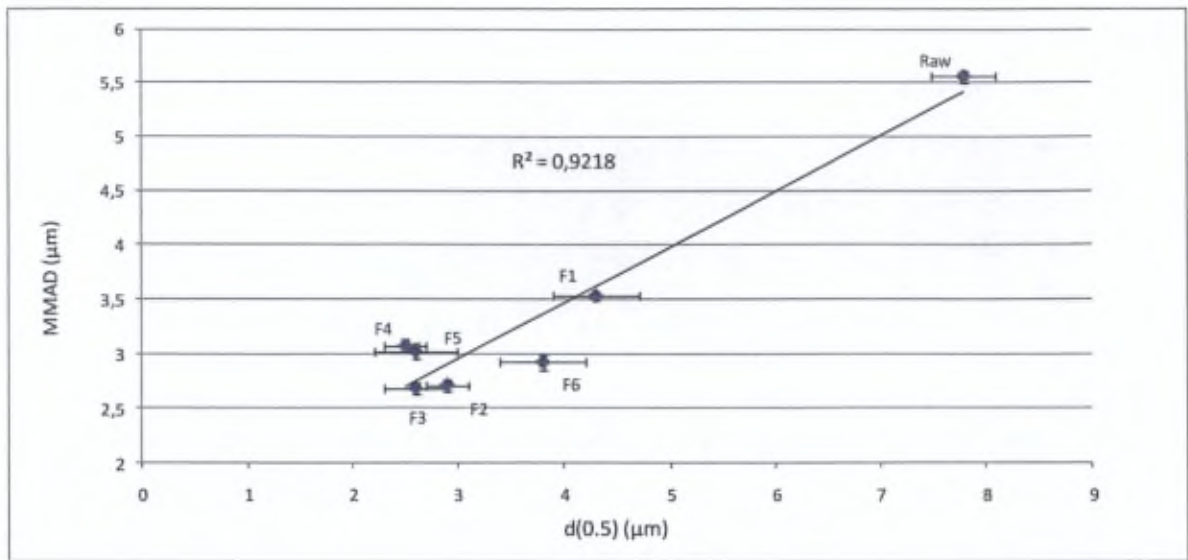


Figure 50. Comparison plot of the results obtained with the Spraytec laser diffraction technique and with the impaction technique. Up: MMAD measured with the MsLI (100 l/min for 2.4 sec, mean \pm SD, n=3) and the d(0.5) measured with the Spraytec (mean \pm SD, n=3) for the raw insulin powder and the F1-F6 formulations, Down: percentages of particles below 5 μ m measured with the MsLI (100 l/min for 2.4 sec, mean \pm SD, n=3) and with the Spraytec (mean \pm SD, n=3) for the raw insulin powder and the F1-F6 formulations.

A comparison of the MMAD results with the Spraytec[®] geometric median diameters was obtained by drawing a comparison plot (one method per axis) (**Figure 50**). It gave a good correlation between the two methods, as previously described in the literature (Pilcer et al., 2008b). A coefficient of determination R^2 of 0.92 was calculated, which does not indicate agreement between the two methods, but measures the strength of the linear relationship between them. The most important difference between the MMAD and $d_{(0.5)}$ results was obtained for the raw insulin powder (5.7 μm vs. 7.8 μm , respectively). This can be explained by the fact that the Copley[®] software used for the determination of the MMAD only takes into account particles with an aerodynamic diameter below 10.1 μm (cut-off diameter of stage 2) whereas the determination of the $d_{(0.5)}$ with the Spraytec[®] includes all particles exiting the device. This effect was mainly visible for the raw insulin powder as it possesses a large fraction of particles with a diameter over 10 μm (see Table X). We also compared the FPF values obtained by impaction with the percentage of particles with a diameter below 5 μm obtained using the Spraytec[®]. Here again, there was a linear relation between the data generated from the two methods ($R^2 = 0.97$) (**Figure 50**). However, the FPF values obtained for the different formulations using the impaction method were lower (46-63%) than for the percentage of particles with a diameter below 5 μm measured with the Spraytec[®] (61-93%).

No significant difference was observed for the fine particle fraction between the F2 uncoated formulation (63 \pm 4%) and the coated formulations with a coating load of up to 30% (F3, F4, and F5 formulations), with FPF values of 61 \pm 4%, 59 \pm 4%, and 59 \pm 3%, respectively (1-way ANOVA test, $p > 0.05$, N.S.). However, the F1 (uncoated) and F6 (40% lipid-coated) formulations both exhibited lower FPF values that were below 50%. For the F1 formulation, the more agglomerated state of the powder was indicated by a higher deposition at stage 2 of the MsLI (cut-off: 10.1 μm) and by fewer particles deposited in the last filter stage of the impinger. As discussed above, this lower performance was probably due to the higher residual moisture content (6.1%) of this formulation. An increase of the lipid content of the formulations to up to 40% (F6) also seemed to induce some particle-sticking because of the softening phenomenon previously explained. This was shown by an increase in the particles impacted in the throat and by a higher powder loss within the inhalation device (see **Figure 49**). It is therefore important to be within the appropriate

Table XIV. Results of a 3-month stability study on the F2 and F4 formulations

	F2 formulation (uncoated)			F4 formulation (20% lipid-coated)		
	t ₀	t _{1month}	t _{3month}	t ₀	t _{1month}	t _{3month}
Fridge						
Insulin Content (%)	99.1 ± 1.3	100.4 ± 0.9	100.2 ± 0.9	99.5 ± 1.5	102 ± 2	102 ± 2
HMWP Content (%)	< 0.4	< 0.4	< 0.4	< 0.4	< 0.4	< 0.4
Water Content (%)	4.9 ± 0.1	6.8 ± 0.1	6.9 ± 0.1	2.6 ± 0.2	3.7 ± 0.1	3.5 ± 0.1
Isopropanol Content (ppm)	2480 ± 30	2330 ± 21	2351 ± 42	2795 ± 25	2722 ± 66	2748 ± 65
UDD (%)	All caps. between 94.3-103.0	All caps. between 89.1-107.5	All caps. between 90.0-108.5	All caps. between 93.3-102.1	All caps. between 88.8-107.5	All caps. between 92.2-105.4
FPF (%)	65 ± 5	64 ± 2	63 ± 3	61 ± 4	59 ± 5	60 ± 5
MMAD (µm)	2.74 ± 0.06	2.75 ± 0.05	2.76 ± 0.06	2.97 ± 0.07	3.00 ± 0.08	2.99 ± 0.08
25°C/60%R.H.						
Insulin Content (%)	99.1 ± 1.3	99.5 ± 1.0	99.6 ± 1.3	99.5 ± 1.5	102.2 ± 1.1	100.1 ± 1.2
HMWP Content (%)	< 0.4	< 0.4	< 0.4	< 0.4	< 0.4	< 0.4
Water Content (%)	4.9 ± 0.1	6.2 ± 0.1	6.4 ± 0.1	2.6 ± 0.2	3.6 ± 0.1	3.5 ± 0.1
Isopropanol Content (ppm)	2480 ± 30	2407 ± 74	2370 ± 52	2795 ± 25	2730 ± 60	2620 ± 70
UDD (%)	All caps. between 94.3-103.0	All caps. between 89.0-105.2	All caps. between 88.1-106.3	All caps. between 93.3-102.1	All caps. between 88.2-104.6	All caps. between 89.0-103.0
FPF (%)	65 ± 5	68 ± 4	64 ± 4	61 ± 4	58 ± 4	60 ± 4
MMAD (µm)	2.74 ± 0.06	2.71 ± 0.05	2.76 ± 0.06	2.97 ± 0.07	3.01 ± 0.07	2.98 ± 0.08
40°C/75%R.H.						
Insulin Content (%)	99.1 ± 1.3	99.2 ± 1.1	101 ± 2	99.5 ± 1.5	98.3 ± 1.5	98.4 ± 2
HMWP Content (%)	< 0.4	< 0.4	< 0.4	< 0.4	< 0.4	< 0.4
Water Content (%)	4.9 ± 0.1	5.7 ± 0.1	6.9 ± 0.2	2.6 ± 0.2	3.7 ± 0.1	3.4 ± 0.1
Isopropanol Content (ppm)	2480 ± 30	2269 ± 79	2200 ± 60	2795 ± 25	2808 ± 74	2720 ± 50
UDD (%)	All caps. between 94.3-103.0	All caps. between 93.3-103.8	All caps. between 92.0-103.5	All caps. between 93.3-102.1	All caps. between 83.3-105.9	All caps. between 86.0-104.9
FPF (%)	65 ± 5	61 ± 5	61 ± 5	61 ± 4	57 ± 5	60 ± 5
MMAD (µm)	2.74 ± 0.06	2.89 ± 0.09	2.90 ± 0.07	2.97 ± 0.07	3.09 ± 0.08	2.97 ± 0.08

residual water content range in order to avoid the apparition of both electrostatic charges and liquid bonds leading to more inter-particle interactions.

The aerodynamic performance of the different formulations tested was very high in comparison with that which could be obtained from other protein formulations for inhalation currently under development. Such other formulations often have an in vitro deposition of around 30%. As an example, the insulin formulation Exubera[®] has shown FPF values between 33% and 45%, depending on the nominal dose (1 mg or 3 mg) (White et al., 2005). Aside from insulin, other proteins, such as growth hormone and parathyroid hormone, have already been formulated for DPI administration using formulations presenting higher particle sizes and low powder densities. They are characterised by FPFs of 38% and 61%, respectively (Codrons et al., 2003; Jalalipour et al., 2008).

Assessment of the uniformity of the delivered dose, performed on the F2 and F4 formulations, showed that all capsules delivered between 94.5% and 102.5% of the mean delivered dose for the F2 formulation and between 93.0% and 101.9% for the F4 formulation (data not shown). The mean delivered doses were 74% and 87% of the loaded doses, respectively. For the two formulations, the uniformity of the delivered dose satisfied the requirements of the European Pharmacopoeia, which specifies that the preparation complies if nine out of ten capsules present a delivered dose between 75% and 125% of the average value and all capsules between 65% and 135%.

IV.1.3.4. Stability study

A three-month stability study was performed on the F2 and F4 formulations. The results exhibited no significant difference between the initial features of the physicochemical characterisation (including HPLC insulin content and HMWP) and aerodynamic behaviour for any of the three conditions tested (**Table XIV**), except for the residual water content. For residual water content, values increased up to 6.9% at $t_{3\text{month}}$ for the F2 formulation in accelerated testing conditions (40 °C/75% RH), while the F4 formulation only showed an increase in water content to 3.4%. Insulin was thus found to be a robust biomolecule as regards its good stability in the dry state, even when no lipid coating was added and despite

the fact that an increased level of residual moisture was present in the uncoated powder during storage. However, the addition of a lipid coating could be of interest for other, more sensitive biomolecules as it was shown to provide good protection against water adsorption by the powder during storage. It is to be noted that the duration of this stability study was intentionally limited to 3 months. This provided preliminary stability results that were needed for the further evaluation of the formulations in a clinical study. However, these encouraging results should be investigated in the future with the realisation of a longer stability study.

IV.1.4. Conclusion

In this study, we evaluated insulin lipid-coated formulations and formulations without excipients, produced using high pressure homogenisation and spray-drying. In the case of lipid-coated formulations, a physiological lipid composition based on a mixture of cholesterol and phospholipids was used, and the resulting powders exhibited a size and shape suitable for the deep lung deposition of drugs.

We were able to obtain good aerodynamic features for the different formulations tested, with fine particle fractions between 46% and 63% versus 11% for raw insulin powder. These are high FPF values in comparison with those obtained for other protein formulations for inhalation currently under development, which often have an in vitro deposition of around 30%. The presence of a lipid coating of up to 30% (w/w) did not significantly improve the aerodynamic behaviour, but the coated formulations exhibited decreased residual moisture content, which was even more noticeable after 3 months' storage. This should be of interest for the long-term stability of protein formulations.

Although the formulations presented good aerodynamic features in vitro, it still remains to be determined whether the formulations give high deep lung deposition results effectively in vivo, and how insulin is absorbed into the systemic blood stream. Therefore, in the following section, a pharmaco-scintigraphic clinical trial was performed on type I diabetic patients to evaluate the deep lung deposition, pharmacokinetics, and bioavailability of the uncoated F2 formulation and the coated F4 formulation.

IV.2. Comparative pharmacoscintigraphic and pharmacokinetic evaluation of two new formulations of inhaled insulin in type 1 diabetic patients

Depreter F., Burniat A., Blocklet D., Lacroix S., Cnop M., Fery F., Van Aelst N., Pilcer G., Deleers M., Goldman S., Amighi K. 2012. *Eur. J. Pharm. Biopharm.* 80(1): 4-13

IV.2.1. Introduction

The number of diabetic patients with poor glycemic control is very high. As a consequence, they develop short- and long-term complications responsible for increased morbimortality. A recent report indicates that in the United States only 57% of diabetic adults achieve the treatment goal of less than 7% glycosylated haemoglobin (HbA1c), and the percentage of patients achieving all three treatment goals (HbA1c < 7%, blood pressure < 130/80 mmHg, and total cholesterol < 200 mg/dl) is even lower, reaching only 12% (Cheung et al., 2009). An important cause of this poor glycemic control is the difficulty in achieving plasma insulin profiles that resemble the natural prandial insulin secretion, despite the broad variety of subcutaneous (s.c.) insulins available (Cheung et al., 2009; American Diabetes Association, 2011). Current s.c. insulin therapies do not provide the optimal pharmacokinetic profile. The absorption of regular human insulin is too slow and its action is too prolonged to mimic early insulin release effectively. In an attempt to overcome some of the limitations of regular insulin, rapid-acting insulin analogues have been developed, but their onset of action is still relatively slow compared with prandial glucose absorption (Richardson and Boss, 2007). In addition, these injected formulations present intra-patient variability in the starting time of insulin action of up to 30% (Richardson and Boss, 2007). This is mainly due to variation in the rate of absorption from the s.c. depot, which depends on the insulin concentration, injection volume, and injection site, as well as on endogenous factors such as skin temperature, local blood flow, muscle activity, and the thickness of the subcutaneous fat layer (Heinemann, 2004).

The ideal prandial insulin would therefore have a pharmacokinetic profile that closely matches the body's normal insulin response to a meal and would be highly reproducible.

In recent years, several attempts have been made to develop insulin formulations that more closely meet these clinical requirements. Inhaled insulins seem particularly promising as many formulations for pulmonary delivery exhibit pharmacokinetic profiles with absorption rates at least as fast as that of the rapid-acting insulin analogue, lispro (Brunner et al., 2001; Rave et al., 2005; Muchmore et al., 2007; Boss and Ellerman, 2008). In spite of the commercial failure of Exubera[®], inhaled insulin might thus get a place in the therapeutic

arsenal. In addition to the pharmacodynamic considerations mentioned above, this type of formulation might address compliance problems observed with s.c. insulin treatments, in particular when multiple daily injections are required or in type 2 diabetic patients, who often require insulin later in life (Pfützner and Forst, 2005).

The objective of this study was to evaluate clinically two new dry powder formulations of insulin developed previously (see part IV.1.). The formulations present a very simple composition with few or no excipients, using only those that are potentially acceptable for inhalation. This is of interest given the limited number of excipients currently accepted for inhalation (Pilcer and Amighi, 2010). The formulations were produced using HPH followed by spray-drying. This formulation strategy could potentially be applied to larger proteins and monoclonal antibodies for which an inhaled dry powder treatment is sought.

An uncoated formulation and a lipid-coated formulation (20% lipids w/w) were chosen. These have an interesting aerodynamic behaviour in vitro, with a high FPF of $63 \pm 4\%$ and $59 \pm 4\%$, respectively. Based on these promising in vitro results, we carried out a scintigraphic and pharmacokinetic evaluation of the formulations after inhalation of a single oral dose in twelve type 1 diabetic patients. Gamma scintigraphic imaging provides information on the level and site of drug deposition in the lungs, while the pharmacokinetic evaluation gives information on the absorption of insulin from the deposition site and on its systemic bioavailability.

This clinical study was combined with the in vitro assessment of the influence of several airflow rates on the aerodynamic properties of the formulations. Finally, a dissolution test specifically designed for pulmonary formulations was performed to investigate whether the differences appearing in the pharmacokinetic profiles of the two formulations could be related to differences in their dissolution rate.

IV.2.2. Materials and Methods

IV.2.2.1. Materials

Two dry powder insulin formulations were selected. The first formulation (F2) consisted of a powder that was micronised without excipient. The formulation was obtained by HPH of a

2% w/v insulin (Incelligent™ AF, Millipore®, MA, USA) suspension in isopropanol, followed by spray-drying, as described in part IV.1.2.2.1.2. The second formulation (F4) consisted of lipid-coated micronised insulin particles. It was also obtained by HPH, followed by spray-drying. The lipids (20% of the insulin mass) were dissolved in a small volume (< 3 ml) of hot isopropanol (55 °C) and added to the suspension just before spray-drying. These lipids were cholesterol (Fagron, The Netherlands) and Phospholipon®90H (Nattermann Phospholipids GmbH, Germany) in a ratio of 75:25 (see IV.1.2.2.1.2.).

Size 3 HPMC capsules (Qualicaps, Spain) were hand-filled and loaded with 2 U insulin/kg body weight (corresponding to 4.86 mg and 5.83 mg of powder for a 70 kg person for the F2 and F4 formulations, respectively). The dry powder inhaler (DPI) device used was the Aerolizer® (Novartis, Switzerland), a passive, breath-actuated, single-dose DPI.

A complete batch analysis of the two formulations, with and without radiolabelling, is presented in **Table XV**. The results were obtained from three different production batches, for both the unlabelled and radiolabelled formulations.

It is to be noted that the insulin raw material used in this study (Incelligent™ AF, Millipore®, MA, USA) was different from the material used in the development of the formulations (Sigma-Aldrich, St. Louis, MO). This is due to the need to use a material with an appropriate safety profile when administration to human subjects is intended. The Federal Agency for Medicines and Health Products (FAMHP) indeed required that the manufacturing facility was GMP compliant and that the insulin was free of animal-origin product. The selected insulin product (see certificate of analysis in **APPENDIX VIII**) was GMP manufactured, FDA approved, and ISO 9001:2000 certified. Moreover, Millipore's Incelligent AF insulin is a fully animal-free product. This means it does not make use of bovine or porcine components in the master cell bank, working cell bank, raw materials, manufacturing process and final product. An important issue regarding animal-origin components is indeed the concern about potential Bovine Spongiform Encephalopathy (BSE) transmission.

Table XV. Batch Analyses of the formulations used for the clinical study

PARAMETERS	METHOD	SPECIFICATIONS	RESULTS			
			F2 formulation		F4 formulation	
			Unlabelled	Radiolabelled	Unlabelled	Radiolabelled
Uniformity of mass	Ph. Eur. 6 th Ed. (2.9.5.)	20 capsules : average 5 mg. No more than 2 capsules with a SD > 10%, No capsule with a SD > 20%	Complies: manual filling of the capsules with 5 ± 0.05 mg powder			
Uniformity of content	Ph. Eur. 6 th Ed. (2.9.6.)	10 capsules, No more than 1 capsule outside 85-115%, No capsule outside 75-125%	Complies: All capsules were between 98-102%	Complies: All capsules were between 97-102%	Complies: All capsules were between 98-102%	Complies: All capsules were between 98-102%
Median particle size	Spraytec [®] diffraction (IV.1.2.2.8.4.)	2.2 – 3.4 µm	2.8 ± 0.2 µm	2.8 ± 0.3 µm	2.5 ± 0.2 µm	2.5 ± 0.4 µm
Median particle size	Laser diffraction (IV.1.2.2.2.)	1.5 – 2.7 µm	2.11 ± 0.03 µm	2.20 ± 0.13 µm	2.32 ± 0.09 µm	2.35 ± 0.12 µm
% < 3 µm	Laser diffraction	≥ 60.0 %	79.7 ± 0.6%	80.2 ± 1.0%	70.2 ± 0.8%	72.5 ± 1.0%
% < 5 µm	Laser diffraction	≥ 90.0 %	98.6 ± 0.9%	98.9 ± 1.1%	94.1 ± 0.6%	95.9 ± 0.9%
Assay of insulin	HPLC (IV.1.2.2.4.)	95.0 – 105.0 % of 26.9 IU/mg	Complies: Results for insulin content is 99.2 ± 1.1% of 26.9 IU/mg	Complies: Results for insulin content is 98.7 ± 1.3% of 26.9 IU/mg	Complies: Results for insulin content is 99.5 ± 1.5% of 26.9 IU/mg	Complies: Results for insulin content is 97.7 ± 2.6% of 26.9 IU/mg
Uniformity of delivered dose	IV.1.2.2.8.2.	10 capsules, not less than 9/10 in the range 75 – 125 %	Complies: All capsules were between 94.5-102.5%, Mean Delivered Dose: 75 ± 4%	Complies: All capsules were between 94-103%, Mean Delivered Dose: 76 ± 4%	Complies: All capsules were between 93.0-101.9%, Mean Delivered Dose: 88 ± 4%	Complies: All capsules were between 94-101%, Mean Delivered Dose: 85 ± 5%
Residual solvents	GC (IV.1.2.2.7.2).	< 5000 ppm	Complies: 2470 ± 30 ppm isopropanol	Complies: 2010 ± 15 ppm isopropanol	Complies: 2810 ± 30 ppm isopropanol	Complies: 2751 ± 54 ppm isopropanol
Residual humidity	TGA (IV.1.2.2.7.1.)	≤ 10.0 %	Complies: 4.9 ± 0.1%	Complies: 4.9 ± 0.1%	Complies: 2.6 ± 0.1 %	Complies: 2.6 ± 0.2 %

High Molecular Weight Proteins	SEC (IV.1.2.2.5.)	<1.0%			Complies: <0.4%	
Microbial quality	Ph. Eur. 6 th Ed. (2.6.12 and 2.6.13)	<ul style="list-style-type: none"> ▪ Total Aerobic Microbial Count (TAMC) ≤ 10² CFU/capsule ▪ Total combined Yeasts/Moulds Count (TYMC) ≤ 10¹ CFU/capsule ▪ Absence of <i>Staphylococcus aureus</i> (1 capsule) ▪ Absence of <i>Pseudomonas aeruginosa</i> (1 capsule) ▪ Absence of bile-tolerant gram-negative bacteria (1 capsule) 	<p>Complies**:</p> <ul style="list-style-type: none"> ▪ TAMC= 0.7 ± 0.8 CFU/caps. ▪ TYMC= 0.2 ± 0.3 CFU/caps. ▪ <i>Staph. aureus</i>: absence of UFC in all batches and replicates ▪ <i>Pseudo. aeruginosa</i>: absence of UFC in all batches and replicates ▪ Bile-tolerant gram-negative bacteria: absence of UFC in all batches and replicates 	Not performed	<p>Complies**:</p> <ul style="list-style-type: none"> ▪ TAMC= 29 ± 10 CFU/caps. ▪ TYMC = 0.2 ± 0.3 CFU/caps. ▪ <i>Staph. aureus</i>: absence of UFC in all batches and replicates ▪ <i>Pseudo. aeruginosa</i>: absence of UFC in all batches and replicates ▪ Bile-tolerant gram-negative bacteria: absence of UFC in all batches and replicates 	Not performed
Radioactive content/capsule	measurement of the activity for each capsule just after production	Between 0.41 MBq/kg and 0.52 MBq/kg b.w. (corresponding to 29.0 and 36.3 MBq per capsule for a 70kg man).	/	Complies	/	Complies
In vitro deposition tests	MsLI (IV.1.2.2.8.3.)	<p>FPF_{metered dose}: 55 – 75 %</p> <p>MMAD : 2.5 – 3.5 µm</p>	<p>FPD (based on a nominal dosis of 5 mg insulin): 2.90-3.28 mg</p> <p>FPF_{metered dose}: 65± 5%</p> <p>MMAD: 2.82 ± 0.15 µm</p>	<p>FPD (based on a nominal dosis of 5mg insulin): 2.94-3.32 mg</p> <p>FPF_{metered dose}: 66± 4%</p> <p>MMAD: 2.80 ± 0.11 µm</p>	<p>FPD (based on a nominal dosis of 5 mg insulin): 2.71-3.09 mg</p> <p>FPF_{metered dose}: 59 ± 4%</p> <p>MMAD: 2.88 ± 0.21 µm</p>	<p>FPD (based on a nominal dosis of 5mg insulin): 2.67-3.04 mg</p> <p>FPF_{metered dose}: 59 ± 4%</p> <p>MMAD: 2.89 ± 0.17 µm</p>

** Detailed results for microbial quality can be found in APPENDIX VIII.

IV.2.2.2. Methods

IV.2.2.2.1. Study design

The study was conducted at Erasme Hospital (Brussels, Belgium) in accordance with the principles stated in the Declaration of Helsinki. Approval was obtained from the ethics committee of Erasme Hospital (Ref.: P2009/154 / 2009-012578-10) and from the Belgian Federal Agency for Medicines and Health Products (FAMHP, Ref.: EudraCT No. 2009-012578-10).

The study design is an open single-dose, two-treatment, two-period cross-over study with a wash-out period of at least 6 days between the two phases of the study. Long-standing type 1 diabetic patients were chosen for the study because of the absence of endogenous insulin production, which allows easy and accurate measurement of the exogenous insulin reaching the systemic circulation after inhalation. This population of patients was preferred to healthy volunteers, in whom the circulating exogenous insulin concentration would need to be calculated based on simultaneous insulin and C-peptide measurements (Becker et al., 2006) or by suppressing endogenous insulin secretion through a continuous infusion of insulin, leading to a stable (and known) insulin serum concentration (Heinemann et al., 1997).

A dose of 2 U/kg b.w. of insulin was chosen for both formulations as the bioavailability of insulin by inhalation was expected to be around 10% of the s.c. bioavailability (Thippawong et al., 2002; Heinemann, 2004). Both formulations were radiolabelled with up to 0.014 mCi/kg or 0.53 MBq/kg of technetium-99m (^{99m}Tc). The maximum effective dose of radioactivity administered to the subjects in this study was estimated to be 8.29 $\mu\text{SV/kg}$.

The patients using multiple insulin injections did not inject their long-acting insulin during the evening preceding a study day to ensure that no residual s.c. exogenous insulin was present at the time of dosing. To limit night and morning hyperglycemia, patients were asked to delay dinner to 10:30 P.M. and to inject short-acting human insulin (Actrapid® 100 IU/ml) thirty minutes before, at the usual dose for the meal. For patients with continuous subcutaneous insulin infusion (CSII), the pump was stopped 6h prior to administration of the inhaled insulin. The subjects fasted for at least 10 hours (food) and 3 hours (drink) before

dosing. The morning of the study, patients received a two-hour intravenous insulin infusion of Actrapid[®] to control glycemia prior to insulin inhalation. Glycemia was assessed every 20 min using a glucometer and the infusion rate was adapted on a case-by-case basis to achieve a target glucose level of 100-200 mg/dl at the end of the infusion period. The infusion was stopped 30 min before dosing to avoid the presence of residual exogenous insulin.

Administration of the formulations took place as follows: after a forced exhalation, subjects were asked to inhale the formulation as fast and deep as possible and to hold their breath for 10 seconds before exhaling through a filter. This filter was used to trap any aerosol particles present in the expired air. The patients were taught to perform this procedure during the 30-min period preceding administration of the formulation.

A standardised meal for diabetic patients was provided 30 min after dosing. Alcohol-, caffeine-, grapefruit- and xanthine-containing food or drink were not allowed during the study period.

IV.2.2.2.2. Patients

Twelve type 1 diabetic patients (plasma C-peptide concentration below 0.2 nmol/L) were recruited (seven men and five women; 44 ± 10 years; body weight 88 ± 14 kg; BMI between 23.2 and 33.6 kg/m²). Patients were physically and psychologically well, based on medical history, clinical examination, and routine laboratory tests performed shortly before experiment, and had stable insulin requirements for at least 6 months before inclusion. Patients with poor diabetes control (requiring hospital admission or presenting repeated serious hypoglycemic episodes in the past 6 months) were excluded.

Pulmonary function was recorded using a disposable spirometer (EasyOne, NDD Medizintechnik AG, Zürich, Switzerland). The values for FEV₁ (forced expiratory volume in one second), FVC (forced vital capacity), and PEF (peak expiratory flow) were > 80% of the predicted value for all patients. Because of the modified absorption of inhaled insulin in smoking subjects (Himmelman et al., 2003), all patients had to be non-smokers for at least 1 year before the study (assessed by medical history and a cotinine urine test). Excluded from this study were patients with any past or active acute or chronic pulmonary disorder,

patients with a total daily insulin dose exceeding 150 U, patients with drug addiction or excessive use of alcohol (daily intake in excess of the equivalent of 25 g pure alcohol) or xanthines (tea, coffee, cocoa), and pregnant or lactating patients. Subjects participating in another study within four weeks of this study were also excluded. Before starting the study, the nature of the clinical trial was explained and written consent was obtained from all patients.

IV.2.2.2.3. Safety assessment

Patients were closely monitored during the whole study period for possible hypoglycemia (by checking physical symptoms and blood glucose levels using a glucometer). If necessary, glucose tablets (Dextro Energy) or a 50% dextrose IV injection (2 cc/kg) were administered. Pulmonary function (PEF, FVC, FEV₁) was recorded before and 30 min after dosing. Patients were monitored for adverse events throughout the study days. Subjects underwent a control visit (physical examination, pulmonary function testing, and routine clinical biology and urine analysis) in the 4 weeks preceding the start and in the 10 days following the end of the study. On this end medical date they were also asked about the occurrence of any adverse effect in the hours and days following the experiment.

IV.2.2.2.4. Radiolabelling of the formulations

A classical method for the radiolabelling of dry powders is by adsorbing the radiolabel onto the formulation particles. This is achieved by wetting the particles with a non-solvent containing the radiolabel, followed by the evaporation of the non-solvent, leaving the radiolabel on the surface of the drug particles (Chan, 2002; Newman et al., 2003; Sebti et al., 2006; Pilcer et al., 2008c). ^{99m}Tc is the most commonly-used γ -ray-emitting radionuclide for the radiolabelling of pharmaceutical aerosols. The γ -ray of ^{99m}Tc has sufficient energy (140 keV) to penetrate body tissues, and its half-life of ^{99m}Tc (6 h) is sufficient for handling and imaging, while limiting the risks of lengthy exposure of subjects to radiation (Clark et al., 2008; Carvalho et al., 2011).

The ^{99m}Tc isotope used in the study was first eluted as sodium pertechnetate in a dedicated area of Erasme Hospital (authorisations n°s AFCN 2349/BHA-2402-B and AFCN 2348/BH-2402-A) using a ^{99}Mo - ^{99m}Tc generator from Covidien (MA, USA). The ^{99m}Tc was then extracted into methylethylketone (MEK) by shaking the pertechnetate solution with an approximately equal volume of MEK. The aqueous and MEK phases were separated in a separating funnel and the MEK phase containing the pertechnetate was evaporated to dryness. After that, the pertechnetate was re-dissolved in a small volume of isopropanol (< 2 ml) and then added to the insulin suspension (containing dissolved lipids when applicable) before spray-drying using a Büchi Mini Spray Dryer B-191 (Büchi Laboratory Techniques, Flawil, Switzerland) with constant stirring using the same procedure as described in part IV.1.2.2.1.2.

IV.2.2.2.5. Validation of the radiolabelling process

A validation procedure was performed for each formulation to ensure that the radiolabel was effectively adsorbed onto the surface of the drug particles, that it had the same aerodynamic behaviour as the drug powder (no dissociation), and that it did not alter the size distribution of the drug. The technique employed is widely used and described in the literature (Newman and Wilding, 1998; Sebti et al., 2006). The aerosols were fractionated by impaction using an MSLI (Copley Scientific, UK). Measurements (n=9) were made at 100 l/min for 2.4 s using an Aerolizer[®] inhaler.

The aerodynamic fine particle fractions (FPF, expressed as a percentage of the total metered dose) and aerodynamic particle size distributions (PSD) of the following three products were compared: the unlabelled drug, to which no radiolabel had been added; the labelled drug, following the addition of the ^{99m}Tc radiolabel (from drug deposition in the MSLI, determined by the HPLC method described in IV.1.2.2.4.); and the radiolabel itself (determined by a γ -counting technique using a Cobra γ -counter [Packard bioscience, UK]). This comparison was made to show the similarity of the products' behaviours. The repeated-measures ANOVA test was used to validate the radiolabelling method.

The insulin content of the formulations was also measured using an HPLC method (IV.1.2.2.4.) to detect any possible degradation of the insulin molecule or any impurity that could be due to the radiolabelling process. The overall quality of the radiolabelled formulations was assessed by measurement of the content in HMWP and residual solvents and measurement of the uniformity of the delivered dose. Microbial quality was also evaluated according to the requirements of the European Pharmacopoeia for the microbiological quality of non-sterile pharmaceutical preparations for inhalation use (5.1.4.).

IV.2.2.2.6. Scintigraphic analysis

Immediately following administration of the radiolabelled aerosol, scintigraphic images were recorded in order to estimate the total amount of drug aerosol reaching the lungs and its deposition pattern. The following views were taken using a DST-XLi dual-headed γ -camera (DHD-SMV, Sopha Medical, France): posterior and anterior views of the upper body (chest and right-turned head) using a 3-minute static acquisition; full scan of the whole body (rate: 14 cm/min). A 2 mCi flat flood source was interposed between the lower detector and the patient's body, and the activity was recorded with the upper detector. This was done to define regions of interest in which activity was measured (Newman et al., 2001; Chan, 2002). A background count was also recorded for each camera head.

Four regions of interest were outlined: the oropharynx and exhalation filter, the oesophagus and trachea, the stomach, and the lungs. In regions where both anterior and posterior images were recorded, the geometric mean of counts in both images was calculated. The lungs were subdivided into perihilar (or central) and peripheral regions of interest, corresponding approximately to large and small airways, respectively. The ratio of peripheral to central lung deposition (P/C ratio) was calculated as an index of regional lung deposition or a lung penetration index (Newman et al., 2003). The dose in each defined area was expressed as a percentage of the loaded dose. Calculations were made as follows: the counts in each area were first expressed as a percentage of total body counts, which represented the emitted dose. This emitted dose was quantified by subtracting the insulin remaining in the Aerolizer[®] device and in the emptied capsule (HPLC method IV.1.2.2.4.)

from the insulin dose initially loaded in the capsule. The dose fraction in each region of interest was then adjusted to correspond to the loaded dose in place of the emitted dose.

A two-tailed paired t test was used to determine whether differences between the deposition patterns for the two test formulations were significant.

IV.2.2.2.7. Pharmacokinetic analysis

For the quantification of serum insulin levels, blood samples were collected according to the following sampling schedule: 25, 15, and 5 min before inhalation, and 10, 20, 30, 40, 50, 60, 70, 80, 90, 100, 110, 120, 135, 150, 165, 180, 210, 240, 270, 300, and 360 min after inhalation. After collection, blood samples were left to coagulate at ambient temperature for at least 30 min. The tubes were then centrifuged for 10 min at 1 500g and serum samples were rapidly stored at -80°C in an upright position until analysis was completed. Insulin was assayed in all relevant serum samples using a commercial ELISA kit for the determination of human insulin (Mercodia[®] Insulin Elisa, Sweden).

The following pharmacokinetic parameters were calculated: peak plasma concentration (C_{max}), time to peak plasma concentration (T_{max}), and area under the curve from administration to the last quantified concentration (AUC_{0-360}), calculated using the linear trapezoidal rule. The geometric mean ($Mean_{geom}$), geometric standard deviation (SD_{geom}), and geometric coefficient of variation ($CV\%_{geom}$) of insulin concentrations were calculated for each time point. These were used in place of arithmetic descriptors because concentration data usually follow a skewed distribution that is best described according to a log-normal rather than a Gaussian statistical model (Buclin, 2009). A Mixed Procedure (REML approach, Harville, 1977) was applied to the log-transformed parameters C_{max} and AUC_{0-360} to calculate the F1/F2 ratios of these parameters as well as the associated 90% confidence intervals (CI) and CV%. The difference between the T_{max} of the two formulations was evaluated using the Hodges-Lehmann estimate of shift parameter, with calculation of the associated 90% CI (Hodges and Lehmann, 1963).

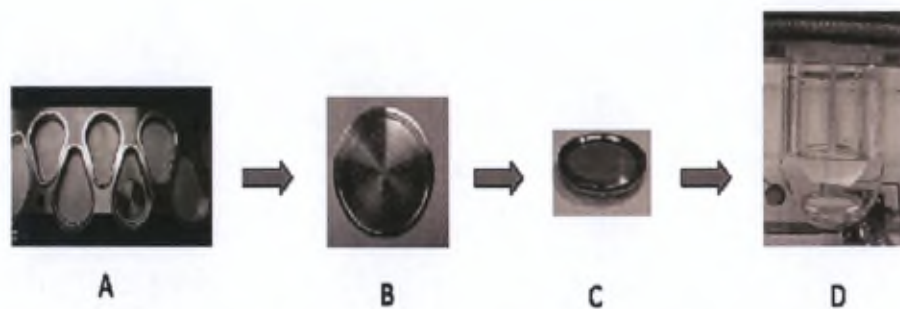


Figure 51. Representation of a dissolution test for inhalation formulations (adapted from Son et al., 2010). A) Disc insert placed in a NGI impactor, B) Particles in a defined size range, collected on the disc insert after impactation, C) Disc insert covered with a polycarbonate membrane, D) Disc insert at the bottom of the vessel of a paddle dissolution apparatus for solid dosage forms

IV.2.2.2.8. In vitro evaluation of the influence of the airflow rate on the aerodynamic behaviour of the formulations

The aerodynamic features of the two formulations, such as the MMAD and the FPF, were described previously (see IV.1.3.3.). These measurements were performed using an air flow rate of 100 l/min, which corresponds to a pressure drop of 4 kPa in the Aerolizer® device. This standardised pressure drop is recommended in European Pharmacopoeia 6.0 for the testing of all dry powder inhaler devices. However, this assumes optimal lung function and optimal inhalation procedure from the patient to obtain a good match between in vitro and in vivo data.

Additional in vitro impaction measurements were therefore made for the two formulations at 30 l/min and 60 l/min to determine the influence of a sub-optimal air flow rate on their aerodynamic properties. These were performed using an MsLI with an acquisition time of 8 s and 4 s for the 30 l/min and 60 l/min flow rates, respectively. The detailed procedure of the impaction measurements was described previously (IV.1.2.2.8.3.).

IV.2.2.2.9. Dissolution test

An in vitro dissolution experiment was performed to compare the dissolution profiles of the two formulations, which might influence their pharmacokinetics. As no official Pharmacopoeia method has yet been established for the testing of inhaled drugs, we used a method adapted from the standard “Paddle over disc” described in European Pharmacopoeia 2.9.4.-2. for the testing of transdermal patches (**Figure 51**) (Son and McConville, 2008). Because only a fraction of the emitted dose of the inhaled formulations enters the lungs and is accessible for dissolution, the whole insulin dose was first fractioned using a Next Generation Impactor (NGI, Copley Scientific Ltd, Nottingham, UK, see IV.1.2.2.8.3.) in order to select only those particles that would deposit in the lungs for the dissolution test. The cup in position 3 of the NGI was chosen to collect particles and was equipped with a removable disc insert in the impaction area. This choice was based on the amount of powder impacted on the different stages of the impactor as stage 3 was found to contain the largest impacted fraction for both formulations. Moreover, at the selected operating flow rate (60 l/min for 4 s), the aerodynamic diameter of the particles collected at

stage 3 was between 2.82 μm and 4.46 μm , values that are compatible with deep lung deposition.

An Aerolizer[®] inhaler was first filled with a single n° 3 HPMC capsule loaded with 50 mg and 60 mg powder for the F2 and F4 formulations, respectively. This difference in powder load was necessary to collect the same insulin dose in the collection cup for each of the two formulations (8.2 \pm 0.1 mg and 8.4 \pm 0.2 mg, respectively). Following size fractionation in the NGI, the disc insert was removed from the collection cup and covered with a polycarbonate membrane with a pore size of 0.4 μm (Millipore, MA, USA), pre-soaked in dissolution fluid and locked in the membrane holder. The disc was then placed at the bottom of the vessel of a paddle dissolution apparatus (Erweka DT6, Heusenstamm, Germany) for solid dosage forms (European Pharmacopoeia 6.0) containing 300 ml of phosphate buffer saline (PBS) as dissolution medium. Simulated lung fluid (SLF) was not used in this case as its pH varies significantly with time (Sdraulig et al., 2008) and the dissolution of insulin is pH-dependent (Fischel-Ghodsian et al., 1988; Lakhiari and Muller, 2004). The use of PBS instead of SLF was found to give results that were similar to the dissolution profiles of budesonide-containing lipid microparticles (Mezzena et al., 2009). The operating conditions were as follows: paddle rotation speed, 75 rpm; temperature of the bath, 37.0 \pm 0.2 $^{\circ}\text{C}$; distance between the blade and the upper face of the disk, 2.5 cm. During dissolution testing, 1 ml samples were withdrawn from the dissolution vessel and replaced with an equivalent volume of fresh dissolution medium at regular intervals up to 180 min. The percentage of dissolved insulin at each time point, and the residual insulin on the membrane and the membrane holder were quantified using HPLC analysis (IV.1.2.2.4.). The total insulin dose considered in the calculation was obtained by adding together the insulin dose obtained at 180 min and the dose collected on the membrane and the membrane holder.

The similarity factor f_2 was used to compare the two dissolution profiles (Shah et al., 1998). It was calculated using only the first nine time points ($P=9$) in order to limit the number of points with a dissolution of the product of over 85% and to avoid bias (f_2 values are sensitive to the number of dissolution time points).

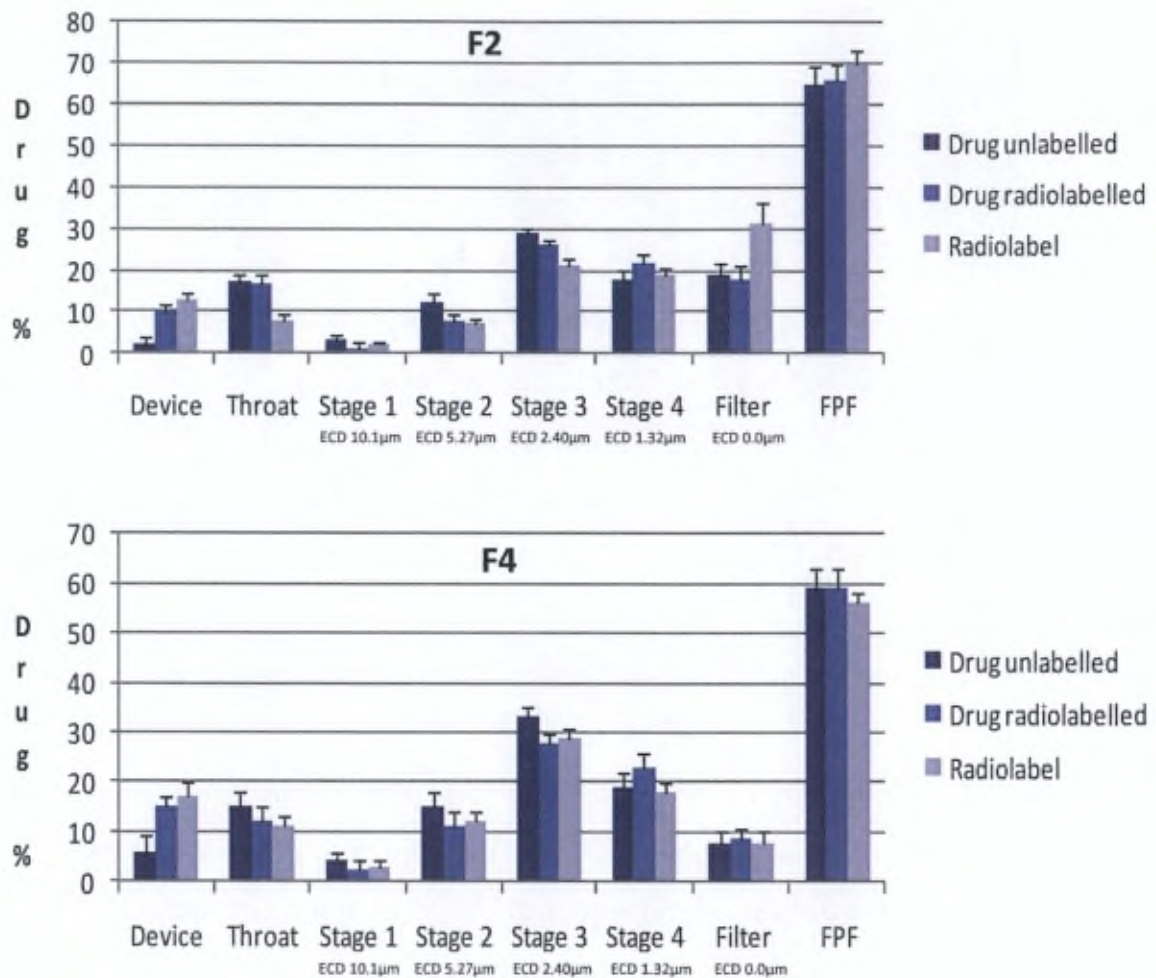


Figure 52. In vitro aerodynamic particle size distributions of F2 (up) and F4 (down) formulations: before labelling, after labelling (drug labelled), and after labelling (radiolabel) with ^{99m}Tc (n=9). Results were obtained using the MSLI, using HPMC capsules loaded with 5 mg powder in an Aerolizer[®] device, with a flow rate of 100 L/min for 2.4 s. The drug % was calculated on the basis of the metered dose of insulin

IV.2.3. Results

IV.2.3.1. Validation of the radiolabelling process

In vitro evaluation of the aerodynamic behaviour of the two insulin formulations with the Aerolizer® device was performed to ensure that the radiolabelling method did not significantly modify the PSD of the aerosol generated by the device. It was also performed to confirm that the distribution of the ^{99m}Tc reflected that of the drug, and that ^{99m}Tc therefore acted as a suitable marker for the two powder formulations.

The MsLI in vitro deposition profiles were compared for unlabelled insulin, labelled insulin, and ^{99m}Tc (Table XVI and Figure 52). Results for the F4 lipid-coated formulation showed no significant differences in the powder impaction at any stage of the MsLI, except for the powder remaining in the device (repeated-measures ANOVA test, $p > 0.05$). This demonstrates that the PSD of the radiolabel and the formulation were well-matched, with no alteration of the aerosol properties after radiolabelling. The FPF results obtained for the F4 formulation before labelling ($59 \pm 4\%$), after labelling ($59 \pm 4\%$), and for the radiolabel ($56 \pm 2\%$) were also not significantly different (repeated-measures ANOVA test, $p > 0.05$).

Table XVI. In vitro aerodynamic particle size distributions of F2 and F4 formulations: before labelling, after labelling (drug labelled), and after labelling (radiolabel) with ^{99m}Tc (n=9).

Results obtained using the MsLI, using HPMC capsules loaded with 5 mg powder in an Aerolizer® device, with a flow rate of 100 L/min for 2.4 s. The drug % was calculated on the basis of the metered dose of insulin

	F2 formulation				F4 formulation			
	Drug unlabelled (%)	Drug labelled (%)	Radiolabel (%)	Statistics (ANOVA, repeated measures)	Drug unlabelled (%)	Drug labelled (%)	Radiolabel (%)	Statistics (ANOVA, repeated measures)
Device	2.2 ± 1.8	10.0 ± 1.9	13.0 ± 1.5	$p < 0.05$	6 ± 3	15 ± 2	17 ± 3	$p < 0.05$
Throat	17 ± 2	16.8 ± 1.9	7.9 ± 1.8	$p < 0.05$	15 ± 3	12 ± 3	11 ± 2	N.S.
Stage 1	3.5 ± 0.8	1.3 ± 1.3	2.0 ± 0.6	N.S.	4.1 ± 1.9	2.5 ± 1.9	2.8 ± 1.5	N.S.
Stage 2	12.5 ± 2.1	7.7 ± 1.9	7.0 ± 1.3	N.S.	15 ± 3	11 ± 3	12 ± 2	N.S.
Stage 3	29.1 ± 1.0	26.2 ± 1.1	20.9 ± 1.9	N.S.	33 ± 2	28 ± 2	29 ± 2	N.S.
Stage 4	18.0 ± 2.0	21.7 ± 2.1	19.0 ± 1.8	N.S.	19 ± 3	23 ± 3	18 ± 2	N.S.
Filter	19 ± 3	18 ± 3	31 ± 5	$p < 0.05$	8 ± 2	8.9 ± 1.8	8 ± 2	N.S.
FPF (%)	65 ± 4	66 ± 4	70 ± 3	N.S.	59 ± 4	59 ± 4	56 ± 2	N.S.
MMAD (µm)	2.82 ± 0.15	2.80 ± 0.11	2.76 ± 0.13	N.S.	2.88 ± 0.21	2.89 ± 0.17	2.92 ± 0.16	N.S.

Table XVII. Evaluation of the lung function (PEF, FVC, and FEV₁) of the patients just before dosing (Pre-) and 30 min after dose (Post-) using a disposable spirometer. Results expressed as a percentage of the predicted value for each subject. A two-tailed paired t test was performed for each parameter, with the values obtained before and after dosing.

Patient	F2 formulation						F4 formulation					
	FVC		FEV1		PEF		FVC		FEV1		PEF	
	Pre-	Post-										
1	104	99	100	97	106	93	106	101	97	95	97	81
2	87	80	81	82	98	101	89	92	80	81	93	92
3	97	100	84	83	89	86	111	101	103	84	82	84
4	80	81	81	80	85	95	83	82	82	80	83	83
5	84	88	80	85	87	81	81	88	87	88	83	80
6	100	90	98	92	84	85	95	86	98	83	81	82
7	98	98	100	98	90	109	105	107	106	106	92	104
8	83	108	83	100	82	98	92	111	86	104	89	103
9	95	121	94	115	82	118	125	123	118	116	102	109
10	98	92	100	99	141	140	98	95	100	102	139	155
11	97	94	98	101	118	125	94	92	97	97	114	112
12	82	122	92	122	90	136	109	127	113	122	108	140
Mean	92	98	91	96	96	106	99	100	97	97	97	102
S.D.	8	14	8	13	18	20	13	14	12	14	17	24
statistics	p = 0.2411 N.S.		p = 0.1335 N.S.		p = 0.0816 N.S.		p = 0.6074 N.S.		p = 0.7905 N.S.		p = 0.1687 N.S.	

On the other hand, results for the F2 uncoated formulation showed significant differences for the powder impaction in the device, the throat, and the filter (**Table XVI** and **Figure 52**). The presence of a lipid coating in the F4 formulation, which is formed at the same time as the radiolabelling process during spray-drying, might have helped the radiolabel to adhere to the particles. However, FPF values obtained for the F2 formulation before labelling ($65 \pm 4\%$), after labelling ($66 \pm 4\%$), and for the radiolabel ($70 \pm 3\%$) were not significantly different ($p > 0.05$), indicating that the radiolabelling process could adequately be used to assess in vivo lung deposition.

The insulin content of the formulations was also measured using an HPLC method (IV.1.2.2.4.) to detect any possible degradation of the insulin molecule or any impurity that could be due to the radiolabelling process. The overall quality of the radiolabelled formulations was also assessed by measurement of the content in HMWP and residual solvents and measurement of the uniformity of the delivered dose. No significant difference was observed with the characteristics of the unlabelled formulations, as can be seen in the batch analysis presented in **Table XV**.

IV.2.3.2. Adverse events

The lung function (PEF, FVC, FEV₁) of patients was evaluated just before dosing and 30 min after dose using a disposable spirometer. For both formulations, mean values for these parameters (expressed as a percentage of the predicted value for each subject) were not significantly different before and after dosing (two-tailed paired t test, $p > 0.05$), as can be seen in **Table XVII**. Measurements were always above 80% of the predicted value for both formulations. Two episodes of mild coughing occurred just after inhalation of the drug (one episode for each formulation), which resolved themselves within 1 minute and did not affect the results of the lung function test.

Mild hypoglycemic episodes (plasma glucose level < 60 mg/dl) occurred in 3 patients for the F2 formulation, and in 1 patient for the F4 formulation. These events were easily resolved using glucose tablets. Hypoglycemia occurred around one hour after dosing. Four and 5

Table XVIII. Distribution of the insulin dose (% of the loaded dose, mean \pm SD) in the lungs, oropharynx, trachea, Stomach, and device for the F2 and F4 insulin formulations in type 1 diabetic patients (n=11)

	F2	F4
Device	2.5 \pm 1.0	5 \pm 2
Oropharynx	18 \pm 9	35 \pm 11
Trachea/oesophagus	4.9 \pm 1.3	6 \pm 2
Stomach	3 \pm 2	5 \pm 3
Whole lung	50 \pm 9	24 \pm 8
1/3 perihilar	25 \pm 5	14 \pm 7
2/3 peripheral	25 \pm 4	10 \pm 2
P/C ratio	1.05 \pm 0.15	0.80 \pm 0.18

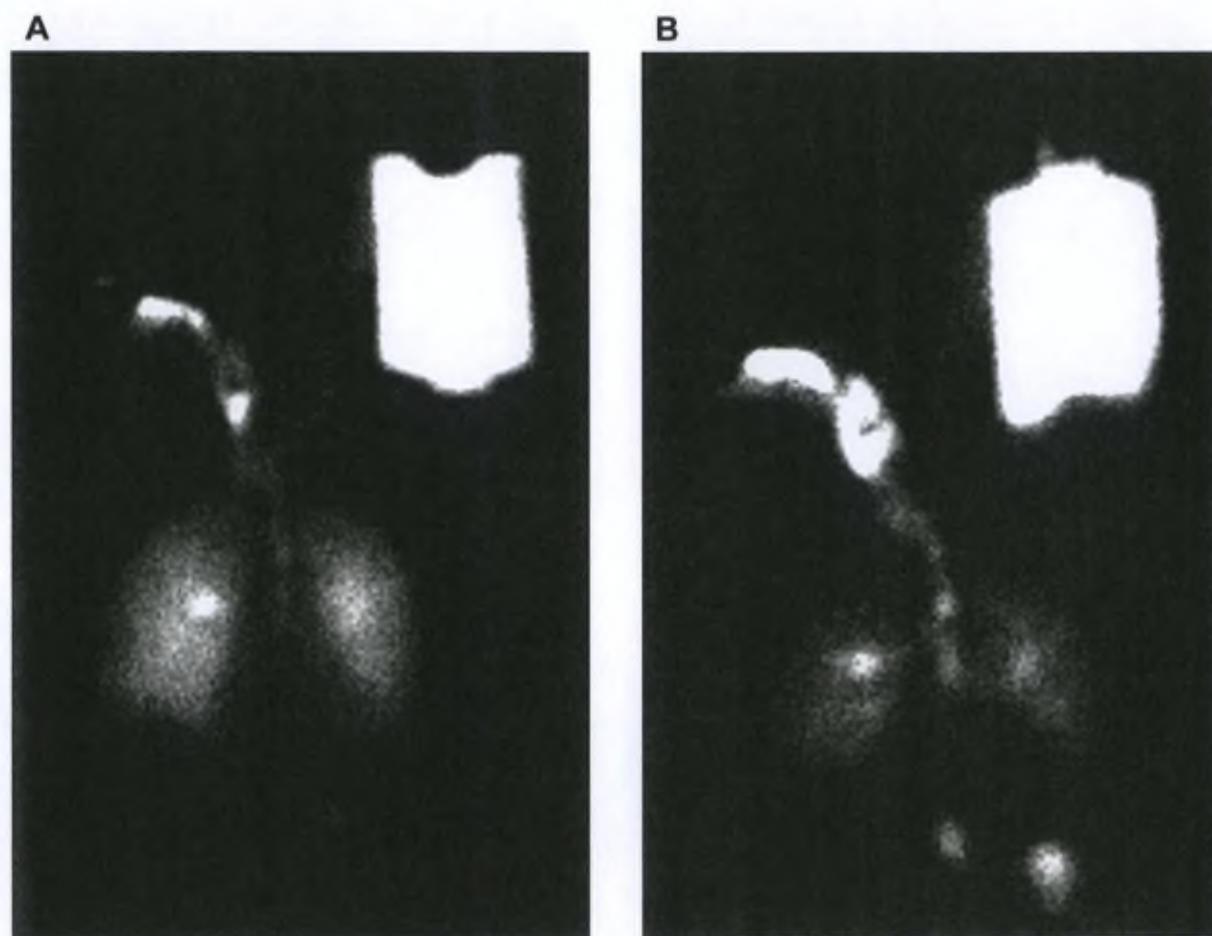


Figure 53. Scintigraphic images obtained for one representative patient after administration of the F2 formulation (A) and F4 formulation (B)

patients for the F2 and F4 formulations, respectively, were hyperglycemic (plasma glucose level > 200 mg/dl) at the end of the study period. When needed, s.c. insulin was administered to correct glycemia after collection of the last blood sample.

One patient presented a headache the day after administration of the two formulations, which might be linked to the taking of the inhaled insulin. No other adverse events were noted in any subject for either formulation.

IV.2.3.3. Scintigraphic results

Analysis of the scintigraphic results was performed on 11 subjects as one of the patients was withdrawn because of poor compliance with the instructions for the inhalation procedure (deep and slow inspiration in place of deep and fast). The percentage of radiolabelled insulin formulation deposited in the device (determined by HPLC) and in the whole lung, oropharynx, trachea (inseparable from the oesophagus), and stomach, as determined by γ -scintigraphy is shown in **Table XVIII**.

The F2 and F4 formulations exhibited a mean lung deposition of $50 \pm 9\%$ and $24 \pm 8\%$, respectively (two-tailed paired t test, $p < 0.0001$). Similar percentages of the insulin dose were deposited in the device ($p > 0.05$), the trachea ($p > 0.05$), and the stomach ($p > 0.05$) for the F2 and F4 formulations, respectively (see **Table XVIII**). The dose impacted in the oropharynx was significantly higher for the F4 formulation than for F2 (35% vs. 18% ($p < 0.01$)).

A representative comparison of the scintigraphic images obtained for the two formulations is shown in **Figure 53**. The powder is homogeneously distributed in the peripheral region of the lungs for the two formulations, and more powder is impacted in the oropharynx and trachea for the F4 formulation. These observations are in accordance with the distribution of the dose obtained in **Table XVIII**. Regional deposition results are also shown in this table. The relative distribution (P/C ratio) of the radiolabel within the central and peripheral airways was higher for the F2 formulation (1.05 vs 0.80, $p < 0.001$), indicating a greater deposition in small-diameter airways and alveoli.

Table XIX. Comparison of the scintigraphic and pharmacokinetic parameters obtained for the F2 and F4 formulations and for other inhaled insulin formulations in selected studies

DPI formulation	Inhalation device	SCINTIGRAPHIC DATA		PHARMACOKINETIC DATA							
		Whole lung deposition (% of loaded dose)	Ref.	n	Dose	T _{max} (min)	C _{max} (mU/l)	AUC ₀₋₃₆₀ (mU h/l)	Dose-normalised C _{max} ¹ (mU/l)	Dose-normalised AUC ₀₋₃₆₀ ¹ (mU h/l)	Ref.
F2 formulation	Aerolizer*	50 ± 9	/	11	2 U/kg b.w. ~ 176 U	26 ± 7 [†]	73 (52) [*]	230 ± 95 [†]	41(52) [*]	131±54 [†]	/
F4 formulation	Aerolizer*	24 ± 8	/	11	2 U/kg b.w. ~ 176 U	16 ± 9 [†]	52 (51) [*]	125 ± 62 [†]	30 (51) [*]	71±35 [†]	/
Exubera* (Pfizer, New York, NY)	Exubera inhaler*	~ 40	Exubera SPC, 2007	10	1 mg (27.5 U)	55.0 [†]	9.7 [*]	27.4 [*]	35.3 [*]	99.7 [*]	Becker et al., 2006
Afrezza* (MannKind, Valencia, CA)	MedTone inhaler*	40 ± 9	Cassidy et al., 2011	16	100 U	19.8 [‡]	241 (52) [*]	219 (43) [*]	241 (52) [*]	219 (43) [*]	Potocka et al., 2011
AIR* (Alkermes, Cambridge, MA)	AIR* inhaler*	51 (18)	Delong et al., 2005	15	5.2 mg =(150 U)	45 [‡]	44 (49) [*]	148 (39) ^{*2}	29.3 (49) [*]	99 (39) ^{*2}	Rave et al., 2007a

^{*} Arithmetic mean ± SD

[‡] Median

^{*} Geometric mean (geometric CV%)

¹ Dose-normalised C_{max} and dose-normalised AUC₀₋₃₆₀ are calculated on the basis of a 100 U dose

² AUC₀₋₆₀₀ in place of AUC₀₋₃₆₀

IV.2.3.4. Pharmacokinetic results

Analysis of the pharmacokinetic results was also performed on 11 subjects. The pharmacokinetic data for the two formulations (**Table XIX**) correlated well with the mean percentage of insulin deposited in the lungs, as determined by γ -scintigraphy. The AUC_{0-360} and C_{max} values were significantly higher for the F2 formulation than for the F4 formulation, with a F2/F4 ratio for AUC_{0-360} of 188% (90% CI: [148; 240], CV% = 32%). In comparison, the F2/F4 ratio of the mean deposition in the lungs, measured by scintigraphy, was around 208%. The F2/F4 ratio for C_{max} was 138% (90% CI: [107; 177], CV% = 34%). The rapid serum concentration peak for the two DPI formulations, followed by a progressive decrease in insulin concentrations over 6 h, is illustrated in **Figure 54**.

The T_{max} of the uncoated formulation (F2) and lipid-coated formulation (F4) occurred at 26 and 16 min, respectively. The Hodges-Lehmann estimation of the median difference in T_{max} was 10 min with a 90% CI of [-10 ; 20]; hence T_{max} was not statistically different for the two formulations. It should be noted that the first blood sample used for the measurement of pharmacokinetics was collected only 10 min after dosing, which could have slightly underestimated the AUC_{0-360} and C_{max} for the F4 formulation.

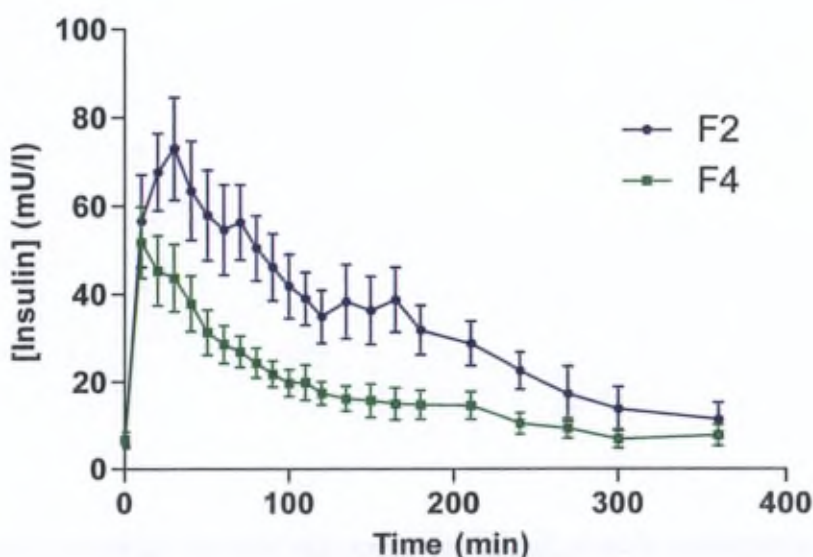


Figure 54. Insulin mean serum concentrations following administration of 2 U/kg b.w. of the F1 and F2 formulations in type 1 diabetic patients (geometric mean \pm SE, n=11)

Table XX. In vitro aerodynamic particle size distributions of F2 and F4 formulations at a flow rate of 30 l/min, 60 l/min, and 100 l/min. Results obtained using the MsLI, with HPMC capsules loaded with 5 mg powder in an Aerolizer[®] device, actuated for 8 s, 4 s, and 2.4 s, respectively. The drug % was calculated on the basis of the metered dose of insulin

	F2 formulation				F4 formulation			
	30 l/min	60 l/min	100 l/min	Statistics (ANOVA, repeated measures)	30 l/min	60 l/min	100 l/min	Statistics (ANOVA, repeated measures)
Device (%)	2.5 ± 2.0	2.0 ± 1.4	2.2 ± 1.8	N.S.	7 ± 2	8 ± 3	6 ± 3	N.S.
Throat (%)	18 ± 3	17 ± 2	17 ± 2	N.S.	25 ± 4	24 ± 4	15 ± 3	p < 0.05
Stage 1 (%)	4.2 ± 1.5	2.8 ± 1.2	3.5 ± 0.8	N.S.	7 ± 2	6 ± 2	4.1 ± 1.9	N.S.
Stage 2 (%)	14 ± 3	10.0 ± 1.0	12.5 ± 2.1	N.S.	13 ± 4	16 ± 4	15 ± 3	N.S.
Stage 3 (%)	28 ± 2	30 ± 2.0	29.1 ± 1.0	N.S.	35 ± 5	31 ± 4	33 ± 2	N.S.
Stage 4 (%)	16.1 ± 1.9	18.2 ± 1.9	18.0 ± 2.0	N.S.	10.1 ± 1.2	12.0 ± 1.3	19 ± 3	p < 0.05
Filter (%)	17 ± 3	22 ± 2	19 ± 3	N.S.	4.0 ± 1.3	3.2 ± 1.1	8 ± 2	p < 0.05
FPF (%)	62 ± 2	67 ± 4	65 ± 4	N.S.	49 ± 3	47 ± 2	59 ± 4	p < 0.05
MMAD (µm)	2.88 ± 0.09	2.79 ± 0.17	2.82 ± 0.15	N.S.	3.50 ± 0.14	3.55 ± 0.10	2.88 ± 0.21	p < 0.05

IV.2.3.5. In vitro aerodynamic evaluation

Additional in vitro deposition tests were performed at 30 l/min and 60 l/min to determine the influence of a sub-optimal air flow rate on the aerodynamic properties of the formulations. For the F2 formulation, the FPF remained constant when decreasing the air flow rate, with values of $65 \pm 4\%$, $67 \pm 4\%$, and $62 \pm 2\%$ at 100 l/min, 60 l/min, and 30 l/min, respectively (Table XX and Figure 55). For the F4 formulation, however, the FPF significantly decreased at a flow rate of 60 l/min compared to 100 l/min ($47 \pm 2\%$ and $59 \pm 4\%$, respectively), but showed no further decrease at 30 l/min ($49 \pm 3\%$). The difference in particle deposition of the F4 formulation at 60 l/min mainly consisted of an increased deposition in the throat of the impinger, while less powder was impacted at stage 4 and in the filter. This indicates that a sub-optimal aspiration flow rate used by the patient (below 100 l/min) results in a decreased disaggregation efficiency of the F4 formulation, whereas the aerodynamic properties of the F2 formulation remain almost unchanged.

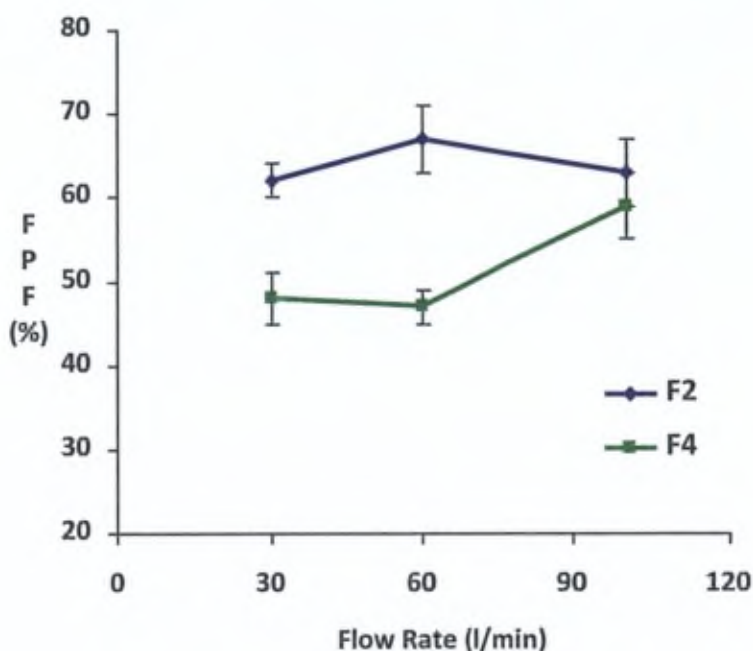


Figure 55. In vitro FPF obtained for the F2 and F4 formulations at 30, 60 and 100 l/min (mean \pm SD, n=3). Results obtained using the MsLI, using HPMC capsules loaded with 5 mg powder in an Aerolizer[®] device, with a flow rate generated for 8 s, 4 s, and 2.4 s, respectively

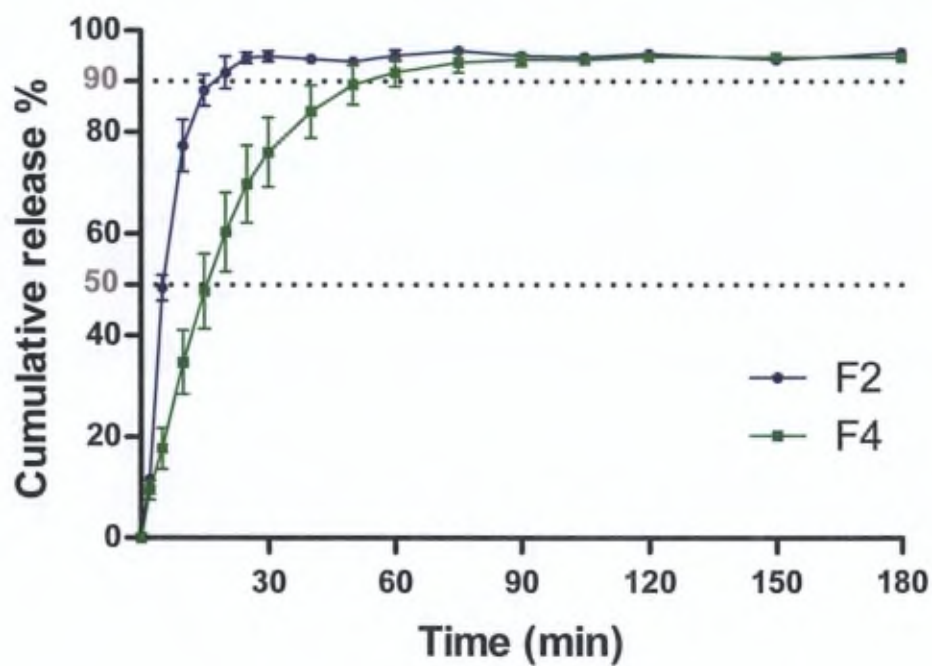


Figure 56. Dissolution profiles obtained for the F2 and F4 formulations (mean \pm S.D., n=6). Results obtained at 37 °C in a paddle dissolution apparatus filled with PBS (paddle rotation speed, 75 RPM). Powder (8.2 ± 0.1 mg and 8.4 ± 0.2 mg for the F2 and F4 formulations, respectively) collected at stage 3 after dose fractionation using a NGI operated at 60 l/min for 4 s (particle size 2.82-4.46 μ m)

IV.2.3.6. Dissolution

The dissolution profiles of the two formulations are shown in **Figure 56**. At the end of the experiment, the fraction of undissolved insulin remaining on the disc insert and membrane was $4.4 \pm 0.2\%$ and $5.3 \pm 0.2\%$ for the F2 and F4 formulations, respectively. This was most probably due to the presence of air bubbles trapped under the membrane, which prevented optimal contact between the powder and the dissolution media. F2 exhibited a faster dissolution rate than F4, with 50% of insulin mass dissolved at 4.8 min and 90% at 17.6 min for the F2 formulation, and 50% dissolved at 15.5 min and 90% at 53.3 min for the F4 formulation.

The difference between the two dissolution profiles was confirmed by the similarity factor ($f_2=28$), which was below the limit value of 50. This difference could be explained by the presence in the F4 formulation of a lipid coating around insulin particles (20% w/w), which is made up of 75% hydrophobic cholesterol. The extent of this sustained-release effect is probably limited by the presence in the coating of 25% Phospholipon[®] 90H, which contains more than 90% amphiphilic phosphatidylcholine.

These results differ from the *in vivo* observations, where insulin absorption rates were similar. This can probably be explained by the relatively thick layer of powder deposited *in vitro* on the disc insert, which could have caused a wettability problem for the F4 formulation because of its hydrophobic lipid-coating. This probably does not occur *in vivo* as the particles disperse over a much larger surface area and alveolar surfactant wets the particles.

IV.2.4. Discussion

The adverse events noted during the study were mainly a mild cough, occurring just after inhalation of the drug. Cough episodes have also been reported in 25% of patients treated with Exubera[®] and Afrezza[®]. They were transient, disappearing with continued treatment, and did not result in discontinuation of treatment (Bellary and Barnett, 2006).

The inhalation of 2 U/kg b.w. of insulin, alone or in the presence of lipids, did not cause immediate bronchoconstriction, suggesting good tolerance of these products. The lipid excipients used in this study had already shown good tolerance in other phase I clinical trials on DPI formulations of budesonide (Sebti et al., 2006) and tobramycin (Pilcer et al., 2008c) in healthy volunteers and cystic fibrosis patients, respectively.

The other adverse events were linked to glycemia. The mild hypoglycemic episodes (3 patients for the F2 formulation, 1 patient for the F4 formulation) were most probably due to a delay in taking the meal. The higher number of patients having undergone hypoglycemia after taking the F2 formulation is in accordance with the higher pulmonary deposition and bioavailability observed with this formulation. The hyperglycemic episodes observed in 4 and 5 patients for the F2 and F4 formulations, respectively, were probably linked to the end of action of the inhaled insulin. Under the study protocol, the patients could not use long-acting insulin in the evening preceding the study days, which could also have contributed to these hyperglycemic events.

Regarding potential long-term toxicity concerns for inhaled insulin, currently available studies for both Exubera[®] (a 3-year study) and Afrezza[®] (a 1-year study) indicate no apparent safety issue, although reversible, non-progressive, and non-pathological effects on lung function have been noted (Skyler et al., 2008; Rosenstock et al., 2010). The assessment of the long-term safety requires more extensive, longer evaluation, including further studies on the manner in which inhaled insulin passes through the alveoli (Bailey and Barnett, 2010).

The γ -scintigraphy results of this study showed that the F2 uncoated insulin formulation leads to an *in vivo* pulmonary deposition around 50%, which corresponds to the *in vitro* impaction results (FPF= $63 \pm 4\%$) (see IV.1.3.3.). However, the F4 lipid-coated formulation showed an *in vivo* deposition around 24%. This latter result was expected neither from the validation experiments (see **Table XVI**) nor from previous *in vitro* data as the FPF of F2 and F4 formulations obtained in MsLI experiments performed at 100 l/min were comparable (FPF of $63 \pm 4\%$ and $59 \pm 4\%$, respectively). The inter-patient variability observed in lung deposition is attributable in part to the fact that very few of the selected patients had prior experience with drug inhalation. It is therefore assumed that many of them did not perform the inhalation procedure optimally, despite brief prior training. The variability observed for the whole lung deposition (CV% of 18% and 33% for the F2 and F4 formulations,

respectively) is, however, in the range of that observed in other pharmacoscintigraphic studies performed with DPI formulations (Newman et al., 2002).

The pharmacokinetic analysis was in keeping with the scintigraphic results, with F2/F4 ratios of lung deposition and the AUC_{0-360} of 208% and 188%, respectively. This agreement indicates that if an equal dose of each formulation had reached the lungs, they would probably have shown comparable bioavailability. This also shows that the higher P/C ratio value obtained with F2 probably did not cause a significant increase in the bioavailability of this formulation. The variability observed in the pharmacokinetic data can, again, be partly attributed to the patients' lack of experience with an inhaled medication.

The results of additional in vitro aerodynamic evaluation showed that the F4 lipid-coated formulation, unlike the F2 formulation, had decreased disaggregation efficiency at a flow rate between 60 and 100 l/min. This resulted in increased powder impaction in the throat of the impinger, and decreased deposition at stage 4 and in the filter (**Table XX**). This effect was also observed in vivo (see **Figure 53** and **Table XVIII**), with higher deposition of F4 in the oropharynx resulting in lower deposition in the peripheral region of the lung. As this decreased disaggregation efficiency was not observed for the F2 formulation, this could at least partly explain the higher lung deposition observed for this formulation, leading to a higher bioavailability. However, the difference in the in vitro FPFs measured at 60 l/min (67% and 47% for the F2 and F4 formulations, respectively) cannot fully explain the in vivo difference observed in lung deposition (50% vs. 24%).

Although the correlation between FPFs and lung deposition was reasonable in many DPI studies, poor agreement was also observed from a variety of drug delivery systems (Newman et al., 2000b). A number of potential causes have been investigated. Firstly, the geometry of the MsLI throat may not be optimal as it typically takes the form of a right angle tube and cannot adequately mimic the anatomical complexity of the human upper airway or the interaction of the aerosol cloud with it. Differences in particle deposition have indeed been shown between the traditional throat model and several human-cast models (Li et al., 1996c; Dunbar et al., 2002). Secondly, the constant airflow profile used in the impactor may not be representative of the clinical inspiratory flow profile since patients instead supply a time-varying flow rate through the device. This unsteady flow can result in enhanced

mouth–throat deposition that can be explained by the higher velocity reached by the particles due to the accelerating flow rate (Grgic et al., 2006). Peak Inspiratory Flow Rate (PIFR) and Flow Increase Rate (FIR) have been shown by various researchers to be important parameters for DPI performance (Grgic et al., 2006). Based on these considerations, future pharmacopoeial recommendations for in vitro DPI testing should take into consideration realistic inhalation profiles. The development of new-generation induction ports that more closely fit physiologic features would also be highly valuable.

In view of the above-mentioned in vitro/in vivo mismatch, this study points out the importance of performing human lung deposition studies in addition to in vitro studies. This provides a much better understanding of the drug delivery process and avoids further misinterpretation of pharmacokinetic and pharmacodynamic data.

As explained previously (IV.1.3.3.), the sticky behaviour of lipid-coated powders had already been observed in other papers and is a function of the percentage of lipid coating and of the cholesterol/Phospholipon®90H ratio (Sebti and Amighi, 2006; Pilcer et al., 2006). However, no dependency on the flow rate had been noted for the aerodynamic properties of the coated powders in these experiments. This difference could be linked to the lower proportion of lipid-coating that was used (up to 5%). Although the presence of a lipid coating in the F4 formulation (20%) seems to induce a lower disaggregation efficiency at a lower inspiratory flow rate, the concept of a lipid-coating around protein particles should still be of interest. It was indeed shown to provide a low residual moisture content in the formulation, and to protect against water adsorption over time (see IV.1.3.1. and IV.1.3.4.), which is a great advantage for the long-term stability of proteins stored in the dry state, as has been shown in several studies (Wang, 2000; Schüle et al., 2008). Moreover, proteins can adsorb at the air–liquid interface of droplets during spray-drying, leading to unfolding and aggregation at the droplet surface. Surfactants such as phospholipids have been shown to reduce this phenomenon by excluding the protein from the interface, which might improve protein integrity after spray-drying (Bosquillon et al., 2004). These properties could be of particular interest for the formulation of large biomolecules such as monoclonal antibodies, which are more likely to undergo degradation than the smaller insulin molecule.

In **Table XIX**, the pharmacokinetic parameters of the F2 and F4 formulations are compared with those of the three inhaled insulin DPI formulations that have reached phase III clinical

investigation, namely Afrezza[®], AIR[®], and Exubera[®] formulations (Becker et al., 2006; Rave et al., 2007a; Potocka et al., 2011). The T_{max} of F2 and F4 (16-26 min) is comparable to that of Afrezza[®] (19.8 min). The fast absorption of Afrezza[®] is thought to result from the highly efficient delivery of the particles to the deep lung due to their low MMAD (2-2.5 μm) and narrow particle size distribution. Particles can then dissolve rapidly due to their large surface area and to the highly soluble fumaryl diketopiperazine (FDKP) residues. This provides high local concentrations of insulin that drive diffusion across the membrane (Lian et al., 2000; Angelo et al., 2009). A low T_{max} (24 ± 19 min) has also been obtained for a pure microcrystalline insulin powder (Heinemann et al., 1997), indicating that short T_{max} can be achieved without the help of an excipient. On the other hand, the AIR[®] and Exubera[®] formulations presented higher T_{max} of 45 min and 55 min, respectively. The presence of lipids (~60% DPPC) in the AIR[®] formulation causes a sustained-release effect, leading to its higher T_{max} (Vanbever et al., 1999). Although the F4 formulation also contains lipids, their proportion might be too low to exhibit this sustained release. The Exubera[®] formulation, which mainly contains mannitol and glycine as excipients, is not intended for sustained release. Its high T_{max} might be related to its particle size distribution. Although Exubera[®] presents whole lung deposition comparable with the other formulations (**Table XIX**), it has a slightly higher MMAD in the range of 2.8-3.4 μm (Harper et al., 2007) and might also have a broader size distribution, leading to lower P/C ratio. Larger particles deposit in the larger bronchioles of the lung and have a thicker epithelium to go through, which could lead to slower absorption. Moreover, these particles dissolve more slowly than smaller ones, which leads to lower local insulin concentration and may also reduce the absorption rate.

The fast release and absorption of insulin observed for the F2, F4, and Afrezza[®] formulations is of great interest for the control of post-prandial glucose excursions as it better corresponds to the natural insulin secretion profile. Indeed, with normal pancreatic beta-cell function, insulin secretion increases rapidly after a meal, with approximately two-thirds of the insulin response occurring in the first 2 h and a return to fasting levels over the course of 3-4 h (Richardson and Boss, 2007). This rapid absorption of insulin is also interesting in comparison with traditional s.c. prandial insulins. In a 1-year trial in patients with type 2 diabetes, the insulin therapy was either a twice-daily premixed biphasic insulin or a bedtime long-acting insulin glargine plus prandial Afrezza[®]. The two groups had similar efficacy regarding reduction of HbA1c, and Afrezza[®] induced slightly lower early postprandial glucose

excursions as well as less weight gain and fewer hypoglycemic episodes (Rosenstock et al., 2010).

The dose-normalised AUC_{0-360} (**Table XIX**) shows that the F2 and F4 formulations seem to have a slightly higher ($AUC_{0-360} = 131$ mU h/l) and slightly lower ($AUC_{0-360} = 71$ mU h/l) bioavailability, respectively, than the Exubera[®] and AIR[®] formulations (both with an AUC_{0-360} around 99 mU h/l). Afrezza[®] exhibits a greater normalised AUC value ($AUC_{0-360} = 219$ mU h/l), indicating a higher bioavailability. Interestingly, this cannot be related to higher whole lung deposition of the powder (Table XIX) but it is again probably related to the lower particle size of this formulation. It should be noted that the F2 and F4 formulations were administered using a commercially-available Aerolizer[®] device. Development of a dedicated DPI device could enhance their bioavailability by improving disaggregation and decrease the sensitivity of the lipid-coated formulation to flow rate variability.

IV.2.5. Conclusion

This phase I study compared the in vivo lung deposition and bioavailability of two new insulin formulations administered by inhalation to type 1 diabetic patients. The formulation with a lipid coating around the insulin particles exhibited a lower lung deposition in comparison with the uncoated formulation. This was found to be related to a decrease in the disaggregation efficiency of the powder at a sub-optimal flow-rate.

The two formulations showed interesting features, with pharmacokinetic profiles that mimic the natural insulin secretion pattern and bioavailability that is within the ranges of two of the three DPI insulins that have reached phase III clinical development. This was achieved using fast, simple production techniques, as well as simple formulations with few or no biocompatible excipients. Moreover, the formulations were administered using a simple, passive commercial device. A new dedicated device could be developed in the future to improve formulation performance.

These observed advantages are obviously of interest for the successful use of inhaled insulin in diabetic patients, as well as for the development of DPI formulations containing proteins or monoclonal antibodies that would benefit an inhaled therapy.

IV.3. Formulation and in vitro evaluation of DPI formulations of an anti-IL13 MAb fragment

IV.3.1. Introduction

In this chapter, a larger protein than insulin was chosen for the development of DPI formulations based on the same production strategy as previously developed. Indeed, insulin – which is a small protein of 5.8 kDa – was found to be a robust molecule. It formed few degradation products, even in relatively harsh production and storage conditions. Due to their more complex primary, secondary, and tertiary structures, larger proteins are likely to undergo degradation to a greater extent or could be affected by other degradation pathways. Therefore a large protein was used to evaluate the potential of the formulation strategy to achieve optimal stability and aerodynamic features. The model molecule chosen was an anti-IL13 monoclonal antibody fragment (code name: CA582), which was provided by our partner, UCB S.A. (Brussels, Belgium), within the framework of the NEOFOR project. As previously mentioned (see “Introduction”), the use of anti-IL13, as well as anti-IL4 and anti-IgE monoclonal antibodies or antibody fragments, could be of interest for the treatment of asthma and COPD. However, in most studies these new products are administered by injection. Local lung delivery could optimise the therapeutic index by increasing local tissue drug concentrations and, at the same time, minimising systemic exposure, and could also increase compliance.

IV.3.2. Materials and methods

IV.3.2.1. Materials

The CA582 molecule (UCB s.a., Brussels, Belgium) is a murine monoclonal antibody Fab fragment directed against interleukin 13 (IL-13). It is constituted of two chains of about 28 kDa and 26 kDa, with a total molecular weight of about 54 kDa. It is provided as a 24 mg/ml solution in 50 mM sodium acetate/125 mM sodium chloride, pH 5.0 buffer. Phosphate Buffered Saline (PBS) pH 7.4 was purchased from Invitrogen, Grand Island, NY, USA. Sucrose, mannitol, α -lactose monohydrate, guanidine HCl, Na glycocholate, palmitic acid, Na acetate and Na chloride were purchased from Sigma-Aldrich, St Louis, MO, USA.

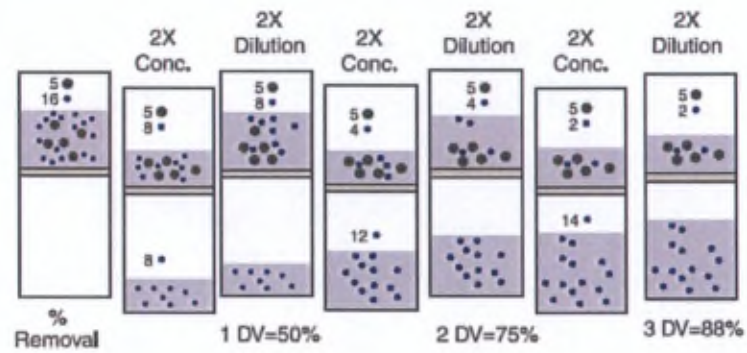


Figure 57. Principle of discontinuous diafiltration. Grey dots represent large molecules (bigger than the pores in the membrane), blue dots represent small molecules (salts or solvent). DV: diafiltration volume (Schwartz, 2003)

IV.3.2.2. Methods

IV.3.2.2.1. Desalting the antibody solution

The antibody is provided in a buffer with a high ionic strength (corresponding to about 36% of weight as salts on a dry basis). However, as the aim is to produce dry powders for inhalation, the strength of the buffer used to ensure the stability of the antibody in solution has to be limited to the minimum. There are, indeed, strong regulatory restrictions on the type and concentration of excipients accepted for pulmonary administration. It is also easier to obtain appropriate aerodynamic properties of powders when only a few, chosen excipients are present. Therefore a desalting procedure was used to replace the initial buffer before processing.

Modified buffering conditions were obtained using **discontinuous diafiltration**. This consists of the use of a semi-permeable membrane, which retains molecules that are larger than the pores of the membrane while smaller molecules, such as salts, solvents, and water, freely pass through the membrane. The device is pressurised to force fluid (and salts) through the membrane. The transport mechanism is convection in place of diffusion and the permeation rate is therefore independent of molecular size. The membrane is selected based on its rejection characteristics for the molecule to be retained. As a general rule, the molecular weight cut-off (MWCO) of the membrane should be 1/3 to 1/6 of the molecular weight of the molecule to ensure complete retention. The closer the MWCO is to that of the sample, the greater the risk of some small product loss during diafiltration (Schwartz, 2003). The sample is first concentrated to a predetermined volume and then diluted back to its original volume with water or replacement buffer. This is repeated until the unwanted salts, solvents or smaller molecules are removed. Each subsequent concentration and dilution removes more of the small molecules (**Figure 57**).

Molecules larger than salts and solvents, but still smaller than the pores in the membrane, can also be washed out. The permeability of these molecules, however, may be less than 100%. In such cases, it will take more liquid, i.e. more diafiltration volumes (DV), to completely wash a partially permeable molecule through the membrane, compared to a

Table XXI. Theoretical salt reduction (%) from a sample using discontinuous diafiltration

Diafiltration volume (2X volume reduction)	100% Permeable molecule	75% Permeable molecule
1	50%	41%
2	75%	65%
3	88%	79%
4	94%	88%
5	96.9%	93%
6	98.4%	95.6%
7	99.2%	97.4%
8	99.6%	98.4%
9	99.8%	99.0%
10	99.9%	99.4%

100% permeable molecule. Typically, the larger the molecule, the lower the permeability and the greater the wash volume required. The permeability of a molecule through a specific membrane can be determined by measuring the concentration of the molecule in the filtrate compared to the concentration in the retentate under specified conditions.

$$\% \text{ permeability} = (\text{Conc. FILTRATE} / \text{Conc. RETENTATE}) \times 100$$

Table XXI shows the relationship between permeability through a membrane and the number of diafiltration volumes required for the removal of permeating species. To remove 99% of a molecule that is 75% permeable to the membrane requires 9 DVs while for a 100% permeable species, only 7 DVs are required. In some cases, the transmission of a small molecule can also be affected by interaction with the molecule to be retained. Citrate, for example, has been shown to interact with a Fab antibody fragment, affecting its clearance (Harinarayan et al., 2008).

The diafiltration device was a 10 ml Stirred Cell 8000 (Millipore, Billerica, MA, USA) equipped with a Biomax PB polyethersulfone membrane with a 5 kDa cut-off (Millipore, Billerica, MA, USA). The device was pressurised with compressed air (4 Bar). The solution was stirred at 120 rpm during diafiltration to avoid adsorption of the CA582 onto the membrane. Seven diafiltration volumes were used to achieve complete replacement of the buffer. Several replacement buffers were tested:

- 50 mM Na acetate/125 mM NaCl, pH 5.0 (initial buffer)
- 5 mM Na acetate/12.5 mM NaCl, pH 5.0
- 1 mM Na acetate/2.5 mM NaCl, pH 5.0
- 5 mM Na phosphate, pH 6.0
- 2 mM Na phosphate, pH 6.0
- 5 mM Na phosphate, pH 7.0
- 2 mM Na phosphate, pH 7.0
- Ultrapure water, pH 7.0

The stability of the CA582 molecule in the new buffering conditions was evaluated after 24h under stirring at room temperature by evaluation of unfolding, soluble and insoluble aggregation, fragmentation, and desamidation (see IV.3.2.2.3.).

Efficacy of the desalting procedure

The efficacy of the desalting procedure was evaluated to ensure that no interaction occurred between the CA582 molecule and the buffer components (sodium acetate and sodium chloride) and to evaluate the number of DVs needed to completely remove the initial buffer. This was achieved by diafiltration with ultrapure water as a replacement solvent followed by dosage of sodium ions in the filtrate. A sodium-selective electrode was used for this purpose. Ion-selective electrodes (ISE) give the activity (A) of an ion (M) in solution by measurement of the voltage at both sides of a membrane that is sensitive to M. Although several types of electrode membranes are available, the most common type is made of glass (composition: $\text{Li}_2\text{O}-\text{Al}_2\text{O}_3-\text{SiO}_2$). It is immersed in water before use, generating a gel-like hydrated silicic acid layer. In aqueous solution, cations are removed from the outer hydrated layer and replaced by ions from the sample. This creates a potential at the boundary layer between the sample solution and the membrane that depends on the activity of M (Bard and Faulkner, 2000). Potentiometry with ISE is based on the Nernst equation:

$$E = P \log A + K$$

Where E is the measured voltage

P is a constant that mainly depends on the ion valence and temperature

K is a constant that depends on the electrode itself but is also influenced by factors such as solution viscosity, ionic strength, and presence of proteins. Diluted solutions are therefore generally required. Moreover, in diluted solutions the activity corresponds to the concentration of the respective ion (Cristol et al., 2007).

Measurements were taken using a sodium-sensitive electrode equipped with a glass membrane (ref. 6.0501.100, Metrohm, Herisau, Switzerland). The measuring range of the electrode lies between 1×10^{-5} and 1 mol/l Na^+ (corresponding to 0.23 mg/l and 22.99 g/l

Na⁺). An Ag/AgCl reference electrode was used (ref. 6.0750.100, Metrohm, Herisau, Switzerland). A calibration curve was established with [Na⁺] between 25 and 300 mg/l. The experiment was conducted on 5 ml of the initial CA582 solution and measurement of [Na⁺] was made on each of 7 successive filtrate fractions (5 ml) after appropriate dilution. Because of the limited availability of CA582, the experiment was run only in triplicate.

IV.3.2.2.2. Production of the formulations

A three-step strategy was used to produce dry formulations of the CA582 antibody from the desalted solution, with or without lipid coating around the particles. Freeze-drying was first used to obtain dry antibody material. High Shear Homogenisation (HSH) and HPH were then used to break up the freeze-dried cake and obtain particles with a size distribution compatible with deep lung deposition. Finally, particles were dried and coated with lipids (when applicable) using spray-drying. A formulation was also produced by direct spray-drying of the antibody from the solution. The physico-chemical stability of the CA582 was evaluated after each production step.

IV.3.2.2.2.1. Freeze-drying

Principle

Freeze-drying is the most common process for making solid protein pharmaceuticals. It consists of the separation of liquid water from a wet solid or from a solution or dispersion in the form of a frozen solid phase, and the subsequent removal of ice by vacuum sublimation, leaving the solutes or substrates in their anhydrous or almost anhydrous states (Franks, 1998). A freeze dryer generally consists of:

- a product chamber in which the substance is placed on shelves that can be heated,
- a vacuum pump to extract air from the product chamber, and

- an ice condenser operating at temperatures from -55 °C to -105 °C (depending on the type of system), which serves to freeze the sample and to extract water vapour from the chamber during drying.

The first step is to cool the product sufficiently to freeze and solidify the formulation, typically below its eutectic crystallization and/or glass transition temperatures (Colandene et al., 2007). As the temperature of a solution is lowered, the ice crystallizes, which results in the concentration of the protein and excipients (termed the freeze-concentrate), which are confined to the spaces between the ice crystals. Theoretically, all solutes in a mixture precipitate in the crystalline state at various stages (eutectic phase separation) during the freeze concentration process when their respective saturation solubilities are reached. When the temperature of the protein formulation further decreases after crystallization of the least soluble component, this component and water crystallize out as a mixture at the same time. The last droplet of liquid then solidifies at a temperature termed the eutectic crystallization/melting temperature (T_{eut}). However, most multicomponent protein formulations do not exhibit clean eutectic phase separation or a T_{eut} during freeze concentration (Wang, 2000). Indeed, the use of excipients that do not readily crystallise from a frozen solution will inhibit the precipitation of other components and cause the freeze concentration process to proceed well beyond the limit of saturation solubility. Freezing then continues but slows down. This is because with decreasing temperature and an increasing degree of supersaturation, the solution viscosity rises until it reaches a point at which ice growth comes to a stop: the 'solution' phase might still contain up to 50% of unfrozen water. The mixture is then said to have undergone a glass transition, characterised by a glass temperature T_g . The product consists of a mass of ice crystals embedded and dispersed in the vitreous, freeze-concentrated solution, with the whole occupying the original solution volume (Franks, 1998; Piedmonte et al., 2007). The rate of cooling during the freezing process may affect the degree of super-cooling and the size/type of ice crystals, which has the potential to affect the drying rate.

The next step after freezing is primary drying, which is sublimation of frozen or unbound water, while maintaining the product below its collapse temperature (T_c). This temperature is usually associated with the T_g of the product, with the T_c about 2°C higher than the T_g (Colandene et al., 2007). This process allows the microscopic structure of solids present in

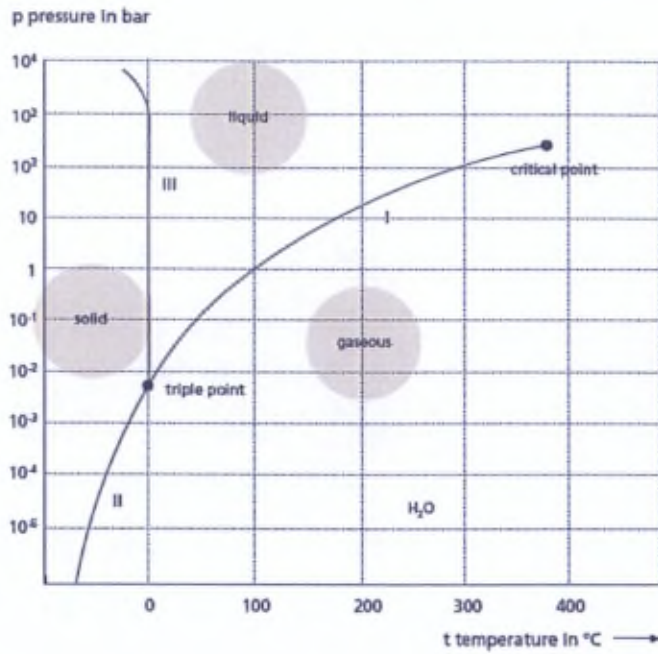


Figure 58. Phase diagram of water (Martin Christ GmbH, 2010)

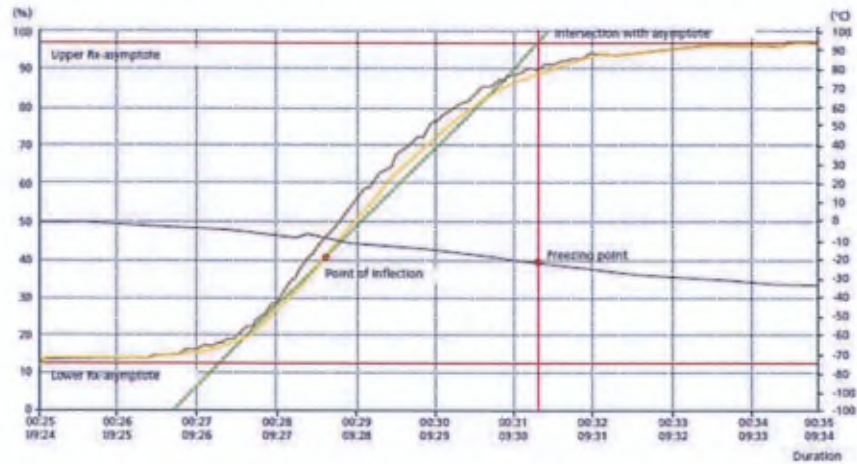


Figure 59. Method for freezing point determination. Blue curve: product temperature ($^{\circ}\text{C}$); Yellow curve: product resistance (%); Green curve: tangent at the inflection point; Red curves: asymptotes to the resistance curve

the frozen solution to be kept intact. These solids eventually make up a freeze-dried cake with a relatively high surface area. Sublimation is achieved by creating low pressure with a vacuum, with pressure typically set to the vapor pressure of ice at the desired product temperature (**Figure 58**). The desired product temperature is dependent on the formulation, since different formulations differ in their collapse temperatures, and is generally set 10°C below the solidification temperature (Colandene et al., 2007). As soon as the sublimation of the ice in the frozen material begins, heat energy is extracted from the material and it is therefore further cooled. At the same time, the shelves supporting the product to be dried are heated to supply the necessary sublimation energy to the product. The vapour extracted during drying freezes on the surfaces of the very cold ice condenser, so that the ice condenser effectively acts as a 'vapour pump'.

A secondary drying step is sometimes added if the goal is to retain the minimum amount of residual moisture, which involves the removal of adsorbed residual water. It is carried out at the lowest possible final pressure and is supported by a raised shelf temperature.

Operating conditions

Desalted antibody solutions (20 mg/ml) containing different concentrations and types of stabilising excipient (see **Tables XXIII, XXIV, and XXV** in "Results and Discussion" section IV.3.3.5.) were frozen at -30°C in the product chamber of the freeze-dryer (Epsilon 1-6, Martin Christ GmbH, Osterode, Germany). The solidification point of a typical composition (CA582/sucrose 70:30 in 2 mM Na phosphate buffer, pH 6) was determined by measuring the product temperature and electrical resistance at the same point during freezing. The electric resistance of the product being dried indeed rises dramatically with the transfer from liquid to solid state due to the reduced mobility of the ions and electrons (see **Figure 59** for the determination method). The solidification point was found to be -14.9°C. A pressure of 0.63 mbar was therefore chosen for the primary drying of all formulations, as it corresponds to a product temperature of -25°C in the ice-pressure curve, which should be far below the solidification point of all formulations. The shelf temperature was set at 5°C. This allowed complete drying within 3-4 hours while avoiding samples collapsing. Drying was

considered to be terminated when the product temperature was above the shelf temperature.

IV.3.2.2.2.2. High pressure homogenisation

In order to obtain a final particle size distribution compatible with pulmonary administration, the particle size of the freeze-dried cakes was reduced using HPH (see IV.1.2.2.1.2.). Powders were suspended in isopropanol (0.5% w/v) containing different types and concentrations of dissolved stabilising agent (see **Table XXX** and **Table XXXI** in "Results and Discussion", section IV.3.3.6.4. and IV.3.3.6.5.). Dispersion of the powders and a preliminary break up of the particles was obtained by 20 min high shear homogenisation in an ice bath using a CAT high speed homogenizer X620 (CAT M. Zipperer, Staufen, Germany) operated at 24 000 rpm. The particle size was then further reduced by HPH using an EmulsiFlex-C5 high-pressure homogeniser (Avestin Inc., Ottawa, Canada). Homogenisation cycles were either 10 cycles at 7 000 PSI and 50 cycles at 12 000 PSI, or 200 cycles at 5 000 PSI. These cycles were conducted by recirculating the processed suspension directly into the sample tank (closed loop). Operations were carried out using a heat exchanger placed ahead of the homogenising valve, with the sample temperature maintained either at 5 ± 1 °C or -20 ± 1 °C.

IV.3.2.2.2.3. Spray-drying

Four formulations (F1-F4) were selected for spray-drying, whose composition (see **Table XXXIV** in "Results and Discussion", section IV.3.3.7.1.) was chosen based on the CA582 stability results obtained for the homogenised suspensions. The same spray-drying equipment as previously described was used (see IV.1.2.2.1.1.)

Spray-drying was first used to produce a formulation directly from a solution of the antibody (F1), without the use of freeze-drying and HPH. The composition of the aqueous solution was as follows: 0.5% (w/v) CA582/sucrose 50:50 (w/w) in 2 mM Na phosphate, pH 6. The spray-drying conditions were: inlet temperature, 120 °C; resulting outlet temperature, 40-42 °C; spraying air flow rate, 800 l/h; drying air flow rate, 35 m³/h; solution feed rate, 3.3 g/min;

nozzle size, 0.75 mm. Following these conditions, the process yield was $45 \pm 5\%$ for a batch size of 100 ml, corresponding to the production of about 225 mg powder formulation.

The formulations F2-F4 were produced by spray-drying after freeze-drying and HPH, with the following parameters: inlet temperature, 70 °C; resulting outlet temperature, 35 °C; spraying air flow rate, 800 l/h; drying air flow rate, 35 m³/h; solution feed rate, 1.7 g/min; nozzle size, 0.75 mm. Following these conditions, the yield for the whole process (HPH and spray-drying) of a batch size of 100 ml, corresponding to the production of about 300 mg powder, was $60 \pm 4\%$, $62 \pm 3\%$, and $60 \pm 4\%$ for the F2, F3, and F4 formulations, respectively.

Because of the limited availability of the CA582 molecule, all formulations were produced only in duplicate.

IV.3.2.2.3. Physico-chemical characterisation

IV.3.2.2.3.1. CA582 assay

The concentration of CA582 in solution was obtained spectrophotometrically, by measuring UV absorbance at 280 nm (A_{280}). Proteins in solution indeed absorb light at this wavelength to a greater or lesser extent in proportion to the type and the number of aromatic (principally tryptophan and tyrosin) residues present and, to a very small extent, in proportion to disulfide bonds. This method can therefore be used to measure the protein concentration providing that no interfering substance is present and that the extinction coefficient (ϵ) at 280 nm has been derived. The Beer-Lambert law can then be used:

$$\text{Product concentration} = A \times D / \epsilon \times l$$

Where A = absorbance reading

D = sample dilution factor

ϵ = extinction coefficient of the protein at 280 nm

l = cuvette path length (in cm).

The extinction coefficient of CA582 at 280 nm provided by UCB s.a. is $1.82 \text{ ml.mg}^{-1}.\text{cm}^{-1}$. The test solutions were diluted in PBS, pH 7.4, (Invitrogen, Grand Island, NY, USA) to a target concentration of 0.5 mg/ml to achieve absorbance readings ≤ 1 . At this concentration, the inter-day CV% of the method was found to be 0.7% ($n=3$ on each day, performed on three successive days). The quantification limit (QL) of the method was determined according to the ICH guidelines (Q2(R1), Validation of analytical procedures) and was found to be 0.05 mg/ml. This concentration corresponds to an absorbance signal that is 10 times higher than the standard deviation of the blank response.

The spectrophotometer was a single beam instrument (Hewlett Packard 8453) with a UV/visible diode array detector (Agilent, CA, USA). Samples for all spectroscopic measurements were analysed in triplicate after filtration through $0.22 \mu\text{m}$ syringe filters with low protein binding (Acrodisc® HT Tuffryn membrane, Pall Life Sciences, NY, USA). Spectra of PBS, pH 7.4 were recorded and subtracted from the experimental samples to correct the background interference in all experiments. The potential occurrence of a matrix effect due to the presence of excipients (buffering agents, sugars, polyols, amino-acids and/or lipids) was evaluated for each formulation. In this purpose, the A_{280} values obtained in samples of known concentrations were compared, with and without addition of the matrix excipients in the same proportions as in the formulation. The A_{280} average values ($n = 3$) were compared for each formulation by the t-test. None of the samples with matrix excipients presented a significant difference with the samples without addition of the matrix excipients. This indicates that no matrix effect occurred for any of the conditions tested.

A study was performed to verify whether absorbance at 280 nm of the CA582 molecule is influenced by the conformational state of the protein. This was done to find out if the method can be considered unbiased for the determination of the antibody concentration regardless of its folding state. Absorbance at 280 nm by aromatic side chains is indeed frequently used to monitor conformational changes in proteins. This is based on the exposure of some aromatic residues buried within the hydrophobic core of the protein to the aqueous solvent during unfolding, giving rise to a decrease in absorbance (Melo et al., 1997; Liu et al., 2009).

Denaturation of the antibody was performed by diluting aliquots of the reference CA582 material in PBS containing 0, 2, 4 or 6 M guanidine hydrochloride (Gdn, Sigma-Aldrich, MO,

USA) to a final concentration of 0.5 mg/ml. Before the measurements were made, samples were incubated at 25°C overnight to reach equilibrium. The equilibrated solutions were then filtered through 0.22 µm syringe filters and scanned from 200 to 300 nm. The baselines of the buffer solutions were subtracted from the corresponding sample absorbance.

IV.3.2.2.3.2. Evaluation of unfolding

The three-dimensional structure of a protein is essential to its biological activity. Structural alterations at this level, namely the unfolding or denaturation of proteins, are frequently responsible for loss of activity. UV absorbance is a common and simple technique for monitoring protein unfolding. However, absorbance at 280 nm of CA582 was found to be little influenced by protein conformation (see "Results and Discussion", section IV.3.3.1.). Absorbance at 230 nm (A_{230}) is also known to be sensitive to protein conformation (Liu et al., 2009). The UV spectra of protein solutions usually show slopes, not peaks, at 230 nm. However, the difference spectra between folded and unfolded conformations commonly show a downward peak at 230 nm; i.e., unfolded proteins have lower A_{230} than folded proteins. Interestingly, the change in A_{230} on unfolding is typically 10-fold greater than the change in A_{280} . Like absorbance at 280 nm, aromatic side chains, especially tryptophan, are known to contribute most to the change in A_{230} on protein unfolding (Liu et al., 2009). However, changes in A_{230} are also influenced by changes in peptide backbone conformation. Indeed, the π electrons in the peptide bond are to some extent delocalised over three atoms: the peptide nitrogen, carbon, and oxygen act at low wavelengths (180-220 nm) because the $\pi \rightarrow \pi^*$ transition in the peptide bond absorbs light (Glazer and Smith, 1961; Kuipers and Gruppen, 2007).

Unfolding was evaluated by using the ratio of A_{230}/A_{280} in place of the absolute A_{230} . This avoids the influence of CA582 concentration on the measurement and allows rapid analysis of test solutions in-line, with determination of the concentration. Samples were diluted in PBS, pH 7.4, (Invitrogen, Grand Island, NY, USA) to a target concentration of 0.15 mg/ml to achieve absorbance readings ≤ 1 for A_{230} . Samples were analysed in triplicate using the same instrumentation and protocol as described in IV.3.2.2.3.1.

IV.3.2.2.3.3. Quantitative evaluation of aggregation

IV.3.2.2.3.3.1. Soluble aggregates

Soluble CA582 aggregates were identified and quantified using size-exclusion HPLC (SEC). The procedure was performed using two columns in series to obtain the required resolution of molecular species (Zorbax GF450, 9.4mm i.d. x 25cm, and Zorbax GF250, 9.4mm i.d. x 25cm, Agilent Technologies, CA, USA). The mobile phase was 0.2 M Phosphate buffer, pH 7/ethanol 90:10. Samples were diluted to a target concentration of 5 mg/ml in 50 mM Na acetate/125mM Na chloride, pH 5.0, and were filtered on 0.22 μ m PVDF syringe filters (Millex-GV, Millipore, MA, USA) before injection. The injection volume was 20 μ l and runs were conducted at a flow rate of 1 ml/min for 30 min. Detection was achieved by absorbance at 280 nm.

The percentage of soluble aggregates was calculated using the following equation:

$$\% \text{ Aggregates} = (\text{Peak Area Aggregates} / \text{Total Chromatogram Peak Area}) \times 100$$

The use of gel filtration for the determination of molecular weight or size, particularly of proteins, is well-documented. In practice it is found that for a series of compounds of similar molecular shape and density a sigmoidal relationship exists between their elution volume (V_e) and the logarithms of their molecular weights (MW) (Barth et al., 1996). Therefore, a molecular weight standard made of globular proteins (Gel filtration standard, Bio-Rad, CA, USA) was used to obtain information on the molecular weight of the detected aggregates. The standard contained bovine thyroglobulin (670 kDa, 5.0 mg), bovine immunoglobulin G (158 kDa, 5.0 mg), chicken ovalbumin (44 kDa, 5.0 mg), equine myoglobin (17 kDa, 2.5 mg), and Vitamin B12 (1.35 kDa, 0.5 mg). It is to be noted that V_e is not sufficient to define the behaviour of the sample substance since this parameter varies with the void volume of the column (V_0). The ratio V_e/V_0 was therefore used for determination of the MW. V_0 corresponds to the elution volume of a molecule that is confined to the mobile phase because it is larger than the largest pores into the stationary phase. The elution volume of Blue dextran (MW: 2000 kDa, Sigma-Aldrich, MO, USA) was taken as V_0 .

To assess the suitability of the system to achieve good separation of the CA582 molecule from its aggregated species, the resolution factor for the IgG (158 kDa) and ovalbumin (44 kDa) was calculated as follows from the chromatogram of molecular weight standards:

$$R_s = \frac{2(T_2 - T_1)}{(W_1 + W_2)}$$

Where

R_s is the resolution factor

T_1 is the retention time of the IgG peak

T_2 is the retention time of the ovalbumine peak

W_1 is the IgG peak width at baseline

W_2 is the ovalbumine peak width at baseline.

Values of R_s greater than about 1.5 indicate baseline separation when the two components are present in approximately equal proportions.

IV.3.2.2.3.3.2. Insoluble aggregates

The various stresses induced by production processes can often lead to the production of insoluble protein aggregates. Quantification of these aggregates was obtained by assay of CA582 by UV absorbance at 280 nm (see IV.3.2.2.3.1.) before and after each production step. As insoluble aggregates produced during the process are removed by filtration before absorbance reading, their percentage can be calculated as follows:

$$\% \text{ insoluble aggregates} = [1 - (\% \text{ CA582}_{\text{after process}} / \% \text{ CA582}_{\text{before process}})] \times 100$$

IV.3.2.2.3.4. Qualitative evaluation of aggregation and fragmentation

SDS-Polyacrylamide gel electrophoresis (SDS-PAGE) was used to evaluate qualitatively the presence of aggregates and fragments of CA582 in the formulations. SDS-PAGE provides additional information on the type (covalent or non-covalent) of aggregates formed and also gives a more accurate estimation of the molecular weight than SEC (Wang, 2005). Gel

electrophoresis is a technique based on the use of an electric field applied to a gel matrix. By placing the molecules in wells in the gel and applying an electric field, the molecules move through the matrix at different rates, determined largely by their mass when the charge to mass ratio (Z) of all species is uniform, toward the anode if negatively charged or toward the cathode if positively charged. However, proteins can have varying charges and complex shapes, and therefore may not migrate in the polyacrylamide gel at similar rates when placing an electric field on the sample. Therefore, proteins are usually unfolded in the presence of a detergent, such as sodium dodecyl sulfate (SDS) or lithium dodecyl sulfate (LDS), which coats the proteins with a negative charge so that the resulting denatured proteins have an overall negative charge and all the proteins have a similar charge to mass ratio. Since denatured proteins have lost their complex tertiary shape, the rate at which the resulting SDS coated proteins migrate in the gel is relative only to their size and not their charge or shape.

To evaluate molecular weight, a molecular weight standard containing a mixture of molecules of known sizes can be run on one lane in the gel parallel to the unknown size samples so that the observed known size bands can be compared to the unknown-size proteins. The relative mobility (R_f) of a protein is inversely proportional to the logarithm of its molecular weight. R_f measurements can be made according to the following equation, in which the dye used is that of the sample buffer (Sadeghi et al., 2003):

$$R_f = \text{distance migrated by protein} / \text{distance migrated by dye}$$

It is also possible to add a reducing agent to the samples such as dithiothreitol (DTT) or mercaptoethanol before migration. Comparison between the results obtained under reduced and non-reduced conditions provides information on the type of aggregates. The reducing agent indeed reduces the disulfide bonds that can be present between covalently-linked aggregates and between the peptide chains of the molecule.

CA582 samples were diluted in PBS, pH 7.4, (Invitrogen, Grand Island, NY, USA) to a concentration of 2.5 mg/ml. Sample buffer was added to the samples (25% v/v, NuPAGE[®] LDS, Invitrogen, CA, USA), which contained LDS, glycerol, and coomassie G250 and Phenol Red as tracking dyes. For tests in reduced conditions, DTT was added (10% v/v,

NuPAGE[®] reducing agent, Invitrogen, CA, USA). Samples were then heated at 70°C for 10 min. PageRuler™ (Fermentas, MA, USA) and SeeBlue[®] Plus2 (Invitrogen, CA, USA) were used as protein molecular weight standards. The samples and the standards (5 µl) were loaded on discontinuous gels, with a gradient concentration of acrylamide in the running gel of 4-12% (NuPAGE[®] Novex[®] Bis-Tris Mini gel, Invitrogen, CA, USA), which is designed to separate small to mid-size molecular weight proteins. The running buffer was a MOPS buffer ([3-(N-morpholino) propane sulfonic acid], NuPAGE[®] MOPS, Invitrogen, CA, USA) containing SDS. Electrophoresis was run with a 125 V voltage applied for 55 min in a XCell SureLock™ Mini-Cell Electrophoresis System (Invitrogen, CA, USA) connected to a PowerEase[®] 500 power supply (Invitrogen, CA, USA).

After electrophoresis was complete, the molecules in the gel were stained to make them visible. Coomassie Brilliant Blue R250 (Sigma-Aldrich, MO, USA) was used for this purpose. A 0.025% (w/w) solution was prepared in methanol/H₂O/glacial acetic acid 10:9:1. The gel was incubated in a staining container with 30 ml of solution and gently shaken for 2 h at room temperature on an orbital shaker. The gel was destained by overnight shaking in a solution of glacial acetic acid (7.5% v/v) and methanol (5% v/v).

IV.3.2.2.3.5. Evaluation of desamidation

Desamidation of proteins involves the hydrolysis of amide side chains on glutamine or asparagine residues and the formation of the corresponding glutamic acid (pKa ~ 4.3) and aspartic acid (pKa ~ 3.9), leading to a modification of the global charge of the molecule. Cation-exchange HPLC (CEX) was therefore used to monitor desamidation. In ion-exchange HPLC, analyte molecules are retained on the column based on electrostatic interactions between charged amino acid side chains and the surface charge of the ion-exchange resin. CEX retains biomolecules by the interaction of negatively charged functional groups, such as sulfonic acid groups, on the surface of the ion-exchange resin with histidine (pKa ~ 6.5), lysine (pKa ~ 10), and arginine (pKa ~ 12) residues. The mobile phase is buffered to maintain the mobile phase below pH 6 or 7 to keep the basic side chains protonated. At higher pH, the basic sidechains begin to deprotonate and retention decreases. Below pH 7, retention is dependent on the net charge of the molecule, which depends on the proportion of basic and

acid amino acids present in the protein. Once the protein is retained on the column, elution can be achieved by increasing the ionic strength of the mobile phase with a displacer ion (i.e. Na^+) that possesses a higher affinity for the stationary phase than the protein. As the ionic strength of the mobile phase increases, salt ions compete for binding to the charges on the ion exchange matrix, displacing the bound macromolecule, and allowing them to elute from the matrix (Kopaciewicz et al., 1983; Malmquist and Lundell, 1992).

The procedure was performed using a Propac SCX-10 column (4 x 250 mm, Dionex, CA, USA) maintained at 25°C. Samples were diluted to a target concentration of 1 mg/ml in 20 mM Na acetate, pH 5.0, and were filtered on 0.22 μm PVDF syringe filters (Millex-GV, Millipore, MA, USA) before injection. The injection volume was 100 μl and runs were conducted at a flow rate of 0.5 ml/min for 64 min. Detection was achieved by absorbance at 280 nm. Mobile phase A (equilibration buffer) was a 20 mM MES buffer, pH 6.2, ([2-(N-Morpholino)ethane sulfonic acid], Sigma-Aldrich, MO, USA) and mobile phase B (elution buffer) was a 20 mM MES buffer, pH 6.2, containing 100 mM NaCl. A mobile phase gradient was applied as follows:

Time (minutes)	Phase A (%)	Phase B (%)
0.0	80.0	20.0
2.0	80.0	20.0
52.0	10.0	90.0
52.5	0.0	100.0
53.5	0.0	100.0
54.0	80.0	20.0
64.0	80.0	20.0

The total relative acidic species in the sample, corresponding to the desamidated species, was calculated using the following equation:

$$\% \text{ desamidated species} = (\text{Acidic species peak area} / \text{Total sample peak area}) \times 100$$

IV.3.2.2.3.6. Crystalline state

PXRD was used to evaluate the crystalline state of the powders after the freeze-drying and spray-drying steps. The same operating parameters as described in IV.1.2.2.6. were used.

IV.3.2.2.3.7. Residual water content

Thermogravimetric Analysis (TGA) was used to evaluate the residual water content of the powders after the freeze-drying and spray-drying steps. The same operating parameters as described in IV.1.2.2.7.1. were used.

IV.3.2.2.3.8. Particle size analysis

Laser diffraction (see also IV.1.2.2.2.1.) was used to determine the geometric size distribution of the particles after the HPH and spray-drying steps. The $d_{(0.5)}$, $D_{[4,3]}$, and $V\% < 5 \mu\text{m}$ were measured using a Malvern Mastersizer 2000 laser diffractometer with a liquid sampling system (Hydro S, Malvern, UK). The particles were measured using the following parameters: refractive index, 1.52; absorption index, 0.1; dispersing liquid, isopropanol containing 0.1% (m/v) Polysorbate 80; agitation rate, 1 750 rpm; obscuration, 4%. This low obscuration level was used to avoid multiple scattering.

IV.3.2.2.4. Stability study

A three-month stability study was performed on the freeze-dried CA582 powders containing different types of stabilising excipient (see **Table XXVI** in "Results and discussion", section IV.3.3.5.5.). Powders were stored at 2-8 °C in 20 ml glass vials (Wheaton, NJ, USA) sealed with aluminium caps containing PTFE septa. The vials were maintained in a desiccator containing silica gel beads. A complete physico-chemical characterisation of the powders was performed at $t = 0, 1, 2,$ and 3 months.

IV.3.2.2.5. Aerodynamic features

Evaluation of the aerodynamic features was performed on the spray-dried formulations (F1-F4).

IV.3.2.2.5.1. Uniformity of the delivered dose

The same technique was used as previously described (see IV.1.2.2.8.2.).

An Aerolizer[®] inhaler (Novartis, Switzerland) was first filled with a size 3 HPMC capsule (Capsugel, Bornem, Belgium) loaded with 5.0 mg of CA582 (corresponding to 10.6, 10.1, 11.1, and 11.1 mg powder for the F1, F2, F3, and F4 formulations, respectively). The airflow rate was set to 100 l/min for 2.4 s or 60 l/min for 4.0 s. After particle deposition, the UDD device was rinsed with PBS, pH 7.4, (Invitrogen, Grand Island, NY, USA) and the liquid was quantitatively collected in a 100.0 ml volumetric flask. This procedure was repeated for 9 other capsules. Drug deposition in the UDD device was then determined by measuring UV absorbance at 230 nm, using the same equipment as described in the CA582 assay (IV.3.2.2.3.1.). A_{230} was measured in place of A_{280} because of the much higher absorbance of the CA582 molecule at 230 nm. This allows better quantification of the CA582 in the UDD experiment, for which high dilution of the molecule occurs. The delivered dose was calculated using an extinction coefficient at 230 nm of $9.55 \text{ ml} \cdot \text{mg}^{-1} \cdot \text{cm}^{-1}$. It was deducted from the measurement of A_{230} of the reference CA582 solution at a concentration of 0.05 mg/ml.

IV.3.2.2.5.2. Impaction measurements

Impaction measurements were performed using an MsLI (see IV.1.2.2.8.2.1.). An Aerolizer[®] inhaler (Novartis, Switzerland) was first filled with a size 3 HPMC capsule (Capsugel, Bornem, Belgium) loaded with 5.0 mg of CA582 (corresponding to 10.6, 10.1, 11.1, and 11.1 mg powder for the F1, F2, F3, and F4 formulations, respectively). Three capsules were taken for each test. The applied air flow rate was either 100 l/min or 60 l/min and the duration of the experiment was 2.4 s or 4.0 s, respectively. At these flow rates, the cut-off diameters for stages 1, 2, 3, and 4 were, respectively, 10.1, 5.3, 2.4, and 1.3 μm at 100 l/min and 13.0, 6.8, 3.1, and 1.7 μm at 60 l/min. The MsLI was filled with 20 ml PBS, pH 7.4, (Invitrogen, Grand Island, NY, USA) in each stage. After particle deposition, fractions were quantitatively collected in 100.0 ml volumetric flasks and the volume adjusted with PBS. Two flasks were also dedicated to the collection of the powder that remained in the inhalation device and in

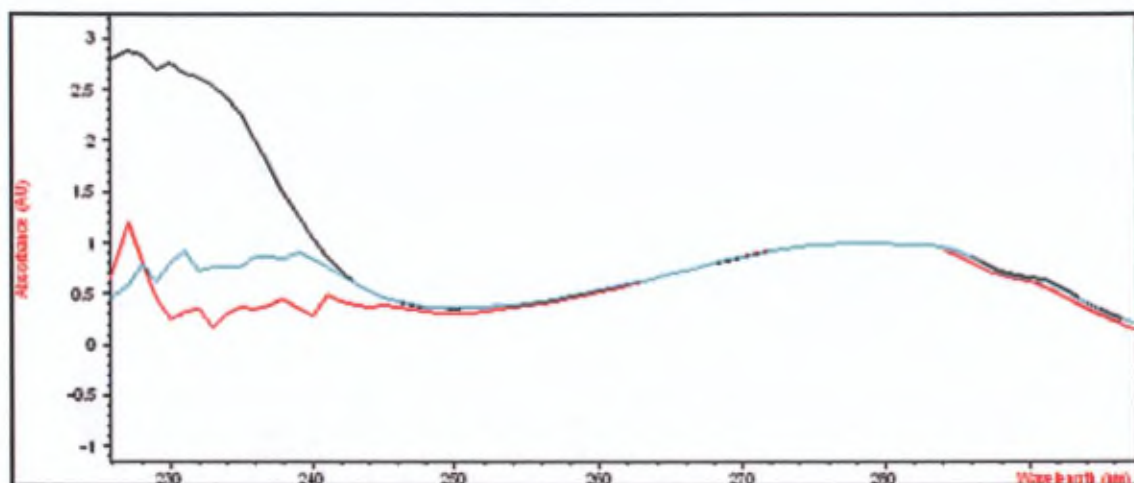


Figure 60. Example of UV absorbance spectra of the CA582 molecule at 0.5 mg/ml incubated in PBS with Gdn in concentrations of 0 M (black curve), 2 M (turquoise curve), and 6 M (red curve)

the throat. Drug deposition in the device, the throat, the four stages, and the filter was determined by measuring UV absorbance at 230 nm as described in the previous section (IV.3.2.2.5.1.). Each test was performed in triplicate. Data interpretation was performed using CITDAS software (Copley Scientific Ltd, Nottingham, UK).

IV.3.2.2.5.3. Spraytec[®] measurements

Geometric particle size distributions of the aerosols under simulated breathing conditions were obtained using the Spraytec[®] device (see IV.1.2.2.8.4.). It was used in-line with the MsLI equipment, which allows simultaneous sizing of the aerosol by the two techniques.

The acquisition parameters were as follows: triggering mode, 10% level; data acquisition rate, 2 500 Hz; acquisition duty cycle, 50%; test duration, 3 000 ms or 4 500 ms at 100 l/min and 60 l/min, respectively; refractive index, 1.50 (standard opaque particles).

IV.3.3. Results and discussion

IV.3.3.1. Influence of the folding state on UV absorbance

Guanidine hydrochloride has been widely used at a concentration of 6 M to obtain protein in a fully unfolded state (Gill and von Hippel, 1989; Del Vecchio et al., 2002; Ruiz et al., 2003). The UV absorbance spectra of the CA582 molecule after overnight incubation with various Gdn concentrations are presented in **Figure 60**.

No significant difference (student t-test, $p > 0.05$, $n=3$) in absorbance at 280 nm was found between the protein in its native conformation (Gdn 0 M, $A_{280} = 0.91 \pm 0.01$) and in the fully unfolded state (Gdn 6 M, $A_{280} = 0.89 \pm 0.01$). It was therefore concluded that UV absorbance at 280 nm can be used to measure the CA582 concentration regardless of the folding state of the protein. However, it was found that absorbance in the far-UV region is strongly influenced by protein denaturation, as samples with increased concentrations of Gdn

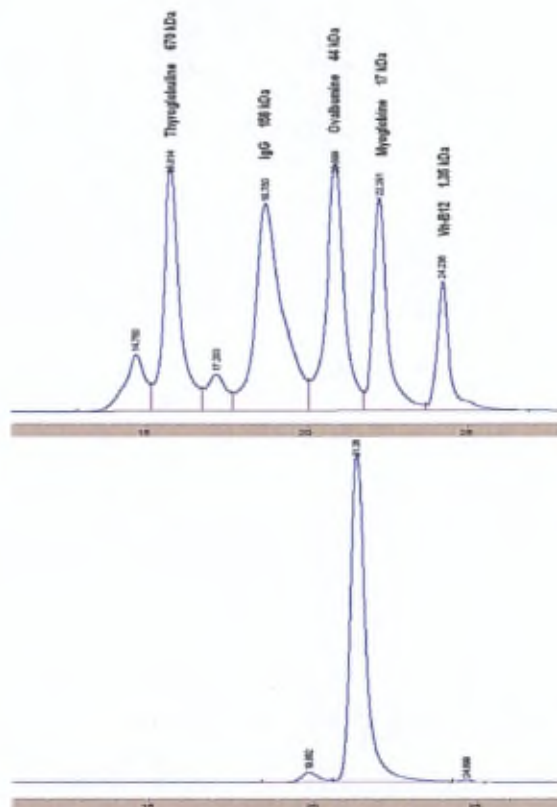


Figure 61. Chromatograms obtained by SEC. Up: molecular weight standards, Down: CA582 reference material (provided as a 24 mg/ml solution in 50 mM sodium acetate/125 mM sodium chloride, pH 5.0 buffer)

exhibited decreased absorbance between 200 and 250 nm. As previously mentioned, this can be explained by changes in the absorbance of aromatic amino-acids and the peptide bonds at these wavelengths, depending on their conformation. Therefore, evaluation of CA582 unfolding was performed by calculation of the A_{230}/A_{280} ratio. A_{230}/A_{280} ratio values were found to be 5.61 ± 0.10 , 1.88 ± 0.11 , 0.24 ± 0.07 , and 0.27 ± 0.04 for the samples in 0 M, 2 M, 4 M, and 6 M Gdn, respectively. This indicates that the CA582 molecule is partially unfolded in Gdn 2 M and fully unfolded in Gdn 4 M and Gdn 6 M and that the A_{230}/A_{280} ratio can be used effectively for monitoring protein unfolding.

IV.3.3.2. Characterisation of the CA582 reference material

Assay of the CA582 reference material by UV absorbance at 280 nm provided a concentration of 24.4 ± 0.6 mg/ml, and an A_{230}/A_{280} ratio of 5.61 ± 0.10 .

The soluble aggregates content of the reference material was assessed by SEC. An example of a chromatogram obtained for the molecular weight standards and for the CA582 reference material can be seen in **Figure 61**.

The R_s factor was found to be 2.3 ± 0.2 , indicating an appropriate resolution of the peaks in this size range. After injection of the CA582 reference material, the major peak in the chromatogram was identified as the monomer peak. The molecular weight of the compound was evaluated to be 32 ± 2 kDa from the calibration curve with the molecular weight standards. A small peak ($1.85 \pm 0.05\%$ of the total peak area) was also visible and was identified as a dimer because of its evaluated molecular weight of 76 ± 2 kDa. It can be noted that the observed molecular weight of CA582 does not correspond to the theoretical molecular weight of CA582 (54 kDa). This could be explained by the fact that the calibration with molecular weight standards is only conclusive if the molecule to be analysed has the same relation between its hydrodynamic diameter and its size as the globular proteins used in the standard. It is possible that the CA582, which is only a fragment of monoclonal antibody, does not behave exactly like a globular protein and its measured molecular weight could therefore be under-estimated by this method.

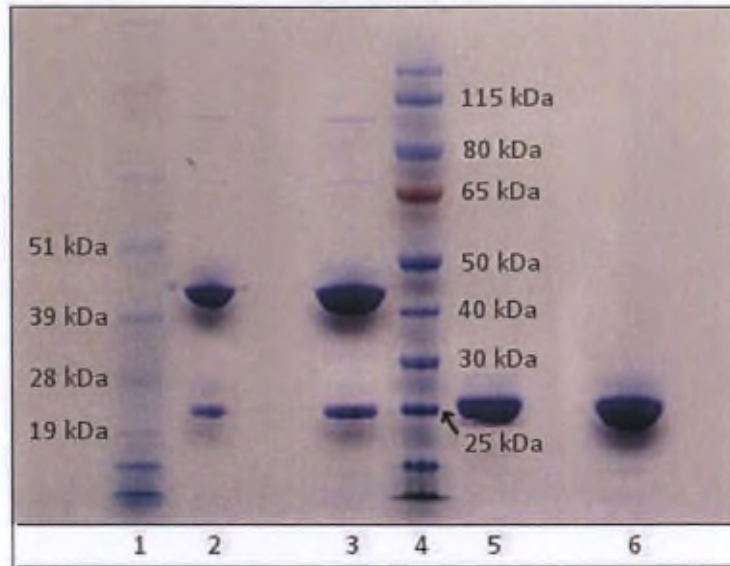


Figure 62. SDS-PAGE of the CA582 reference material in reduced and non-reduced conditions. 1: SeeBlue Plus2 molecular weight standard; 2 and 3: CA582 reference material in non-reduced conditions; 4: PageRuler molecular weight standard; 5 and 6: CA582 reference material in reduced conditions

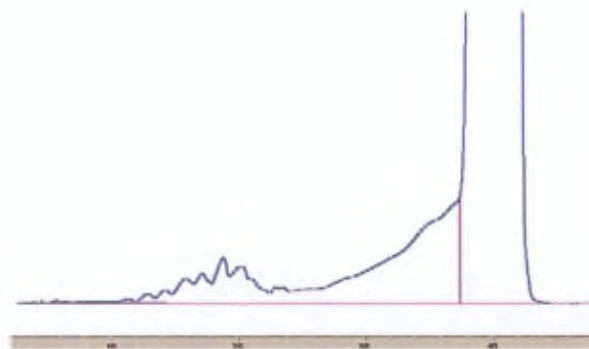


Figure 63. Chromatograms obtained by CEX after injection of the CA582 reference material

The results of SDS-PAGE for the CA582 reference material are presented in **Figure 62**. They exhibit a molecular weight of about 45 kDa for the protein, which is much more in agreement with the theoretical value (54 kDa) than the value obtained by SEC. In reduced conditions, a single band at about 25 kDa can be seen, which is in agreement with the structure of CA582 and corresponds to the two separated peptide chains (theoretical molecular weight of 28 and 26 kDa). It can be noted that this band is also present to a much lesser extent for the un-reduced sample, indicating that the CA582 reference material contains a small proportion of dissociated peptide chains. Interestingly, a weak band corresponding to the CA582 dimer is present around 100 kDa in the un-reduced sample, which had also been detected by SEC. This band disappears in the reduced sample, indicating that the dimer is disulfide-bonded.

The CEX results for the CA582 reference material are presented in **Figure 63**. The major peak in the chromatogram was identified as the native CA582 peak. However, a number of small peaks ($25.0 \pm 0.8\%$ of the total peak area) were also visible and were identified as desamidated species of CA582. It is well-known from the literature that not all Asn residues have the same tendency to undergo desamidation (Huang et al., 2005). Asn residues that are surrounded by residues with a low steric effect are indeed more likely to react. In the primary structure of CA582, which contained 15 Asn residues, we found 1 Asn residue with a high desamidation potential (glycine in C-terminal position) and 6 Asn residues with an intermediate potential tendency to desamidation (serine or other small amino-acids in C-terminal position). The number and relative intensities of the small peaks observed in the chromatogram show that among the desamidated species, most have only a few Asn residues modified, which is consistent with this theoretical assumption. However, it can be seen that a small proportion of CA582 presents desamidation of more Asn residues. Considering the number of the peaks, it is likely that small populations of desamidated compounds with 1 up to the 15 Asn residues are present.

IV.3.3.3. Efficacy of the desalting procedure

The efficacy of the desalting procedure was evaluated by potentiometric dosage of Na^+ in the filtrate fractions during diafiltration of the initial antibody solution with ultrapure water.

Table XXII. Influence of the buffering conditions on the stability of the CA582 molecule in solution

(Results obtained after 24 h stirring at room temperature)

	Unfolding (A_{230}/A_{280})	Aggregation (% soluble dimer)	Aggregation (% insoluble aggregates)	Desamidation (% acid species)	Aggregation/ Fragmentation (SDS-PAGE)
Reference CA582 (50 mM Na acetate/ 125 mM NaCl pH 5)	5.61 ± 0.10	1.84 ± 0.06	/	25.1 ± 0.9	Major band 45kDa Weak band 25kDa Weak band 100kDa
t24h					
50 mM Na acetate/ 125 mM NaCl pH 5	5.59 ± 0.09	1.77 ± 0.04	0.0 ± 0.1	25.2 ± 1.1	No change with Ref.
5 mM Na acetate/ 12.5 mM NaCl pH 5	5.54 ± 0.10	1.96 ± 0.04	1.1 ± 0.9	25.8 ± 1.0	No change with Ref.
1 mM Na acetate/ 2.5 mM NaCl pH 5	4.91 ± 0.10	2.10 ± 0.07	2.9 ± 0.5	24.4 ± 1.0	Fragmentation bands mainly at 10 kDa, 35 kDa
2 mM Na phosphate pH 6	5.62 ± 0.11	1.91 ± 0.09	1.0 ± 0.6	24.8 ± 0.7	No change with Ref.
5 mM Na phosphate pH 6	5.62 ± 0.07	1.83 ± 0.01	0.1 ± 0.1	25.1 ± 0.4	No change with Ref.
2 mM Na phosphate pH 7	5.55 ± 0.10	1.81 ± 0.06	0.5 ± 0.2	25.0 ± 0.4	No change with Ref.
5 mM Na phosphate pH 7	5.68 ± 0.15	1.79 ± 0.06	0.0 ± 0.2	25.4 ± 0.9	No change with Ref.
Ultrapure water pH 7	4.83 ± 0.18	2.08 ± 0.05	8.8 ± 0.9	24.9 ± 1.2	Fragmentation bands mainly at 10 kDa, 35 kDa

The cumulated fraction of Na^+ in the successive fractions was plotted as a function of the number of DVs (**Figure 64**). Measurement of the $[\text{Na}^+]$ in initial buffer (50 mM sodium acetate/125 mM sodium chloride, pH 5.0, buffer) was also taken and was considered as 100% in the calculation of the cumulated fraction of Na^+ recovered in the filtrate. The concentration of Na^+ in the initial buffer was found to be $4\,175 \pm 19$ mg/l, which is in agreement with the calculated value (4 025 mg/l). In Figure 64, it can be seen that the cumulated fraction of Na^+ recovered in the filtrate is in agreement with the theoretical values mentioned in **Table XXI** for a 100% permeable molecule. This indicates that the diafiltration procedure used can efficiently remove sodium acetate and sodium chloride from the initial buffer and that no interaction of the buffer with the protein occurs.

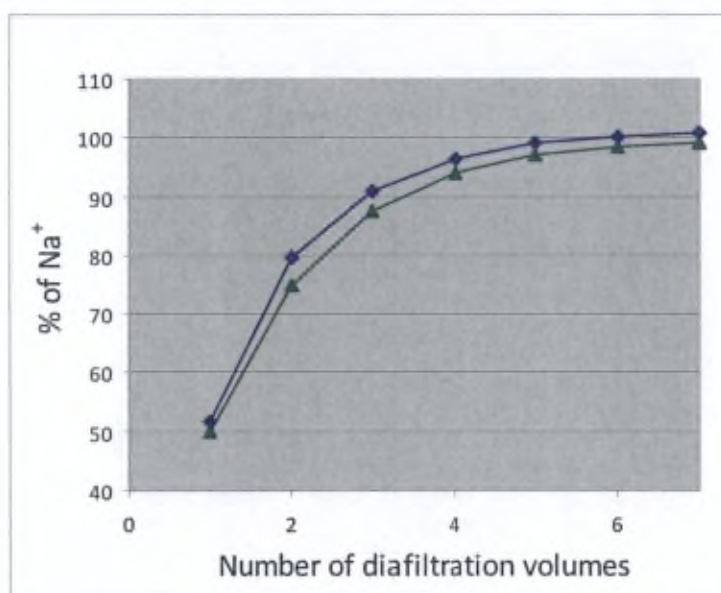


Figure 64. Cumulated % of Na^+ in the filtrate after diafiltration with ultrapure water. **Green curve: theoretical values; blue curve: experimental values.** Results obtained using a sodium-sensitive electrode equipped with a glass membrane and an Ag/AgCl reference electrode. Measurements performed with $[\text{Na}^+]$ between 25 and 300 mg/l after appropriate dilution of the samples. Experiment run in triplicate.

IV.3.3.4. Stability of the desalted CA582 solutions

A number of replacement buffers (**Table XXII**) were evaluated for maintaining CA582 stability after 24 h stirring at room temperature. An experiment was also performed using

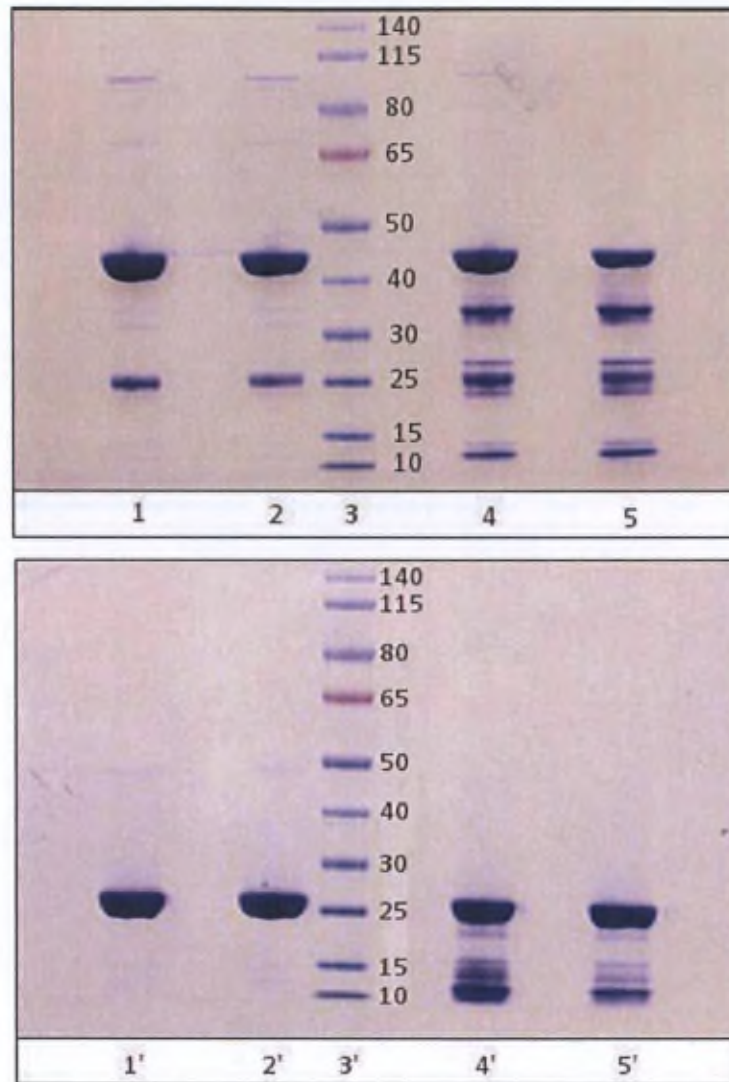


Figure 65. SDS-PAGE of the CA582 molecule in different buffering conditions after 24 h stirring at room temperature. Up: unreduced samples, Down: reduced samples. 1 and 1', 50 mM Na acetate/125 mM NaCl, pH 5; 2 and 2', 5 mM Na acetate/12.5 mM NaCl, pH 5; 3 and 3', PageRuler molecular weight standard; 4 and 4', 1 mM Na acetate/2.5 mM NaCl, pH 5; 5 and 5', Ultrapure water, pH 7

the initial buffer as a replacement buffer to evaluate the impact of the desalting procedure itself on the physico-chemical stability of the CA582 molecule.

Evaluation of unfolding exhibited no significant change with CA582 reference (initial CA582 solution) for any of the tested conditions, except for the solutions in 1 mM Na acetate/2.5 mM NaCl, pH 5 and in ultrapure water, pH7 (Student t-test, $p < 0.05$). These exhibited a decrease in the A_{230}/A_{280} ratio, indicating the presence of unfolded species. Evaluation of aggregation by SEC exhibited the presence of a soluble dimer for all conditions in a percentage that was not significantly different from the CA582 reference (Student t-test, $p > 0.05$). Evaluation of the insoluble aggregate content was performed by visual inspection and measurement of A_{280} in the desalted solutions at $t = 0$ h and $t = 24$ h. All solutions remained limpid at $t = 24$ h, except the solutions in 1 mM Na acetate/2.5 mM NaCl, pH 5 and in ultrapure water, pH7, in which the presence of insoluble aggregates could be seen. This was confirmed by UV absorbance, with measurement of a percentage of insoluble aggregates of 2.9 ± 0.5 % and 8.8 ± 0.9 %, respectively. Although measurements by spectrophotometry also indicated low percentages of insoluble aggregates for the other tested conditions, it is likely that these values do not reflect the presence of aggregates but are due to experimental error in the measurement method. No change was detected by CEX for the desamidated species content for any condition. The results of the SDS-PAGE indicated the presence of fragmentation for the solutions in 1 mM Na acetate/2.5 mM NaCl, pH 5 and in ultrapure water, pH7 (**Figure 65**), with apparition of bands mainly at 35 kDa and 12 kDa in both cases. Interestingly, the sum of the sizes of these two fragments roughly corresponds to the size of the whole CA582 molecule (45 kDa). It can also be seen that the 35 kDa fragment is no longer detected under reduced conditions. These observations tend to indicate that fragmentation mainly occurred at one point in the primary sequence of one of the two chains of the CA582 molecule (28 and 26 kDa), with the formation of one large fragment (35 kDa) made up of the intact chain disulfide-bonded with the remaining part of the fragmented chain, and one small fragment (12 kDa) constituting the other part of the fragmented chain.

From these results, it was concluded that the conditions of 1 mM Na acetate/2.5 mM NaCl, pH 5 and ultrapure water, pH7, which constituted the lightest buffered or unbuffered

Table XXIII. Influence of the buffering conditions on the stability of the CA582 molecule in the freeze-dried powders

	Unfolding (A_{230}/A_{280})	Aggregation (% soluble dimer)	Aggregation (% insoluble aggregates)	Desamidation (% acid species)	Aggregation/Fragmentation (SDS-PAGE)
Reference CA582 (50 mM Na acetate/ 125 mM NaCl pH 5)	5.61 ± 0.10	1.85 ± 0.05	/	24.9 ± 0.8	Major band 45kDa Weak band 25kDa Weak band 100kDa
2 mM Na phosphate pH 5	5.53 ± 0.13	3.10 ± 0.04	1.0 ± 1.0	25.7 ± 0.4	No change with Ref.
2 mM Na phosphate pH 6	5.50 ± 0.11	3.11 ± 0.04	0.0 ± 0.9	25.3 ± 0.4	No change with Ref.
2 mM Na phosphate pH 7	4.81 ± 0.11	3.28 ± 0.04	0.0 ± 1.0	29.3 ± 0.5	No change with Ref.
10 mM Na phosphate pH 6	5.52 ± 0.10	2.26 ± 0.03	1.0 ± 1.4	24.8 ± 0.3	No change with Ref.

conditions, were not appropriate for ensuring 24 h stability of the CA582 molecule. All other conditions conserved the short-term physico-chemical stability of the antibody and were therefore considered to be adequate replacement buffers for further processing of the formulations. It was also shown that the desalting procedure itself did not induce any degradation of the molecule, as can be seen from the unchanged results obtained from the replacement of the initial buffer with the same buffer (see Table XXII).

IV.3.3.5. Freeze-drying of the CA582 molecule

IV.3.3.5.1. Influence of the buffering conditions on CA582 stability

In the previous section, it was shown that Na phosphate buffer at pH 6 or 7 provides adequate short-term stabilisation of the CA582 in solution at buffer concentrations as low as 2 mM. Na phosphate buffer was therefore chosen as a replacement buffer for further processing of the formulations by freeze-drying. The influence of the pH and concentration of the buffer on the stability of the CA582 in the freeze-dried cakes was evaluated and is presented in **Table XXIII**.

It could be seen that the CA582 molecule presented no change in its physico-chemical stability when freeze-dried in the presence of 2 mM Na phosphate buffer, pH 5, or in the presence of 2 mM or 10 mM Na phosphate buffer, pH 6, except for an increase in the soluble dimer content from 1.85% (before freeze-drying) to 3.10, 3.11, and 2.26%, respectively. On the other hand, freeze-drying in the presence of 2 mM Na phosphate buffer, pH 7 induced the formation of 3.28% soluble dimer as well as the formation of more unfolded and desamidated species in comparison to the reference CA582 molecule (Student t-tests, $p < 0.05$). This indicates that a buffering pH above pH 6 is not suitable for stabilisation of the CA582 molecule in the dry state. On the other hand, a buffering pH under 6 is to be avoided because low pH is not recommended for formulations intended for inhalation (Adjei et al., 1996). Therefore, Na phosphate buffer, pH 6 was selected for further processing of the formulations. The 2 mM buffer concentration was chosen in place of the 10 mM concentration because the latter would result in a high salt concentration in the dry product of up to 7% w/w.

Table XXIV. Influence of the stabilising sugar content on the stability of the CA582 molecule in the freeze-dried powders

	Unfolding (A_{230}/A_{280})	Aggregation (% soluble dimer)	Aggregation (% insoluble aggregates)	Desamidation (% acid species)	Aggregation/ Fragmentation (SDS-PAGE)	Residual water (%)
Reference CA582 (50 mM Na acetate/ 125 mM NaCl pH 5)	5.55 ± 0.09	1.87 ± 0.07	/	24.9 ± 0.7	Major band 45kDa Weak band 25kDa Weak band 100kDa	/
2 mM Na phosphate pH 6 CA582/sucrose 80:20	5.44 ± 0.14	2.27 ± 0.02	1.9 ± 1.2	25.4 ± 0.5	No change with Ref.	4.3 ± 0.3
2 mM Na phosphate pH 6 CA582/sucrose 70:30	5.51 ± 0.10	1.91 ± 0.04	0.0 ± 1.5	25.4 ± 0.5	No change with Ref.	5.4 ± 0.3
2 mM Na phosphate pH 6 CA582/sucrose 50:50	5.59 ± 0.11	1.92 ± 0.03	0.0 ± 1.2	24.8 ± 0.5	No change with Ref.	4.6 ± 0.1
2 mM Na phosphate pH 6 CA582/sucrose 20:80	5.51 ± 0.15	1.93 ± 0.01	0.6 ± 1.0	25.0 ± 0.3	No change with Ref.	4.9 ± 0.2

IV.3.3.5.2. Influence of the concentration of stabilising sugar on CA582 stability

It is to be noted that the best buffering conditions did not fully preserve CA582 stability (increase in soluble dimers). Therefore addition of another stabilising agent is required. Saccharides and polyols have been shown to enhance stability of proteins in the dry state due to their glass-forming ability and/or a water replacement effect (see "Introduction" II.2.2.2). We then added increasing concentrations (20% to 80% w/w of the solid content) of sucrose to the CA582 solution before freeze-drying to evaluate the influence of the content in stabilising sugar on the physico-chemical stability of the CA582 molecule (**Table XXIV**).

The results showed that a sucrose concentration between 30% and 80% (w/w) provided optimal stabilisation of the CA582 molecule with no significant difference from the reference for any of the degradation products (Student t-tests, $p > 0.05$, N.S.). However, with a 20% sucrose concentration, a slightly increased soluble dimer aggregates content was still detectable. This finding is consistent with what is found in the literature, where the level of stabilisation afforded by sugars or polyols generally depends on their concentrations (Wang 2000). For example, freezing rabbit muscle lactate dehydrogenase (LDH) in water caused a 64% loss of protein activity, and in the presence of 5, 10 or 34.2% sucrose, the respective losses were 27, 12, and 0% (Nema and Avis, 1992). In another study, it was demonstrated that saccharides protected catalase during freeze-drying by direct interaction with the protein and that a concentration of saccharides sufficient to form a monomolecular layer on the protein surface was the minimum required to achieve the optimal stabilisation (Tanaka et al., 1991).

The residual water content of the cakes was measured by TGA. It was comprised between 4.3% and 5.4% and was not significantly different for the various sucrose concentrations (1-way ANOVA test, $p > 0.05$, N.S.). No secondary drying step was used during freeze-drying as this range of residual water content was considered to be appropriate for ensuring stability of the protein. Indeed, proteins in an aqueous solution are fully hydrated, which means they have a monolayer of water covering their surface, termed the hydration shell. The amount of water in full hydration is 0.3-0.35 g/g protein, corresponding to 30-35% water (Wang, 2000). Therefore freeze-drying – which leads to much lower residual water contents – removes part

of the hydration shell. This may disrupt the native state of a protein and cause unfolding. A hydrated protein, when exposed to a water-poor environment during dehydration, tends to transfer protons to ionised carboxyl groups and thus abolishes as many charges as possible in the protein. The decreased charge density may facilitate protein–protein hydrophobic interaction, causing protein aggregation (Wang, 2000).

IV.3.3.5.3. Influence of the type of stabilising excipient on CA582 stability

Although appropriate stabilisation of the CA582 molecule during freeze-drying was achieved with addition of at least 30% (w/w) sucrose, the influence of other stabilisers on CA582 stability during freeze-drying was also investigated (Table XXV). These could indeed present other interesting features for stabilisation of the molecule during HPH or spray-drying, or provide better aerodynamic properties to the final powder formulations. Mannitol and α -lactose monohydrate were chosen because of their accepted status as an excipient for the inhaled route. Moreover, these are also widely used as protein stabilising excipients both during freeze-drying and spray-drying (see “Introduction” II.2.2.2.2.).

Table XXV. Influence of the type of stabilising sugar on the stability of the CA582 molecule in the freeze-dried powders

	Unfolding (A_{230}/A_{280})	Aggregation (% soluble dimer)	Aggregation (% insoluble aggregates)	Desamidation (% acid species)	Aggregation/ Fragmentation (SDS-PAGE)	Residual water (%)
Reference CA582 (50 mM Na acetate/ 125 mM NaCl pH 5)	5.59 ± 0.10	1.86 ± 0.05	/	25.1 ± 0.7	Major band 45kDa Weak band 25kDa Weak band 100kDa	/
2 mM Na phosphate pH 6 CA582/sucrose 70:30	5.51 ± 0.10	1.91 ± 0.04	0.0 ± 1.5	25.4 ± 0.5	No change with Ref.	5.4 ± 0.3
2 mM Na phosphate pH 6 CA582/mannitol 70:30	5.51 ± 0.11	2.00 ± 0.09	1.8 ± 1.6	25.6 ± 0.6	No change with Ref.	3.1 ± 0.3
2 mM Na phosphate pH 6 CA582/lactose 70:30	5.61 ± 0.10	1.94 ± 0.08	1.8 ± 1.8	25.5 ± 0.2	No change with Ref.	5.6 ± 0.2
2 mM Na phosphate pH 6 CA582/sucrose/mann itol 70:15:15	5.60 ± 0.07	1.91 ± 0.09	0.0 ± 1.7	25.6 ± 0.2	No change with Ref.	3.3 ± 0.1

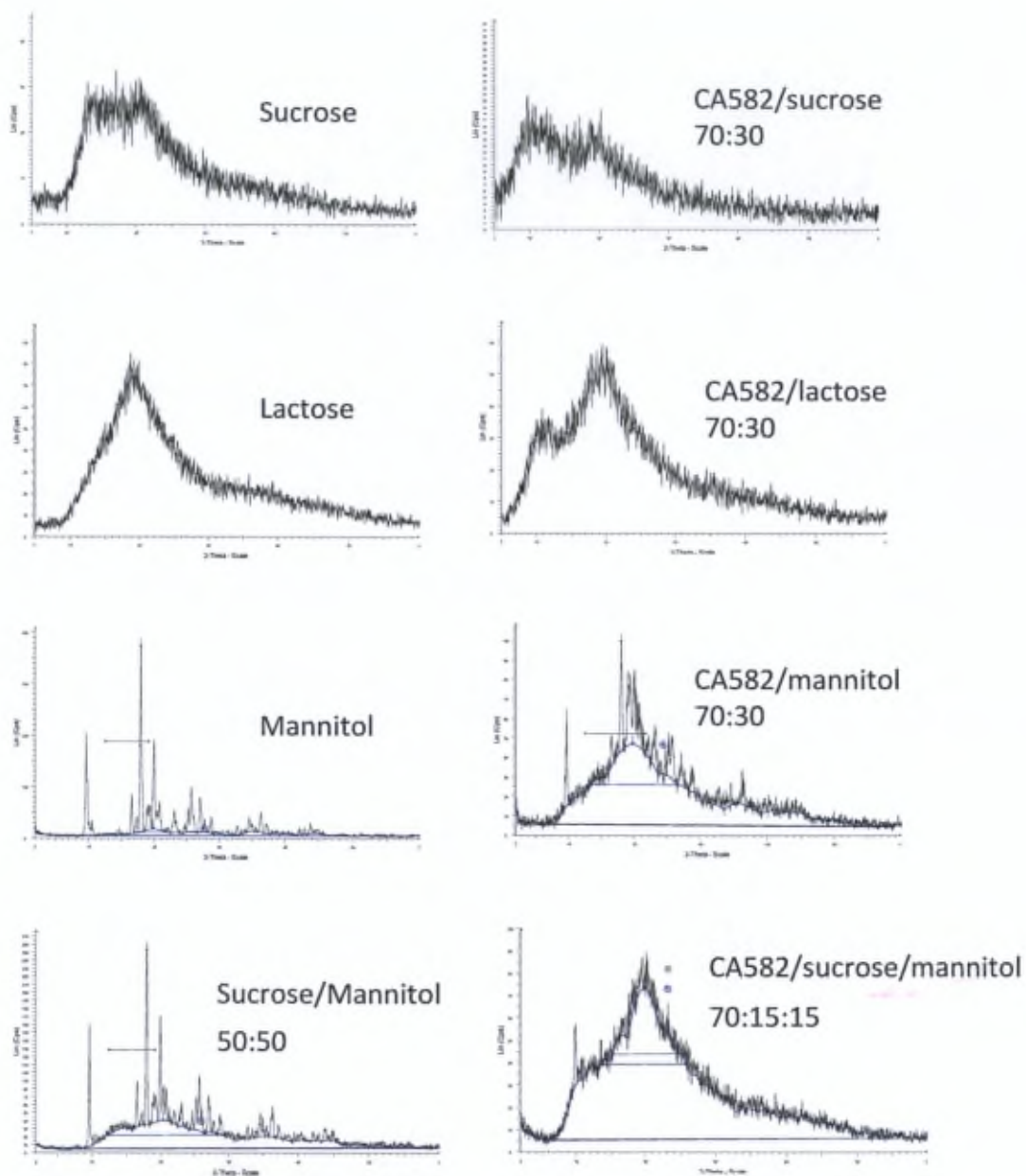


Figure 66. X-ray powder diffraction patterns of the freeze-dried excipients alone (left) and of the freeze-dried CA582 molecule with excipients (right). Freeze-dried excipients alone were produced using the same freeze-drying parameters and excipient concentration as in the freeze-dried CA582 powders. Modelling of the amorphous and crystalline areas was performed using a pseudo-Voigt function.

The results exhibited no significant difference between the different sugars in the stabilisation of CA582 during freeze-drying, indicating that sucrose, mannitol, and lactose might all be appropriate stabilisers to use for further processing of the formulations (HPH and spray-drying). However, the residual water contents of the freeze-dried powders containing mannitol were significantly lower than those containing sucrose (Student t-test, $p < 0.05$).

IV.3.3.5.4. Crystalline state of the freeze-dried powders

PXRD diffraction patterns of the freeze-dried CA582 with the different types of stabilising excipients are presented in **Figure 66**. The spectra of the stabilising excipients freeze-dried alone were also obtained using the same freeze-drying parameters and excipient concentration as in the freeze-dried CA582 powders. Diffraction patterns exhibited a fully amorphous structure for the sucrose and lactose excipients, alone or in the presence of the CA582 molecule. However, the freeze-dried mannitol excipient presented partial crystallisation (76% crystalline peak areas) and crystalline structures were also found in the freeze-dried CA582 with mannitol in a proportion that is in accordance with the mannitol content of the powder (19% and 6% crystalline peak areas for the powders containing 30% and 15% mannitol, respectively).

The crystallisation of mannitol during freeze-drying has been reported in the literature. It is dependent on the processing conditions employed and generally increases with increased mannitol concentrations (Franks, 1998; Andya et al., 1999; Chan et al., 2004). This can be attributed to the low T_g of mannitol (4 °C in the anhydrous state) in comparison with sucrose (68 °C in the anhydrous state) and lactose (108 °C in the anhydrous state) (Andya et al., 1999; Kawai et al., 2005). The spectrum obtained for the mannitol excipient was compared with α , β , δ , and hemihydrate crystalline mannitol reference spectra and crystals were found to be at least partly of the metastable hemihydrate type, a form that is typically produced during freeze-drying of mannitol (Yu et al., 1999; Lee et al., 2011b).

Table XXVI. Influence of the type of stabilising sugar on the 3-month stability of the CA582 molecule in the freeze-dried powders (Powders stored at 2-8°C in 20 ml glass vials (Wheaton, NJ, USA) sealed with aluminium caps containing PTFE septa. Vials maintained in a dessicator containing silica gel beads.

	Unfolding				Aggregation				Aggregation				Desamidation				Residual water			
	(A ₂₃₀ /A ₂₈₀)				(% soluble dimer)				(% insoluble aggregates)				(% acid species)				(%)			
Reference CA582 (50 mM Na acet./ 125 mM NaCl pH 5)	5.62 ± 0.09				1.86 ± 0.05				/				25 ± 1				/			
	t0	t1m	t2m	t3m	t0	t1m	t2m	t3m	t0	t1m	t2m	t3m	t0	t1m	t2m	t3m	t0	t1m	t2m	t3m
2 mM Na phosph. pH 6 CA582 alone	5.50 ± 0.11	5.50 ± 0.10	5.20 ± 0.14	4.72 ± 0.19	3.11 ± 0.04	3.90 ± 0.11	4.83 ± 0.15	5.54 ± 0.15	0.0 ± 0.9	0.0 ± 0.4	0.3 ± 0.8	0.9 ± 0.9	25.3 ± 0.4	25.6 ± 0.4	26.3 ± 0.1	27.3 ± 0.3	5.2 ± 0.4	5.2 ± 0.3	5.5 ± 0.4	5.9 ± 0.3
2 mM Na phosph. pH 6 CA582/sucrose 70:30	5.51 ± 0.10	5.54 ± 0.09	5.51 ± 0.10	5.50 ± 0.13	1.91 ± 0.04	2.04 ± 0.09	2.19 ± 0.10	2.0 ± 0.2	0.0 ± 1.5	1.1 ± 1.2	0.8 ± 0.6	0.0 ± 1.4	25.4 ± 0.5	25.7 ± 0.5	26.1 ± 0.2	25 ± 1	5.4 ± 0.3	5.3 ± 0.5	5.8 ± 0.3	6.1 ± 0.4
2 mM Na phosph. pH 6 CA582/mannitol 70:30	5.51 ± 0.11	5.21 ± 0.07	4.95 ± 0.11	4.90 ± 0.06	2.00 ± 0.09	2.22 ± 0.15	2.41 ± 0.11	2.6 ± 0.2	1.8 ± 1.6	1.8 ± 1.4	0.3 ± 0.8	1.2 ± 1.0	25.6 ± 0.6	25.5 ± 0.2	25.3 ± 0.5	26.6 ± 0.5	3.1 ± 0.3	4.0 ± 0.4	4.1 ± 0.3	5.9 ± 0.1
2 mM Na phosph. pH 6 CA582/lactose 70:30	5.61 ± 0.10	5.60 ± 0.16	5.51 ± 0.15	5.55 ± 0.11	1.94 ± 0.08	2.11 ± 0.08	2.21 ± 0.13	2.23 ± 0.14	1.8 ± 1.8	1.7 ± 1.6	1.7 ± 0.9	1.2 ± 0.2	25.5 ± 0.2	26.0 ± 0.2	28.9 ± 0.1	29 ± 2	5.6 ± 0.2	5.4 ± 0.4	7.2 ± 0.2	7.3 ± 0.4
2 mM Na phosph. pH 6 CA582/sucr./mann. 70:15:15	5.60 ± 0.07	5.55 ± 0.05	5.50 ± 0.14	5.01 ± 0.08	1.91 ± 0.09	2.00 ± 0.08	2.32 ± 0.12	2.02 ± 0.10	0.0 ± 1.7	0.0 ± 0.4	0.1 ± 1.0	0.8 ± 0.7	25.6 ± 0.2	25.6 ± 0.1	26.3 ± 0.2	25 ± 2	3.3 ± 0.1	3.4 ± 0.7	4.2 ± 0.3	5.2 ± 0.2

IV.3.3.5.5. Stability study on the freeze-dried powders

A three-month stability study was performed on the freeze-dried powders containing 30% of the different types of stabilising excipients (**Table XXVI**). This was done to estimate the potential long-term stability of the final spray-dried formulations with these different stabilisers. Due to the large amounts of CA582 material needed to produce a single batch by spray-drying, it was not possible to perform the study with spray-dried formulations and it may be hypothesised that the dry state stability of the formulations will be comparable whether these have been produced by freeze-drying or spray-drying.

The results show that the powder that does not contain a stabilising sugar or polyol excipient presents an increased degradation of the CA582 molecule over time, with significant formation of unfolded species and an increase in soluble dimers to up to 5.5% at $t = 3$ months. On the other hand, the powder containing 30% sucrose provided optimal stabilisation of the antibody, with no significant change between $t = 0$ and $t = 3$ months for any of the tested parameters. Interestingly, the powder containing mannitol as a stabiliser presented a slight but progressive increase in unfolded species and soluble dimer of CA582 (2.6% at $t = 3$ months), which could also be suspected for the powder containing both sucrose and mannitol even if no significant difference was obtained from $t = 0$ for this powder (Student t -test, $p > 0.05$). The failure of mannitol to prevent degradation of the antibody is probably due to crystallisation of this excipient during freeze-drying as amorphous systems are known to provide better stabilisation of proteins in the dry state. A similar deleterious effect was, for example, observed in the stabilisation of several other proteins such as L-asparaginase, LDH, and β -galactosidase during freeze-drying in the presence of increasing concentrations of mannitol, which was also attributed to mannitol crystallisation (Izutsu et al., 1994).

The high T_g of sucrose and lactose may provide an advantage over mannitol in the stabilisation of CA582 due to a better maintained glassy state in powders with an increased amount of moisture. The type of mannitol crystals formed during freeze-drying also could have influenced the degradation of the antibody because hemihydrate crystals are known to

Table XXVII. Evaluation of CA582 stability after 2h stirring in isopropanol. Results obtained on a CA582 formulation containing 30% (w/w) sucrose, freeze-dried from a 2 mM Na phosphate, pH 6 buffer

	Unfolding (A_{230}/A_{280})		Aggregation (% soluble dimer)		Aggregation (% insoluble aggregates)		Desamidation (% acid species)		Aggregation/ Fragmentation (SDS-PAGE)	
	t0	t2h	t0	t2h	t0	t2h	t0	t2h	t0	t2h
Reference CA582 (50 mM Na acet./ 125 mM NaCl pH 5)	5.62 ± 0.09		1.86 ± 0.05		/		25 ± 1		Major band 45kDa Weak band 25kDa Weak band 100kDa	
2 mM Na phosph. pH 6 CA582/sucrose 70:30	5.51 ± 0.10	5.52 ± 0.08	1.91 ± 0.04	2.1 ± 0.2	0.0 ± 1.5	0.7 ± 0.9	25.5 ± 0.5	25.9 ± 0.6	No change with ref.	No change with ref

be metastable, converting to anhydrous polymorphs of mannitol upon heating or exposure to moisture (Yu et al., 1999). The hydrate water can then be released and redistributed to the amorphous drug and thus increase the potential for chemical and physical changes.

Results also showed that the powder containing lactose as a stabiliser did not provide appropriate stabilisation of the CA582 molecule after 3 months' storage. This powder indeed presented a significant increase in its desamidated species content to up to 29% at $t = 3$ months. It is likely that these "desamidated species" are in fact glycated species. These could be produced by a reaction between lactose, which is a reducing sugar, and the primary amine of lysine residues in the protein (Maillard reaction). As glycation affects the global charge of the molecule, it also affects the retention time of these species in CEX, producing an acidic shift. Similar degradation has, for example, been reported during storage of spray-dried recombinant human deoxyribonuclease formulated with lactose (Clark et al., 1996; Andya et al., 1999).

Therefore, sucrose was considered to be the best stabilising sugar for further processing of the powders by HPH. HPH was performed to break up the freeze-dried cakes and obtain particle size distributions compatible with lung deposition of the particles.

IV.3.3.6. High pressure homogenisation of the freeze-dried CA582

IV.3.3.6.1. Evaluation of CA582 stability in isopropanol

As the HPH process was performed in isopropanol, the stability of the freeze-dried CA582 molecule in this solvent was first evaluated (**Table XXVII**). A 0.5% suspension in isopropanol was realised with the powder (CA582/sucrose 70:30) and stirred for 2 hours at room temperature. The powder was then recovered after filtration on a ceramic filter and overnight drying under vacuum.

The results showed that no degradation of the antibody occurred after 2 hours ($p > 0.05$) in isopropanol, indicating that this solvent can be used for the HPH process.

Table XXVIII. Particle size characteristics of the homogenised suspensions obtained by laser diffraction (mean \pm S.D., n=10, performed on the freeze-dried powder 2 mM Na phosph., pH 6 CA582/sucrose 70:30)

	Particle size characteristics		
	<i>d</i> (0.5)	<i>D</i> [4, 3]	% < 5.0 μ m
	(μ m)	(μ m)	(%)
20 min HSH at 24 000 rpm	34 \pm 2	42 \pm 3	8 \pm 1
20 min HSH at 24 000 rpm + 10 cycles HPH at 7 000 PSI	15.2 \pm 0.9	18.5 \pm 1.2	18.2 \pm 1.0
20 min HSH at 24 000 rpm + 10 cycles HPH at 7 000 PSI + 20 cycles at 12 000 PSI	8.5 \pm 0.2	10.0 \pm 0.1	30.7 \pm 0.9
20 min HSH at 24 000 rpm + 10 cycles HPH at 7 000 PSI + 50 cycles at 12 000 PSI	3.43 \pm 0.05	3.74 \pm 0.05	76.6 \pm 0.2
20 min HSH at 24 000 rpm + 200 cycles at 5 000 PSI	3.41 \pm 0.08	3.70 \pm 0.06	77.7 \pm 0.3

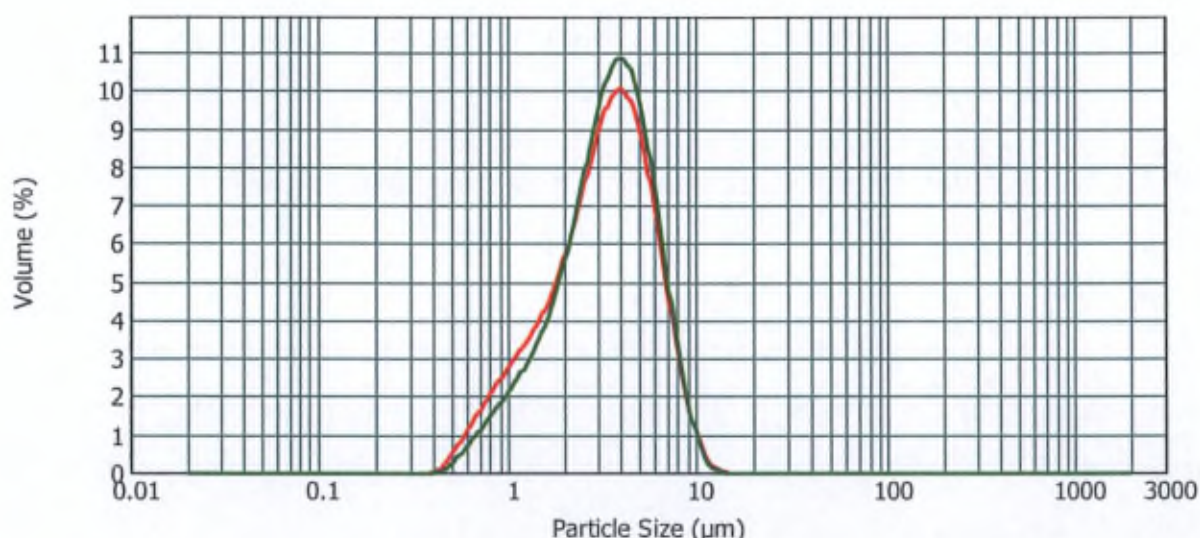


Figure 67. Particle size distributions measured by laser diffraction of the homogenised suspensions after 10 cycles at 7 000 PSI and 50 cycles at 12 000 PSI (green curve), and after 200 cycles at 5 000 PSI (red curve)

IV.3.3.6.2. Particle size distribution of the CA582 homogenised suspensions

Determination of the HPH processing conditions was performed with the freeze-dried powder (CA582/sucrose 70:30). As a first step, the suspensions were processed by 20 min HSH to break up the freeze-dried cakes. Then HPH was applied and evaluation of the particle size distribution was performed after 10 cycles at 7 000 PSI and 10, 20, 30, 40 or 50 cycles at 12 000 PSI. Evaluation was also performed after 50, 100, 150 or 200 cycles at 5 000 PSI. In all the conditions tested, HPH was conducted at 5°C on 0.5% w/v suspensions. Adequate particle size distribution compatible with lung deposition of the powder was obtained after HPH at 10 cycles at 7 000 PSI and 50 cycles at 12 000 PSI (**Table XXVIII**). Similar particle size distribution was obtained after 200 cycles at 5 000 PSI (**Table XXVIII** and **Figure 67**), indicating that these two protocols may be used for processing the antibody. However, as the process with 200 cycles at 5 000 PSI is more time-consuming (60 min vs. 30 min, for 20 ml suspension), it was not chosen for the production of the suspensions but was used to investigate the effect of using a lower processing pressure on CA582 stability (see IV.3.3.6.6.).

It is to be noted that the use of an operating pressure higher than 12 000 PSI was not investigated because proteins are likely to be degraded in harsh environmental conditions such as high pressures. Moreover, HPH processing at high pressure is much more time-consuming.

IV.3.3.6.3. Influence of the type of stabilising excipient on CA582 stability and particle size after HPH

Although sucrose provided the best stabilisation of the antibody in the freeze-dried state, HPH was also performed on the CA582 powders that were freeze-dried with lactose and mannitol excipients as these might provide better protection of the antibody during the HPH process (**Table XXIX**). Evaluation of the addition of glycine in the freeze-dried powder (15% w/w) or addition of a small proportion of water (1% v/v) in the isopropanol dispersant was also carried out. The stability of the CA582 molecule after HPH was evaluated on the powder recovered after filtration on a ceramic filter and overnight drying under vacuum.

Table XXIX. Influence of the type of stabilising excipient on the stability of the CA582 molecule and particle size in the homogenised suspensions. Results obtained on the freeze-dried powders suspended in isopropanol (0.5% w/v) after 20 min HSH, followed by 10 cycles HPH at 7 000 PSI and 50 cycles HPH at 12 000 PSI.

	Unfolding (A_{230}/A_{280})	Aggregation (% soluble dimer)	Aggregation (% insoluble aggregates)	Desamidation (% acid species)	Particle size d(0.5) (μm)
Reference CA582 (50 mM Na acetate/ 125 mM NaCl pH 5)	5.60 ± 0.14	1.84 ± 0.06	/	25.2 ± 0.6	/
2 mM Na phosphate pH 6 CA582/sucrose 70:30	5.52 ± 0.10	3.5 ± 0.2	15 ± 2	34 ± 3	3.43 ± 0.05
2 mM Na phosphate pH 6 CA582/mannitol 70:30	4.67 ± 0.11	6.8 ± 0.1	19 ± 2	43 ± 4	3.49 ± 0.07
2 mM Na phosphate pH 6 CA582/lactose 70:30	5.51 ± 0.10	3.4 ± 0.2	24 ± 4	50 ± 6	3.39 ± 0.07
2 mM Na phosphate pH 6 CA582/sucrose/mannitol 70:15:15	5.50 ± 0.11	3.7 ± 0.1	23 ± 2	35 ± 4	3.40 ± 0.05
2 mM Na phosphate pH 6 CA582/sucrose/glycine 55:30:15	5.33 ± 0.12	4.2 ± 0.4	33 ± 4	48 ± 3	3.48 ± 0.05
2 mM Na phosphate pH 6 CA582/sucrose 70:30 1% v/v ultrapure water	5.54 ± 0.09	3.3 ± 0.2	29 ± 3	52 ± 3	3.5 ± 0.2

The main consequence of HPH was the formation of insoluble aggregates in all of the tested conditions, which were also detected visually. It is known from the literature that high pressure can cause protein unfolding and facilitate protein aggregation due to increased hydrophobic interactions. This has been observed for a recombinant human interleukin-1 receptor antagonist above 180 MPa (~ 26 000 PSI) (Seefeldt et al., 2005) and β -lactoglobulin B above 500 MPa (~ 70 000 PSI) (Considine et al., 2007). Pressure treatment can also generate chemically linked aggregates since high pressure can expose reactive groups that are normally well-covered under atmospheric pressure (Huppertz et al., 2006; Wang et al., 2010).

Although the differences in insoluble aggregates formed with the use of sucrose, mannitol, and lactose were not significantly different (15%, 19%, and 24%, respectively, ANOVA test, $p > 0.05$), sucrose again provided the best global stabilising effect. Mannitol indeed led to the formation of unfolded species and of more soluble aggregates (6.8%) whereas lactose presented a high content of desamidated - or more likely, glycated - species (50%). Surprisingly, addition of glycine, which was tested because small amino acids are also known to provide stabilisation of proteins under the dry state (see section II.2.2.2.2.), exhibited a particularly high insoluble aggregates and desamidated species content. The same tendency was seen with the addition of a small fraction of ultrapure water, which was tested because it might have helped the protein to maintain its hydration shell during processing, avoiding protein-protein hydrophobic interactions.

It is to be noted that the type of stabilising excipient had no influence on the particle size distribution obtained after HPH.

IV.3.3.6.4. Influence of the type of liquid-phase dispersing agent on CA582 stability and particle size after HPH

As the use of 30% sucrose in the CA582 freeze-dried powder did not provide optimal stabilisation of the molecule during the HPH process, different dispersing agents (see **Table XXX**) were tested that were dissolved in isopropanol. These were surfactive agents, which could also help avoid aggregation of the protein (see section II.2.2.2.2.). Na glycocholate was chosen because a previous work realized in our laboratory had shown it is a particularly

Table XXX. Influence of the type of liquid-phase dispersing agent on CA582 stability and particle size after HPH. Results obtained on the freeze-dried powders suspended in isopropanol (0.5% w/v) after 20 min HSH, followed by 10 cycles HPH at 7 000 PSI and 50 cycles HPH at 12 000 PSI.

	Unfolding (A_{230}/A_{280})	Aggregation (% soluble dimer)	Aggregation (% insoluble aggregates)	Desamidation (% acid species)	Particle size d(0.5) (μm)
Reference CA582 (50 mM Na acetate/ 125 mM NaCl pH 5)	5.54 ± 0.15	1.84 ± 0.07	/	25.2 ± 0.5	/
2 mM Na phosphate pH 6 CA582/sucrose 70:30	5.52 ± 0.10	3.5 ± 0.2	15 ± 2	34 ± 3	3.43 ± 0.05
2 mM Na phosphate pH 6 CA582/sucrose 70:30 2% Phospholipon® 90H	5.54 ± 0.14	3.2 ± 0.2	25 ± 3	33 ± 4	3.50 ± 0.11
2 mM Na phosphate pH 6 CA582/sucrose 70:30 2% Polysorbate 80	5.50 ± 0.11	3.5 ± 0.1	23 ± 2	39 ± 1	3.44 ± 0.08
2 mM Na phosphate pH 6 CA582/sucrose 70:30 2% Na glycocholate	5.59 ± 0.13	3.0 ± 0.1	16 ± 1	29 ± 2	3.37 ± 0.07
2 mM Na phosphate pH 6 CA582/sucrose 70:30 2% Palmitic acid	5.50 ± 0.09	3.4 ± 0.1	16 ± 3	30 ± 1	3.40 ± 0.05

effective surface active agent for the stabilisation of nanosuspensions of tobramycin during HPH (Pilcer et al., 2009). Moreover, Na glycocholate seems to be relatively well tolerated in the respiratory tract (Yamamoto et al., 1997). It also presents a high melting point (130 °C), which is useful for further processing, such as spray-drying, to avoid partial melting or softening of the excipient. Palmitic acid was chosen because it was shown to provide the stabilising effect of β -lactoglobulin B under pressure stress (Considine et al., 2007). Moreover, palmitic acid is part of the composition of Survanta[®], which is a surfactant replacement therapy used for the prevention and treatment of ARDS. It should therefore be easily accepted as an excipient for inhalation. It also presents a relatively high melting temperature (63-64 °C), which should allow spray-drying. Due to its hydrophobic nature, it could also provide a hydrophobic coating around the particles after spray-drying, which could help maintain the long-term stability of the protein and could possibly provide sustained release.

This experiment was performed with the freeze-dried powder containing 30% sucrose. The surfactive agents were dissolved at 60 °C in isopropanol (2% w/w of the powder weight) before addition of the CA582 freeze-dried powder. The physico-chemical stability of the CA582 molecule after HPH was evaluated on the powder recovered after filtration on a ceramic filter and overnight drying under vacuum.

Results indicated that addition of 2% Phospholipon[®] 90H or polysorbate 80 to isopropanol did not improve the stability of the CA582 molecule. In both cases, a significant increase was even noted in the insoluble aggregate content in comparison with the powder without addition of a liquid-phase dispersing agent, with a percentage of $25 \pm 3\%$, $23 \pm 2\%$, and $15 \pm 2\%$ insoluble aggregates, respectively (Student t-test, $p < 0.05$). With the use of polysorbate 80, a significant increase in desamidated species was also noted in comparison with the powder without addition of surfactant ($39 \pm 1\%$ vs. $34 \pm 3\%$, Student t-test, $p < 0.05$). On the other hand, addition of 2% sodium glycocholate or palmitic acid could improve stabilisation, with a slight, insignificant decrease in the content of desamidated species formed in comparison with the powder obtained without addition of surfactant ($29 \pm 2\%$, $30 \pm 1\%$, and $34 \pm 3\%$, respectively, Student t-test, $p > 0.05$).

Table XXXI. Influence of the concentration of the liquid-phase dispersing agent on CA582 stability and particle size after HPH. Results obtained on the freeze-dried powders suspended in isopropanol (0.5% w/v) after 20 min HSH, followed by 10 cycles HPH at 7 000 PSI and 50 cycles HPH at 12 000 PSI.

	Unfolding (A_{230}/A_{280})	Aggregation (% soluble dimer)	Aggregation (% insoluble aggregates)	Desamidation (% acid species)	Particle size d(0.5) (μm)
Reference CA582 (50 mM Na acetate/ 125 mM NaCl pH 5)	5.55 ± 0.15	1.92 ± 0.11	/	25.4 ± 0.7	/
2 mM Na phosphate pH 6 CA582/sucrose 70:30	5.52 ± 0.10	3.5 ± 0.2	15 ± 2	34 ± 3	3.43 ± 0.05
2 mM Na phosphate pH 6 CA582/sucrose 70:30 10% Na glycocholate	5.51 ± 0.09	3.4 ± 0.2	10 ± 3	27 ± 1	3.44 ± 0.04
2 mM Na phosphate pH 6 CA582/sucrose 70:30 10% Palmitic acid	5.52 ± 0.08	3.5 ± 0.1	11 ± 3	30 ± 1	3.51 ± 0.10

No significant difference was obtained for the content in unfolded species and in soluble aggregates for any of the surfactants tested in comparison with the powder without addition of surfactant. Particle size distributions of the suspensions were also not influenced by the addition of surfactive agent in the dispersing isopropanol, whatever the type of surfactant.

IV.3.3.6.5. Influence of the concentration of liquid-phase dispersing agent on CA582 stability

As a stabilising effect of sodium glycocholate and palmitic acid was suspected, as stated in the previous section (IV.3.3.6.4.), another experiment was conducted, with the concentration of these two excipients increased to 10% (**Table XXXI**).

Increasing the concentration of Na glycocholate and palmitic acid to 10% also led to a slight, but not significant, decrease in the content of insoluble aggregates in comparison with the powder without addition of surfactant ($10 \pm 3\%$ and $11 \pm 3\%$ vs. $15 \pm 2\%$, respectively, Student t-test, $p > 0.05$). A decrease in the content of desamidated species was also obtained, with values of $27 \pm 1\%$ ($p < 0.05$) and $30 \pm 1\%$ ($p > 0.05$) vs. $34 \pm 3\%$, respectively. This decrease was significant for Na glycocholate but not for palmitic acid. However, it is to be noted that these results were obtained with a small number of batches ($n=3$). An increase in the number of batches tested could allow a significant difference to be obtained for palmitic acid as well.

Due to these results, Na glycocholate and palmitic acid in a concentration of 10% (w/w of the powder weight) were selected for further processing of the formulations by spray-drying.

IV.3.3.6.6. Influence of the processing pressure and temperature on CA582 stability

The influence of the operating pressure during HPH was tested by using a sequence of 200 cycles at 5 000 PSI in place of the 10 cycles at 7 000 PSI and 50 cycles at 12 000 PSI. An experiment has also been conducted using a decreased temperature of the sample during

Table XXXII. Influence of the processing pressure and temperature during HPH on CA582 stability

	Unfolding (A_{230}/A_{280})	Aggregation (% soluble dimer)	Aggregation (% insoluble aggregates)	Desamidation (% acid species)
Reference CA582 (50 mM Na acetate/ 125 mM NaCl pH 5)	5.62 ± 0.12	1.91 ± 0.01	/	25.3 ± 0.6
2 mM Na phosphate pH 6 CA582/sucrose 70:30 10% Na glycocholate 10 c. 7 000 PSI, 50 c. 12 000 PSI, 5°C	5.51 ± 0.09	3.4 ± 0.2	10 ± 3	27 ± 1
2 mM Na phosphate pH 6 CA582/sucrose 70:30 10% Na glycocholate 200 cycles at 5 000 PSI, 5°C	5.50 ± 0.06	3.3 ± 0.2	16 ± 3	35 ± 5
2 mM Na phosphate pH 6 CA582/sucrose 70:30 10% Na glycocholate 10 c. 7 000 PSI, 50 c. 12 000 PSI, -20°C	5.54 ± 0.16	3.2 ± 0.2	15 ± 2	29 ± 2

Table XXXIII. Influence of the stabilising excipient content on CA582 stability after HPH.

Results obtained on the freeze-dried powders suspended in isopropanol (0.5% w/v) after 20 min HSH, followed by 10 cycles HPH at 7 000 PSI and 50 cycles HPH at 12 000 PSI.

	Unfolding (A_{230}/A_{280})	Aggregation (% soluble dimer)	Aggregation (% insoluble aggregates)	Desamidation (% acid species)
Reference CA582 (50 mM Na acetate/125 mM NaCl pH 5)	5.59 ± 0.08	1.95 ± 0.06	/	25.0 ± 0.6
2 mM Na phosphate pH 6 CA582/sucrose 70:30 10% Na glycocholate	5.51 ± 0.09	3.4 ± 0.2	10 ± 3	27 ± 1
2 mM Na phosphate pH 6 CA582/sucrose 50:50 10% Na glycocholate	5.51 ± 0.09	2.32 ± 0.08	8 ± 2	28.0 ± 0.7
2 mM Na phosphate pH 6 CA582/sucrose 20:80 10% Na glycocholate	5.50 ± 0.14	2.50 ± 0.07	10 ± 3	30 ± 2
2 mM Na phosphate pH 6 CA582/sucrose 70:30 10% Palmitic acid	5.52 ± 0.08	3.5 ± 0.1	11 ± 3	30 ± 1
2 mM Na phosphate pH 6 CA582/sucrose 50:50 10% palmitic acid	5.57 ± 0.11	2.43 ± 0.05	7 ± 3	31 ± 3
2 mM Na phosphate pH 6 CA582/sucrose 20:80 10% palmitic acid	5.55 ± 0.10	2.48 ± 0.13	12 ± 3	31 ± 3

processing (-20 °C in place of 5 °C) as low temperature can, in some cases, decrease the mobility of proteins and reduce aggregation (Wang et al., 2010). These two experiments were conducted on the powder containing 30% sucrose and 10% Na glycocholate in the dispersing medium (Table XXXII).

The results indicated no improvement in CA582 stability in any of the two modified operating conditions, so the previous parameters were maintained (sample temperature, 5°C; operating pressure, 10 cycles at 7 000 PSI and 50 cycles at 12 000 PSI).

IV.3.3.6.7. Influence of the content of stabilising excipient on CA582 stability

To limit the amount of excipients in the formulations, all previous HPH experiments were conducted with powders containing 30% sucrose as a stabilising excipient. However, it had been found in section IV.3.3.5.2. that this ratio corresponds to the minimum required to provide stabilisation of the CA582 in the freeze-dried powder and that no destabilisation of the molecule occurred with sucrose ratios up to 80%. Therefore, higher sucrose ratios (50% and 80%) were included during freeze-drying to evaluate their influence on the stabilisation of the antibody during HPH (Table XXXIII). This was performed in the presence of either 10% Na glycocholate or palmitic acid in isopropanol.

It was found that for the suspensions obtained with both Na glycocholate and palmitic acid, a content of 50% sucrose in place of 30% sucrose in the powder allowed the soluble dimer content to be decreased to 2.32% and 2.43%, respectively, in place of 3.4% and 3.5% when 30% sucrose was used. The values obtained are close to that of the reference CA582 material (1.95%). This also allowed the insoluble aggregate content to be further decreased to values of 8% and 7%, respectively, in place of 10% and 11%, respectively. The use of 80% sucrose, however, did not provide any additional stabilisation effect. A sucrose ratio of 50% was therefore finally selected for further processing of the formulations by spray-drying.

Table XXXV. Particle size characteristics of the formulations, obtained by laser diffraction
(liquid dispersion, mean \pm S.D., n=2)

	Particle size characteristics			
	Before spray-drying (suspension)	After spray-drying (powder)		
	<i>d</i> (0.5) (μm)	<i>d</i> (0.5) (μm)	<i>D</i> [4, 3] (μm)	%< 5.0 μm (%)
F1	/	13.35 \pm 0.10	23.22 \pm 0.11	27.1 \pm 0.6
F2	3.45 \pm 0.06	3.27 \pm 0.06	3.58 \pm 0.05	78.1 \pm 0.4
F3	3.27 \pm 0.04	3.40 \pm 0.05	3.70 \pm 0.07	76.8 \pm 0.6
F4	3.59 \pm 0.07	3.49 \pm 0.08	3.85 \pm 0.05	73.9 \pm 0.6

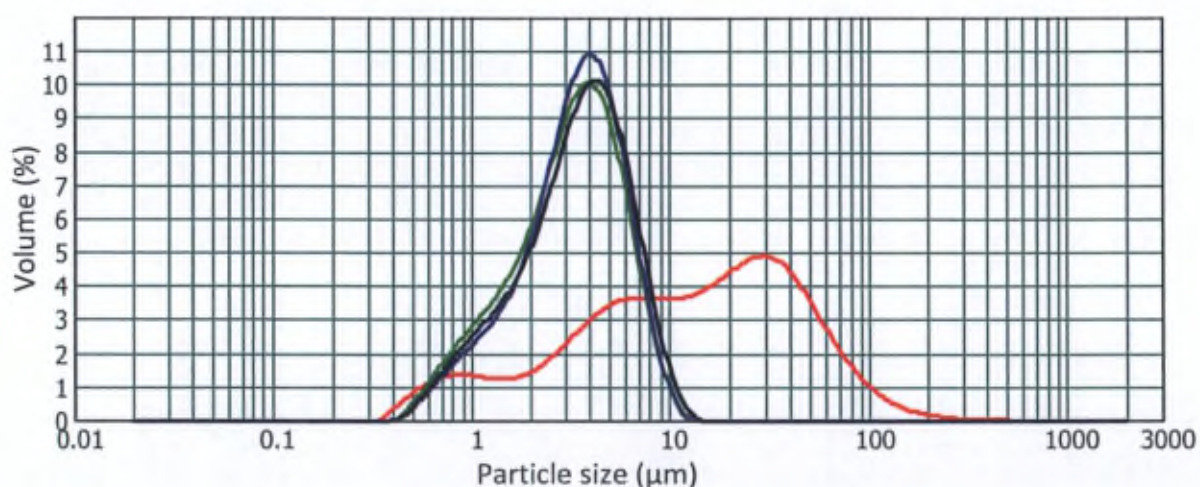


Figure 68. Particle size distributions measured by laser diffraction of formulation F1 (red line), formulation F2 (green line), formulation F3 (blue line), and formulation F4 (black line)

IV.3.3.7. Spray-drying of the CA582 formulations

IV.3.3.7.1. Selection and composition of the formulations

Four different formulations were selected for spray-drying to obtain dry powders for inhalation (Table XXXIV). In all cases, a CA582/sucrose ratio of 50:50 was selected as it provided the best stabilisation of the antibody during freeze-drying and HPH. A concentration of 0.5% w/v solid content in the liquid was also used in the four formulations. To evaluate the influence of the spray-drying process itself on the antibody, the F1 formulation was produced by direct spray-drying from a solution without previous freeze-drying and HPH steps. The F2, F3, and F4 formulations were spray-dried after freeze-drying and HPH in presence of no surfactant, 10% Na glycocholate, and 10% palmitic acid, respectively.

Table XXXIV. Composition of the formulations before and after spray-drying

Physical state (before spray-drying)	Liquid composition (before spray-drying)					Solid composition (after spray-drying)				
	CA582	Sucr.	Na Gly.	Palm. Ac.	Na Phosph.	CA582	Sucr.	Na Gly.	Palm. Ac.	Na Phosph.
	(% w/v)					(% w/w)				
F1 solution	0.25	0.25	/	/	0.0286	47.3	47.3	/	/	5.4
F2	0.25	0.25	/	/	0.007	49.3	49.3	/	/	1.4
F3 suspension	0.25	0.25	0.05	/	0.007	44.9	44.9	9.0*	/	1.2
F4	0.25	0.25	/	0.05	0.007	44.9	44.9	/	9.0*	1.2

*corresponding to 10% w/w when expressed as a percentage of the CA582/sucrose particles. Sucr.: sucrose, Na Gly.: sodium glycocholate, Palm. Ac.: palmitic acid, Na Phosph.: sodium phosphate buffer

IV.3.3.7.2. Particle size of the formulations

Particle size distribution of the F1 formulation (see Table XXXV and Figure 68) was found to be polydispersed, with a population in the nanometer size range, a population with a median particle size around 5 μm , and a population with a median size around 30 μm . This resulted in a % < 5.0 μm as low as 27%. This could be due to the relatively low concentration of solids (0.5% w/v) used in the solution before spray-drying, which was chosen to obtain a sufficient processing volume during HPH of the other formulations. For the F1 formulation,

Table XXXVI. Physico-chemical stability of the CA582 formulations after spray-drying

	Unfolding (A_{230}/A_{280})	Aggregation (% soluble dimer)	Aggregation (% insoluble aggregates)	Desamidation (% acid species)	Aggregation/ Fragmentation (SDS-PAGE)	Water content (%)
Reference CA582 (50 mM Na acetate/ 125 mM NaCl pH 5)	5.59 ± 0.11	1.96 ± 0.05	/	26.0 ± 0.8	Major band 45kDa Weak band 25kDa Weak band 100kDa	/
F1	5.50 ± 0.12	2.33 ± 0.03	1.3 ± 1.1	42.2 ± 0.4	No change with Ref.	4.70 ± 0.09
F2	5.54 ± 0.10	2.51 ± 0.03	14.7 ± 0.4	37 ± 4	No change with Ref.	4.20 ± 0.10
F3	5.50 ± 0.09	1.76 ± 0.05	6.0 ± 1.3	30.2 ± 1.3	No change with Ref.	4.14 ± 0.10
F4	5.45 ± 0.13	1.90 ± 0.01	16 ± 2	39 ± 5	No change with Ref.	3.27 ± 0.13

this low concentration could have led to the formation of very small nanometric particles during spray-drying, which present very high cohesive forces resulting in aggregation of the particles. On the other hand, the F2, F3, and F4 formulations exhibited monodispersed size distributions that were not significantly different between the three formulations. Moreover, for each formulation, the median particle size was not significantly different before or after spray-drying (Student t-test, $p > 0.05$, N.S.), indicating that a single particle was contained in each droplet during spray-drying of the suspensions and that no aggregation of particles occurred.

IV.3.3.7.3. Stability of the formulations

The physico-chemical stability of the formulation produced is presented in **Table XXXVI**. It can be seen that the F1 formulation, which was produced by direct spray-drying, did not produce a significant amount of insoluble aggregates ($1.3 \pm 1.1\%$, negative by visual inspection), indicating that spray-drying is a more conservative process than HPH for the formation of insoluble aggregates of the CA582 molecule. However, the F1 formulation presented a slight increase in soluble dimers and a high level of desamidated species (42%) produced during spray-drying. The F2 formulation produced after HPH without addition of a liquid-phase dispersing agent exhibited values similar to F1 for soluble dimers and desamidated species, but presented 15% insoluble aggregates. The F3 formulation spray-dried after HPH in the presence of 10% Na glycocholate presented a lower insoluble aggregate content that was comparable to the formulation before spray-drying that was presented in Table XXXIII (6% vs. 8%, respectively), indicating that Na glycocholate effectively inhibited the formation of insoluble aggregates during spray-drying. The F3 formulation also presented a lower desamidated species content, comparable to the level before spray-drying presented in Table XXXIII (30% vs. 28%, respectively) and non-significantly higher than the reference CA582 material ($p > 0.05$). The soluble dimer content for the F3 formulation was also as low as in the reference CA582 material. Na glycocholate was thus found to be particularly efficient in stabilising the CA582 molecule during spray-drying. The F4 formulation spray-dried after HPH in the presence of 10% palmitic acid presented an increased insoluble aggregates content compared to the formulation before spray-drying

(16% vs. 7%), which was comparable to the level obtained with the F2 formulation spray-dried without a liquid-phase dispersant. The F4 formulation also presented an increased desamidated species content compared to the formulation before spray-drying (39% vs. 31%), which was comparable to the F2 formulation. However, the soluble dimer content in the F4 formulation was as low as in the reference CA582 material. This indicates that palmitic acid was effective in avoiding the formation of soluble dimers during spray-drying but could not protect the molecule from insoluble aggregation and desamidation. However, it is to be recalled that palmitic acid also provided a stabilising effect on the antibody during HPH.

Although all the formulations spray-dried after HPH presented a low insoluble aggregate content, the level of insoluble aggregate that is allowed in a formulation for inhalation is not clearly defined and should be very dependent on the molecule administered and the potential immunogenicity of its aggregates. It is still to be determined if CA582 aggregates produce *in vivo* toxicity. As the F1 formulation possesses a high desamidated species content but has the advantage of not presenting insoluble aggregates, the addition of Na glycocholate to the formulation, which is a water-soluble compound, could be of interest to avoid desamidation of formulation F1.

The results of SDS-PAGE in non-reducing and reducing conditions exhibited no change from the reference for any of the formulations, despite the presence of insoluble aggregates in the F2-F4 formulations. Addition of the denaturing agent during the experiment indeed led to the dissolution of the insoluble aggregates that were therefore observed in the monomer band. This indicates that these aggregates were due to protein-protein hydrophobic interactions and were not disulfide-linked.

The water content of the formulation was slightly higher for the F1 formulation (4.7%), which is attributed to the fact that this formulation was produced from a water solution in place of an isopropanol suspension. On the other hand, the water content of the F4 formulation (3.3%) was lower than for the F2 and F3 formulations, which could be attributed to the presence of a hydrophobic coating made up of palmitic acid around the particles. This may avoid formation of aggregates or other degradation products during long-term storage

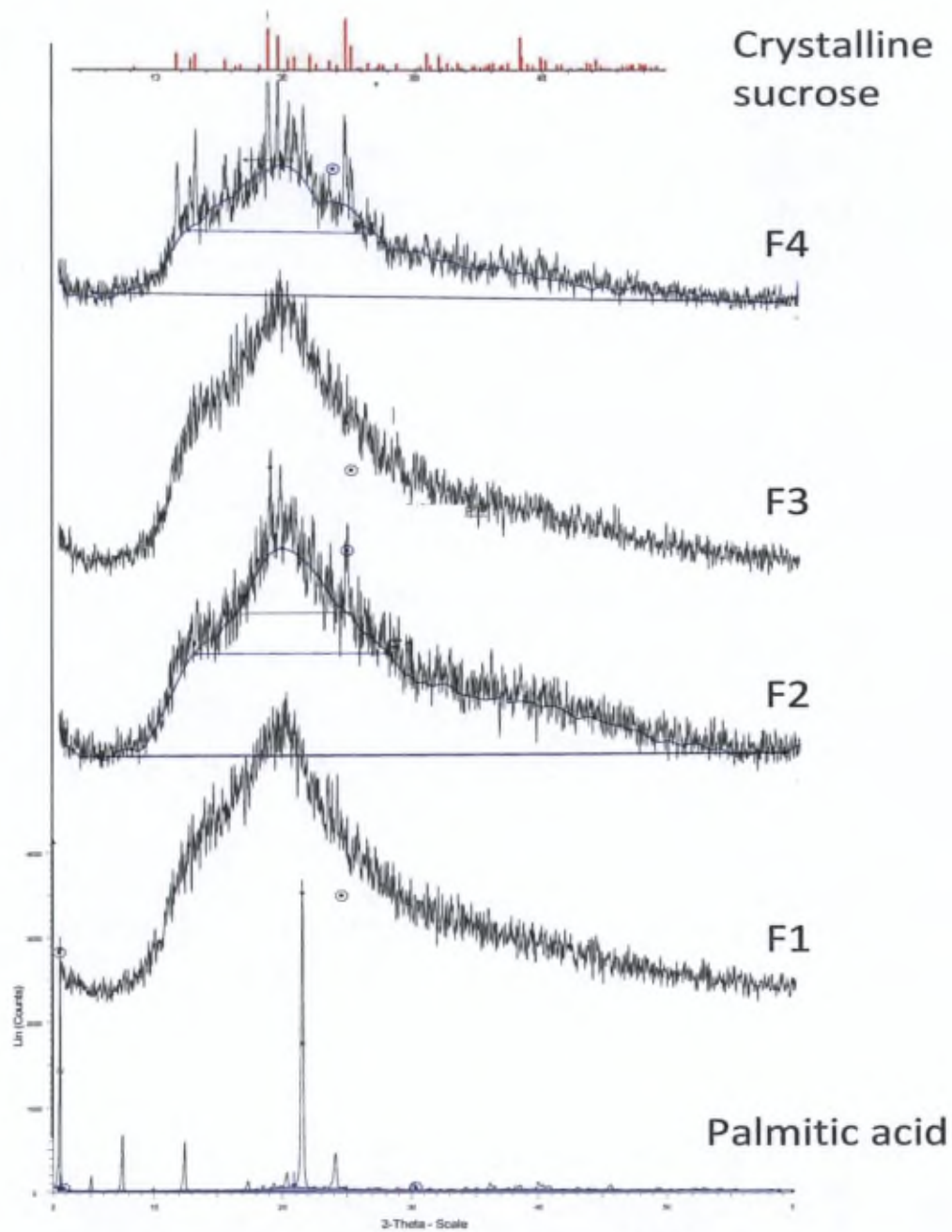


Figure 69. X-ray powder diffraction patterns of the formulations after spray-drying. Modelling of the amorphous and crystalline areas was performed using a pseudo-Voigt function.

of the formulation. As no hydrophobic coating can be included in the F1 formulation because of poor solubility of hydrophobic compounds in water, hydrophobic coating in this formulation could be achieved by performing a second spray-drying step in isopropanol containing the dissolved excipient. As this formulation presents no insoluble aggregates, this strategy could constitute a good solution for stabilisation during processing and for long-term storage of the molecule.

PXRD patterns of the formulations are presented in **Figure 69**. It can be seen that the F1 and F3 formulations presented fully amorphous structures, whereas the F2 and F4 formulations presented crystalline structures in ratios of 9% and 12%, respectively. In both formulations, the peaks could be attributed to the presence of crystalline sucrose. As sucrose in the freeze-dried CA582 powders was fully amorphous, it was concluded that some recrystallisation of sucrose occurred during the HPH or spray-drying process. Interestingly, no crystalline sucrose was found in the F3 formulation, indicating that Na glycocholate prevented this recrystallisation phenomenon. This was not the case for the F4 formulation, indicating that palmitic acid did not provide the same protection against recrystallisation. This finding could explain why Na glycocholate provided better stabilisation of the CA582 molecule, as proteins are generally better protected in an amorphous matrix. It can be noted that the palmitic acid starting material contained 76% crystalline phase. As no peak of palmitic acid was recovered in the F4 formulation, it is likely that the palmitic acid was in amorphous state in the coating formed during spray-drying. Therefore, stability studies should be performed in the future to assess the physical stability of this formulation, as crystalline structures could appear upon storage.

Table XXXVII. Dry powder formulations particle size characteristics: $d_{(0.5)}$, $D_{[4,3]}$, and $V\% < 5 \mu\text{m}$ (mean \pm S.D., $n=2$), measured with the Spraytec[®] laser diffractometer.

Results obtained at 100 l/min for 2.4 s using an Aerolizer[®] device. Acquisition parameters: triggering mode, 10% level; data acquisition rate, 2 500 Hz; acquisition duty cycle, 50%; test duration, 3 000 ms; refractive index, 1.50 (standard opaque particles).

	$d_{(0.5)}$ (μm)	$D_{[4,3]}$ (μm)	$\% < 5.0 \mu\text{m}$ (%)
F1	27 \pm 3	37 \pm 4	24.4 \pm 1.7
F2	3.8 \pm 0.2	4.8 \pm 0.3	66 \pm 2
F3	4.5 \pm 0.3	5.2 \pm 0.3	57 \pm 5
F4	3.3 \pm 0.2	4.1 \pm 0.3	73 \pm 3

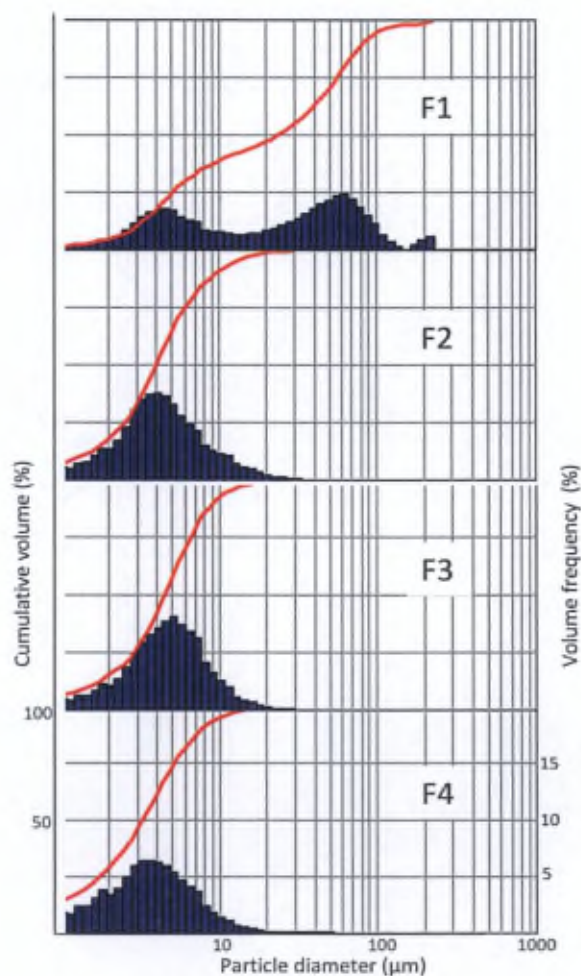


Figure 70. Particle size distributions of the CA582 formulations, measured with the Spraytec[®] laser diffractometer

IV.3.3.7.4. Dispersion properties and aerodynamic features of the dry powder formulations

Particle size distributions observed with the Spraytec® laser diffraction technique (Table XXXVII and Figure 70) exhibited a polydispersed curve for the F1 formulation, which is in accordance with what was observed by classical laser diffraction (Table XXXV). The values obtained for the $d_{(0.5)}$ and $D_{[4,3]}$ were, however, higher with the Spraytec® measurement, indicating that the F1 particles are even more aggregated in simulated breathing conditions. Particle size distributions obtained for the F2, F3, and F4 formulations were not significantly different (ANOVA, $p > 0.05$) although the F4 formulations seemed to present a slightly lower particle size. Results also showed a good correlation with the classical laser diffraction results. This indicates that the particles in these formulations are easily dispersed and almost fully individualised upon aerosolisation. The F2, F3, and F4 formulations presented a $d_{(0.5)}$ of $3.8 \pm 0.2 \mu\text{m}$, $4.5 \pm 0.3 \mu\text{m}$, and $3.3 \pm 0.2 \mu\text{m}$, respectively, which should allow lung deposition of the powders to be achieved.

Impaction measurements were performed on the four formulations using an MsLI. Measurements were conducted at 60 l/min and 100 l/min in order to detect any possible loss of deaggregation efficiency of the formulations at a suboptimal flow rate. The results at 100 l/min (Table XXXVIII and Figure 71) exhibited a lower FPF for the F1 formulation (25%) than for the F2, F3, and F4 formulations (36%, 42%, and 35%, respectively), resulting in more powder impacted in the first stage of the impinger. On the other hand, the F3 formulation presented a significantly higher FPF in comparison with the F2 and F4 formulations, which was mainly characterised by a decreased impaction of powder in the “throat”, and an increased impaction in stage 3 of the impinger. The FPFs obtained for the F2, F3, and F4 formulations were in the same range as those obtained for most commercial DPI formulations used in asthma therapy, which were found to have FPFs between 23% and 39% (Steckel and Müller, 1997).

The poorer aerodynamic performance of the F1 formulation fits very well with the observations obtained by the two laser diffraction techniques, with a $\% < 5.0 \mu\text{m}$ of 27.1% and 24.2% obtained by classical laser diffraction and Spraytec laser diffraction, and an FPF of 25% obtained by impaction. Optimisation of the spray-drying parameters for the formulation

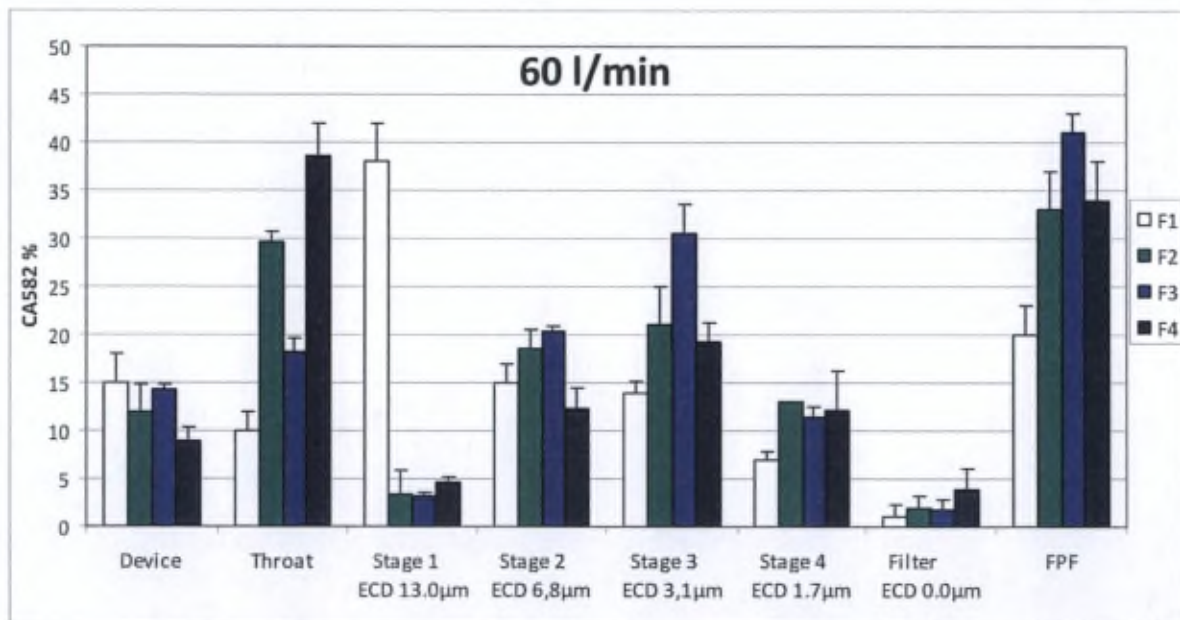
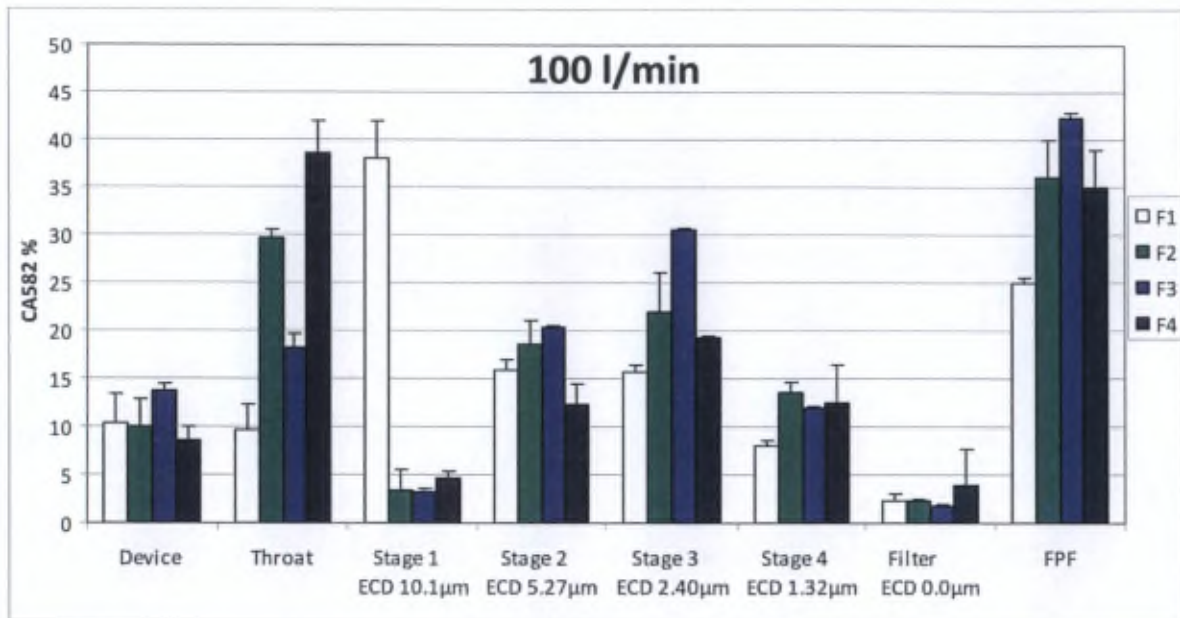


Figure 71. In vitro deposition patterns (MsLI) of the different CA582 formulations at 100 l/min (up) and 60 l/min (down) (n=2). Results obtained with a nominal CA582 dose of 5.0 ± 0.5 mg loaded in HPMC capsules. The inhalation device (Aerolizer[®]) was used with a flow rate of 100 l/min for 2.4 s or of 60 l/min for 4 s. The drug % was calculated on the basis of the metered dose of CA582. ECD: Effective Cut-off Diameter of each stage of the MsLI.

Table XXXVIII. In vitro deposition characteristics of the different formulations measured at 100 l/min using an MsLI and corresponding to a nominal CA582 dose of 5.0 mg
(Mean \pm S.D., n=2, results obtained using an Aerolizer® device operated at a flow rate of 100 l/min for 2.4 s)

	F1	F2	F3	F4
FPD (mg)	1.10 \pm 0.02	1.4 \pm 0.2	1.95 \pm 0.01	1.4 \pm 0.2
MMAD (μ m)	4.13 \pm 0.12	3.8 \pm 0.2	3.92 \pm 0.01	3.2 \pm 0.3
Metered dose (mg)	4.42 \pm 0.16	3.8 \pm 0.2	4.59 \pm 0.04	3.9 \pm 0.3
FPF (%)	25.0 \pm 0.5	36 \pm 4	42.4 \pm 0.5	35 \pm 4
DD (%)	66 \pm 6	68 \pm 5	79 \pm 4	70 \pm 4
UDD (%)	All capsules between 83.0 - 116.1	All capsules between 87.4 - 110.2	All capsules between 93.3 - 107.5	All capsules between 92.6 - 109.3

Table XXXIX. In vitro deposition characteristics of the different formulations measured at 60 l/min using an MsLI and corresponding to a nominal CA582 dose of 5.0 mg
(Mean \pm S.D., n=2, results obtained using an Aerolizer® device operated at a flow rate of 60 l/min for 4.0 s)

	F1	F2	F3	F4
FPD (mg)	0.91 \pm 0.1	1.39 \pm 0.2	1.84 \pm 0.05	1.36 \pm 0.2
MMAD (μ m)	4.3 \pm 0.2	3.9 \pm 0.2	3.93 \pm 0.02	3.2 \pm 0.2
Metered dose (mg)	4.53 \pm 0.12	4.21 \pm 0.15	4.50 \pm 0.09	4.01 \pm 0.11
FPF (%)	20 \pm 3	33 \pm 4	41 \pm 2	34 \pm 4
DD (%)	63 \pm 5	62 \pm 3	74 \pm 3	70 \pm 2
UDD (%)	All capsules between 80.0 - 114.0	All capsules between 83.1 - 115.4	All capsules between 90.2 - 111.9	All capsules between 89.4 - 113.7

(increased solid content in the solution) could improve its aerodynamic features. Concerning the formulations obtained after HPH, the better results obtained for the F3 formulation might be due to the modification of surface properties of the particles by the formation of a layer of Na glycocholate around the particles. The F4 formulation containing palmitic acid presented a FPF comparable to the F2 formulation without coating, indicating that the presence of a hydrophobic coating made up of 10% palmitic acid did not influence the FPF of the powder. However, it is to be noted that the MMAD of the F4 formulation ($3.2 \pm 0.3 \mu\text{m}$) was significantly lower than for the F1, F2, and F3 formulations ($4.13 \pm 0.12 \mu\text{m}$, $3.8 \pm 0.2 \mu\text{m}$, and $3.92 \pm 0.01 \mu\text{m}$, respectively). This was also observed for the $d_{(0.5)}$ measured by the Spraytec® technique (see Table XXXVII), even if no significant difference could be found. However, the F4 formulation presents a FPF that is lower than the F3 formulation. This observation is due to the fact that the MMAD calculation is based on the total powder mass recovered from stage 1 to the filter, excluding the powder impacted in the device and in the throat. Similarly, the Spraytec measurements do not take into account the particles impacted in the device and throat. As can be seen in **Figure 71**, the F4 formulation presented a higher powder impaction in the throat of the impactor in comparison with the F3 formulation, which explains its lower FPF. However, the lower MMAD of the F4 formulation in comparison with the F3 formulation indicates that the F4 powder that is not impacted in the throat of the impactor can penetrate the lungs more deeply than the F3 formulation.

Impaction results performed at 60 l/min (**Table XXXIX** and **Figure 71**) presented no significant difference in the FPFs from those obtained at 100 l/min for any of the formulations, although slightly lower mean values were obtained. This is of particular interest for the F4 formulation, which is coated with palmitic acid, as it did not present a decrease in its desaggregation efficiency in contrast to the insulin formulation, which was coated with 20% (w/w) of cholesterol and phospholipids 75:25 (see section IV.2.3.5.). For this formulation, a significant decrease in the FPF was obtained at a flow rate of 60 l/min compared to 100 l/min ($47 \pm 2\%$ and $59 \pm 4\%$, respectively, see Table XX). The difference between the CA582 formulation coated with palmitic acid and the insulin formulation coated with cholesterol and phospholipids could be due to the lower percentage of hydrophobic coating used (10% vs. 20%) or to the intrinsic properties of palmitic acid.

The delivered dose was not significantly different between the four formulations and was also similar at a lower flow rate, with values between 66% and 79% of the loaded dose at 100 l/min and between 62% and 74% at 60 l/min. For all formulations, the UDD results satisfied the requirements of the European Pharmacopoeia, which specifies that a preparation for inhalation complies if nine out of ten capsules present a delivered dose of between 75% and 125% of the average value and all capsules present a delivered dose of between 65% and 135%.

IV.3.4. Conclusion

In the present study, we developed and evaluated DPI formulations of an antibody fragment that were produced using, successively, freeze-drying, high pressure homogenisation, and spray-drying. This allowed to isolate the CA582 molecule in the dry state, reduce the particle size to achieve size distribution compatible with lung deposition, and finally obtain DPI formulations. Formulations with or without addition of a hydrophobic coating around the particles were produced.

It was possible to achieve adequate physico-chemical stabilisation of the antibody in the dry state using freeze-drying with appropriate buffering conditions and adding 30% sucrose as a stabilising excipient. However, the HPH process produced different types of degradation products that could partly be avoided by increasing the sucrose content to 50% in the powder and adding 10% Na glycocholate or palmitic acid as dispersing agents to the liquid phase during HPH. However, the presence of a small fraction of insoluble aggregates could not be fully avoided. Spray-drying of the formulations produced an increased formation of the different degradation products. Na glycocholate was found to be particularly effective in protecting the antibody during spray-drying, which was found to be at least partly related to its ability to inhibit sucrose recrystallisation. However, the best formulation still presented a small fraction of insoluble aggregates (6%).

The aerodynamic evaluation of the formulations showed FPFs that were compatible with lung deposition, with the formulation containing Na glycocholate presenting the highest FPF (42%). This is within the range of FPFs obtained for most DPI formulations for asthma therapy. The formulation containing palmitic acid, although it presented a lower FPF (35%)

than that using Na glycocholate, presented the lowest MMAD, indicating that this formulation can probably penetrate deeper into the lungs.

Depending on the accepted aggregation level in the formulation, the production of protein powders for inhalation using HPH could be of interest as it should allow a higher production yield and easier scaling up than with the use of spray-drying, and the possibility to produce coated formulations, providing hydrophobic protection of the molecule to avoid long-term stability issues. To this purpose, palmitic acid could be a promising coating material. Although it only provided partial protection of the antibody against degradation occurring during processing, it indeed provided unmodified aerosolisation properties to the powder, even at a sub-optimal inspiratory flow rate of 60 l/min.

Alternatively, a formulation was also produced from an aqueous solution using only spray-drying. It led to a high desamidated species content but had the advantage of not presenting insoluble aggregates. The addition of Na glycocholate to the formulation, which is a water-soluble compound, could be of interest to avoid desamidation of this formulation. As no hydrophobic coating can be included in the F1 formulation because of the poor solubility of hydrophobic compounds in water, a hydrophobic coating in this formulation could be achieved by performing a second spray-drying step. This strategy may constitute an alternative means of stabilising the molecule both during processing and for long-term storage.

In the future, the formulations developed should be further tested in a long-term storage study to evaluate the efficacy of a lipid coating in maintaining the physico-chemical stability of the protein. Moreover, a method should also be used to assess the conservation of the biological activity of the molecule. It is to be noted that *in vivo* evaluation of the lung deposition of the developed formulations was not performed in man because of the murine origin of the antibody fragment, which may induce immunogenicity issues.

V. GENERAL CONCLUSION

GENERAL CONCLUSION

In this work, we aimed to develop formulations for either local or systemic delivery of proteins that presented optimal aerodynamic features and stability. Insulin and an anti-IL13 monoclonal antibody fragment were used as model proteins. The formulation strategy was to stabilise the proteins under the dry state, as water is involved in most of the protein degradation processes. Moreover, the use of DPI formulations is of interest in comparison with the liquid inhalation systems (nebulisers and pMDIs), as DPIs are small and portable, environmentally friendly, and they require short treatment time and no patient coordination.

A combination of micronisation techniques (high speed and high pressure homogenisations) and drying techniques (spray-drying, freeze-drying) was used for production of the dry powder formulations. Lipid excipients were used to form a coating around the protein particles to prevent protein degradations during processing and/or storage and possibly improve the aerodynamic properties of the powders.

The insulin formulations developed presented high FPF values in comparison with those obtained for other protein formulations for inhalation currently under development, which often have an *in vitro* deposition of around 30%. Insulin presented a good stability in the dry state, even when no lipid coating was added, without formation of degradation products. The presence of a lipid coating made up of cholesterol and phospholipids did not significantly improve the aerodynamic behaviour, but the coated formulations exhibited decreased residual moisture content, and lower water adsorption upon storage, which is of interest for the long term stability of the protein.

Evaluation of an uncoated formulation and a formulation with 20% (w/w) lipid coating was performed in a pharmaco-scintigraphic study in type 1 diabetic patients. A decreased lung deposition was observed for the lipid-coated formulation, which was related to a lower deaggregation performance of this formulation at a sub-optimal inspiratory flow rate. However, lung deposition of this formulation should be improved by training of the patients to the inhalation procedure. Moreover, the two formulations showed interesting features, with pharmacokinetic profiles that mimic the natural insulin secretion pattern and

bioavailability that is within the ranges of two of the three dry powder insulins that have reached phase III clinical development.

The dry powder formulations of the anti-IL13 antibody fragment were produced using, successively, freeze-drying, HPH, and spray-drying. The freeze-drying step was first needed because the molecule was provided as a solution to the contrary of the insulin raw material. For the antibody fragment, a desalting procedure was also required before formulation. Due to its more elaborated structure, the antibody fragment was found to be more sensitive than insulin to physico-chemical degradation. Different types and concentrations of stabilizing excipients were evaluated for each production step. The formulation that provided the best stabilisation of the molecule and at the same time the best aerodynamic properties contained 50% sucrose, and a coating made up of Na glycocholate (10% w/w). However, a low percentage (6%) of insoluble aggregates in the formulation could not be avoided. This formulation presented a FPF around 42%. On the other hand, a formulation containing 50% sucrose and a coating made up of palmitic acid (10% w/w) led to a FPF around 35% that did not decrease with a decreased inhalation flow rate. This formulation also provided a hydrophobic coating around the particles, and low residual water content in the powder.

As a conclusion, the formulation work performed with the insulin and the antibody fragment molecules provided the proof-of-concept that it is possible to obtain dry powder protein formulations with appropriate aerodynamic properties and good physico-chemical stability, using a combination of freeze-drying, high pressure homogenisation, and spray-drying techniques. The use of HPH for the production of these formulations seems particularly interesting, as it allows obtention of coated particles when used in-line with spray-drying. Moreover, HPH processes can be easily scaled up. The presence of a lipid coating around the particles, although it did not improve the aerodynamic properties of the powders, provided low residual water content in the powders and limited moisture uptake during storage. This is of interest for the long term-stability of biomolecules, as most degradation pathways of proteins are water mediated.

Perspectives of this work include the realisation of long-term stability studies in ICH conditions to confirm the potential of hydrophobic coating to provide protein stabilisation.

These should also compare different packaging solutions, from bulk powder in a standard multi-dose container to individual aluminium blisters providing full protection against environmental water and gases. This should provide information on the usefulness of hydrophobic coatings in limiting packaging costs by decreasing the need to use elaborated multiple-layer blister materials. On the other hand, an issue with insulin and the anti-IL13 molecules is that they are used in the treatment of chronic diseases, which is also the case of many other inhaled proteins under investigation. It is therefore required to evaluate the long-term safety of the excipients used. In particular, bile salts such as Na glycocholate have been suspected to cause lung inflammation due to their ability to interact with epithelial membranes. However, this toxicity is strongly expected to be dose-dependent and could not be an issue in our formulations due to the low percentage of excipient involved. Finally, the use of other coating and stabilising excipients could be investigated that would provide better aerosolisation properties to the formulations. Small biocompatible molecules such as amino-acids or amino-acid derivatives with hydrophobic properties could be tested. As an example, trileucine has recently been shown to inhibit various protein degradation pathways during spray-drying due to surface-active properties and due to the formation of amorphous structures with high glass transition temperature. It also provides superior aerosol performance by modification of the particle morphology and by providing a hydrophobic surface to the particles. In the future development of formulations, implementation of statistically-assisted design of experiment should also be envisaged to help in defining the formulation parameters of most influence, and achieve good time-quality balance.

The formulation strategy presented in this work could be of interest for the future development of other inhaled proteins for local or systemic applications. Developments for systemic applications should be partly dependent on the acceptance or refusal of the Afrezza® inhaled insulin product by the FDA. In case of positive outcome, other molecules could be launched such as calcitonine, GH, PTH, FSH, EPO, and TSH, for which the experimental data on inhaled alternatives are often promising. However, it is to be noted that there are only little data regarding the long-term effects of these inhaled macromolecules and a commercial product of one of these molecules is therefore not expected before several years. On the other hand, several molecules against interleukin 4 and interleukin 13 are being developed for the treatment of asthma and seem particularly

promising (MAb fragments, soluble receptors and receptor antagonists). Finally, another potential application of inhaled proteins is vaccination. In comparison to parenteral vaccination, pulmonary delivery indeed provides ease of administration and has shown superior mucosal and systemic immunity. It could therefore be particularly useful in children and for mass vaccination of third-world populations by limiting the number of medical acts and avoiding the need of cold-chain storage.

VI. REFERENCES

Abdul-Fattah A.M., Kalonia D.S., Pikal M.J. 2007. The challenge of drying method selection for protein pharmaceuticals: product quality implications. *J. Pharm. Sci.* 96: 1886-1916.

Abra R.M., Mihalko P.J., Schreier H. 1990. The effect of lipid composition upon the encapsulation and in vitro leakage of metaprotenol sulfate from 0.2 mm diameter, extruded, multilamellar liposomes. *J. Controlled Release* 14: 71-78.

Adcock I.M., Caramori G., Chung K.F. 2008. New targets for drug development in asthma. *Lancet* 372: 1073-1087.

Adi H., Young P.M., Chan H.K., Stewart P., Agus H., Traini D. 2008. Cospray dried antibiotics for dry powder lung delivery. *J. Pharm. Sci.* 97: 3356-3366.

Adjei A.L., Ciu Y., Gupta P.K. 1996. Bioavailability and pharmacokinetics of inhaled drugs. In: Hickey A.J. (Ed), *Inhalation aerosols, Physical and biological basis for therapy.* vol. 94, Marcel Dekker, New York, NY, pp. 197-231.

Adler M., Unger M., Lee G. 2000. Surface composition of spray-dried particles of bovine serum albumin/trehalose/surfactant. *Pharm. Res.* 17: 863-870.

Agu R.U., Ugwoke M.I., Armand M., Kinget R., Verbeke N. 2001. The lung as a route for systemic delivery of therapeutic proteins and peptides. *Respir. Res.* 2: 198-209.

Alberti K.G., Zimmet P.Z. 1998. Definition, diagnosis and classification of diabetes mellitus and its complications. Part 1: diagnosis and classification of diabetes mellitus. *Diabet. Med.* 15: 539-553.

American Diabetes Association. 2011. Standards of medical care in diabetes. *Diabetes Care* 34(Suppl.1): S11-S61.

Andya J.D., Maa Y-F, Costantino H.R., Nguyen P-A, Dasovich N., Sweeney T.D., Hsu C.C., Shire S.J. 1999. The effect of formulation excipients on protein stability and aerosol performance of spray-dried powders of a recombinant humanized anti-IgE monoclonal antibody. *Pharm. Res.* 16(3): 350-358.

Angelo R., Rousseau K., Grant M, Bay A.L., Richardson P. 2009. Technosphere® Insulin: Defining the Role of Technosphere Particles at the Cellular Level. *J. Diabetes Sci. Technol.* 3(3): 545-554.

Antosova Z., Mackova M., Kral V., Macek T. 2009. Therapeutic application of peptides and proteins: parenteral forever? *Trends Biotech.* 27(11): 628-635.

Armstrong D.J., Elliott P.N.C., Ford J.L., Gadson D., McCarthy G.P., Rostron C., Worsley M.D. 1996. Poly-(D,L-lactic acid) microspheres incorporating histological dyes for intra-pulmonary histopathological investigations. *J. Pharm. Pharmacol.* 48: 258-262.

Arnolds S., Heise T. 2007. Inhaled insulin. *Best Pract. Res. Cl. En.* 21(4): 555-571.

Asthma, 2012. www.asthma.ca/images/adults/treatment/turbuhaler.gif. Retrieved 2012-04-05.

Bailey C.J., Barnett A.H. 2010. Inhaled insulin: new formulation, new trial, *Lancet* 375: 2199-2201.

Balda M.S., Matter K. 2007. Size-selective assessment of tight junction paracellular permeability using fluorescently labelled dextrans. Division of Cell Biology, UCL Institute of Ophthalmology, London, UK, Application Note 146.

Balwani G., Boyd B., Whatley J., Thippawong J., Morishige R., Okikawa J., Otulana B., Tamches E., Buclin T., Biollaz J., Spertini F., Gonda I. 2002. Evaluation of the AERx® system for the pulmonary delivery of recombinant human interferon ALFA-2b to healthy subjects, 29th Annual Meeting of the Controlled Release Society, Seoul, South Korea.

- Bard J., Faulkner L. 2000.** *Electrochemical Methods: Fundamentals and Applications*. John Wiley & Sons, New York, USA.
- Barnes P. J. 1997.** Current Therapies for Asthma, Promise and Limitations. *CHEST* 111(2): 175-265.
- Barnes P.J. 2003.** Theophylline: new perspectives for an old drug. *Am. J. Respir. Crit. Care Med.* 167(6): 813-8.
- Barnes P.J. 2006a.** Corticosteroids: the drugs to beat. *Eur. J. Pharmacol.* 533(1-3): 2-14.
- Barnes P.J. 2006b.** New therapies for asthma. *Trends Mol. Med.* 12: 515-20.
- Barth H.G., Boyes B.E., Jackson C. 1996.** Size Exclusion Chromatography. *Anal. Chem.* 68: 445R-466R.
- Bartow R.A., Brogden R.N. 1998.** Formoterol. An update of its pharmacological properties and therapeutic efficacy in the management of asthma. *Drugs* 55(2): 303-22.
- Bateman E.D., Boushey H.A., Bousquet J., Busse W.W., Clark T.J.H., Pauwels R.A., Pedersen S.E. 2004.** Can guideline-defined asthma control be achieved? The Gaining Optimal Asthma Control Study. *Am. J. Respir. Crit. Care Med.* 170: 836-44.
- Becker A., Bérubé D., Chad Z., Dolovich M., Ducharme F., D'Urzo T., Ernst P., Ferguson A., Gillespie C., Kapur S., Kovesi T., Lyttle B., Mazer B., Montgomery M., Pedersen S., Pianosi P., Reisman J.J., Sears M., Simons E., Spier S., Thivierge R., Watson W., Zimmerman B. 2005.** Canadian Pediatric Asthma Consensus Guidelines, 2003 (updated to December 2004): Pharmacotherapy — add-on therapies. *CMAJ* 173:537-538.
- Becker R.H.A., Sha S., Frick A.D., Fountaine R.J. 2006.** The effect of smoking cessation and subsequent resumption on absorption of inhaled insulin. *Diabetes Care* 29: 277-282.
- Bellary S., Barnett A. H. 2006.** Inhaled insulin: new technology, new possibilities. *Int. J. Clin. Pract.* 60(6) 728-734.
- Berger M. 1985.** Pharmacokinetics of subcutaneously injected insulin: the miscibility of short and long-acting insulin preparations. In: Crepaldi G., Tiengo A., Baggio G. (Eds.), *Diabetes, obesity and hyperlipidemias*, Elsevier, Amsterdam, The Netherlands, pp. 427-431.
- Bhatnagar B.S., Bogner R.H., Pikal M.J. 2007.** Protein stability during freezing: separation of stresses and mechanisms of protein stabilization. *Pharm. Dev. Technol.* 12: 505-523.
- Biotech, 2011.** http://www.biotech-weblog.com/50226711/inhalable_insulin_exubera_approved_by_fda.php. Retrieved 2011-10-11.
- Bissinger R.L., Carlson C.A. 2006.** Surfactant. *NAINR* 6 (2): 87-93.
- Bitonti A.J., Dumont J.A., Low S.C., Peters R.T., Kropp K.E., Palombella V.J., Stattel J.M., Lu Y., Tan C.A., Song J.J., Garcia A.M., Simister N.E., Spiekermann G.M., Lencer W.I., Blumberg R.S. 2004.** Pulmonary delivery of an erythropoietin Fc fusion protein in non-human primates through an immunoglobulin transport pathway. *Proc Natl Acad Sci USA* 101: 9763-9768.
- Bitonti A.J., Dumont J.A. 2006.** Pulmonary administration of therapeutic proteins using an immunoglobulin transport pathway. *Adv. Drug Deliv. Rev.* 58(9-10): 1106-1118.
- Bjermer L., Diamant Z. 2004.** Current and emerging nonsteroidal anti-inflammatory therapies targeting specific mechanisms in asthma and allergy. *Treat. Respir. Med.* 3(4): 235-46.
- Blair J., Mao L., Hodgers E. 2000.** *Modification of the Pulmonary Absorption of Cyclosporin using SoliDose Technology*. Serentec Press, Raleigh, NC.

Borgström L. 2001. On the use of dry powder inhalers in situations perceived as constrained. *J. Aerosol Med.* 14: 281-287.

Borish L.C., Nelson H.S., Lanz M.J., Claussen L., Whitmore J.B., Agosti J.M., Garrison L. 1999. Interleukin-4 receptor in moderate atopic asthma, a phase I/II randomized, placebo-controlled trial. *Am. J. Respir. Crit. Care Med.* 160: 1816-1823.

Bosquillon C., Rouxhet P.G., Ahimou F., Simon D., Culot C., Pr at V., Vanbever R. 2004. Aerosolization properties, surface composition and physical state of spray-dried protein powders. *J. Control. Release* 99: 357-367.

Boss A. H. 2006. Technospheres Insulin as effective as sc rapid acting insulin analogue in providing glycemic control in both patients with type 1 and type 2 diabetes. Presented at the Sixth Annual Diabetes Technology Meeting, November 2-4, 2006, Atlanta, GA.

Boss A.H., Yu W., Ellerman K. 2008. Prandial insulin: is inhaled enough? *Drug Dev. Res.* 69: 138-142.

Bousquet J., Aubier M., Sastre J., Izquierdo J.L., Adler L.M., Hofbauer P., Rost K.D., Harnest U., Kroemer B., Albrecht A., Bredenbr oker D. 2006. Comparison of roflumilast, an oral anti-inflammatory, with beclomethasone dipropionate in the treatment of persistent asthma. *Allergy* 61(1): 72-78.

Brambilla G., Cocconi D., Armani A., Smith S., Lye E., Burge S. 2006. Designing a novel dry powder inhaler: the NEXTTM DPI (Part 1). In: Dalby et al. (Eds.), *Respiratory Drug Delivery X*, Davis Horwood International, UK, pp. 553-555.

Brange J. 1987. Galenics of insulin: the physico-chemical and pharmaceutical aspects of insulin and insulin preparations. Springer-Verlag, Berlin.

Brange J., Owens D.R., Kang S., Volund A. 1990. Monomeric insulins and their experimental and clinical implications. *Diabetes Care* 13: 923-954.

Breen E.D., Curley J.G., Overcashier D.E., Hsu C.C., Shire S.J. 2001. Effect of moisture on the stability of a lyophilized humanized monoclonal antibody formulation. *Pharm. Res.* 18: 1345-1353.

British Thoracic and Tuberculosis Association. 1975. Inhaled corticosteroids compared with oral prednisone in patients starting long-term corticosteroid therapy for asthma. *Lancet* 2(7933): 469-73.

Brown B.A.S., Rasmussen J.A., Becker D.P., Friend D.R. 2004. A piezo-electric inhaler for local and systemic application. *Drug Deliv. Technol.* 4(8): 90-93.

Brunner G.A., Balent B., Ellmerer M., Schaupp L., Siebenhofer A., Jendle J.H., Okikawa J., Pieber T.R. 2001. Dose-response relation of liquid aerosol inhaled insulin in type I diabetic patients. *Diabetologia* 44: 305-308.

Buchi. 2008. www.buchi.com. Retrieved in 2008.

Buclin T. 2009. Pharmacology. In: *Clinical trials handbook*. Shayne Cox Gad (Ed.), John Wiley, New Jersey, pp. 985-986.

Bundgaard M. 1984. The three-dimensional organization of tight junctions in a capillary endothelium revealed by serial-section electron microscopy. *J. Ultrastruct. Res.* 88: 1-17.

Bur M., Huwer H., Lehr C-M, Hagen N., Guldbrandt M., Kim K-J, Ehrhardt C. 2006. Assessment of transport rates of proteins and peptides across primary human alveolar epithelial cell monolayers. *Eur. J. Pharm. Sci.* 28: 196-203.

- Bush L., Webb C., Bartlett L., Burnett B. 1998.** The formulation of recombinant factor IX: stability, robustness, and convenience. *Semin. Hematol.* 35: 18-21.
- Byron P.R. 1986.** Prediction of drug residence times in regions of the human respiratory tract following aerosol inhalation. *J. Pharm. Sci.* 75: 433-438.
- Cal K., Sollohub K. 2010.** Spray Drying Technique. I: Hardware and Process Parameters. *J. Pharm. Sci.* 99(2): 575-86.
- Caporal-Gautier J., Nivet J.M., Algranti P., Guilloteau M., Histe M., Lallier M., N'Guyen-Huu J.J., Russotto R. 1992.** Guide de validation analytique – Rapport d'une commission SFSTP, STP Pharma. *Pract.* 2: 205-226.
- Caramori G., Groneberg D., Ito K., Casolari P., Adcock I.M., Papi A. 2008.** New drugs targeting Th2 lymphocytes in asthma. *J. Occup. Med. Toxicol.* 3(Suppl 1): S6.
- Carden D.L., Alexander J.S., George R.B. 1998.** The pathophysiology of the acute respiratory distress syndrome, *Pathophysiology* 5: 1-13.
- Carvalho T.C., Peters J.I., Williams R.O. 2011.** Influence of particle size on regional lung deposition – What evidence is there? *Int. J. Pharm.* 406: 1-10.
- Cassidy J.P., Amin N., Marino M., Gotfried M., Meyer T., Sommerer K., Baughman R.A. 2011.** Insulin lung deposition and clearance following Technosphere® insulin inhalation powder administration. *Pharm. Res.* 28(9): 2157-64.
- Cazzola M., Matera M.G., Lotvall J. 2005.** Ultra long-acting beta2-agonists in development for asthma and chronic obstructive pulmonary disease. *Expert Opin Invest Drugs* 14(7): 775-83.
- Cazzola M., Matera M.G. 2008.** Novel long-acting bronchodilators for COPD and asthma. *Br J Pharmacol.* 155(3): 291-299.
- Cerqueira M.F., Ferreira J.A., Adriaenssens G.J. 2000.** Structural studies and influence of the structure on the electrical and optical properties of microcrystalline silicon thin films produced by RF sputtering. *Thin Solid Films* 370: 128-136.
- Chan H.K., Clark A., Gonda I., Mumenthaler M., Hsu C. 1997.** Spray dried powders and powder blends of recombinant human deoxyribonuclease (rhDNase) for aerosol delivery. *Pharm. Res.* 14: 431 -7.
- Chan H.K. 2002.** Radiolabeling of pharmaceutical aerosols and γ -scintigraphic imaging for lung deposition. In: *Encyclopedia of Pharmaceutical Technology*, Marcel Dekker, New York, pp. 2365-2374.
- Chan H-K., Clark A.R., Feeley J.C., Kuo M-C, Lehrman R., Pikal-Cleland K., Miller D.P., Vehring R., Lechuga-Ballesteros D. 2004.** Physical Stability of Salmon Calcitonin Spray-Dried Powders for Inhalation. *J. Pharm. Sci.* 93(3): 792-804.
- Chang B.S., Kendrick B.S., Carpenter J.F. 1996a.** Surface-induced denaturation of proteins during freezing and its inhibition by surfactants. *J. Pharm. Sci.* 85: 1325-1330.
- Chang B.S., Beauvais R.M., Dong A., Carpenter J.F. 1996b.** Physical factors affecting the storage stability of freeze-dried interleukin-1 receptor antagonist: glass transition and protein conformation. *Arch. Biochem. Biophys.* 331: 249-258.
- Chang B.S., Reeder G., Carpenter J.F. 1996c.** Development of a stable freeze-dried formulation of recombinant human interleukin-1 receptor antagonist. *Pharm. Res.* 13: 243-249.
- Chang L., Pikal M.J. 2009.** Mechanisms of Protein Stabilization in the Solid State. *J. Pharm. Sci.* 98(9): 2886-908.

- Chelius D., Rehder D.S., Bondarenko P.V. 2005.** Identification and characterization of deamidation sites in the conserved regions of human immunoglobulin gamma antibodies. *Anal. Chem.* 77: 6004-6011.
- Chen B., Bautista R., Yu K., Zapata G.A., Mulkerrin M.G., Chamow S.M. 2003.** Influence of histidine on the stability and physical properties of a fully human antibody in aqueous and solid forms. *Pharm Res* 20: 1952-1960.
- Cheung B.M., Ong K.L., Cherny S.S., Sham P.C., Tso A.W., Lam K.S. 2009.** Diabetes prevalence and therapeutic target achievement in the United States, 1999 to 2006. *Am. J. Med.* 122: 443-453.
- Chew N.Y.K., Tang P., Chan H-K, Raper J.A. 2005.** How much particle surface corrugation is sufficient to improve aerosol performance of powders? *Pharm. Res.* 22(1): 148-152.
- Chimote G., Banerjee R. 2010.** In Vitro Evaluation of Inhalable Isoniazid-Loaded Surfactant Liposomes as an Adjunct Therapy in Pulmonary Tuberculosis. *J. Biomed. Mater. Res. B.* 94B(1): 1-10.
- Chono S., Fukuchi R., Seki T., Morimoto K. 2009.** Aerosolized liposomes with dipalmitoyl phosphatidylcholine enhance pulmonary insulin delivery. *J. Controlled Release* 137: 104-109.
- Chowdhury T.A., Mijovic C.H., Barnett A.H. 1999.** The aetiology of Type 1 diabetes. *Baillieres Best Pract Res Clin Endocrinol Metab.* 13(2): 181-195.
- Chrystyn H. 2007.** The Diskus TM : a review of its position among dry powder inhaler devices. *Int. J. Clin. Pract.* 61(6): 1022-1036.
- Chung F. K. 2006.** Phosphodiesterase inhibitors in airways disease. *Eur. J. Pharmacol.* 533(1-3): 110-7.
- Clark T.J. 1972.** Effect of beclomethasone dipropionate delivered by aerosol in patients with asthma. *Lancet* 1(7765): 1361-4.
- Clark A.R., Dasovich N., Gonda I., Chan H-K. 1996.** The balance between biochemical and physical stability for inhalation protein powders. rhDNase as an example. In: Darby R.N., Byron P.R., Farr S.J. (eds.), *Respiratory Drug Delivery V.* Interpharm Press, Buffalo Grove, pp. 167-174.
- Clark A., Kuo M.C., Newman S., Hirst P., Pitcairn G., Pickford M. 2008.** A comparison of the pulmonary bioavailability of powder and liquid aerosol formulations of salmon calcitonin. *Pharm. Res.* 25: 1583-1590.
- Cleland J.L., Lam X., Kendrick B., Yang J., Yang T-H, Overcashier D., Brooks D., Hsu C., Carpenter J.F. 2001.** A specific molar ratio of stabilizer to protein is required for storage stability of a lyophilized monoclonal antibody. *J Pharm Sci* 90: 310-321.
- Coates M.S., Fletcher D.F., Chan H.K., Raper J.A. 2004.** Effect of design on the performance of a dry powder inhaler using computational fluid dynamics. Part 1: Grid structure and mouthpiece length. *J. Pharm. Sci.* 93(11): 2863-2876.
- Codrons V., Vanderbist F., Verbeeck R.K., Arras M., Lison D., Pr at V., Vanbever R. 2003.** Systemic delivery of parathyroid hormone (1-34) using inhalation dry powders in rats. *J. Pharm. Sci.* 92: 938-950.
- Colandene J.D., Maldonado L.M., Creagh A.T., Vrettos J.S., Goad K.G., Spitznagel T.M. 2007.** Lyophilization Cycle Development for a High-Concentration Monoclonal Antibody Formulation Lacking a Crystalline Bulking Agent. *J. Pharm. Sci.* 96(6): 1598-1608.
- Colice G.L. 2011.** Emerging Therapeutic Options for Asthma. *J. Manag. Care.* 17: S82-S89.
- Condos R., Hull F.P., Schluger N.W., Rom W.N., Smaldone G.C. 2004.** Regional deposition of aerosolized interferon- γ in pulmonary tuberculosis. *Chest* 125: 2146-2155.

- Considine T., Patel H.A., Singh H., Creamer L.K. 2007.** Influence of binding conjugated linoleic acid and myristic acid on the heat- and high-pressure-induced unfolding and aggregation of β -lactoglobulin B. *Food Chem.* 102: 1270-1280.
- Cook R.O., Pannu R.K., Kellaway I.W. 2005.** Novel sustained release microspheres for pulmonary drug delivery. *J. Controlled Release* 104: 79-90.
- Copley Scientific. 2010.** Quality Solutions for inhaler testing. 2010 Edition. <http://www.copleyscientific.co.uk/documents/ww/Inhaler%20Brochure%202010%20%28High%20Res%29.pdf>. Retrieved 2011-08-21.
- Corren J., Lemanske R.F., Hanania N.A., Korenblat P.E., Parsey M.V., Arron J.R., Harris J.M., Scheerens H., Wu L.C., Su Z., Mosesova S., Eisner M.D., Bohen S.P., Matthews J.G. 2011.** Lebrikizumab Treatment in Adults with Asthma. *N. Engl. J. Med.* 365: 1088-1098.
- Costantino H.R., Griebenow K., Mishra P., Langer R., Klibanov A.M. 1995a.** Fourier-transform infrared spectroscopic investigation of protein stability in the lyophilized form. *Biochim. Biophys. Acta* 1253: 69-74.
- Costantino H.R., Langer R., Klibanov A.M. 1995b.** Aggregation of a lyophilized pharmaceutical protein, recombinant human albumin: effect of moisture and stabilization by excipients. *Biotechnology* 13: 493-496.
- Costantino H.R., Schwendeman S.P., Griebenow K., Klibanov A.M., Langer R. 1996.** The secondary structure and aggregation of lyophilized tetanus toxoid. *J. Pharm. Sci.* 85: 1290-1293.
- Costantino H.R., Andya J.D., Nguyen P.A., Dasovich N., Sweeney T.D., Shire S.J., Hsu C.C., Maa Y.F. 1998.** Effect of mannitol crystallization on the stability and aerosol performance of a spray dried pharmaceutical protein, recombinant humanized anti-IgE monoclonal antibody. *J. Pharm. Sci.* 87: 1406-1411.
- Courrier H.M., Butz N., Vandame T.F. 2002.** Pulmonary Drug Delivery Systems: Recent Developments and Prospects. *Crit. Rev. Ther. Drug. Carrier. Syst.* 19: 425-498.
- Cristol J.P., Balint B., Canaud B., Daurés M.F. 2007.** Sodium determination in biological fluids. *Nephrol. Ther.* 3(Suppl 2): S104-111.
- Crowder T.M., Louey M.D., Sethuraman V.V., Smyth H.D.C., Hickey A.J. 2001.** An odyssey in inhaler formulations and design. *Pharm. Technol.* 25(7): 99-113.
- Daniher D.I., Zhu J. 2008.** Dry powder platform for pulmonary drug delivery. *Particuology* 6: 225-238.
- Daugherty A.L., Mrsny R.J. 2006.** Formulation and delivery issues for monoclonal antibody therapeutics. *Adv. Drug Deliver. Rev.* 58: 686-706.
- Davis S.N., Thompson C.J., Brown M.D., Home P.D., Alberti K.G. 1991.** A comparison of the pharmacokinetics and metabolic effects of human regular and NPH insulin mixtures. *Diabetes Res Clin Pract* 13: 107-117.
- de Boer A.H., Hagedoorn P., Gjaltema D., Goede J., Frijlink H.W. 2003.** Air classifier technology (ACT) in dry powder inhalation. Part 1. Introduction of a novel force distribution concept (FDC) explaining the performance of a basic air classifier on adhesive mixtures. *Int. J. Pharm.* 260: 187-200.
- de Boer A.H., Chan H.K., Price R. 2011.** A critical view on lactose-based drug formulation and device studies for dry powder inhalation: Which are relevant and what interactions to expect? *Adv. Drug Deliv. Rev.* doi:10.1016/j.addr.2011.04.004.
- Defronzo R.A., Bergenstal R.M., Cefalu W.T., Pullman J., Lerman S., Bode B.W., Phillips L.S. 2005.** Efficacy of inhaled insulin in patients with type 2 diabetes not controlled with diet and exercise: a 12-week, randomized, comparative trial. *Diabetes Care* 28: 1922-8.

- Defetos L.J., Nolan J.J., Seely B.L., Clopton P.L., Cote G.J., Whitham C.L., Florek L.J., Christensen T.A., Hill M.R. 1997.** Intrapulmonary drug delivery of salmon calcitonin. *Calcif. Tissue Int.* 61: 345-347.
- Dellamary L.A., Tarara T.E., Smith D.J., Woelk C.H., Adractus A., Costello M.L., Gill H., Weers, J.G. 2000.** Hollow porous particles in metered dose inhalers. *Pharm. Res.* 17: 168-174.
- DeLong M., Wright J., Dawson M., Meyer T., Sommerer K., Dunbar C. 2005.** Dose delivery characteristics of the AIR® pulmonary delivery system over a range of inspiratory flow rates. *J. Aerosol. Med.* 18(4): 452-459.
- Del Vecchio P., Graziano G., Granata V., Barone G., Mandrich L., Rossi M., Manco G. 2002.** Denaturing action of urea and guanidine hydrochloride towards two thermophilic esterases. *Biochem. J.* 367: 857-863.
- Deng W., Klemic J.F., Li X., Reed M.A., Gomez A. 2006.** Increase of electrospray throughput using multiplexed microfabricated sources for the scalable generation of monodisperse droplets. *Aerosol Science* 37: 696-714.
- Desai T.R., Hancock R.E.W., Finlay W.H. 2003.** Delivery of liposomes in dry powder form: aerodynamic dispersion properties. *Eur. J. Pharm. Sci.* 20: 559-567.
- Deshpande D., Toledo-Velasquez D., Wang L.Y., Malanga C.J., Ma J.K.H., Rojanasakul Y. 1994.** Receptor mediated peptide delivery in pulmonary epithelial monolayers. *Pharm. Res.* 11(8): 1121-1126.
- de Swart R.L., LiCalsi C., Quirk A.V., van Amerongen G., Nodelman V., Alcock R., Yüksel S., Ward G.H., Hardy J.G., Vos H., Witham C.L., Grainger C.I., Kuiken T., Greenspan B.J., Gard T.G., Osterhaus A.D.M.E. 2007.** Measles vaccination of macaques by dry powder inhalation. *Vaccine* 25: 1183-1190.
- Diamant Z., Sampson A.P. 1999.** Anti-inflammatory mechanisms of leukotriene modulators. *Clin. Exp. Allergy* 29(11): 1449-53.
- Diamant Z., Boot J.D., Virchow J.C. 2007.** Summing up 100 years of asthma. *Resp. Med.* 101: 378-388.
- Dolovich M. 1993.** Lung Dose, Distribution, and Clinical Response to Therapeutic Aerosols. *Aerosol Sci. Tech.* 18(3): 230-240.
- Dolovich M.B., Dhand R. 2011.** Aerosol drug delivery: developments in device design and clinical use. *Lancet* 377: 1032-45.
- Duddu S.P., Sisk S.A., Walter Y.H., Tarara T.E., Trimble K.R., Clark A.R., Eldon M.A., Elton R.C., Pickford M., Hirst P.H., Newman S.P., Weers J.G. 2002.** Improved lung delivery from a passive dry powder inhaler using an Engineered PulmoSphere powder. *Pharm. Res.* 19(5): 689-695.
- Dumont J.A., Bitonti A.J., Clark D., Evans S., Pickford M., Newman S.P. 2005.** Delivery of an Erythropoietin-Fc Fusion Protein by Inhalation in Humans through an Immunoglobulin Transport Pathway. *J. Aerosol Med.* 18(3): 294-303.
- Dunbar C.A., Hickey A.J., Holzner P. 1998.** Dispersion and characterization of pharmaceutical dry powder aerosols. *Kona* 16: 7-45.
- Dunbar C.A., Scheuch G., Sommerer K., DeLong M., Verma A., Batycky R. 2002.** In vitro and in vivo dose delivery characteristics of large porous particles for inhalation. *Int. J. Pharm.* 245: 179-189.
- Dunne M., Corrigan O.I., Ramtoola Z. 2000.** Influence of particle size and dissolution conditions on the degradation properties of polylactide-co-glycolide particles. *Biomaterials* 21: 1659-1668.
- Edwards D.A., Hanes J., Caponetti G., Hrkach J., Ben-Jebria A., Eskew M-L, Mintzes J., Deaver D., Lotan N., Langer R. 1997.** Large porous particles for pulmonary delivery. *Science* 276: 1868-1871.

- El-Baseir M.M., Kellaway I.W. 1998.** Poly(l-lactic acid) microspheres for pulmonary drug delivery: release kinetics and aerosolisation studies. *Int. J. Pharm.* 175: 135-145.
- Elhissi A.M.A., Faizi M., Naji W.F., Gill H.S., Taylor K.M.G. 2007.** Physical stability and aerosol properties of liposomes delivered using an air-jet nebulizer and a novel micropump device with large mesh apertures. *Int. J. Pharm.* 334: 62-70.
- Elias J.A., Zhu Z., Chupp G., Homer R.J. 1999.** Airway remodeling in asthma. *J. Clin. Invest.* 104: 1001-1006.
- Endo K., Amikawa S., Matsumoto A., Sahashi N., Onoue S. 2005.** Erythritol-based dry powder of glucagon for pulmonary administration. *Int. J. Pharm.* 290: 63-71.
- Essayan D.M. 2001.** Cyclic nucleotide phosphodiesterases. *J. Allergy Clin. Immunol.* 108: 671-680.
- Exubera SPC. 2007.** Retrieved 2007-12-20. http://www.ema.europa.eu/docs/en_GB/document_library/EPAR_-_Product_Information/human/000588/WC500054704.pdf
- Fahy J.V., Cockcroft D.W., Boulet L-P, Wong H.H., Deschesnes F., Davis E.E., Ruppel J., Su J.Q., Adelman D.C. 1999.** Effect of Aerosolized Anti-IgE (E25) on Airway Responses to Inhaled Allergen in Asthmatic Subjects. *Am. J. Respir. Crit. Care Med.* 160: 1023-1027.
- Fatouros A., Osterberg T., Mikaelsson M. 1997.** Recombinant factor VIII SQ—influence of oxygen, metal ions, pH and ionic strength on its stability in aqueous solution. *Int. J. Pharm.* 155: 121-131.
- Fink A.L. 1998.** Protein aggregation: folding aggregates, inclusion bodies and amyloid. *Fold Des.* 3: R9-R23.
- Fischel-Ghodsian F., Brown L., Mathiowitz E., Brandenburg D., Langer R. 1988.** Enzymatically controlled drug delivery. *Proc. Natl. Acad. Sci.* 85: 2403-2406.
- Fleming F.S. 2007.** Flexible, smart and low cost: the Microdose DPI, a true platform inhaler. *ONdrugDelivery*. <http://www.mdtx.com/mdtx/wp-content/uploads/pdf/MicroDoseDPIDrugDeliveryAug2007.pdf>. Retrieved 2011-09-10.
- Folkesson H.G., Westrom B.R., Pierzynowski S.G., Svendsen J., Karlsson B.W. 1993.** Lung to blood passage of albumin and a nonapeptide after intratracheal instillation in the young developing pig. *Acta Physiol. Scand.* 147: 173-178.
- Franks F. 1998.** Freeze-drying of bioproducts: putting principles into practice. *Eur. J. Pharm. Biopharm.* 45: 221-229.
- Fransson J.R. 1997.** Oxidation of human insulinlike growth factor I in formulation studies. 3. Factorial experiments of the effects of ferric ions, EDTA, and visible light on methionine oxidation and covalent aggregation in aqueous solution. *J Pharm Sci* 86: 1046-1050.
- Fukuda Y., Tsuji T., Fujita T., Yamamoto A., Muranishi S. 1995.** Susceptibility of insulin to proteolysis in rat lung homogenate and its protection from proteolysis by various protease inhibitors. *Biol. Pharm. Bull.* 18: 891-894.
- Garcia-Contreras L., Sarubbi D., Flanders E., Smart J., Newcomer C., Hicke A.J. 2001.** Immediate and short-term cellular and biochemical responses to pulmonary single-dose studies of insulin and H-MAP. *Pharm. Res.* 18: 1685-1693.
- Gelfand R.A., Schwartz S.L., Horton M., Law C.G., Pun E.F. 2000.** Pharmacological reproducibility of inhaled human insulin in patients with type 2 diabetes mellitus. *Diabetologia* 43: 773.
- Gill S.C., von Hippel P.H. 1989.** Calculation of Protein Extinction Coefficients from Amino Acid Sequence Data. *Anal. Biochem.* 182: 319-326.

Global Initiative for Asthma, 2010. GINA Report, Global Strategy for Asthma Management and Prevention. Available from: <http://www.ginasthma.org/>.

Glazer A.N., Smith E.L. 1961. Studies on the Ultraviolet Difference Spectra of Proteins and Polypeptides. *JBC* 236(11): 2942-2947.

Goldstein J. 2003. Scanning electron microscopy and x-ray microanalysis, Volume 1. Springer Verlag, Berlin, Germany.

Gomez A. 2002. The electrospray and its application to targeted drug inhalation. *Respir Care* 47(12): 1419-1433.

Gonda I. 2004. Targeting by deposition. In: Hickey A.J. (Ed.), *Pharmaceutical Inhalation Aerosol Technology*. Marcel Dekker, New York, NY, pp. 65-88.

Gordon G.S., Moses A.C., Silver R.D., Flier J.S., Carey M.C. 1985. Nasal absorption of insulin: enhancement by hydrophobic bile salts. *Proc. Natl. Acad. Sci.* 82: 7419-7423.

Grgic B., Martin A.R., Finlay W.H. 2006. The effect of unsteady flow rate increase on in vitro mouth-throat deposition of inhaled boluses. *J. Aerosol Sci.* 37: 1222-1233.

Griese M., von Bredow C., Birrer P., Schams A. 2001. Inhalation of $\alpha(1)$ -Protease Inhibitor in Cystic Fibrosis does not affect Surfactant Convertase and Surface Activity. *Pulm. Pharmacol. Ther.* 14: 461-467.

Griffiths H.R. 2000. Antioxidants and protein oxidation. *Free Radic. Res.* 33 (Suppl.): S47-S58.

Groneberg D.A., Rabe K.F., Fischer A. 2006. Novel concepts of neuropeptide-based drug therapy: vasoactive intestinal polypeptide and its receptors. *Eur. J. Pharmacol.* 533: 182-194.

Gross N.J. 2006. Anticholinergic agents in asthma and COPD. *Eur. J. Pharmacol.* 533(1-3): 36-9.

Guchardi R., Frei M., John E., Kaerger J.S. 2008. Influence of fine lactose and magnesium stearate on low dose dry powder inhaler formulations. *Int. J. Pharm.* 348: 10-17.

Guillaume C., Delepine P., Mercier B., Gobin E., Leroy J.P., Morin V., Ferec C. 2000. Phosphonocationic lipids in protein delivery to mice lungs. *J. Pharm. Sci.* 89: 639-645.

Guntur V.P., Dhand R. 2007. Inhaled Insulin: Extending the Horizons of Inhalation Therapy. *Resp. Care* 52(7): 911-922.

Hallas-Möller K., Petersen K., Schlichtkrull J. 1952. Crystalline and amorphous insulin-zinc compounds with prolonged action. *Science* 116: 394-396.

Halme M., Maasilta P., Mattson K., Cantell K. 1994. Pharmacokinetics and toxicity of inhaled human natural interferon-beta in patients with lung cancer. *Respiration* 61: 105-107.

Haney S., Hancox R.J. 2005. Rapid onset of tolerance to beta-agonist bronchodilation. *Respir. Med.* 99(5): 566-71.

Harinarayan C., Skidmore K., Kao Y., Zydney A.L., van Reis R. 2009. Small molecule clearance in ultrafiltration/diafiltration in relation to protein interactions: Study of citrate binding to a Fab. *Biotechnol. Bioeng.* 102(6): 1718-22.

Harper N.J., Gray S., De Groot J., Parker J.M., Sadrzadeh N., Schuler C., Schumacher J.D., Seshadri S., Smith A.E., Steeno G.S., Stevenson C.L., Taniere R., Wang M, Bennett D.B. 2007. The design and performance of the exubera pulmonary insulin delivery system. *Diabetes Technol. Ther.* 9(s1): S16-S27.

Harville D.A. 1977. Maximum likelihood approaches to variance component estimation and to related problems. *JASA* 72(358): 320-338.

Haynes A., Shaik M.S., Krapup H., Singh M. 2004. Evaluation of the Malvern Spraytec® with inhalation cell for the measurement of particle size distribution from metered dose inhalers. *J. Pharm. Sci.* 93(2): 349-363.

Hecq J. 2006. Development, characterization and evaluation of crystalline nanoparticles for enhancing the solubility, the dissolution rate and the oral bioavailability of poorly water-soluble drugs. Thesis presented at Université Libre de Bruxelles, Bruxelles, Belgium.

Heinemann L., Traut T., Heise T. 1997. Time-action profile of inhaled insulin. *Diabet. Med.* 14: 63-72.

Heinemann L., Klappoth W., Rave H., Hompesch B., Linkeschowa R., Heise T. 2000. Intra-individual variability of the metabolic effect of inhaled insulin together with an absorption enhancer. *Diabetes Care* 23: 1343-1347.

Heinemann L., Heise T. 2004. Current status of the development of inhaled insulin. *Br. J. Diabetes Vasc. Dis.* 4: 295-301.

Heinemann L. 2004. Influences on time-action profiles. In: *Time-action Profiles of Insulin Preparations.* Kirchheim (eds), Mainz, Germany, pp. 85-105.

Hendeles L., Asmus M., Chesrown S. 2004. Evaluation of cytokine modulators for asthma. *Paediatr. Respir. Rev.* 5(Suppl. A): S107-S112.

Henry R.R., Mudaliar S.R.D., Howland W.C., Chu N., Kim D., An B., Reinhardt R.R. 2003. Inhaled insulin using the AERx insulin diabetes management system in healthy and asthmatic subjects. *Diabetes Care* 26: 764-769.

Hersey S.J., Jackson R.T. 1987. Effect of bile salts on nasal permeability in vitro. *J. Pharm. Sci.* 76: 876-879.

Hess D., Fisher D., Williams P., Pooler S., Kacmarek R.M. 1996. Medication nebulizer performance: Effects of diluent volume, nebulizer flow, and nebulizer brand. *Chest* 110: 498-505.

Himmelmann A., Jendle J., Mellen A., Petersen A.H., Dahl U.L., Wollmer P. 2003. The impact of smoking on inhaled insulin. *Diabetes Care* 26: 677-82.

Hinds W.C. 1999. *Aerosol technology: properties, behavior, and measurement of airborne particles*, 2nd edition. John Wiley & Sons, New York, USA.

Hodges J.L., Lehmann E.L. 1963. Estimation of location based on ranks. *Ann. Math. Statist.* 34: 598-611.

Høiby N., Ciofu O., Bjarnsholt T. 2010. *Pseudomonas aeruginosa* biofilms in cystic fibrosis. *Future Microbiol.* 25(11): 1663-1674.

Holgate S.T., Davies D.E., Lackie P.M., Wilson S.J., Puddicombe S.M., Lordan J.L. 2000. Epithelial-mesenchymal interactions in the pathogenesis of asthma. *J Allergy Clin Immunol.* 105: 193-204.

Holgate S.T., Buhl R., Bousquet J., Smith N., Panahloo Z., Jimenez P. 2009. The use of omalizumab in the treatment of severe allergic asthma: A clinical experience update. *Resp. Med.* 103: 1098-113.

Hollander P.A., Blonde L., Rowe R., Mehta A.E., Milburn J.L., Hershon K.S., Chiasson J.L., Levin S.R. 2004. Efficacy and safety of inhaled insulin (exubera) compared with subcutaneous insulin therapy in patients with type 2 diabetes: results of a 6-month, randomized, comparative trial. *Diabetes Care* 27: 2356-62.

Hora M.S., Rana R.K., Smith F.W. 1992a. Lyophilized formulations of recombinant tumor necrosis factor. *Pharm. Res.* 9: 33-36.

- Hora M.S., Rana R.K., Wilcox C.L., Katre N.V., Hirtzer P., Wolfe S.N., Thomson J.W. 1992b.** Development of a lyophilized formulation of interleukin-2. *Dev. Biol. Stand.* 74: 295-303.
- Hsu C.C., Ward A.C., Pearlman R., Nguyen H.M., Yeung D.A., Curley J.G. 1991.** Determining the optimum residual moisture in lyophilized protein pharmaceuticals. *Dev. Biol. Stand.* 74: 255-271.
- Huang L., Lu J., Wroblewski V.J., Beals J.M., Riggin R.M. 2005.** In Vivo Deamidation Characterization of Monoclonal Antibody by LC/MS/MS. *Anal. Chem.* 77: 1432-1439.
- Huang W-H, Yang Z-J, Wu H., Wong Y-F, Zhao Z-Z, Liu L. 2010.** Development of Liposomal Salbutamol Sulfate Dry Powder Inhaler Formulation. *Biol. Pharm. Bull.* 33(3): 512-517.
- Huff T., Hannappel E. 1997.** Oxidation and reduction of thymosin β 4 and its influence on the interaction with G-actin studied by reverse-phase HPLC and post-column derivatization with fluorescamine. *Anal. Chim. Acta* 352(1-3): 249-255.
- Huland E., Heinzer H., Huland H., Yung R. 2000.** Overview of interleukin-2 inhalation therapy. *Cancer J. Sci. Am.* 6: S104-S112.
- Huppertz T., Kelly A.L., Fox P.F. 2006.** High pressure-induced changes in ovine milk. 2: Effects on casein micelles and whey proteins. *Milchwissenschaft* 61: 394-397.
- Hussain A., Arnold J.J., Khan M.A., Ahsan F. 2004.** Absorption enhancers in pulmonary protein delivery. *J. Controlled Release* 94: 15-24.
- Ikehata M., Yumoto R., Kato Y., Nagai J., Takano M. 2009.** Mechanism of insulin uptake in rat alveolar type II and type I-like epithelial cells. *Biol Pharm Bull.* 32: 1765-1769.
- Irvin C.G. 2009.** Pulmonary Physiology. In: Barnes P.J., Drazen J., Rennand S.I., Thomson N.C. (Eds.). *Asthma and COPD: Basics Mechanisms and Clinical Management*, 2nd Ed. Elsevier, CA, USA, pp. 55-69.
- Islam N., Gladki E. 2008.** Dry powder inhalers (DPIs) – a review of device reliability and innovation. *Int. J. Pharm.* 360 (1-2): 1-11.
- Iwase H., Kobayashi M., Nakajima M., Takatori T. 2001.** The ratio of insulin to C-peptide can be used to make a forensic diagnosis of exogenous insulin overdose. *Forensic Sci. Int.* 115(1-2): 123-127.
- Izutsu K., Yoshioka S., Terao T. 1994.** Effect of mannitol crystallinity on the stabilization of enzymes during freeze-drying. *Chem. Pharm. Bull.* 42: 5-8.
- Jackson L.D., Polygenis D., McIvor R.A., Worthington I. 1999.** Comparative efficacy and safety of inhaled corticosteroids in asthma. *Can. J. Clin. Pharmacol.* 6: 26-37.
- Jalalipour M., Gilani K., Tajerzadeh H., Najafabadi A. R., Barghi M. 2008.** Characterization and aerodynamic evaluation of spray dried recombinant human growth hormone using protein stabilizing agents. *Int. J. Pharm.* 352: 209-216.
- Janeway C.A., Travers P., Walport M., Shlomchik M. 2001.** *Immunobiology*, 5th ed. Garland Publishing, New York, USA.
- Jaspart S., Bertholet P., Piel G., Dogne J-M, Delattre L., Evrard B. 2007.** Solid lipid microparticles as a sustained release system for pulmonary drug delivery. *Eur. J. Pharm. Biopharm.* 65: 47-56.
- Ji Y., Liu C., Pei, Y-Y. 2007.** Artificial pulmonary surfactant as a carrier for intratracheally instilled insulin. *Acta Pharmacol. Sin.* 28(5): 744-750.

Johansson F., Hjertberg E., Eirefelt S., Tronde A., Bengtsson U.H. 2002. Mechanisms for absorption enhancement of inhaled insulin by sodium taurocholate. *Eur. J. Pharm. Sci.* 17: 63-71.

Johnson M. 1995. Salmeterol. *Med Res Rev* 15(3): 225-57.

Johnson K.A. 1997. Preparation of peptide and protein powders for inhalation. *Adv. Drug. Deliv. Rev.* 26: 3-15.

Jonas D., Van Scoyoc E., Gerrald K., Wines R., Amick H., Runge T., Triplette M. 2011. Drug class review: Newer diabetes medications, TZDs, and combinations. <http://derp.ohsu.edu/about/final-document-display.cfm> . Retrieved 2011-09-10

Junghanns J-U.A.H., Müller R.H. 2008. Nanocrystal technology, drug delivery and clinical applications. *Int. J. Nanomed.* 3(3): 295-309.

Katakam M., Banga A.K. 1995. Aggregation of insulin and its prevention by carbohydrate excipients. *PDA J. Pharm. Sci. Technol.*49: 160-165.

Kattwinkel J. 2005. Synthetic Surfactants: The Search Goes on. *Pediatrics* 115: 1075-1076.

Kawai K., Hagiwara T., Takai R., Suzuki T. 2005. Comparative Investigation by Two Analytical Approaches of Enthalpy Relaxation for Glassy Glucose, Sucrose, Maltose, and Trehalose. *Pharm. Res.* 22(3): 490-5.

Keck C.M., Müller R.H. 2006. Drug nanocrystals of poorly soluble drugs produced by high pressure homogenization. *Eur. J. Pharm. Biopharm.* 62(1): 3-16.

Kerwin B.A., Heller M.C., Levin S.H., Randolph T.W. 1998. Effects of Tween 80 and sucrose on acute short-term stability and long-term storage at -20 °C of a recombinant hemoglobin. *J. Pharm. Sci.* 87: 1062-1068.

Kim H., Park H., Lee J., Kim T.H., Lee E.S., Oh K.T., Lee K.C., Youn Y.S. 2011. Highly porous large poly(lactic-co-glycolic acid) microspheres adsorbed with palmityl-acylated exendin-4 as a long-acting inhalation system for treating diabetes. *Biomaterials* 32: 1685-1693.

Kipp J.E. 2004. The role of solid nanoparticle technology in the parenteral delivery of poorly water-soluble drugs. *Int. J. Pharm.* 295: 269-281.

Kirkham P., Rahman I. 2006. Oxidative stress in asthma and COPD: antioxidants as a therapeutic strategy. *Pharmacol. Ther.* 111: 476-94.

Knip M., Veijola R., Virtanen S. M., Hyoty H., Vaarala O., Akerblom H. K. 2005. Environmental Triggers and Determinants of Type 1 Diabetes. *Diabetes* 54: S125-S136.

Knip M., Siljander H. 2008. Autoimmune mechanisms in type 1 diabetes. *Autoimmun. Rev.* 7: 550-557.

Knip M. 2009. Diet, Gut, and Type 1 Diabetes: Role of Wheat-Derived Peptides? *Diabetes* 58: 1723-1724.

Kobayashi S., Konda S., Juni K. 1994. Study on pulmonary delivery of salmon calcitonin in rats: effects of protease inhibitors and absorption enhancers. *Pharm. Res.* 11: 1239-1243.

Kobayashi S., Konda S., Juni K. 1996. Pulmonary delivery of salmon calcitonin dry powders containing absorption enhancers in rats. *Pharm. Res.* 13: 80-83.

Koh W.J., Kwon O.J., Suh G.Y., Chung M.P., Kim H., Lee N.Y., Kim T.S., Lee K.S. 2004. Six-month therapy with aerosolized interferon- γ for refractory multidrug-resistant pulmonary tuberculosis. *J. Korean Med. Sci.* 19: 167-171.

- Kohler D. 2004.** The Novolizers: overcoming inherent problems of dry powder inhalers. *Resp. Med. Suppl. A:* S17-S21.
- Kolleck I., Wissel H., Guthmann F., Schlame M., Sinha P., Rustow B. 2002.** HDL-holoparticle uptake by alveolar type II cells: effect of vitamin E status. *Am. J. Respir. Cell Mol. Biol.* 27: 57-63.
- Komada F., Iwakawa S., Yamamoto N., Sakakibara H., Okumura K. 1994.** Intratracheal delivery of peptide and protein agents: absorption from solution and dry powder by rat lung. *J. Pharm. Sci.* 83: 863-867.
- Kopaciewicz W., Rounds M.A., Fausnaugh J., Regnier F.E. 1983.** Retention Model for High-Performance Ion-Exchange Chromatography. *J. Chrom.* 266: 3-21.
- Kreilgaard L., Frokjaer S., Flink J.M., Randolph T.W., Carpenter J.F. 1998a.** Effects of additives on the stability of recombinant human factor XIII during freeze-drying and storage in the dried solid. *Arch. Biochem. Biophys.* 360: 121-134.
- Kreilgaard L., Jones, L.S., Randolph T.W., Frokjaer S., Flink J.M., Manning M.C., Carpenter J.F. 1998b.** Effect of Tween 20 on freeze-thawing-and agitation-induced aggregation of recombinant human factor XIII. *J. Pharm. Sci.* 87: 1597-1603.
- Kuipers B.J.H., Gruppen H. 2007.** Peptides Using UV Absorption of the Constituent Amino Acids at 214 nm To Enable Quantitative Reverse Phase High-Performance Liquid Chromatography/Mass Spectrometry Analysis. *J. Agric. Food Chem.* 55: 5445-5451.
- Kumon M., Suzuki M., Kusai A., Yonemochi E., Terada K. 2006.** Novel approach to DPI carrier lactose with mechanofusion process with additives and evaluation by IGC. *Chem. Pharm. Bull.* 54: 1508-1514.
- Kurtzhals P., Havelund S., Jonassen I., Ribel U., Markussen J. 1996.** Mode of action of fatty acid acylated insulin: a novel type of soluble, long-acting insulin analogues. *Diabetes* 45(Suppl. 2): 222A.
- Lai Y-L, Mehta R.C., Thacker A.A., Yoo S-D, McNamara P.J., DeLuca P.P. 1993.** Sustained bronchodilation with isoproterenol poly(glycolide-co-lactide) microspheres, *Pharm. Res.* 10: 119-125.
- Lai M.C., Topp E.M. 1999.** Solid-state chemical stability of proteins and peptides. *J. Pharm. Sci.* 88: 489-500.
- Lakhiari H., Muller D. 2004.** Insulin adsorption on coated silica based supports grafted with N acetylglucosamine by liquid affinity chromatography. *J. Chromatogr. B* 808: 35-41.
- Lauweryns, J.M., Baert, J.H. 1977.** Alveolar clearance and the role of the pulmonary lymphatics. *Am. Rev. Respir. Dis.* 115: 625-683.
- Lee H-K, Kwon J-H, Park S-H, Kim C-W. 2006.** Insulin microcrystals prepared by the seed zone method. *J. Cryst. Growth* 293: 447-451.
- Lee K.C., Chae S.Y., Kim T.H., Lee S., Lee E.S., Youn Y.S. 2009.** Intrapulmonary potential of polyethylene glycol-modified glucagon-like peptide-1s as a type 2 anti-diabetic agent. *Regul. Peptides* 152: 101-107.
- Lee H.J., McAuley A., Schilke K.F., McGuire J. 2011a.** Molecular origins of surfactant-mediated stabilization of protein drugs. *Adv Drug Deliv Rev.* 63(13): 1160-71.
- Lee Y.Y., Wu J.X., Yang M., Young P.M., van den Berg F., Rantanen J. 2011b.** Particle size dependence of polymorphism in spray-dried mannitol. *Eur J Pharm Sci.* 44(1-2): 41-8.
- Leone-Bay A., Grant M. 2006.** Technosphere technology: a platform for inhaled protein therapeutics. *ONdrugDelivery* 8-11. <http://www.ondrugdelivery.com/publications/Pulmonary.pdf>. Retrieved 2010-10-09.

- Li S., Schoneich C., Wilson G.S., Borchardt R.T. 1993.** Chemical pathways of peptide degradation. V. Ascorbic acid promotes rather than inhibits the oxidation of methionine to methionine sulfoxide in small model peptides. *Pharm Res* 10: 1572-1579.
- Li S., Schoneich C., Borchardt R.T. 1995.** Chemical pathways of peptide degradation. VIII. Oxidation of methionine in small model peptides by prooxidant/ transition metal ion systems: Influence of selective scavengers for reactive oxygen intermediates. *Pharm Res* 12: 348-355.
- Li Y., Mitra A.K. 1996.** Effect of phospholipids chain length, concentration, charge, and vesicle size on pulmonary insulin absorption. *Pharm. Res.* 13: 76-79.
- Li S., Patapoff T.W., Nguyen T.H., Borchardt R.T. 1996.** Inhibitory effect of sugars and polyols on the metal-catalyzed oxidation of human relaxin. *J Pharm Sci* 85: 868-872.
- Li S., Patapoff T.W., Overcashier D., Hsu C., Nguyen T.H., Borchardt R.T. 1996b.** Effects of reducing sugars on the chemical stability of human relaxin in the lyophilized state. *J Pharm Sci* 85: 873-877.
- Li W-I, Perzl M., Heyder J., Langer R., Brain J.D., Englmeier K-H, Niven R.W., Edwards D.A. 1996c.** Aerodynamics and aerosol particle deaggregation phenomena in model oral-pharyngeal cavities. *J. Aerosol Sci.* 27(8): 1269-1286.
- Li S., Zhao B., Wang F., Wang M., Xie S., Wang S., Han C., Zhu L., Zhou W. 2010a.** Yak interferon-alpha loaded solid lipid nanoparticles for controlled release. *Res. Vet. Sci.* 88: 148-153.
- Li Y-Z, Sun X., Gong T., Liu J., Zuo J., Zhang Z-R. 2010b.** Inhalable Microparticles as Carriers for Pulmonary Delivery of Thymopentin-Loaded Solid Lipid Nanoparticles. *Pharm. Res.* 27: 1977-1986.
- Lian H., Steiner S.S., Sofia R.D., Woodhead J.H., Wolf H.H., White H.S., Shen G.S., Rhodes C.A., McCabe R.T. 2000.** A self-complementary, self-assembling microsphere system: application for intravenous delivery of the antiepileptic and neuroprotectant compound felbamate. *J. pharm. sci.* 89(7): 867-875.
- Linzer J.F. 2007.** Review of Asthma: Pathophysiology and Current Treatment Options. *Clin. Ped. Emerg. Med.* 8: 87-95.
- Lisanti M.P., Scherer P.E., Vidugiriene J., Tang Z.L., Hermanowski-Vosatka A., Tu Y.H., Cook R.F., Sargiacomo M. 1994.** Characterization of caveolin-rich membrane domains isolated from an endothelial-rich source: Implications for human disease. *J Cell Biol.* 126(1): 111-26.
- Liu R., Langer R., Kibanov A.M. 1991.** Moisture induced aggregation of lyophilized proteins in the solid state. *Biotechnolgy Bioeng.* 37: 177-184.
- Liu F., Shao .Z, Kildsig D.O., Mitra A.K. 1993.** Pulmonary delivery of free and liposomal insulin. *Pharm. Res.* 10: 228-232.
- Liu P-F, Avramova L.V., Park C. 2009.** Revisiting absorbance at 230 nm as a protein unfolding probe. *Anal. Biochem.* 389: 165-170.
- Lock S.H., Kay A.B., Barnes N.C. 1996.** Double-blind, placebo controlled study of cyclosporin A as a corticosteroid-sparing agent in corticosteroid-dependent asthma. *Am. J. Respir. Crit. Care* 153: 509-514.
- Lohrmann M., Kappl M., Butt H-J, Urbanetz N.A., Lippold B.C. 2007.** Adhesion forces in interactive mixtures for dry powder inhalers – Evaluation of a new measuring method. *Eur. J. Pharm. Biopharm.* 67: 579-586.
- Louey M.D., Van Oort M., Hickey A.J. 2006.** Standardized entrainment tubes for the evaluation of pharmaceutical dry powder dispersion. *Aerosol Science* 37: 1520 -1531.

- Lu D., Garcia-Contreras L., Muttill P., Padilla D., Xu D., Liu J., Braunstein M., McMurray D.N., Hickey A.J. 2010.** Pulmonary immunization using antigen 85-B polymeric microparticles to boost tuberculosis immunity. *AAPS J.* 12: 338-347.
- Ma X., Wang D.Q., Bouffard R., MacKenzie A. 2001.** Characterization of murine monoclonal antibody to tumor necrosis factor (TNF-MAb) formulation for freeze-drying cycle development. *Pharm. Res.* 18: 196-202.
- Maa Y.F., Hsu S.W. 1996.** Effect of high shear on proteins. *Biotech. and Bioeng.* 51: 458-465.
- Maa Y.F., Nguyen P.A., Hsu S.W. 1998.** Spray-drying of air-liquid interface sensitive recombinant human growth hormone. *J. Pharm. Sci.* 87: 152-159.
- Machida M., Hayashi M., Awazu S. 2000.** The effects of absorption enhancers on the pulmonary absorption of recombinant human granulocyte colony-stimulating factor (rhG-CSF) in rats. *Biol. Pharm. Bull.* 23: 84-86.
- Malik R., Roy I. 2011.** Probing the mechanism of insulin aggregation during agitation. *Int. J. Pharm.* 413(1-2): 73-80.
- Malmquist G., Lundell N. 1992.** Characterization of the influence of displacing salts on retention in gradient elution ion-exchange chromatography of proteins and peptides. *J. Chrom.* 627: 107-124.
- Maltesen M.J., van de Weert M. 2008.** Drying methods for protein pharmaceuticals. *Drug Discov. Today Technol.* 5(2-3): e81-e88.
- MannKind, 2010.** <http://www.mannkindcorp.com/news-and-events-media-room-photos.htm>. Retrieved 2010-12-21.
- Mansfield E., Kar A., Quinn T.P., Hooker S.A. 2010.** Quartz Crystal Microbalances for Microscale Thermogravimetric Analysis. *Anal. Chem.* 82: 9977-9982.
- Marino M.T., Costello D., Baughman R., Boss A., Cassidy J., Damico C., van Marle S., van Vliet A., Richardson P.C. 2010.** Pharmacokinetics and pharmacodynamics of inhaled GLP-1 (MKC253): proof-of-concept studies in healthy normal volunteers and in patients with type 2 diabetes. *Clin. Pharmacol. Ther.* 88(2): 243-50.
- Markussen J., Andersen A.S., Vad K. 1996.** Synthesis of the soluble, long-acting insulin NN304. *Diabetes* 45(Suppl. 2): 220A.
- Martin Christ GmbH. 2010.** Smart Freeze Drying: Basic principles, optimum procedures and applications. http://www.martinchrist.de/fileadmin/my_uploads/christ/en/Christ_Theorie_Katalog_en_web.pdf. Retrieved 2011-05-14.
- Mastrandrea L. D., Quattrin T. 2006.** Clinical evaluation of inhaled insulin. *Adv. Drug Deliver. Rev.* 58: 1061-1075.
- Matsubara K., Abe K., Irie T., Uekama K. 1995.** Improvement of nasal bioavailability of luteinizing hormone-releasing hormone agonist, buserelin, by cyclodextrin derivatives in rats. *J. Pharm. Sci.* 84: 1295-1300.
- Mattern M., Winter G., Kohnert U., Lee G. 1999.** Formulation of proteins in vacuum-dried glasses. II. Process and storage stability in sugar-free amino acid systems. *Pharm. Dev. Technol.* 4: 199-208.
- McAlpine R.R., Morris A.D., Emslie-Smith A., James P., Evans J.M. 2005.** The annual incidence of diabetic complications in a population of patients with type 1 and type 2 diabetes. *Diabet. Med.* 22(3): 348-352.
- McFarlane S.I., Shin J.J., Rundek T., Bigger J.T. 2003.** Prevention of type 2 diabetes. *Curr Diab Rep* 3(3): 235-241.
- McIvor R., Pizzichini E., Turner MO, Hussack P, Hargreave FE, Sears M.R. 1998.** Potential masking effects of salmeterol on airway inflammation in asthma. *Am. J. Respir. Crit. Care Med.* 158(3): 924-30.

- Melo E.P., Aires-Barros M.R., Costa S.M.B, Cabral J.M.S. 1997.** Thermal unfolding of proteins at high pH range studied by UV absorbance. *J. Biochem. Biophys. Methods* 34: 45-59.
- Mezzena M., Scalia S., Young P.M., Traini D. 2009.** Solid lipid budesonide microparticles for controlled release inhalation therapy. *AAPS Journal* 11(4): 771-778.
- Mokdad A.H., Ford E.S., Bowman B.A., Dietz W.H., Vinicor F., Bales V.S., Marks J.S. 2003.** Prevalence of obesity, diabetes, and obesity related health risk factors, 2001. *JAMA* 289(1): 76-79.
- Morimoto K., Uehara Y., Iwanaga K., Kakemi M. 2000.** Effects of sodium glycocholate and protease inhibitors on permeability of TRH and insulin across rabbit trachea. *Pharm. Acta Helv.* 74: 411-415.
- Moss M., Burnham E.L. 2006.** Alcohol abuse in the critically ill patient. *Lancet* 368: 2231-42.
- Muchmore D.B., Silverman B., De La Pena A., Tobian J. 2007.** The AIR® inhaled insulin system : system components and pharmacokinetic/glucodynamic data, *Diabetes Technol. Ther.* 9(Suppl. 1): S41-S46.
- Müller R.H., Jacobs C., Kayser O. 2001.** Nanosuspensions as particulate drug formulations in therapy. Rationale for development and what we can expect for the future. *Adv. Drug. Deliv. Rev.* 47(1): 3-19.
- Murphy K.P., Bhakuni V., Xie D., Freire E. 1992.** Molecular basis of cooperativity in protein folding. III. Structural identification of folding units and folding intermediates. *J. Mol. Biol.* 227: 293-306.
- Muttill P., Prego C., Garcia-Contreras L., Pulliam B., Fallon J.K., Wang C., Hickey A.J., Edwards D. 2010.** Immunization of Guinea pigs with novel hepatitis B antigen as nanoparticle aggregate powders administered by the pulmonary route. *AAPS J.* 12: 330-337.
- Narhi L.O., Philo J.S., Sun B., Chang B.S., Arakawa T. 1999.** Reversibility of heat-induced denaturation of the recombinant human megakaryocyte growth and development factor. *Pharm. Res.* 16: 799-807.
- Nave R., Zech K., Bethke T.D. 2005.** Lower oropharyngeal deposition of inhaled ciclesonide via hydrofluoroalkane metered-dose inhaler compared with budesonide via chlorofluorocarbon metered-dose inhaler in healthy subjects. *Eur. J. Clin. Pharmacol.* 61: 203-208.
- Nelson H.S., Weiss S.T., Bleecker E.R., Yancey S.W., Dorinsky P.M. 2006.** The salmeterol multicenter asthma research Trial: a comparison of usual pharmacotherapy for asthma or usual pharmacotherapy plus salmeterol. *Chest* 129(1): 15-26.
- Nelson H.S., Busse W.W., Sanger M., Cutler G., Ellwanger C., Chipman J.J. 2009.** Short-term safety of somatropin inhalation powder in adults with mild to moderate asthma. *Allergy Asthma Proc.* 30(3): 325-32.
- Nema S., Avis K.E. 1992.** Freeze-thaw studies of a model protein, lactate dehydrogenase, in the presence of cryoprotectants. *J. Parenter. Sci. Technol.* 47: 76-83.
- Newhouse M., Hirst P., Duddu S., Walter Y., Tarara T., Clark A., Weers J. 2003.** Inhalation of a dry powder tobramycin pulmosphere formulation in healthy volunteers. *Chest.* 124: 360-366.
- Newman S.P. 1985.** Aerosol deposition considerations in inhalation therapy. *Chest* 88(Suppl):152S-160S.
- Newman S.P., Wilding R. 1998.** Gamma scintigraphy an in vivo technique for assessing the equivalence of inhaled products. *Int. J. Pharm.* 170: 1-9.
- Newman S.P., Pitcairn G., Hirst P., Bacon R.E., O'Keefe E., Reiners M., Hermann R. 2000a.** Scintigraphic comparison of budesonide deposition from two dry powder inhalers. *Eur. Respir. J.* 16(1): 178-83.

- Newman S.P., Wilding I.R., Hirst P.H. 2000b.** Human lung deposition data: the bridge between in vitro and clinical evaluations for inhaled drug products? *Int. J. Pharm.* 208: 49-60.
- Newman S.P., Pitcairn G.R., Hirst P.H. 2001.** A brief history of gamma scintigraphy. *J. Aerosol. Med.* 14: 139-145.
- Newman S.P., Busse W.W. 2002.** Evolution of dry powder inhaler design, formulation, and performance. *Respir. Med.* 96: 293-304.
- Newman S.P., Malik S., Hirst P., Pitcairn G., Heide A., Pabst J., Dinkelaker A., Fleischer W. 2002.** Lung deposition of salbutamol in healthy human subjects from the MAGhaler dry powder inhaler. *Respir. Med.* 96: 1026-1032.
- Newman S.P., Pitcairn G.R., Hirst P.H., Rankin L. 2003.** Radionuclide imaging technologies and their use in evaluating asthma drug deposition in the lungs. *Adv. Drug Deliv. Rev.* 55: 851-867.
- Newman S.P. 2004.** Dry powder inhalers for optimal drug delivery. *Expert Opin Biol Ther.* 4:23-33.
- Newman S.P. 2005.** Principles of Metered-Dose Inhaler design. *Resp. Care.* 50(9): 1177-1190.
- Nolan C.J., Damm P., Prentki M. 2011.** Type 2 diabetes across generations: from pathophysiology to prevention and management. *Lancet* 378: 169-181.
- Nowak D. 2006.** Management of asthma with anti-immunoglobulin E: A review of clinical trials of omalizumab. *Resp. Med.* 100: 1907-1917.
- Ohmori Y., Maruyama S., Kimura R., Onoue S., Matsumoto A., Endo K., Iwanaga T., Kashimoto K., Yamada S. 2004.** Pharmacological effects and lung-binding characteristics of a novel VIP analogue, [R15, 20, 21, L17]-VIP-GRR (IK312532). *Regul. Pept.* 123: 201-7.
- Ohtake S., Martin R., Saxena A., Pham B., Chiueh G., Osorino M., Kopecko D., Xu DQ., Lechuga-Ballesteros D., Truong-Le V. 2011.** Room temperature stabilization of oral, live attenuated *Salmonella enterica* serovar Typhi-vectored vaccines. *Vaccine* 29(15): 2761-2771.
- Okumura K., Iwakawa S., Yoshida T., Seki T., Komada F. 1992.** Intratracheal delivery of insulin. Absorption from solution and aerosol by rat lung. *Int. J. Pharm.* 88: 63-73.
- Onoue S., Yamada S., Yajima T. 2007.** Bioactive analogues and drug delivery systems of vasoactive intestinal peptide (VIP) for the treatment of asthma/COPD. *Peptides* 28: 1640-50.
- Onoue S., Hashimoto N., Yamada S. 2008.** Dry powder inhalation systems for pulmonary delivery of therapeutic peptides and proteins. *Expert Opin. Ther. Patents* 18(4): 429-442.
- Onoue S., Yamamoto K., Kawabata Y., Hirose M., Mizumoto T., Yamada S. 2009.** Novel dry powder inhaler formulation of glucagon with addition of citric acid for enhanced pulmonary delivery. *Int. J. Pharm.* 382(1-2): 144-150.
- Onoue S., Aoki Y., Matsui T., Kojo Y., Misaka S., Mizumoto T., Yamada S. 2011.** Formulation design and in vivo evaluation of dry powder inhalation system of new vasoactive intestinal peptide derivative ([R15, 20, 21, L17, A24,25, des-N28]-VIP-GRR) in experimental asthma/COPD model rats. *Int. J. Pharm.* 410: 54-60.
- Onoue S., Sato H., Ogawa K., Kojo Y., Aoki Y., Kawabata Y., Wada K., Mizumoto T., Yamada S. 2012.** Inhalable dry-emulsion formulation of cyclosporine A with improved anti-inflammatory effects in experimental asthma/COPD model rats. *Eur. J. Pharm. Biopharm.* 80(1): 54-60.
- Orlando R. A., Rader K., Authier F., Yamazaki H., Posner B. I., Bergeron J. J. M., Farquhar M. G. 1998.** Megalin is an Endocytic Receptor for Insulin. *J. Am. Soc. Nephrol.* 9: 1759-1766.

Owens D.R., Zinman B., Bolli G. 2003. Alternative routes of insulin delivery. *Diabet. Med.* 20: 886-898.

Patent US5284656, 1994. Amgen. Pulmonary administration of granulocyte colony stimulating factor.

Patent US5558085, 1996. Aradigm Corp. Intrapulmonary delivery of peptide drugs.

Patent WO9741831, 1997. Cornell Research Foundation. Stimulation of immune response with low doses of IL-2.

Patent US5780014, 1998. Nektar Therapeutics. Method and apparatus for pulmonary administration of dry powder alpha 1-antitrypsin.

Patent US6080721, 2000. Nektar Therapeutics. Pulmonary delivery of active fragments of parathyroid hormone.

Patent WO0061178, 2000. Nektar Therapeutics. Pulmonary administration of dry powder formulations for treating infertility.

Patent US6423344, 2002. Nektar Therapeutics. Dispersible macromolecule compositions and methods for their preparation and use.

Patent US6596261, 2003. Aeropharm Technology. Method of administering a medicinal aerosol formulation.

Patent US6589560, 2003. Nektar Therapeutics. Stable glassy state powder formulations.

Patent US6506724, 2003. Amylin Pharmaceuticals. Use of exendins and agonists thereof for the treatment of gestational diabetes mellitus.

Patent US6506377, 2003. Amarillo Biosciences. Interferon-alpha mediated upregulation of aquaporin expression.

Patent WO0448401, 2004. Itoham Foods. Peptides and medicinal compositions containing the same.

Patent US6780839, 2004. Pharmagene Laboratories. Use of secretin-receptor ligands in treatment of cystic fibrosis (CF) and chronic obstructive pulmonary disease (COPD).

Patent US6784156, 2004. Enanta Pharmaceuticals. Cyclosporins for the treatment of respiratory diseases.

Patent US6743429, 2004. Sherbrooke University. Use of calcitonin gene-related peptide in the prevention and alleviation of asthma and related bronchospastic pulmonary diseases.

Patent US6720407, 2004. Eli Lilly. Method for administering insulinotropic peptides.

Patent US6759393, 2004. Pfizer. Growth hormone and growth hormone releasing hormone compositions.

Patent US6797258, 2004. Nektar Therapeutics. Compositions and methods for the pulmonary delivery of aerosolized macromolecules.

Patent WO0535088, 2005. Baxter International. Method for preparing small spherical by controlled phase separation.

Patent US6964761, 2005. New York University. Method of treating idiopathic pulmonary fibrosis with aerosolized IFN-gamma.

Patent US6887462, 2005. Chiron Corp. HSA-free formulations of interferon-beta.

Patent US7166575, 2007. Natestch Pharmaceutical Co. Compositions and methods for enhanced mucosal delivery of peptide YY and methods for treating and preventing obesity.

Patton J.S., Platz R.M. 1992. Pulmonary delivery of peptides and proteins for systemic action. *Adv. Drug Deliv. Rev.* 8(179): 196-179.

Patton J.S., Trincherio P., Platz R.M. 1994. Bioavailability of pulmonary delivered peptides and proteins: α -interferon, calcitonins and parathyroid hormones. *J. Controlled Rel.* 28: 19-85.

Patton J.S. 1996. Mechanisms of macromolecule absorption by the lungs. *Adv. Drug Deliv. Rev.* 19: 3-36.

Patton J.S., Bukar J., Nagarajan S. 1999. Inhaled insulin. *Adv. Drug Deliver. Rev.* 35: 235-247.

Patton J.S. 2000. Pulmonary delivery of drugs for bone disorders. *Adv. Drug Deliv. Rev.* 42: 239 -48.

Patton J.S., Bukar J.G, Eldon M.A. 2004. Clinical pharmacokinetics and pharmacodynamics of inhaled insulin. *Clin. Pharmacokinet.* 43: 781-801.

Patton J.S., Byron P.R. 2007. Inhaling medicines: delivering drugs to the body through the lungs. *Nat. Rev. Drug Discovery* 6: 67-74.

Pearce F.L. 1993. Effect of nedocromil sodium on mediator release from mast cells. *J. Allergy Clin. Immunol.* 92(1, Part2): 155-8.

Pecharsky V.K., Zavalij P.Y. 2009. Fundamentals of powder diffraction and structural characterization of materials. Springer Verlag, Berlin, Germany.

Pfützner A., Forst T. 2005. Pulmonary insulin delivery by means of the Technosphere drug carrier mechanism. *Expert Opin. Drug Deliv.* 2(6): 1097-1106.

Piedmonte D.M., Summers C., McAuley A., Karamujic L., Ratnaswamy G. 2007. Sorbitol Crystallization Can Lead to Protein Aggregation in Frozen Protein Formulations. *Pharm. Res.* 24(1): 136-146.

Piercenet. 2012. <http://www.piercenet.com/browse.cfm?fldID=F6556788-5056-8A76-4EAC-3683B8E3197A>. Retrieved 2012-01-20.

Pikal M.J., Dellerman K.M., Roy M.L., Riggan R.M. 1991. The effects of formulation variables on the stability of freeze-dried human growth hormone. *Pharm. Res.* 8: 427-436.

Pilcer G., Sebti T., Amighi K. 2006. Formulation and characterization of lipid-coated tobramycin particles for dry powder inhalation. *Pharm. Res.* 23(5): 931-40.

Pilcer G. 2008a. New highly effective dry powder tobramycin formulations for inhalation in the treatment of cystic fibrosis. Thesis presented at Université Libre de Bruxelles, Bruxelles, Belgium.

Pilcer G., Vanderbist F., Amighi K. 2008b. Correlations between cascade impactor analysis and laser diffraction techniques for the determination of the particle size of aerosolised powder formulations. *Int. J. Pharm.* 358: 75-81.

Pilcer G., Goole J., Van Gansbeke B., Blocklet D., Knoop C., Vanderbist F., Amighi K. 2008c. Pharmacoscintigraphic and pharmacokinetic evaluation of tobramycin DPI formulations in cystic fibrosis patients. *Eur. J. Pharm. Biopharm.* 68(2): 413-21.

Pilcer G., Vanderbist F., Amighi K. 2009. Preparation and characterization of spray-dried tobramycin powders containing nanoparticles for pulmonary delivery. *Int. J. Pharm.* 365(1-2): 162-169.

- Pilcer G., Amighi K. 2010.** Formulation strategy and use of excipients in pulmonary drug delivery. *Int. J. Pharm.* 392: 1-19.
- Pilcer G., Wauthoz N., Amighi K. 2011.** Lactose characteristics and the generation of the aerosol. *Adv. Drug Deliv. Rev.* doi:10.1016/j.addr.2011.05.003.
- Polonsky K.S., Given B.D., Hirsch L.J., Hirsch L.J., Tillil H., Shapiro E.T., Beebe C., Frank B.H., Galloway J.A., Van Cauter E. 1988.** Abnormal patterns of insulin secretion in non-insulin-dependent diabetes mellitus. *N. Engl. J. Med.* 318: 1231-1239.
- Potocka E., Baughman R.A., Derendorf H. 2011.** Population pharmacokinetic model of human insulin following different routes of administration. *J. Clin. Pharmacol.* 51:1015-1024.
- Qian F., Mathias N., Moench P., Chi C., Desikan S., Hussain M., Smith R.L. 2009.** Pulmonary delivery of a GLP-1 receptor agonist, BMS-686117. *Int. J. Pharm.* 366: 218-220.
- Quattrin T., Belanger A., Bohannon N.J., Schwartz S.L. 2004.** Efficacy and safety of inhaled insulin (Exubera) compared with subcutaneous insulin therapy in patients with type 1 diabetes: results of a 6-month, randomized, comparative trial. *Diabetes Care* 27: 2622-7.
- Radkiewicz J.L., Zipse H., Clarke S., Houk K.N. 2001.** Neighboring side chain effects on asparaginyl and aspartyl degradation: an ab initio study of the relationship between peptide conformation and backbone NH acidity. *J. Am. Chem. Soc.* 123: 3499-3506.
- Raehs S.C., Sandow J., Wirth K., Merkle H.P. 1988.** The adjuvant effect of bacitracin on nasal absorption of gonadorelin and buserelin in rats. *Pharm. Res.* 5: 689-693.
- Rave K., Bott S., Heinemann L., Sha S., Becker R.H.A., Willavize S.A., Heise T. 2005.** Time-action profile of inhaled insulin in comparison with subcutaneously injected insulin lispro and regular human insulin. *Diabetes Care* 28(5): 1077-1082.
- Rave K., De la Pena A., Tibaldi F.S., Zhang L., Silverman B., Hausmann M., Heinemann L., Muchmore D.B. 2007a.** AIR inhaled insulin in subjects with chronic obstructive pulmonary disease: pharmacokinetics, glucodynamics, safety, and tolerability. *Diabetes Care* 30(7): 1777-1782.
- Rave K., Heise T., Boss A.H. 2007b.** Inhaled Technosphere/Insulin in comparison to subcutaneous regular human insulin: favorable time action profile and low variability in subjects with type 2 diabetes. *J. Diabetes Sci. Technol.* 2: 205-211.
- Reid D.W., Ward C., Wang N., Zheng L., Bish R., Orsida B., Walters E.H. 2003.** Possible anti-inflammatory effect of salmeterol against interleukin-8 and neutrophil activation in asthma in vivo. *Eur. Respir. J.* 21(6): 994-9.
- Rhoades R.A., Pflanzer R.G. 2002.** *Human Physiology*, 4th ed. Thomson Learning, Pacific Grove, CA.
- Richardson P.C., Boss A.H. 2007.** Technosphere insulin technology. *Diabetes Technol. Ther.* 9(Suppl. 1): S65-S72.
- Risérus U., Willett W.C., Hu F.B. 2009.** Dietary fats and prevention of type 2 diabetes. *Prog. Lipid Res.* 48(1): 44-51.
- Robertson C., Drexler A.J., Vernillo A.T. 2003.** Update on diabetes diagnosis and management. *JADA* 134: 16S-23S.
- Robinson N.E., Robinson A.B. 2004.** Prediction of primary structure deamidation rates of asparaginyl and glutaminyl peptides through steric and catalytic effects. *J. Pept. Res.* 63: 437-448.

- Rohatagi S., Calic F., Harding N., Ozoux M-L, Bouriot J-P, Kirkesseli S., DeLeij L., Jensen B. K. 2000.** Pharmacokinetics, Pharmacodynamics, and Safety of Inhaled Cyclosporin A (ADI628) after Single and Repeated Administration in Healthy Male and Female Subjects and Asthmatic Patients. *J. Clin. Pharmacol.* 40: 1211-1226.
- Rosenstock J., Zinman B., Murphy L.J., Clement S.C., Moore P., Bowering C.K., Hendler R., Lan S-P, Cefalu W.T. 2005.** Inhaled insulin improves glycemic control when substituted for or added to oral combination therapy in type 2 diabetes: a randomized, controlled trial. *Ann. Intern. Med.* 143: 549-58.
- Rosenstock J., Lorber D.L., Gnudi L., Howard C.P., Bilheimer D.W., Chang P-C, Petrucci R.E., Boss A.H., Richardson P.C. 2010.** Prandial inhaled insulin plus basal insulin glargine versus twice daily bipart insulin for type 2 diabetes: a multicentre randomised trial. *Lancet* 375: 2244-53.
- Rosenwasser L.J., Nash D.B. 2003.** Incorporating omalizumab into asthma treatment guidelines: Consensus panel recommendations. *Pharmacy and Therapeutics* 28: 400-410.
- Rother K.I. 2007.** Diabetes treatment—bridging the divide. *NEJM* 356(15): 1499-501.
- Roux K. 1999.** Immunoglobulin structure and function as revealed by electron microscopy. *Int. Arch. Allergy Immunol.* 120(2): 85-99.
- Rowlett R. 2005.** How Many? A Dictionary of Units of Measurement. Center for Mathematics and Science Education, University of North Carolina at Chapel Hill. Retrieved 2011-10-08.
- Roy I., Gupta M.N. 2004.** Freeze-drying of proteins: some emerging concerns. *Biotechnol. Appl. Biochem.* 39: 165-177.
- Ruiz J.L., Ferrer J., Pire C., Llorca F.I., Bonete M.J. 2003.** Denaturation Studies by Fluorescence and Quenching of Thermophilic Protein NAD-Glutamate Dehydrogenase from *Thermus thermophilus* HB8. *J. Protein Chem.* 22(3): 295-301.
- Rxlist, 2011.** <http://www.rxlist.com/foradil-drug/medication-guide.htm>. Retrieved 2011-07-10.
- Sackner M.A., Kim C.S. 1985.** Recent advances in the management of obstructive airways disease. Auxiliary MDI aerosol delivery systems. *Chest* 88(2 Suppl): 161S-170S.
- Sadeghi M., Hajivandi M., Bogoev R., Amshey J. 2003.** Molecular weight estimation of proteins by gel electrophoresis revisited. *Focus®* 25(3): 35-39. <http://www.invitrogen.jp/focus/253035.pdf>. Retrieved 2011-09-28.
- Salas-Salvado J., Martinez-Gonzalez M.A., Bullo M., Ros E. 2011.** The role of diet in the prevention of type 2 diabetes. *Nutr. Metab. Cardiovasc. Dis.* 21(Suppl 2): B32-48.
- Salnikova M.S., Middaugh R., Rytting J.H. 2008.** Stability of lyophilized human growth hormone. *Int. J. Pharm.* 358(1-2): 108-113.
- Saluja V., Amorij J-P, Kapteyn J.C., de Boer A.H., Frijlink H.W., Hinrichs W.L.J. 2010.** A comparison between spray drying and spray freeze drying to produce an influenza subunit vaccine powder for inhalation. *J. Control.Release* 144: 127-133.
- Sane S.U., Wong R., Hsu C.C. 2004.** Raman spectroscopic characterization of drying-induced structural changes in a therapeutic antibody: Correlating structural changes with long-term stability. *J. Pharm. Sci.* 93: 1005-1018.
- Sangwan S., Agosti J.M., Bauer L.A., Otulana B.A., Morishige R.J., Cipolla D.C., Blanchard J.D., Smaldone G.C. 2001.** Aerosolized protein delivery in asthma: gamma camera analysis of regional deposition and perfusion. *J. Aerosol Med.* 14: 185-195.

- Sanna V., Kirschvink N., Gustin P., Gavini E., Roland I., Delattre L., Evrard B. 2003.** Preparation and In Vivo Toxicity Study of Solid Lipid Microparticles as Carrier for Pulmonary Administration. *AAPS PharmSciTech* 5(2) Article 27.
- Sarciaux J.M., Mansour S., Hageman M.J., Nail S.L. 1999.** Effects of buffer composition and processing conditions on aggregation of bovine IgG during freeze-drying. *J. Pharm. Sci.* 88: 1354-1361.
- Sauerborn M., Brinks V., Jiskoot W., Schellekens H. 2010.** Immunological mechanism underlying the immune response to recombinant human protein therapeutics. *Trends Pharmacol. Sci.* 31(2): 53-59.
- Sausse Lhernould M., Pierobon M., Mathys P., Lambert P. 2009.** Determination of EHD Generated Droplet Size: Review of Models and Experimental Tools. *European Aerosol Conference 2009, Karlsruhe, Germany, Abstract T065A01.*
- Scheuch G. 2006.** Lung physiology and biophysics for optimal drug delivery. In: *Achievements and trends in pulmonary delivery, international association for pharmaceutical technology, Marburg, Germany, Course No. 6057 on 9th November 2006.*
- Scheuch G., Siekmeier R. 2007.** Novel approaches to enhance pulmonary delivery of proteins and peptides. *J. Physiol. Pharmacol.* 58 (S5): 615-625.
- Scheuch G., Brand P., Meyer T., Herpich C., Müllinger B., Brom J., Weidinger G., Kohlhäufel M., Häussinger K., Spannagl M., Schramm W., Siekmeier R. 2007.** Anticoagulative effects of the inhaled low molecular weight heparin certoparin in healthy subjects. *J. Physiol. Pharmacol.* 58(Suppl 5): 603-614.
- Schipper N.G.M., Verhoef J.C., De Lannoy L.M., Romeijn S.G., Brakkee J.H., Wiegant V.M., Gispens W.H., Merkus F.W.H.M. 1993.** Nasal administration of an ACTH[4-9] peptide analogue with dimethyl- β -cyclodextrin as an absorption enhancer: pharmacokinetics and dynamics. *Br. J. Pharmacol.* 110: 1335-1340.
- Schnitzer J.E., Oh P., Jacobson B.S., Dvorak A.M. 1995.** Caveolae from luminal plasmalemma of rat lung endothelium: Microdomains enriched in caveolin, Ca⁺⁺-ATPase, and inositol trisphosphate receptor. *Proc Natl Acad Sci U S A.* 92(5): 1759-1763.
- Schüle S., Schulz-Fademrecht T., Garidel P., Bechtold-Peters K., Frieß W. 2008.** Stabilization of IgG1 in spray dried powders for inhalation. *Eur. J. Pharm. Biopharm.* 69: 793-807.
- Schurch S., Gehr P., Im Hof V., Geiser M., Green F. 1990.** Surfactant displaces particles toward the epithelium in airways and alveoli. *Respir. Physiol.* 80: 17-32.
- Schutte B.C., Mc Cray P.B.Jr. 2002.** Beta-defensins in lung hosts defense. *Annu. Rev. Physiol.* 64: 709-748.
- Schwartz L. 2003.** Diafiltration: A Fast, Efficient Method for Desalting, or Buffer Exchange of Biological Samples. Scientific & Technical Report PN 33289, Pall Life Sciences. http://site.pall.com/pdf/02.0629_Buffer_Exchange_STR.pdf. Retrieved 2009-08-12.
- Sdraulig S., Franich R., Tinker R.A., Solomon S., O'Brien R., Johnston P.N. 2008.** In vitro dissolution studies of uranium bearing material in simulated lung fluid. *J. Environ. Radioactiv.* 99: 527-538.
- Sebti T., Amighi K. 2006.** Preparation and in vitro evaluation of lipidic carriers and fillers for inhalation. *Eur. J. Pharm. Biopharm.* 63(1): 51-58.
- Sebti T., Pilcer G., Van Gansbeke B., Goldman S., Michils A., Vanderbist F., Amighi K. 2006.** Pharmacoscintigraphic evaluation of lipid dry powder budesonide formulations for inhalation. *Eur. J. Pharm. Biopharm.* 64(1): 26-32.

- Seefeldt M.B., Kim Y-S, Tolley K.P., Seely J., Carpenter J.F., Randolph T.W. 2005.** High-pressure studies of aggregation of recombinant human interleukin-1 receptor antagonist: Thermodynamics, kinetics, and application to accelerated formulation studies. *Protein Sci.* 14: 2258-2266.
- Serrano A.G., Perez-Gil J. 2006.** Protein-lipid interactions and surface activity in the pulmonary surfactant system. *Chem. Phys. Lipids* 141: 105-118.
- Shah V.P., Tsong Y., Sathe P., Liu J-P. 1998.** In vitro dissolution profile comparison statistics and analysis of the similarity factor f_2 . *Pharm. Res.* 15(6): 889-896.
- Shao Z., Krishnamoorthy R., Mitra A.K. 1992.** Cyclodextrins as nasal absorption promoters of insulin: mechanistic evaluations. *Pharm. Res.* 9: 1157-1163.
- Shao Z., Li Y., Mitra A.K. 1994.** Cyclodextrins as mucosal absorption promoters of insulin III: pulmonary route of delivery. *Eur. J. Pharm. Biopharm.* 40: 283-288.
- Shaw J. 2004.** Aerogen impacts pulmonary drug delivery in the acute care setting. *Drug Deliv. Technol.* 4(6): 1-3.
- Shaw J.E., Sicree R.A., Zimmet P.Z. 2010.** Global estimates of the prevalence of diabetes for 2010 and 2030. *Diabetes Res. Clin. Pract.* 87: 4-14.
- Shen Z., Cheng Y., Zhang Q., Wei S., Li R., Wang K. 2000.** Lanthanides enhance pulmonary absorption of insulin. *Biol. Trace Elem. Res.* 75: 215-225.
- Siekmeier R., Scheuch G. 2008.** Inhaled insulin – Does it become reality? *J. Physiol. Pharmacol.* 59(Suppl. 6): 81-113.
- Siekmeier R., Scheuch G. 2009.** Treatment of systemic diseases by inhalation of biomolecule aerosols. *J. Physiol. Pharmacol.* 60(Suppl. 5): 15-26.
- Siekmeier R. 2010.** Lung deposition of inhaled alpha-1-proteinase inhibitor (alpha 1-P1) – problems and experience of alpha 1-P1 inhalation therapy in patients with hereditary alpha 1-P1 deficiency and cystic fibrosis. *Eur. J. Med. Res.* 15(2): 164-74.
- Singh R.R., Rao A.G.A. 2002.** Reductive unfolding and oxidative refolding of a Bowman-Birk inhibitor from horsegram seeds (*Dolichos biflorus*): evidence for 'hyperreactive' disulfide bonds and rate-limiting nature of disulfide isomerization in folding. *BBA Protein Struct. M.* 1597(2): 280-291.
- Skoog D.A., West D.M., Holler F.J. 1997.** *Chimie analytique*, 7th edition. De Boeck and Larcier, Bruxelles, Belgium.
- Skubitz K.M., Anderson P.M. 2000.** Inhalational interleukin-2 liposomes for pulmonary metastases: a phase I clinical trial. *Anticancer Drugs* 11: 555-563.
- Skyler J.S. 2004.** Insulin treatment. In: Lebrovitz H.E. (Ed.). *Therapy for Diabetes Mellitus and related disorders*, 4th Ed. American diabetes association, Alexandria, VA, pp. 207-223.
- Skyler J.S., Weinstock R.S., Raskin P., Yale J.F., Barrett E., Gerich J.E., Gerstein H.C. 2005.** Use of inhaled insulin in a basal/bolus insulin regimen in type 1 diabetic subjects: a 6-month, randomized, comparative trial. *Diabetes Care* 28(7): 1630-5.
- Skyler J.S., Hollander P.A., Jovanovic L., Klioze S., Krasner A., Riese R.J., Reis J., Schwartz P., Duggan W. 2008.** Safety and efficacy of inhaled human insulin (Exubera®) during discontinuation and readministration of therapy in adults with type 1 diabetes: A 3-year randomized controlled trial. *Diabetes Res. Clin. Pract.* 82: 238-246.
- Son Y-J, McConville J.T. 2008.** Dissolution testing for inhalation formulations. *Inhalation* 2(6) : 8-11.

- Son Y.-J., Horng M., Copley M., McConville J. T. 2010.** Optimization of an In Vitro Dissolution Test Method For Inhalation Formulations. *Dissolution Technol.* 17(2): 6-13.
- Sou T., Meeusen E.N., de Veer M., Morton D.A.V., Kaminskas L.M., McIntosh M.P. 2011.** New developments in dry powder pulmonary vaccine delivery. *Trends Biotechnol.* 29(4): 191-198.
- Sridhar A.V., McKean M. 2006.** Nedocromil sodium for chronic asthma in children. *Cochrane Database Syst. Rev.* 3: CD004108.
- Stalh K., Claesson M., Lilliehorn P., Linden H., Backstrom K. 2002.** The effect of process variables on the degradation and physical properties of spray dried insulin intended for inhalation. *Int. J. Pharm.* 233: 227-237.
- Starke A.A.R., Heinemann L., Hohmann A., Berger M. 1989.** The action profiles of human NPH insulin preparations. *Diabetic Med.* 6: 239-244.
- Steckel H., Muller B.W. 1997.** In vitro evaluation of dry powder inhalers 1: drug deposition of commonly used devices. *Int. J. Pharm.* 154: 19-29.
- Steiner D.F., Oyer P.E. 1967.** The biosynthesis of insulin and a probable precursor of insulin by a human islet cell adenoma. *Proc. Natl. Acad. Sci. U.S.A.* 57(2): 473-480.
- Steiner S., Pfutzner A., Wilson B.R., Harzer O., Heinemann L., Rave K. 2002.** Technosphere/Insulin: proof of concept study with a new insulin formulation for pulmonary delivery. *Exp. Clin. Endocrinol. Diabetes* 110: 17-21.
- Strack T.R. 2006.** Inhaled human insulin. *Drugs Today* 42(4): 207.
- Suarez S., Garcia-Contreras L., Sarubbi D., Flanders E., O'Toole D., Smart J., Hickey A.J. 2001.** Facilitation of pulmonary insulin absorption by H-MAP: Pharmacokinetics and pharmacodynamics in rats. *Pharm. Res.* 18: 1677-1684.
- Suckale J., Solimena M. 2008.** Pancreas islets in metabolic signaling - focus on the beta-cell. *Front. Biosci.* 13: 7156-7171.
- Suzuki M., Machida M., Adachi K., Otabe K., Sugimoto T., Hayashi M., Awazu S. 2000.** Histopathological study of the effects of a simple intratracheal instillation of surface active agents on lung in rats. *J. Toxicol. Sci.* 25(1): 49-55.
- Szefler S.J., Phillips B.R., Martinez F.D., Chinchilli V.M., Lemanske R.F., Strunk R.C., Zeiger R.S., Larsen G., Spahn J.D., Bacharier L.B., Bloomberg G.R., Guilbert T.W., Heldt G., Morgan W.J., Moss M.H., Sorkness C.A., Taussig L.M. 2005.** Characterization of within-subject responses to fluticasone and montelukast in childhood asthma. *J. Allergy Clin. Immunol.* 115: 233-42.
- Takemoto L., Fujii N., Boyle D. 2001.** Mechanism of Asparagine Deamidation During Human Senile Cataractogenesis. *Exp. Eye Res.* 72(5): 559-563.
- Tanaka K., Takeda T., Miyajima K., 1991.** Cryoprotective effect of saccharides on denaturation of catalase by freeze-drying. *Chem. Pharm. Bull.* 39: 1091-1094.
- Tang G., White J.E., Gordon R.J., Lumb P.D., Tsan M.F. 1993.** Polyethylene glycol-conjugated superoxide dismutase protects rats against oxygen toxicity. *J. Appl. Physiol.* 74: 1425-31.
- Tang K., Gomez A. 1995.** Generation of monodisperse water droplets from electrosprays in a Corona-assisted cone-jet mode. *J. Colloid Interface Sci.* 175: 326-332.

- Tang X., Pikal M.J. 2004.** Design of freeze-drying processes for pharmaceuticals: practical advice. *Pharm. Res.* 21(2): 191-200.
- Terray M. 2007.** Initiation au développement de méthode pour les poudres et les suspensions en voie liquide, Présentation Malvern Instruments, Université Libre de Bruxelles, Bruxelles, Belgium
- Thippawong J., Otulana B., Clauson P., Okikawa J., Farr S.J. 2002.** Pulmonary insulin administration using the AERx insulin diabetes system. *Diabetes Technol. Ther.* 4: 499-504.
- Thippawong J. 2006.** Inhaled cytokines and cytokine antagonists. *Adv. Drug Delivery Rev.* 58: 1089-1105.
- Thorens B., Porret A., Buhler L., Deng S.P., Morel P., Widmann C. 1993.** Cloning and functional expression of the human islet GLP-1 receptor. Demonstration that exendin-4 is an agonist and exendin-(9-39) an antagonist of the receptor. *Diabetes* 42: 1678-82.
- Tian F., Sane S., Rytting J.H. 2006.** Calorimetric investigation of protein/amino acid interactions in the solid state. *Int J Pharm* 310: 175-186.
- Tian F., Middaugh C.R., Offerdahl T., Munson E., Sane S., Rytting J.H. 2007.** Spectroscopic evaluation of the stabilization of humanized monoclonal antibodies in amino acid formulations. *Int. J. Pharm.* 335: 20-31.
- Timsina M.P., Martin G.P., Marriott C., Ganderton D., Yianneskis M. 1994.** Drug delivery to the respiratory tract using dry powder inhalers. *Int. J. Pharm.* 101: 1-13.
- Tobyn M., Staniforth J., Morton D., Harmer Q., Newton M. E. 2004.** Active and intelligent inhaler device development. *Int. J. Pharm.* 277(1-2): 31-37.
- Todo H., Okamoto H., Lida K., Danjo K. 2001.** Effect of additives on insulin absorption from intratracheally administered dry powders in rats. *Int. J. Pharm.* 220: 101-110.
- Townsend M.W., Byron P.R., DeLuca P.P. 1990.** The effects of formulation additives on the degradation of freeze-dried ribonuclease A. *Pharm. Res.* 7: 1086-1091.
- Tzannis S.T., Prestrelski S.J., 1999.** Moisture effects on protein-exipient interactions in spray-dried powders. Nature of destabilizing effects of sucrose. *J. Pharm. Sci.* 88: 360-370.
- Uversky V.N., Karnoup A.S., Khurana R., Segel D.J., Doniach S., Fink A.L. 1999.** Association of partially folded intermediates of staphylococcal nuclease induces structure and stability. *Protein Sci.* 8: 161-173.
- Vanbever R., Mintzes J.D., Wang J., Nice J., Chen D., Batycky R., Langer R., Edwards D.A. 1999.** Formulation and physical characterization of large porous particles for inhalation. *Pharm. Res.* 16: 1742-1753.
- Vehring R. 2008.** Pharmaceutical particle engineering via spray drying. *Pharm. Res.* 25: 999-1022.
- Voss A., Finlay W.H. 2002.** Deagglomeration of dry powder pharmaceutical aerosols. *Int. J. Pharm.* 248: 39-59.
- Waldeck B. 2002.** [β]-Adrenoceptor agonists and asthma—100 years of development. *Eur. J. Pharmacol.* 445(1 and 2): 1-12.
- Wang W. 2000.** Lyophilization and development of solid protein pharmaceuticals. *Int. J. Pharm.* 203:1-60.
- Wang Z., Zhang Q. 2004.** Transport of proteins and peptides across human cultured alveolar A549 cell monolayer. *Int. J. Pharm.* 269: 451-456.
- Wang W. 2005.** Protein aggregation and its inhibition in biopharmaceutics. *Int. J. Pharm.* 289: 1-30.

Wang W., Nema S., Teagarden D. 2010. Protein aggregation—Pathways and influencing factors. *Int. J. Pharm.* 390: 89-99.

Wang S.H., Thompson A.L., Hickey A.J., Staats H.F. 2012. Dry powder vaccines for mucosal administration: critical factors in manufacture and delivery. In: Kozlowski P.A. (Ed.). *Current topics in microbiology and immunology*, volume 354. Springer Verlag, Berlin, Germany, pp. 121-156.

Ward J. 2005. Physiology of breathing I. *Surgery* 23(11): 419-423.

Watanabe Y., Matsumoto Y., Kikuchi R., Kiriya M., Nakagawa K., Nomura H., Maruyama K., Matsumoto M. 1995. Pharmacokinetics and pharmacodynamics of recombinant human granulocyte colony-stimulation factor [rhG-CSF] following intranasal administration to rabbits. *J. Drug Targeting* 3: 231-238.

Watts A.B., McConville J.T., Williams R.O. 2008. Current Therapies and Technological Advances in Aqueous Aerosol Drug Delivery. *Drug Dev. Ind. Pharm.* 34: 913-922.

Webb S.D., Golledge S.L., Cleland J.L., Carpenter J.F., Randolph T.W. 2002. Surface adsorption of recombinant human interferon-gamma in lyophilized and spray-lyophilized formulations. *J. Pharm. Sci.* 91: 1474-1487.

Wechsler M.E., Lehman E., Lazarus S.C., Lemanske Jr R.F., Boushey H.A., Deykin A., Fahy J.V., Sorkness C.A., Chinchilli V.M., Craig T.J., DiMango E., Kraft M., Leone F., Martin R.J., Peters S.P., Szeffler S.J., Liu W., Israel E. 2006. Beta-Adrenergic receptor polymorphisms and response to salmeterol. *Am. J. Respir. Crit. Care Med.* 173(5): 519-26.

Weers J.G., Tarara T.E., Clark A.R. 2007. Design of fine particles for pulmonary drug delivery. *Expert Opin. Drug Deliv.* 4: 297-313.

Wenzel S., Wilbraham D., Fuller R., Getz E.B., Longphre M. 2007. Effect of an interleukin-4 variant on late phase asthmatic response to allergen challenge in asthmatic patients: results of two phase 2a studies. *Lancet* 370(9596): 1422-1431.

Westphal S., Kästner S., Taneva E., Leodolter A., Dierkes J., Luley C. 2004. Postprandial lipid and carbohydrate responses after the ingestion of a casein-enriched mixed meal. *Am J Clin Nutr* 80: 284 -90.

White S., Bennett D. B., Cheu S., Conley P. W., Guzek D. B., Gray S., Howard J., Malcolmson R., Parker J. M., Roberts P., Sadrzadeh N., Schumacher J. D., Seshadri S., Sluggett G. W., Stevenson C. L., Harper N. J. 2005. EXUBERA®: Pharmaceutical Development of a Novel Product for Pulmonary Delivery of Insulin, *Diabetes Technol. Ther.* 7(6): 896-906.

Wiederrecht G., Lam E., Hung S., Martin M., Sigal N. 1993. The mechanism of action of FK-506 and cyclosporin A. *Ann. NY Acad. Sci.* 696: 9-19.

Won C.M., Molnar T.E., McKean R. E., Spenlehauer G. A. 1998. Stabilizers against heat induced aggregation of RPR, 114849, an acidic fibroblast growth factor (AFGF). *Int. J. Pharm.* 167: 25-36.

Woof J. M., Burton D. R. 2004. Human antibody-Fc receptor interactions illuminated by crystal structures. *Nat. Rev. Immunol.* 4(2): 89-99.

World Health Organization. 2009. General policies for monoclonal antibodies. <http://www.who.int/medicines/services/inn/Generalpoliciesformonoclonalantibodies2009.pdf>. Retrieved 2010-06-08.

Wright J.R. 1990. Clearance and recycling of pulmonary surfactant. *Am. J. Physiol.* 259: L1-L12.

Xie M., Schowen R.L. 1999. Secondary Structure and Protein Deamidation. *J. Pharm. Sci.* 88(1): 8-13.

- Yamamoto A., Umemori S., Muranishi S. 1994.** Absorption enhancement of intrapulmonary administered insulin by various absorption enhancers and protease inhibitors in rats. *J. Pharm. Pharmacol.* 46: 14-18.
- Yamamoto A., Okumura S., Fukuda Y., Fukui M., Takahashi K., Muranishi S. 1997.** Improvement of the pulmonary absorption of [Asu1,7]-eel calcitonin by various absorption enhancers and their pulmonary toxicity in rats. *J. Pharm. Sci.* 86: 1144-1146.
- Yang M., Velag S., Yamamoto H., Takeuchi H., Kawashima Y., Hovgaard L., van de Weert M., Frokjaer S. 2007.** Characterisation of salmon calcitonin in spray-dried powder for inhalation: Effect of chitosan. *Int. J. Pharm.* 331: 176-181
- Yang W., Peters J.I., Williams R.O. 2008.** Inhaled nanoparticles—A current review. *Int. J. Pharm.* 356: 239-247.
- Yapicioğlu H., Yildizdaş D., Bayram I., Sertdemir Y., Yilmaz H.L. 2003.** The use of surfactant in children with acute respiratory distress syndrome: efficacy in terms of oxygenation, ventilation and mortality. *Pulm. Pharmacol. Ther.* 16(6): 327-33.
- Yeadon M., Diamant Z. 2000.** New and exploratory therapeutic agents for asthma. 1st ed. Marcel Dekker, New York, NY.
- Young P., Thomson J., Woodcock D., Aydin M., Price R. 2004.** The development of a novel high-dose pressurised aerosol dry powder device (PADD) for the delivery of pumactant for inhalation therapy. *J. Aerosol Med.* 17: 123-128.
- Young P.M., Edge S., Traini D., Jones M.D., Price R., El-Sabawi D., Urry C., Smith C. 2005.** The influence of dose on the performance of dry powder inhalation systems, *Int. J. Pharm.* 296: 26-33.
- Yu J., Chien Y.W. 1997.** Pulmonary drug delivery: physiologic and mechanistic aspects. *Crit. Rev. Ther. Drug Carr. Syst.* 14: 395-453.
- Yu L., Milton N., Groleau E.G., Mishra D.S., Vansickle R.E. 1999.** Existence of a mannitol hydrate during freeze-drying and practical implications. *J. Pharm. Sci.* 88: 196-198.
- Zaru M., Mourtas S., Klepetsanis P., Fadda A.M., Antimisias S.G. 2007.** Liposomes for drug delivery to the lungs by nebulization. *Eur. J. Pharm. Biopharm.* 67: 655-666.
- Zeng X.M., Martin G.P., Marriott C. 2001.** Medicinal aerosols. In: Zeng X.M., Martin G.P., Marriott C. (Eds.), *Particulate Interactions in Dry Powder Formulations for Inhalation*. Taylor & Francis, New York, NY, pp. 65-102.
- Zhang Y., Zhang Y. 2007.** Formation and reduction of acrylamide in Maillard reaction: A review based on the current state of knowledge. *Crit Rev Food Sci Nutr* 47: 521-542.
- Zhang J., Wu L., Chan H-K, Watanabe W. 2011a.** Formation, characterization, and fate of inhaled drug nanoparticles. *Adv. Drug Delivery Rev.* 63: 441-455.
- Zhang H., Fan Q., Wang Y.E., Neal C.R., Zuo Y.Y. 2011b.** Comparative study of clinical pulmonary surfactants using atomic force microscopy. *Biochim. Biophys. Acta* 1808: 1832-1842.
- Zhou Q.T., Morton D.A.V. 2011.** Drug-lactose binding aspects in adhesive mixtures: Controlling performance in dry powder inhaler formulations by altering lactose carrier surfaces. *Adv. Drug Deliv. Rev.* doi:10.1016/j.addr.2011.07.002.

VII. APPENDICES

APPENDIX I: Current DPI devices available on the market

(Islam and Gladki, 2008)

Device	DPI type	Company	Delivery method	Drugs	Diseases
Breath actuated Unit-dose and Multiple-unit dose DPIs					
Spinhaler	Unit-dose	Aventis	Capsule	SC	Asthma
Rotahaler	Unit-dose	GlaxoSmithKline	Capsule	SS, BDP, SS+BDP	Asthma
Inhalator	Unit-dose	Boehringer-Ingelheim	Capsule	Fenoterol	Asthma
Cyclohaler	Unit-dose	Pharmachemie	Capsule	SS, BDP, IB, BUD	Asthma
Handihaler	Unit-dose	Boehringer-Ingelheim	Capsule	Tiotropium	COPD
Aerolizer	Unit-dose	Novartis	Capsule	F, BUD, BDP	Asthma
FlowCaps	Unit-dose	Hovione	Capsule	NA	Asthma
TwinCaps	Unit-dose	Hovione	Capsule	Neuraminidase inhibitors	Influenza
Diskhaler	Multiple-unit dose	GlaxoSmithKline	Blister disk	SX, BDP, FP, zanamivir	Asthma, Influenza
Diskus/ Accuhaler	Multiple-unit dose	GlaxoSmithKline	Blister strip	SS, SX, FP, SX + FP	Asthma
Aerohaler	Multiple-unit dose	Boehringer-Ingelheim	-	IB	Asthma
Eclipse	Multiple-unit dose	Aventis	Capsule	SC	Asthma
Breath actuated Multi-dose DPIs					
Turbohaler	Multi-dose	Astra Zeneca	Reservoir	SS, TS, BUD, F, F+BUD	Asthma
Easyhaler	Multi-dose	Orion Pharma	Reservoir	SS, BDP	Asthma
Ultrahaler	Multi-dose	Aventis	Reservoir		Asthma
Pulvinal	Multi-dose	Chiesi	Reservoir	SS, BDP	Asthma
Novolizer	Multi-dose	Meda	Reservoir cartridge	BUD, SS, F	Asthma, COPD
MAGhaler	Multi-dose	Boehringer-Ingelheim	Reservoir	SS	Asthma
Clickhaler	Multi-dose	Innoveta Biomed	Reservoir	SS, BDP	Asthma
Asmanex Twisthaler	Multi-dose	Schering-Plough Corporation	Reservoir	MF	Asthma
Taifun	Multi-dose	LAB Pharma	Reservoir	SS	Asthma
Active DPIs					
Inhance	Unit-dose	Inhale Therap.	Blister	Insulin	Diabetes
Airmax	Multi-dose	Norton Healthcare	Reservoir	F, BUD	Asthma, COPD

MF: Mometasone furoate, SS: Salbutamol sulphate, SX: Salmeterol xinafoate, FP: Fluticasone propionate, BUD: Budesonide, TS: Terbutaline sulphate, F: Formoterol, IB: Ipratropium bromide, SC: Sodium cromoglycate, BDP: Beclomethasone dipropionate

APPENDIX II: Future/next generation DPIs (in development stage)

(Islam and Gladki, 2008)

Device	DPI type	Company	Delivery method	Drugs	Diseases
Omnihaler Active	Unit-dose	Innoveta Biomed Ltd	–	–	–
Actispire Active	Unit-dose	Britania	Powder	Pumactant	
DirectHaler	Unit-dose	Direct-Haler	Premetered	–	Asthma/COPD
Turbospin	Unit-dose	PH & T	Capsule	–	Asthma
AIR	Unit-dose	Alkermes	Capsule	Insulin	Diabetes
CONIX ONE	Unit-dose	Cambridge Consultant	Foil seal	Vaccines ...	Avian flue, COPD, Asthma
Microhaler passive	Unit-dose	Harris Pharmaceutical	Capsule	SC	Asthma
Twincer	Unit-dose	University of Groningen	Blister	Colistin, tobramycin, insulin, hemin, morphine, ciclosporin, vaccines	Multi purpose
Technohaler Passive	Multiple-unit dose	Innoveta Biomed Ltd.	Blister	–	Asthma
Spiros/ Breath activated active	Multiple-unit dose	Dura	Blister	Albuterol sulphate	Asthma
Prohaler	Multiple-unit dose	Valois	Blister	–	Asthma
MF-DPI Passive	Multiple-unit dose	–	Reservoir	MF	Asthma
MicroDose/ electronic breath activated	Unit or Multiple-unit dose	MicroDose Technologies	Blister	Insulin, beta agonists, corticosteroids	Multi purpose
NEXT	Multi-dose	Chiesi	Reservoir	–	Asthma, COPD
Bulkhaler Passive	Multi-dose	Asta Medica	Reservoir	–	Asthma
Miat-Haler Passive	Multi-dose	MiatSpA	Reservoir	Formoterol, Fluticasone, BUD	Asthma, COPD
Aspirair Active	Multi-dose	Vectura	Reservoir	Apomorphine hydrochloride	Erectile dysfunction
Taifun	Multi-dose	Focus Inhalation	Reservoir	Fentanyl	Cancer pain
JAGO	Multi-dose	SkyPharma	Reservoir	SS	Asthma
Cyclovent	Multi-dose	Pharmachemie	Reservoir	Opioids (Morphine)	Dyspnoea, pain
Dispohaler	Multi-dose	AC Pharma	–	–	–
Otsuka DPI/breath actuated	–	Otsuka Pharmaceutical Co. Ltd.	Compact cake	–	Asthma
Acu-Breath	Multi-dose	Respirics	Reservoir	Fluticasone propionate	Asthma
Swinhaler	Multi-dose	Otsuka Pharmaceutical	Reservoir	Procaterol, BUD	Asthma
Certihaler/breath actuated	Multi-dose	Novartis /Skye Pharma	Reservoir	Formoterol	Asthma

MF: Mometasone furoate, SS: Salbutamol sulphate, BUD: Budesonide, SC: Sodium cromoglycate

APPENDIX III: Relative efficacy and toxicity of various agents in promoting pulmonary protein absorption

(Hussain et al., 2004)

Enhancer	Concentration	Animal model	Efficacy ^a	Toxicity ^b	Reference
Sodium taurocholate	8 mM	In vivo (beagle dog)	2.5	1	Johannson et al., 2002
	16 mM		6.1	2	
	32 mM		8.9	4	
Sodium glycocholate	10 mM	In-situ (rat trachea)	2.4		Okumura et al., 1992
	50 mM		5.1		
	10 mM		4	0	
Surfactin	1 mM		1.1		Okumura et al., 1992
	10 mM		6.1		
Span 85	1%		3.1		
Lauryl- β -D-maltoside	1 mM		3.4	0	Yamamoto et al., 1997
	5 mM		5.7	3	
	10 mM		6.2	5	
<i>Fatty acids</i>					
Palmitic acid	0.5%		1.2		Kobayashi et al., 1994
Palmitoleic acid			2.5		
Stearic acid			1		
Oleyl alcohol			1		
Oleic acid	25 μ g/dose		1.2		Kobayashi et al., 1996
	250 μ g/dose		1.6		
Lecithin	25 μ g/dose		1.1		
	250 μ g/dose		1.5		
Sodium oleate	0.5%		2.2		Kobayashi et al., 1994
Ethyl oleate			1.2		
PE oleyl ether			2.6		
Sorbitantrioleate			1.8		
PE sorbitan trioleate			1.5		
Glycerol trioleate			1		
Linoleic acid			2.5		
linoleic acid – hydrogen castor oil	10 mM	In-situ (rat trachea)	3.9	0	Yamamoto et al., 1997
Dimethyl- β -cyclodextrin	25 μ g/dose		1.2		Kobayashi et al., 1996
	250 μ g/dose		2.4		
Liposomes	14 mg/ml		1.8	4	Liu et al., 1993
<i>Lanthanides</i>					
CeCl ₃	0.2 mg/kg	In-situ (rat trachea)	4.3		Shen et al., 2000
GdCl ₃			4.4		
LaCl ₃			2.3		
LuCl ₃			1.2		
EDTA	10 mM		1.8	1	Yamamoto et al., 1997
	100 mM		0.6		Okumura et al., 1992
Salicylate	100 mM		0.5		
Carboxymethyl cellulose	0.5%		1.1		
Gelatin	1%		0.4		
HMAP ^c	16 mg/kg	In vivo (rats)	2.2	2	Suarez et al., 2001; Garcia-Contreras et al., 2001

^a Expressed as a ratio of the AUC of the test formulation to the AUC of the control. ^b Graded on scale 1-5 (lowest to highest toxicity; 0, non-toxic). ^c HMAP: hydroxy methyl amino propionic acid

APPENDIX IV: Examples of inhibition of protein aggregation in the dry state (Wang, 2005)

Processes/protein	Protein formulations	Study conditions	Results	References
examples				
Freezing/drying				
GDH	0.1 mg/ml in 10 mM citrate, pH 6.5	Quench freezing and thawing	A500 > 0.05	Chang et al. (1996a, 1996b, 1996c)
	+ 0.01% Tween 80		A500 < 0.01	
Hemoglobin	50 mg/ml in PBS, pH 7.4	Freeze-thawing for 5 times (-20°C)	Particles ≥ 2 μm ~ 1.4 x 10 ⁴ ml ⁻¹	Kerwin et al. (1998)
	+ 0.0125% Tween 80		Particles ≥ 2 μm ~ 2 x 10 ³ ml ⁻¹	
	+ 0.1 M sucrose		Particles ≥ 2 μm ~ 7 x 10 ³ ml ⁻¹	
Bovine IgG	1 mg/ml in 0.22 M NaCl and 10 mM phosphate, pH 7.1	Freeze-drying	A350 = 0.54	Sarciaux et al. (1999)
	+ 0.02% (w/w) Tween 80		A350 = 0.18	
Bovine insulin	1 mg/ml in phosphate, pH 7.4	Freeze-drying	Light scattering >1300	Katakam and Banga (1995)
	+ 1 mg/ml dextrose		Light scattering <300	
LDH	0.1 mg/ml in 10 mM citrate, pH 6.5	Quench freezing and thawing	A500 = 0.11	Chang et al. (1996a, 1996b, 1996c)
	+ 0.01% Tween 80		A500 < 0.01	
rhMAb	10 mg/ml	Spray-drying	Aggregated by ~5.6%	Andya et al. (1999)
	+ Trehalose at 100 mol:1 mol protein		Aggregated by <1%	
	+ Lactose at the same ratio		Aggregated by ~1%	
	+ Mannitol at the same ratio		Aggregated by ~2.6%	
Trypsinogen	20 mg/ml in 1 mM HCl, pH 3.1	Spray-drying	Dimerisation = 8%	Tzannis and Prestrelski (1999)
	+ 1% sucrose		Dimerisation <2%	
	+ 2% sucrose		Dimerisation <0.5%	
Solid storage				
Factor IX	0.5 mg/ml rFIX in 1% sucrose, 255 mM glycine, 0.005% Tween 80, and 10 mM phosphate, pH 7.0	Incubation (lyophilised) at 30°C for 3 months	>2.5% aggregation	Bush et al. (1998)
	Replacing phosphate with histidine		<0.2% aggregation	
Factor XIII	2 mg/ml in 0.1 mM EDTA and 10 mM Tris, pH 8	Incubation (lyophilised) at 40°C for 1 month	Aggregated (soluble) by ~60%	Kreilgaard et al. (1998a, 1998b)
	+ 3.5% dextran		Aggregated by ~50%	
	+ 100 mM mannitol, trehalose, or sucrose		Aggregated by ~40%, <10% or <5%	
hGH	2 mg/ml in phosphate buffer, pH 7.4	Incubation (lyophilised) at 25°C for 2 months	~6% aggregated	Pikal et al. (1991)
	+ 2 mg/ml glycine		~3.5% aggregated	
	+ 2 mg/ml glycine and 10 mg/ml mannitol		~2.5% aggregated	
rhIL-1ra	10 mg/ml in 2% glycine and 10 mM citrate, pH 6.5	Incubation (lyophilised) at 50°C for 1 week	Turbidity A500 = 0.075	Chang et al. (1996a, 1996b, 1996c)
	+ 1% maltose, trehalose, sucrose, or sorbitol		A500 = 0.003, 0.005, 0.008, or 0.037	
	+ 1% sucrose and 4% mannitol, 4% alanine, or 2% glycine		A500 = 0.006, 0.021 or 0.008	
rHA	1 mg/ml, pH 7.3	Incubation (lyophilised) at 37°C and 96% RH for a day	Aggregated by 81%	Costantino et al. (1995a, 1995b)
	+ Dextran at 1:6, 1:1, or 3:1 (g dextran:g protein)		Aggregated by 63%, 12%, or 6%	
rHA	1 mg/ml, pH 7.3	Incubation (lyophilised) at 37°C and 96% RH for a day	Aggregated by ~80%	Costantino et al. (1995a, 1995b)
	+ Sorbitol at a ratio of 1:50, 1:6, 1:1 (g sorbitol:g rHA)		Aggregated by ~80%, ~40%, or <5%	
	+ D-glucuronic acid, D-glucamine, NaCl, or lactic acid at a ratio of 1:6		Aggregated by ~20%, <5%, <5%, or <5%	
Tetanus toxoid	1 mg/ml, pH 7.3	Incubation (lyophilised) at 37°C and 86% RH for 9 days	Aggregated by 88%	Costantino et al. (1996)
	+ NaCl or sorbitol at a ratio of 1:5 (1 g:5 g protein)		Aggregated by 58% or 21%	
rhMAb	10 mg/ml	Incubation (spray-dried) at 30°C	Aggregation rate constant = 0.0022 day ⁻¹	Costantino et al. (1998)
	+ Mannitol at a ratio of 1:9 or 1:4 (g mannitol:g protein)		Aggregation rate constant = 0.0013 or 0.0009 per day	
TNF	0.25 mg/ml in 1% mannitol and 10 mM citrate, pH 6.5	Incubation (lyophilised) at 37°C for 1 month	Dimerisation by 1.5%	Hora et al. (1992a, 1992b)
	+ 2% trehalose		Dimerisation by 0.2%	
	+ 2% dextran, 2% PEG-6000, or 0.5% sucrose		Dimerisation not detectable	

A₃₅₀ and A₅₀₀ : optical density at 350 nm and 500 nm, respectively

APPENDIX V: Effect of absorption enhancers on pulmonary insulin absorption.
(Siekmeier and Scheuch, 2008)

Substance	Species	Dosage form	Concentration or pH value	Efficacy ¹	Reference
Sodium taurocholate	Beagle dog	Solution	8 mM, 16 mM, 32 mM	2.5, 6.1, 8.9	Johansson et al., 2002
Sodium glycocholate	Rat	Solution	10 mM, 50 mM	2.4, 5.1	Komada et al., 1994; Okumura et al., 1992
Sodium glycocholate	Rat	Solution	10 mM	4.2	Yamamoto et al., 1994
Bile salt	Human	Dry powder	1.028 µg/87.2 U insulin	1.6	Heinemann et al., 2000
Surfactin	Rat	Solution	1 mM, 10 mM	1.1, 6.1	Okumura et al., 1992
Span 85	Rat	Solution	1%	1.1, 6.1	Okumura et al., 1992
Span 85	Rat	Solution	1%	7.2	Todo et al., 2001
Span 85	Rat	Dry powder	160 µg/dose	0.7	Todo et al., 2001
N-Lauryl-β-D-maltopyranoside	Rat	Solution	5 mM	7.1	Yamamoto et al., 1994
MM ²	Rat	Solution	10 mM	2.5	Yamamoto et al., 1994
Liposomes	Rat	Solution	14 mg/ml	1.8	Li and Mitra, 1996 ; Liu et al., 1993
Cyclodextrins	Rat	Solution	Hydroxypropyl-β-cyclodextrin: 5% γ-cyclodextrin: 5% β-cyclodextrin: 1% α-cyclodextrin: 5% Dimethyl-β-cyclodextrin: 5%	Hydroxypropyl-β-cyclodextrin: 1.2 γ-cyclodextrin: 1.7 β-cyclodextrin: 2.0 α-cyclodextrin: 2.3 Dimethyl-β-cyclodextrin: 2.8	Shao et al., 1994
Lanthanides (CeCl ₃ , GdCl ₃ , LaCl ₃ , LuCl ₃)	Rat	Solution	0.2 mg/kg	CeCl ₃ : 4.2, GdCl ₃ : 4.4, LaCl ₃ : 2.3, LuCl ₃ : 1.2	Shen et al., 2000
EDTA ³	Rat	Solution	100 mM	0.6	Okumura et al., 1992
Salicylate	Rat	Solution	100 mM	0.5	Okumura et al., 1992
Citrate	Rat	Solution	pH 3.0; pH 5.0	4.5, 3.4	Todo et al., 2001
Citrate	Rat	Dry powder	36 µg/dose citric acid	2.1	Todo et al., 2001
Citrate	Rat	Solution	pH 3.0	3.2	Komada et al., 1994
Citrate	Rat	Dry powder	0.5 mg/dose citrate	2.7	Komada et al., 1994
Carboxy methylcellulose	Rat	Solution	0.5%	1.1	Okumura et al., 1992
Gelatin	Rat	Solution	1.0%	0.4	Okumura et al., 1992
HMAP ⁴	Rat	Solution	16 mg/kg	2.2	Garcia-Contreras et al., 2001; Suarez et al., 2001

¹Efficacy: Ratio of the area under the curve (AUC) or biological response between the dosage form with absorption enhancer and that without absorption enhancer; ²MM: Mixed micelles of linoleic acid and HCO60 (hydrogenated castor oil); ³EDTA: Ethylene diamine tetraacetic acid; ⁴HMAP: Hydroxymethyl amino propionic acid.

APPENDIX VI: Discontinued formulation/device systems for inhaled administration of insulin

(modified from Siekmeier and Scheuch, 2008)

Trade name	Status before discontinuation	Formulation/device	Selected clinical data
AIR® insulin system (Alkermes/Eli Lilly)	Phase III	DPI. Large porous particles of low density obtained by spray-drying, containing insulin within an excipient matrix composed of DPPC and albumin (Vanbever et al., 1999). AIR passive DPI with capsule's spin motion during inhalation (Muchmore et al., 2007). Geometric diameter of 5–30 µm (MMAD of ~ 3 µm)	Studies in patients with types 1 and 2 diabetes mellitus. Formulation with sustained release (PK similar to an intermediate insulin such as Humulin L) Bioavailability: 10-16 %
AERx® iDMS (Aradigm/Novo Nordisk)	Phase III	Nebulised insulin. Liquid insulin packed into single-use strips. Regulation of the breathing movement by means of microprocessors and electronic optimisation of insulin release within the inspiratory flow. MMAD of ~ 2 µm	More rapid absorption and onset of action than s.c. regular insulin. Variability of PD in type 1 diabetics similar to s.c. insulin. Similar quality of metabolic adjustment in type 2 diabetics than with s.c. regular insulin. Bioavailability: 10-16 %
Microdose DPI® (Microdose Tech./Elan Corporation)	Phase II	Dry powder insulin packed into blisters. Desaggregation by means of a piezo-vibrator. MMAD of ~ 1.5 µm, 84% of the particles < 4.7 µm	Little clinical data; well tolerated in clinical studies, bioavailability about 18% compared with s.c. insulin; more rapid absorption than s.c. regular insulin
Unknown (Abbott)	Phase II	Insulin crystals administered by means of a hand-held breath actuated inhaler (BAI) driven by a propellant	Comparison to Lantus® (insulin glargine) revealed a comparable effectiveness in controlling blood glucose concentrations
Aerodose® (Aerogen)	Phase II (stopped in 2003)	Liquid insulin. Administration in a breath-activated multiple dose inhaler. Mean particle diameter of 3.2 µm, 87% of the particles between 1-6 µm	More rapid onset of action than s.c. regular insulin. Reproducibility of PK similar to s.c. insulin. Linear dose-response-relationship of PD. Bioavailability: 10 - 22 %
Bio-Air® (BioSante Pharmaceuticals)	Phase I	Coated dry particles based on calcium phosphate nanoparticle carriers. Administration by means of a calcium phosphate nanoparticulate delivery system.	Little data available; preclinical studies demonstrated an extension of the hypoglycemic effect after insulin inhalation.
Alveair® (CoreMed/Fosun and Xuzhou)	Phase I	Liquid insulin. Administration by means of a generic hand-held device	Little clinical data; the manufacturer states a very high level of

			Bioavailability.
Unknown (Epic Therapeutics)	Phase I	Microspheres of recombinant human insulin (PROtein MAtRiX microspheres; ProMaxx®) Administration by means of a DPI (Cyclohaler) < 10% excipients 95% of particles with MMAD between 0.95–2.1 µm (mean: 1.5 µm)	Little clinical data; well-tolerated in a phase I trial, bioavailability > 12% compared with s.c. insulin; more rapid absorption than s.c. regular insulin
Spiros® (Elan Pharm.)	Phase I (stopped in 2004)	Dry powder insulin packed into blisters Release by means of a hand-held battery driven multiple dose inhaler. Development of a novel powder dispersion system (Spiros-S2) without electromechanical components for administration at low inspiratory flow rates (15–30 l/min)	Small number of studies only in healthy individuals. Administered doses consistent over a wide range of inspiratory flow rates

PK: Pharmacokinetics, PD: Pharmacodynamics

APPENDIX VII: Validation of the HPLC method used for the dosage of insulin

Linearity

Mean regression curve

N= 18

		concentration (mg/ml)	Signal	Var	(xij - xm)	(yij - ym)	ij - xm)*(yij - y	(xij - xm) ²	(yij - ym) ²
Day 1	Solution 1	0,01	90,08	9,29E+02	-0,71	-6,85E+03	4,85E+03	0,50	4,70E+07
		0,01	92,15		-0,71	-6,85E+03	4,85E+03	0,50	4,69E+07
		0,02	143,88		-0,70	-6,80E+03	4,77E+03	0,49	4,62E+07
Day 1	Solution 2	0,05	482,76	3,31E+04	-0,67	-6,46E+03	4,31E+03	0,45	4,17E+07
		0,05	487,58		-0,67	-6,46E+03	4,31E+03	0,45	4,17E+07
		0,08	800,26		-0,64	-6,14E+03	3,94E+03	0,41	3,77E+07
Day 1	Solution 3	0,10	963,42	9,08E+04	-0,62	-5,98E+03	3,69E+03	0,38	3,58E+07
		0,10	963,67		-0,62	-5,98E+03	3,69E+03	0,38	3,58E+07
		0,15	1485,59		-0,56	-5,46E+03	3,08E+03	0,32	2,98E+07
Day 1	Solution 4	0,50	4790,02	2,28E+06	-0,21	-2,15E+03	4,62E+02	0,05	4,64E+06
		0,50	4876,57		-0,22	-2,07E+03	4,59E+02	0,05	4,27E+06
		0,77	7450,09		0,05	5,07E+02	2,46E+01	0,00	2,57E+05
Day 1	Solution 5	1,01	9660,28	9,06E+06	0,29	2,72E+03	7,84E+02	0,08	7,38E+06
		0,99	9860,44		0,27	2,92E+03	7,97E+02	0,07	8,51E+06
		1,53	14971,00		0,81	8,03E+03	6,54E+03	0,66	6,44E+07
Day 1	Solution 6	2,01	19050,90	3,24E+07	1,29	1,21E+04	1,57E+04	1,68	1,47E+08
		1,98	19621,30		1,26	1,27E+04	1,60E+04	1,60	1,61E+08
		3,06	29184,50		2,35	2,22E+04	5,22E+04	5,51	4,95E+08
Means		0,72	6943,03						
Stand. deviation (Sxij and Syij)		0,89	8588,94						
Sum		12,92	124974,49		0,00	0,00	130451,43	13,58	1,25E+09

Mean regression curve			
Slope	9608,404392	48,27822941	Y-intercept
Slope S.D.	55,00887053	61,97184549	Y-intercept S.D.
r ²	0,99947585	16	DF.
F	30509,6405	657329,3328	Resid. sum squares
Reg. sum squares	1253430102		

Manual calculation

Slope = b	$\Sigma ((x_{ij} - x_m) * (y_{ij} - y_m)) / \Sigma (x_{ij} - x_m)^2$	=	9608,404392
Y-intercept = a	$y_m - b * x_m$	=	48,27822941
Xij and Yij Covariance	$\Sigma ((x_{ij} - x_m) * (y_{ij} - y_m)) / (N - 1)$	=	7673,613586
Corr. Coeff.r	$S_{xijyij} / (S_{xij} * S_{yij})$	=	0,999737891
Corr. Coeff.r ²	$r * r$	=	0,99947585
S ² R	$(\Sigma (y_{ij} - y_m)^2 - b^2 * \Sigma (x_{ij} - x_m)^2) / (N - 2)$	=	41083,0833
Y-intercept variance = S ² a	$S^2R * (1/N + (x_m^2 / (\Sigma (x_{ij} - x_m)^2)))$	=	3840,509633
Y-intercept S.D. = Sa	$\sqrt{S^2a}$	=	61,97184549

Slope Var. = S^2b $S^2R / S(x_{ij} - \bar{x}_m)^2$ - 3025,975837
 Slope S.D. = Sb $\sqrt{S^2b}$ - 55,00887053

Linearity

Comparison Y-intercept with 0

Following inequality is controlled : $(|a| / S_a) < t(\alpha; N-2)$

$|a| / S_a =$ 0,779034883
 $t_{\text{tabulated}}(0.05; 16) =$ 2,119905285

So Y-intercept is not significantly different from 0 at 0.05 level

Intra-groups variances homogeneity test (Cochran test)

Following inequality is controlled : $(S^2_{\text{max}} / \sum S^2_j) < C(\alpha; \text{nbre de groupes}; n-1)$

Group j (= "Solution")	1	2	3	4	5	6		
n_j	3	3	3	3	3	3		
S^2_j	9,29E+02	3,31E+04	9,08E+04	2,28E+06	9,06E+06	3,24E+07		

$\sum S^2_j =$ 43881218

$C = S^2_{\text{max}} / \sum S^2_j =$ 7,39E-01

$C_{\text{tabulated}}(0.05; 6; 2) =$ 0,6161

So variances are inhomogeneous at 0.05 level

Intra-groups variances homogeneity test (Bartlett test)

- For each group, variance = sum of the squared residuals / (effectif-1) = $SCE_i / (n_i - 1)$
- Sum of the squared residuals relative to all data = $SCE = \text{sum of } SCE_i$
- Total variance = $\sigma^2_{\text{est.}} = SCE / (n-p)$ where $(n-p) = (\text{total nbre of observations} - \text{groups number})$

Null hypothesis : equality of the variances : $\rightarrow \sigma^2_1 = \sigma^2_2 = \sigma^2_3 = \dots = \sigma^2_p$

If null hypothesis is true, $\sigma^2_{\text{est.}}$ is a non biased estimation of σ^2

Following inequality is controlled $\chi^2_{\text{obs}} = \frac{(n-p) * \ln(\sigma^2_{\text{est.}}) - \sum [(n_i-1) * \ln(\sigma^2_i)]}{1 + (1 / \{3 * (n-1)\}) * (\sum [1 / (n_i-1)] - 1 / (n-p))}$ $< \chi^2(1-\alpha; p-1)$

When effectives are constant and equivalent to n , expression can be simplified:

Following inequality is controlled $\chi^2_{\text{obs}} = \frac{2.3026 * (n-1) * [p * \log(SCE / p) - \sum \log(SCE_i)]}{1 + \{(p+1) / [3 * p * (n-1)]\}}$ $< \chi^2(1-\alpha; p-1)$

Group j (= "Solution")	1	2	3	4	5	6	Sums
nj	3	3	3	3	3	3	18
nj-1	2	2	2	2	2	2	12
SCEj	1,86E+03	6,62E+04	1,82E+05	4,57E+06	1,81E+07	6,48E+07	8,78E+07
log (SCEj)	3,269084718	4,820862782	5,259322382	6,65980334	7,258171242	7,811731358	35,07897582
Variance σ^2	9,29E+02	3,31E+04	9,08E+04	2,28E+06	9,06E+06	3,24E+07	—
log σ^2	2,968054723	4,519832787	4,958292386	6,358773345	6,957141247	7,510701362	—
1/(nj-1)	0,5	0,5	0,5	0,5	0,5	0,5	3

Variance related to all observations: $\sigma^2_{est} = SCE / (n - p)$

= 7313536,284

log (σ^2_{est}) =

= 6,86412742

$\chi^2_{obs} = \frac{2,3026 * (n-1) * [p * \log(SCE / p) - \sum [\log(SCE_j)]]}{1 + ((p+1) / [3 * p * (n-1)])}$

= 30,50472402

p = 1,17308E-05

$\chi^2_{(1-\alpha; p-1)}$

= 11,07

Table

11,07049775

Excel calculation

So, the variances are not homogeneous at 0.05 level

Intra-group variances homogeneity test (Harvey test)

When batch number is constant and equal to n

Following inequality is controlled: $H_{obs} = (SCE_{max} / SCE_{min}) < H(1-\alpha; \text{nbre of groups}; \text{ddl}n-1 \text{ of the estimated variances})$

Group j (= "Solution")	1	2	3	4	5	6	Somme
nj	3	3	3	3	3	3	18
nj-1	2	2	2	2	2	2	12
SCEj	1,86E+03	6,62E+04	1,82E+05	4,57E+06	1,81E+07	6,48E+07	87762435,41
Variance σ^2	9,29E+02	3,31E+04	9,08E+04	2,28E+06	9,06E+06	3,24E+07	—

$H_{obs} = 34885,61557$

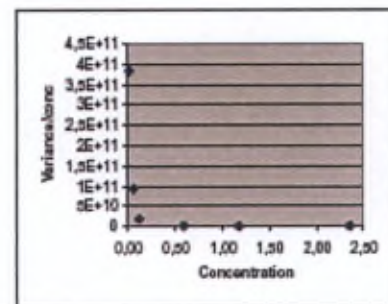
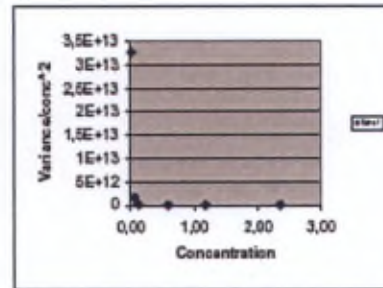
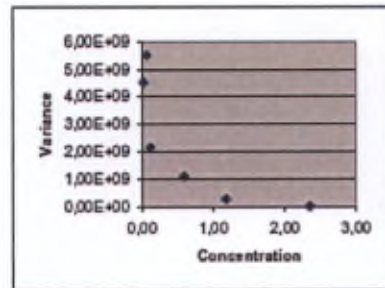
$H_{(1-\alpha; k; n)}$

So, the variances are not homogeneous at 0.05 level

Determination of the adequate transformation

Variance vs [] If constant: weighting 1 or no transformation
 Variance / [] vs [] If constant: weighting 1 / [] or square root transformation for X and Y
 Variance / []² vs [] If constant: weighting 1 / []² or log transformation for X and Y

Solution	Conc.	Variance	Variance / Conc.	Variance / Conc. ²
1	0,01	4,54E+09	3,85581E+11	3,27749E+13
2	0,06	5,52E+09	93906658283	1,59648E+12
3	0,12	2,17E+09	18407200960	1,56165E+11
4	0,59	1,10E+09	1877830794	3192449626
5	1,18	2,63E+08	223429951,4	189951074,5
6	2,35	6,84E+06	2907053,672	1235712



Conclusion: we have to proceed to a 1 / []² weighting or a log X and log Y transformation

Transformed data

N =

18

Linearity

		log Conc.	log Signal	(xij - xm)	(yij - ym)	(xij - xm)*(yij - ym)	(xij - xm) ²	(yij - ym) ²	Variance	m(yj)	(yij - m(yj)) ²
Day 1	Solution 1	-2,00	1,95	-1,342	-1,374	1,844	1,801	1,889	0,013149362	2,03	0,005053103
2	1	-2,00	1,96	-1,349	-1,365	1,840	1,819	1,862			0,003745696
3	1	-1,81	2,16	-1,159	-1,171	1,358	1,344	1,372			0,017499924
1	2	-1,30	2,68	-0,643	-0,645	0,415	0,413	0,417	0,015750985	2,76	0,005565966
2	2	-1,31	2,69	-0,650	-0,641	0,417	0,422	0,411			0,004940894
3	2	-1,12	2,90	-0,480	-0,426	0,196	0,212	0,181			0,02099511
1	3	-1,00	2,98	-0,342	-0,345	0,118	0,117	0,119	0,011784629	3,05	0,003935176
2	3	-1,00	2,98	-0,346	-0,345	0,119	0,120	0,119			0,003921248
3	3	-0,81	3,17	-0,159	-0,157	0,025	0,025	0,025			0,015712835
1	4	-0,30	3,68	0,357	0,351	0,125	0,127	0,123	0,011788367	3,75	0,004426692
2	4	-0,31	3,69	0,350	0,359	0,126	0,123	0,129			0,003452377
3	4	-0,12	3,87	0,540	0,543	0,292	0,291	0,295			0,015697665
1	5	0,00	3,98	0,658	0,656	0,432	0,433	0,430	0,011528011	4,05	0,00440751
2	5	0,00	3,99	0,651	0,665	0,433	0,424	0,442			0,003304272
3	5	0,19	4,18	0,841	0,846	0,711	0,707	0,716			0,015344241
1	6	0,30	4,28	0,959	0,951	0,912	0,920	0,904	0,010701149	4,35	0,004358158
2	6	0,30	4,29	0,952	0,964	0,918	0,907	0,929			0,002830673
3	6	0,49	4,47	1,142	1,136	1,297	1,304	1,291			0,014213507
Means		-0,66	3,23								
Standard Dev. (Sxj and Syj)		0,82	0,83								
Sum		-11,80	59,92	0,000	0,000	11,579	11,508	11,653			0,149405047

Mean regression curve			
Slope	1,00616184	3,988526362	Y-intercept
Slope S.D.	0,00394565	0,004079177	Y-intercept S.D.
r ²	0,999754012	16	D.F.
F	65027,7364	0,002866539	Resid. sum squares
Reg. sum squares	11,65028514		

Manual calculation

Slope = b	$\Sigma ((x_{ij} - x_m) * (y_{ij} - y_m)) / \Sigma (x_{ij} - x_m)^2$	=	1,00616184
Y-intercept = a	$y_m - b * x_m$	=	3,988526362
Kij and Yij Covariance	$\Sigma ((x_{ij} - x_m) * (y_{ij} - y_m)) / (N - 1)$	=	0,681113975
Corr. Coeff.r	$S_{xijyij} / (S_{xij} * S_{yij})$	=	0,999876998
Corr. Coeff.r ²	$r * r$	=	0,999754012
S ² R	$(\Sigma (y_{ij} - y_m)^2 - b^2 * \Sigma (x_{ij} - x_m)^2) / (N - 2)$	=	0,000179159
Y-intercept variance = S ² a	$S^2R * (1/N + (x_m^2 / (\Sigma (x_{ij} - x_m)^2)))$	=	1,66397E-05
Y-intercept S.D. = S _a	$\sqrt{S^2a}$	=	0,004079177
Slope Var. = S ² b	$S^2R / \Sigma (x_{ij} - x_m)^2$	=	1,55682E-05
Slope S.D. = S _b	$\sqrt{S^2b}$	=	0,00394565

Intra-groups variances homogeneity test (Cochran test)

Following inequality is controlled : $(S^2_{max} / \sum S^2_j) < C$ (a; nbre de groupes; n-1)

Group j (= "Solution")	1	2	3	4	5	6		
n _j	3	3	3	3	3	3		
S ² _j	0.013149362	0.016750995	0.011784629	0.011788367	0.011528011	0.010701169		

$\sum S^2_j =$ 0.074702623

$C = S^2_{max} / \sum S^2_j =$ 0.210849437

C tabulated (0.05 ; 6; 2) = 0.6161

So variances are homogeneous at 0.05 level

Intra-groups variances homogeneity test (Bartlett test)

- For each group, variance = sum of the squared residuals / (effectif-1) = SCE_j / (n_j-1)
- Sum of the squared residuals relative to all data = SCE = sum of SCE_j
- Total variance = $\sigma^2_{est.} = SCE / (n-p)$ where (n-p) = (total nbre of observations - groups number)

Null hypothesis : equality of the variances : $\rightarrow \sigma^2_1 = \sigma^2_2 = \sigma^2_3 = \dots = \sigma^2_p$

If null hypothesis is true, $\sigma^2_{est.}$ is a non biased estimation of σ^2

Following inequality is controlled $\chi^2_{obs} = \frac{(n-p) * \ln(\sigma^2_{est.}) - \sum [(n_i-1) * \ln(\sigma^2_i)]}{1 + \{1 / [\sum (n_i-1)]\} * \{ \sum [1 / (n_i-1)] - 1 / (n-p) \}}$ < χ^2 (1- α ; p-1)

When effectives are constant and equivalent to n, expression can be simplified:

Following inequality is controlled $\chi^2_{obs} = \frac{2.3026 * (n-1) * [p * \log(SCE / p) - \sum \log(SCE_i)]}{1 + \{ (p+1) / [3 * p * (n-1)] \}}$ < χ^2 (1- α ; p-1)

Group j (= "Solution")	1	2	3	4	5	6	Sums
n _j	3	3	3	3	3	3	18
n _j -1	2	2	2	2	2	2	12
SCE _j	2,63 E-02	3,16 E-02	2,36 E-02	2,36 E-02	2,31 E-02	2,14 E-02	1,49 E-01
log (SCE _j)	-1,580069331	-1,501662289	-1,627654079	-1,627516344	-1,637219612	-1,66963879	-9,643662441
Variance σ^2_j	0,013149362	0,016750995	0,011784629	0,011788367	0,011528011	0,010701169	---
log σ^2_j	-1,881096326	-1,802692281	-1,928634075	-1,92854634	-1,938245697	-1,970563786	---
1/(n _j -1)	0,5	0,5	0,5	0,5	0,5	0,5	3

Variance related to all observations $\sigma^2_{est} = SCE / (n - p)$	=	0,012459421	
$\log(\sigma^2_{est}) =$	=	-1,904816978	
$\chi^2_{obs} = \frac{2.3026 * (n-1) * [p * \log(SCE / p) - \sum \log(SCE_{ij})]}{1 + [(p+1) / (3 * p * (n-1))]}$	=	0,080721205	$p = 0,999904322$
$\chi^2_{(1-\alpha; p; n)}$	=	11,07 11,07049775	Table Excel calculation

So, the variances are homogeneous at 0.05 level

Intra-group variances homogeneity test (Hardley test)

When batch number is constant and equal to n

Following inequality is controled $H_{obs} = (SCE_{max} / SCE_{min}) < H(1-\alpha; n; n-1 \text{ of the estimated variances})$

Group j (= "Solution")	1	2	3	4	5	6	Somme
n _j	3	3	3	3	3	3	18
n _j -1	2	2	2	2	2	2	12
SCE _j	2,63 E-02	3,16 E-02	2,36 E-02	2,36 E-02	2,31 E-02	2,14 E-02	0,149405047
Variance σ^2_j	0,013143962	0,015795935	0,011794629	0,011795367	0,011828911	0,010791169	—

$H_{obs} = 1,471893897$

$H(1-\alpha; n; n) > 29,5$

So, the variances are homogeneous at 0.05 level

Signification of the slope test

This test compares the variations due to regression (S2I) to the variation due to experimental and adjustment errors (S2R)

Following inequality is controled: $F = S2I / S2R > F(\alpha; 1; N-2)$

Variations	DF	Sum of squares	Variances	F calculated
total	N-1	$\Sigma T^2 - \Sigma (y_i - \bar{y})^2$		
due to regression	1	$\Sigma T^2 - b^2 * \Sigma [n_j * (x_j - \bar{x})^2]$ $= b^2 * \Sigma (x_j - \bar{x})^2$	$S^2 I = \Sigma T^2 / 1$	
residual (due to errors)	N-2	$\Sigma R^2 = \Sigma T^2 - \Sigma I^2$	$S^2 R = \Sigma R^2 / (N-2)$	$S^2 I / S^2 R$

Variations	DF	Sum of squares	Variances	F calculated
total	17	11,653		
due to regression	1	11,65028514	11,65028514	
residual (due to errors)	16	0,003	0,000179159	65027,7364

Fobs =	6,9027,7364
F _{0,20; 1; 16} =	4,493998418

p (Fobs) = 2,63307E-30

There is a significant slope (and a linear relation) at 0,05 level.

Validity of the regression line test

This test compares adjustment errors (S'L) and experimental errors (S'E):

Following inequality is controlled: $F = S'L / S'E < F(\alpha; k-2; N-k)$

N = nbre of observations	18
k = nbre of groups	6

Variations	DF	Sum of squares	Variances	F calculated
Exp. error	N-k	$\sum E^2 = \sum (y_{ij} - m(y_j))^2$	$S'E = \sum E^2 / (N-k)$	
Regr. error	k-2	$\sum L^2 = \sum R^2 - \sum E^2$	$S'L = \sum L^2 / (k-2)$	$= S'L / S'E$

m(y_j) = mean of y inside each group

Variations	DF	Sum of squares	Variances	F calculated
Exp. error	12	0,149405047	0,012450421	
Regr. error	4	0,147	0,036634627	2,942440914

Fobs =	2,942440914
F _{0,20; 4; 12} =	3,259166727

p (Fobs) = 0,065740319

Adjustment is considered as valid at 0,05 level

Accuracy

Accuracy

		Xi	Yi
Regression curve day 1	Solution 1	0,01	90,08
	2	0,05	482,76
	3	0,10	963,42
	4	0,50	4790,02
	5	1,01	9660,28
	6	2,01	19050,90
		Slope	9483,03
	Y-intercept	19,94	Amt = (Area - 19,94277232) / 9483,03134
	r ²	1,00	Recovery = (Amt / Xi) * 100
Regression curve day 2	Solution 1	0,01	92,15
	2	0,05	487,58
	3	0,10	963,67
	4	0,50	4876,57
	5	0,99	9860,44
	6	1,98	19621,30
		Slope	9917,90
	Y-intercept	-10,64	
	r ²	1,00	
Regression curve day 3	Solution 1	0,02	143,88
	2	0,08	800,26
	3	0,15	1485,59
	4	0,77	7450,09
	5	1,53	14971,00
	6	3,06	29184,50
		Slope	9540,33
	Y-intercept	89,04	
	r ²	1,00	

Accuracy

		x_i	Y_i	$m(Y_j)$	s	var	$(Y_{ij}-Y_m)^2$	$(Y_j - m(Y_j))^2$
Day 1	Solution 1	0,01	73,50	71,88	33,58	1127,36	671,82	2,63
	2	0,01	104,61				26,97	1071,60
	3	0,02	37,52				3831,69	1180,49
2	2	0,05	97,00	98,57	2,46	6,04	5,84	2,46
	2	0,05	101,40				3,95	8,03
	3	0,08	97,31				4,45	1,60
3	3	0,10	98,87	97,63	1,83	3,33	0,30	1,54
	2	0,10	98,48				0,87	0,73
	3	0,15	95,53				15,10	4,39
4	4	0,50	99,98	100,05	0,62	0,39	0,31	0,01
	2	0,50	99,47				0,00	0,34
	3	0,77	100,71				1,67	0,43
5	5	1,01	101,05	101,11	0,68	0,47	2,67	0,00
	2	0,99	100,46				1,08	0,43
	3	1,53	101,82				5,78	0,51
6	6	2,01	99,74	99,73	0,20	0,04	0,11	0,00
	2	1,98	99,92				0,25	0,04
	3	3,06	99,51				0,25	0,04
Mean			99,42					
Sum							42,64	20,54

Results obtained with solution 1 will not be taken into account

Intra-group variances homogeneity test (Cochran test)

Following inequality is controlled: $(S^2_{\max} / \sum S^2_j) < C_{(\alpha; n; \text{nr group}; s-1)}$

Group j (= "Solution")	2	3	4	5	6
n_j	3	3	3	3	3
S^2_j	6,04	3,33	0,39	0,47	0,04

$$\sum S^2_j = 10$$

$$C = S^2_{\max} / \sum S^2_j = 0,588363024$$

$$C_{\text{tabulated}}(0,05; 5; 2) = 0,6838$$

Variances are homogeneous at 0.05 level

Intra-groups variances homogeneity test (Bartlett test)

- For each group, variance = sum of the squared residuals / (effectif-1) = SCEi / (ni-1)
- Sum of the squared residuals relative to all data = SCE = sum of SCEi
- Total variance = $\sigma^2_{est.} = SCE / (n-p)$ where (n-p) = (total nbre of observations - groups number)

Null hypothesis : equality of the variances : $\rightarrow \sigma^2_1 = \sigma^2_2 = \sigma^2_3 = \dots = \sigma^2_p$
 Full hypothesis is true, $\sigma^2_{est.}$ is a non biased estimation of σ^2

Following inequality is controlled $\chi^2_{obs} = \frac{(n-p) * \ln(\sigma^2_{est.}) - \sum [(ni-1) * \ln(\sigma^2_i)]}{1 + \{1 / [3 * (p-1)]\} * \{\sum [1 / (ni-1)] - 1 / (n-p)\}}$ $< \chi^2_{(1-\alpha; p-1)}$

When effectives are constant and equivalent to n, expression can be simplified:

$\chi^2_{obs} = \frac{2.3026 * (n-1) * \{p * \log(SCE / p) - \sum [\log(SCE_i)]\}}{1 + \{(p+1) / [3 * p * (n-1)]\}}$ $< \chi^2_{(1-\alpha; p-1)}$

Group j (= "Solution")	2	3	4	5	6	Sums
nj	3	3	3	3	3	15
nj-1	2	2	2	2	2	10
SCEj	1,21E+01	6,66E+00	7,77E-01	9,35E-01	8,31E-02	2,05E+01
log (SCEj)	1,082398895	0,823662016	-0,109725394	-0,029067138	-1,080269478	0,686998902
Variance σ^2_j	6,04	3,33	0,39	0,47	0,04	--
log σ^2_j	0,781368899	0,52263202	-0,41075539	-0,330097133	-1,381299473	--
1/(nj-1)	0,5	0,5	0,5	0,5	0,5	2,5

Variance related to all observations $\sigma^2_{est.} = SCE / (n-p) = 2,054724143$
 $\log(\sigma^2_{est.}) = 0,312753524$
 $\chi^2_{obs} = \frac{2.3026 * (n-1) * \{p * \log(SCE / p) - \sum [\log(SCE_i)]\}}{1 + \{(p+1) / [3 * p * (n-1)]\}} = 9,141009983 \quad p = 0,103570213$
 $Z^2_{(1-\alpha; p-1)} = 9,49 \quad \text{Table}$
 $9,487729037 \quad \text{Excel calculation}$

So, the variances are homogeneous at 0.05 level

Intra-group variances homogeneity test (Hardley test)

When batch number is constant and equal to n

Following inequality is controlled $H_{obs} = (SCE_{max} / SCE_{min}) < H(1-\alpha; n; \text{nbre of groups}; ddln-1 \text{ of the estimated variances})$

Group j (= "Solution")	2	3	4	5	6	Sums
n _j	3	3	3	3	3	15
n _j -1	2	2	2	2	2	10
SCE _j	1,21E+01	6,66E+00	7,77E-01	9,35E-01	8,31E-02	20,54724143
Variance σ ² _j	6,04	3,33	0,39	0,47	0,04	--

H_{obs} = 145,4348117

H_(1-0,05; 3; 2)

So, the variances are homogeneous at 0.05 level

test of the validity of the means

This test compares inter-groups errors and intra-groups errors.

Following inequality is controlled: $F = S^C / S^E < F(\alpha; k-1; N-k)$

Variations	DF	Sum of squares	Variances	F calculated
total	N-1	$\Sigma T^2 = \Sigma (Y_{ij} - Y_m)^2$		
intra-groups	N-k	$\Sigma E^2 = \Sigma [Y_{ij} - m(Y_j)]^2$	$S^E = \Sigma E^2 / (N-k)$	
inter-groups	k-1	$\Sigma C^2 = \Sigma T^2 - \Sigma E^2$	$S^C = \Sigma C^2 / (k-1)$	S^C / S^E

Variations	DF	Sum of squares	Variances	F calculated
total	14	42,64		
intra-groups	10	20,54	2,05403225	
inter-groups	4	22,10	5,525224066	2,68994027

F_{obs} = 2,68994027
 F_(0,05; 4; 10) = 3,478049691

-> Variations between the different groups are due to experimental errors

Estimation of the mean recovery

- Taking each group into account:

Mean recovery	=			94,83
S.D.	=			15,71
Confidence interval	$\pm [t_{(\alpha;N-1)} * s] / \sqrt{N} =$			7,81
From		87,02	to	102,64

- Taking groups 2 to 6 into account:

Mean recovery	=			99,42
S.D.	=			1,74
Confidence interval	$\pm [t_{(\alpha;N-1)} * s] / \sqrt{N} =$			0,96
From		98,45	to	100,38

Precision

2 Factors Analysis of variance with paired results

3 standard concentrations, measured in triplicate for 3 different days

	Day 1	Day 2	Day 3	Mean	
insulin 0,1 mg/ml	0,10 0,11 0,10	0,10 0,10 0,10	0,11 0,11 0,10	0,10	
insulin 1 mg/ml	1,05 1,06 1,05	1,06 1,06 1,06	1,08 1,08 1,08	1,06	Sample variation SD ² 1,03 CMe 9,28 SCEe 18,55 = SD ² * nj * nrep. = CMe * (ne-1)
insulin 2 mg/ml	2,12 2,12 2,11	2,13 2,13 2,12	2,16 2,16 2,15	2,13	
Mean	1,09	1,10	1,11	1,10	Total variation mean for all samples 0,71 SD ² tot = total variance 18,56 SCE tot = total sum of squared deviations = variance * (N-1)
	Day variation SD ² 0,00 CMj 0,00 SCEj 0,00 = SD ² * ne * nrep. = CMj * (nj-1)				

Residual deviation (from sum of squared deviations for each group e i)

Σd^2	0,000	0,000	0,000	0,00	SCEr = Σd^2
	0,000	0,000	0,000	0,00	CMr = SCEr / (ne * nj * (n rep - 1))
	0,000	0,000	0,000		

ANOVA Table

ANOVA	DF	SCE	CM	F	F observed probability	Signification	Variance	CV %	F table (p = 0.05)	F table (p = 0.01)	F table (p = 0.001)
D	2	0,00	0,00	3,94	0,113490781	NS	0,00	0,91	6,94	18,00	61,25
S	2	18,55	9,28	30355,74	4,34031E-09	***	0,77	79,91	6,94	18,00	61,25
DS	4	0,00	0,00	14,98	1,48401E-05	***	0,00	0,89	2,93	4,58	7,46
R	18	0,00	0,00				0,00	0,41			
T	26	18,56									

Conclusions

1. There is no "day" effect
2. There is a "sample" effect, which is normal
3. There is a "day-sample" interaction

CV% intra-day =	0,41
CV% total ("between") =	1,00

Appendix VIII: Certificate of analysis of the raw insulin Incelligent AF



Certificate of Analysis/Origin

Catalog number: 4506
Lot number: KA7CN9115A

Incelligent™ AF (Insulin, Recombinant Human, EP, USP)

Manufactured Novo Nordisk, Denmark
Novo Nordisk Product Number: 306-8890
Novo Nordisk Lot Number: TQ1HHP020
Millipore Lot Number: KA7CN9115A
Date of manufacture: 22 March 2007
Expiration Date: 22 March 2012

Storage: -20°C

Test By Method	Specification	Result
Identification A by Assay	Complies	Complies
Identification B by Peptide mapping	Complies	Complies
High molecular proteins	≤0.4%	0.16%
Related Proteins:		
A21 desamido human insulin	≤1.0%	0.3%
Human insulin related impurities	≤1.0%	0.3%
Zinc (calculated on a dried basis)	0.3 – 0.6%	0.36%
Loss on drying	≤10.0%	5.3%
Sulphated ash (calculated on a dried basis)	≤ 2.0%	0.5%
Microbiological control:		
Total viable count	≤ 300 CFU/g	≤ 20 CFU/g
Bacterial endotoxins	< 10 IU/mg	< 0.4 IU/mg
Assay as is	N/A	26.9 USP U/mg
Assay (calculated on a dried basis)	≥ 27.5 USP U/mg	28.4 USP U/mg
Assay (calculated on a dried basis)	95.0 – 105.0%	98.7%
Bioidentity ¹	≥ 15 USP U/mg	Complies
Host cell-derived proteins ²	≤ 10 ppm	Complies
Insulin human methyl ester ²	< 0.2%	Complies
Insulin human precursor ²	< 0.1%	Complies
Proinsulin content ³	None	None

- 1) Tested on one batch a quarter. Last quarterly lot complies for bioidentity.
- 2) Tested in-process.
- 3) Not formed in the biosynthetic process.

Not for therapeutic use. This is to certify that biosynthetic human insulin is produced by recombinant DNA technology in a fermentation system using yeast as the production organism. It is isolated and purified under Good Manufacturing Practice conditions.

Millipore certifies that the information contained in this certificate of analysis is a true and accurate transcription of the information contained in the manufacturer's certificate of analysis.

Cheryl Meents
Manager, Quality Control
14 May 2009

Page 1 of 1

290 Concord Rd. ■ Billerica, MA 01821 ■ 800.645.5476 or 781.533.6000 ■ orders@millipore.com
The product described here is intended for manufacturing and development and must not be administered to humans, or used for any drug or diagnostic purposes. Except as specifically stated in the Certificate of Analysis, MILLIPORE MAKES NO OTHER WARRANTY EXPRESSED, OR IMPLIED, OR STATUTORY, INCLUDING BUT NOT LIMITED TO WARRANTIES ON MERCHANTABILITY, FITNESS OR PERFORMANCE.

Appendix IX: Assessment of the microbial quality of the insulin formulations used in the pharmacoscintigraphic study

UNIVERSITE LIBRE DE BRUXELLES.
Institut de Pharmacie.
Unité de Microbiologie et d'Hygiène. C.P. 205/2.
Boulevard du Triomphe. B-1050 Bruxelles.

Le 22 mars 2010.

Rapport

Contrôle de qualité microbiologique de deux formulations sèches d'insuline pour inhalation :

- **Dénombrement de germes viables totaux**
- **Recherche de microorganismes spécifiés**

Demandeur : Prof. Karim Amighi, Institut de Pharmacie, Service de Pharmacie Galénique et Biopharmacie, Campus de la Plaine, Bâtiment BC, CP 207, Boulevard du Triomphe, 1050 Bruxelles, Belgique.

Nature des échantillons : gélules

a) Identification du laboratoire : Laboratoire de Microbiologie et Hygiène
Université Libre de Bruxelles,
Institut de Pharmacie
CP 205/2
Prof. Véronique Fontaine

b) Identification des échantillons :

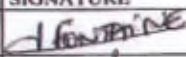
Fabricant : Flore Depreter, Institut de Pharmacie, Service de Pharmacie Galénique et Biopharmacie, Campus de la Plaine, Bâtiment BC, CP 207, Boulevard du Triomphe, 1050 Bruxelles, Belgique.

Date de réception : le 1 février et le 1 mars 2010.

Identification : gélules taille n°3 en HPMC contenant 5.0 ± 0.1 mg de poudre, numérotées :

- o F1 (3 lots, formulation d'insuline sans excipients) : F1L1, F1L2, F1L3
- o F2 (3 lots, formulation d'insuline avec des excipients lipidiques) : F2L1, F2L2, F2L3

Conditions de stockage : à température ambiante à l'abri de la lumière

	NOM	FONCTION	SIGNATURE
Rédigé le 22/03/2010	Fontaine, Véronique	Responsable unité Microbiologie	
Validé le 24/03/2010	Dehaye, Jean-Paul	Chef de Service	

Ce rapport ne peut être reproduit, même partiellement sans l'approbation écrite du laboratoire d'analyses.

c) Conditions expérimentales :

Période d'analyse : du 1 février au 19 mars 2010.

Prise d'essai : Etant donné que la taille des lots est inférieure à 100, la poudre d'une gélule entière (5 mg) est utilisée par test ; les tests ont été réalisés en duplicate pour les essais d'applicabilité et de recherche de germes vivants. Les essais d'applicabilité ont été réalisés sur un lot et les recherches de germes vivants sur 3 lots.

Identification des souches utilisées dans le test d'applicabilité de la méthode pour le dénombrement des germes aérobies totaux (DGAT) et les tests de fertilité:

Staphylococcus aureus ATCC 6538
Pseudomonas aeruginosa ATCC 9027
Echerichia coli ATCC 8739

d) Résultats des contrôles (UFC= unité formant une colonie)

Fertilité des milieux :

Milieux	Observations
Gélose TSA	Croissance de <i>S. aureus</i> , <i>P. aeruginosa</i> et <i>E. coli</i>
Milieu TSB	Croissance de <i>S. aureus</i> et <i>P. aeruginosa</i>
Gélose Cétrimide	Croissance de <i>P. aeruginosa</i> , absence de croissance de <i>S. aureus</i>
Gélose Sabouraud-dextrosé	Croissance de <i>Candida albicans</i>
Gélose Violet Rouge Bile Glucose	Croissance d' <i>E. coli</i>
Gélose Baird-Parker	Croissance de <i>S. aureus</i>
Bouillon lactose	Croissance d' <i>E. coli</i>

Contrôle de la stérilité et des conditions d'aseptie :

Milieux	Observations
Gélose TSA	0 UFC
Rédigé le 22/03/2010	NOM Fontaine, Véronique
	FONCTION Responsable unité Microbiologie
Validé le 24/03/2010	Dehaye, Jean-Paul
	Chef de Service

Ce rapport ne peut être reproduit, même partiellement sans l'approbation écrite du laboratoire d'analyses.

UNIVERSITE LIBRE DE BRUXELLES.
 Institut de Pharmacie.
 Unité de Microbiologie et d'Hygiène. C.P. 205/2.
 Boulevard du Triomphe. B-1050 Bruxelles.

Milieu TSB	0 UFC
Gélose Cétrimide	0 UFC
Gélose Sabouraud-dextrosé	0 UFC
Violet Red Bile Glucose agar	0 UFC
Bouillon EEB	0 UFC
Diluant	0 UFC
Solution tampon peptonée	0 UFC
Bouillon lactosé	0 UFC
Gélose Baird-Parker	0 UFC

e) **Résultats des essais d'applicabilité de la méthode pour le DGAT** (UFC= unité formant une colonie)

essai 1 :

Echantillons	Nbre UFC de <i>S. aureus</i>	Nbre UFC de <i>P. aeruginosa</i>
Pas de gélules	300	320
Gélules F1L1	450	470
Gélules F2L1	400	450

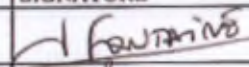
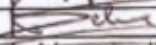
Remarque : problème de solubilité des préparations dans la solution tampon peptonée, donc difficulté de distinguer la différence entre résidu de précipité et UFC, d'où l'explication pour un nombre surévalué en CFU en présence de précipité.

essai 2 (en présence de 10g/l Tween 80):

Echantillons	Nbre UFC de <i>S. aureus</i>	Nbre UFC de <i>P. aeruginosa</i>
Pas de gélules	2	9
Gélules F1L1	3	4
Gélules F2L1	3	8

Résultats : le test est applicable aux préparations

f) **Résultats du dénombrement des germes aérobies totaux** : (UFC= unité formant une colonie)

	NOM	FONCTION	SIGNATURE
Rédigé le 22/03/2010	Fontaine, Véronique	Responsable unité Microbiologie	
Validé le 24/03/2010	Dehaye, Jean-Paul	Chef de Service	

Ce rapport ne peut être reproduit, même partiellement sans l'approbation écrite du laboratoire d'analyses.

essai 1 :

Echantillon	DGAT
Pas de gélule	0 et 0 UFC
Gélules F1L1	0 et 0UFC
Gélules F1L2	1 et 0 UFC
Gélules F1L3	3 et 0 UFC
Gélules F2L1	26 et 27 UFC
Gélules F2L2	25 et 16 UFC
Gélules F2L3	47 et 34 UFC

Les nombres d'UFC obtenus avec les préparations avec l'excipient lipidique (F2) sont probablement surévalués étant donné la présence de résidus insolubles pouvant avoir la même apparence que des UFC.

Essai 2 (en présence de 10g/ml Tween 80):

Echantillon	DGAT
Gélules F1L1	0 et 1UFC
Gélules F2L1	0 et 0 UFC

Résultats : < 100 germes aérobies totaux/gélule analysée

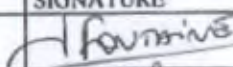
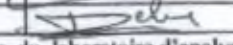
Les échantillons sont conformes

g) Résultats du dénombrement des moisissures et levures totales (DMLT):

(UFC= unité formant une colonie)

essai 1 :

Echantillon	DMLT
Pas de gélule	0 et 0 UFC
Gélules F1L1	0 et 0UFC
Gélules F1L2	0 et 0 UFC
Gélules F1L3	1 et 0 UFC
Gélules F2L1	0 et 1 UFC
Gélules F2L2	0 et 0 UFC

	NOM	FONCTION	SIGNATURE
Rédigé le 22/03/2010	Fontaine, Véronique	Responsable unité Microbiologie	
Validé le 24/03/2010	Dehaye, Jean-Paul	Chef de Service	

Ce rapport ne peut être reproduit, même partiellement sans l'approbation écrite du laboratoire d'analyses.

UNIVERSITE LIBRE DE BRUXELLES.
 Institut de Pharmacie.
 Unité de Microbiologie et d'Hygiène. C.P. 205/2.
 Boulevard du Triomphe. B-1050 Bruxelles.

F2L2	Gélose Cétrimide	0 UFC
F2L3	Gélose Cétrimide	0 UFC

Résultats : Absence *Pseudomonas aeruginosa* /gélule analysée. Les échantillons satisfont à l'essai.

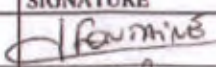
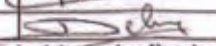
j) Recherche de bacilles à Gram négatif résistantes aux sels biliaires(UFC= unité formant une colonie)

Echantillon	Milieu	Observation de la culture
F1L1	Gélose Bile-Violet-Rouge-Glucose	0 UFC
F1L2	Gélose Bile-Violet-Rouge-Glucose	0 UFC
F1L3	Gélose Bile-Violet-Rouge-Glucose	0 UFC
F2L1	Gélose Bile-Violet-Rouge-Glucose	0 UFC
F2L2	Gélose Bile-Violet-Rouge-Glucose	0 UFC
F2L3	Gélose Bile-Violet-Rouge-Glucose	0 UFC

Résultats : Absence de bacilles à Gram négatif résistants aux sels biliaires /gélule analysée. Les échantillons satisfont à l'essai.

CONCLUSIONS DES ANALYSES EFFECTUEES :

Les gélules de deux formulations sèches d'insulines (avec ou sans excipients lipidiques) qui ont été analysées satisfont aux contrôles de qualité microbiologique, comme décrits ci-dessus.

	NOM	FONCTION	SIGNATURE
Rédigé le 22/03/2010	Fontaine, Véronique	Responsable unité Microbiologie	
Validé le 24/03/2010	Dehay, Jean-Paul	Chef de Service	

Ce rapport ne peut être reproduit, même partiellement sans l'approbation écrite du laboratoire d'analyses.

UNIVERSITE LIBRE DE BRUXELLES.
 Institut de Pharmacie.
 Unité de Microbiologie et d'Hygiène. C.P. 205/2.
 Boulevard du Triomphe. B-1050 Bruxelles.

Gélules F2L3	0 et 0 UFC
--------------	------------

Essai 2 :

Echantillon	DMLT
Gélules F1L1	0 et 1UFC
Gélules F2L1	0 et 0 UFC

Résultats : < 10 moisissures et levures totales/gélule analysée
Les échantillons sont conformes

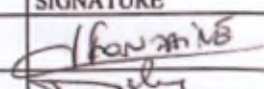
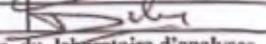
h) Recherche de *Staphylococcus aureus* (UFC= unité formant une colonie)

Echantillon	Milieu	Observation de la culture
F1L1	Gélose Baird-Parker	0 UFC
F1L2	Gélose Baird-Parker	0 UFC
F1L3	Gélose Baird-Parker	0 UFC
F2L1	Gélose Baird-Parker	0 UFC
F2L2	Gélose Baird-Parker	0 UFC
F2L3	Gélose Baird-Parker	0 UFC

Résultats : Absence de *Staphylococcus aureus* /gélule analysée. Les échantillons satisfont à l'essai.

i) Recherche de *Pseudomonas aeruginosa* (UFC= unité formant une colonie)

Echantillon	Milieu	Observation de la culture
F1L1	Gélose Cétrimide	0 UFC
F1L2	Gélose Cétrimide	0 UFC
F1L3	Gélose Cétrimide	0 UFC
F2L1	Gélose Cétrimide	0 UFC

	NOM	FONCTION	SIGNATURE
Rédigé le 22/03/2010	Fontaine, Véronique	Responsable unité Microbiologie	
Validé le 24/03/2010	Dehaye, Jean-Paul	Chef de Service	

Ce rapport ne peut être reproduit, même partiellement sans l'approbation écrite du laboratoire d'analyses.

